Anthrax outbreak investigation 2.0 – Improving bioforensics and detection of the notorious pathogen *Bacillus anthracis*

Dissertation

Zur Erlangung des Doktorgrades

der Naturwissenschaften

(Dr. rer. nat.)

der Fakultät für Biologie

der Ludwig-Maximilians-Universität München

vorgelegt von

Peter Braun

am

09. März 2022

1. Gutachter: Prof. Dr. Ralf Heermann, JGU Mainz

2. Gutachter: Prof Dr. Heinrich Jung, LMU München

Datum der Abgabe: 09.03.2022

Datum der mündlichen Prüfung: 04.07.2022

Eidesstattliche Erklärung

Ich versichere hiermit an Eides statt, dass die vorgelegte Dissertation von mir selbstständig und ohne unerlaubte Hilfe angefertigt wurde. Des Weiteren erkläre ich, dass ich nicht anderweitig ohne Erfolg versucht habe, eine Dissertation einzureichen oder mich der Doktorprüfung zu unterziehen. Die folgende Dissertation liegt weder ganz, noch in wesentlichen Teilen einer anderen Prüfungskommission vor.

München, den 09.03.2022 Peter Braun

Statutory Declaration

I declare that I have authored this thesis independently, that I have not used other than the declared sources/references. As well, I declare that I have not submitted a dissertation without success and not passed the oral exam. The present dissertation (neither the entire dissertation nor parts) has not been presented to another examination board.

Munich, 09.03.2022 Peter Braun

Content

Abbreviations

bp	base pairs
Br.	Branch
canSNP	canonical SNP
CFU	colony forming units
Ct	cycle threshold
DNA	deoxyribonucleic acid
dPCR	digital PCR
EF	edema factor
ELPRA	enzyme-linked phage receptor binding protein assay
FISH	fluorescence in situ hybridization
LB	lysogeny broth
LF	lethal factor
PA	protective antigen
PAGE	polyacrylamide gel electrophoresis
PCR	polymerase chain reaction
RBP	receptor binding protein
RNA	ribonucleic acid
rRNA	ribosomal RNA
RT	reverse transcription
s.l.	*sensu lato*
SNP	single nucleotide polymorphisms
tRNA	transfer RNA
WGS	whole genome sequencing

Publications and manuscripts presented in this thesis

Chapter 2:

Peter Braun[1], Mandy Knüpfer[1], Markus Antwerpen[1], Dagmar Triebel[2], and Gregor Grass[1#] - A Rare Glimpse into the Past of the Anthrax Pathogen *Bacillus anthracis. Microorganisms* 2020, 8, 298

Chapter 3:

Peter Braun[1], Fee Zimmermann[1], Mathias C. Walter[1], Sonja Mantel[1], Karin Aistleitner[1], Inga Stürz[1], Gregor Grass[1#*] and Kilian Stoecker[1*] - In-Depth Analysis of *Bacillus anthracis* 16S rRNA Genes and Transcripts Reveals Intra- and Intergenomic Diversity and Facilitates Anthrax Detection. *mSystems* 2022, Volume 7 Issue 1

Chapter 4:

Peter Braun[1], Martin Duy-Thanh Nguyen[1], Mathias C. Walter[1] and Gregor Grass[1#] - Ultrasensitive Detection of *Bacillus anthracis* by Real-Time PCR Targeting a Polymorphism in Multi-Copy 16S rRNA Genes and Their Transcripts. *Int. J. Mol. Sci*. 2021, 22, 12224

Chapter 5:

Peter Braun[1], Immanuel Wolfschläger[1], Leonie Reetz[1], Lilia Bachstein[1], Ana Clara Jacinto[1], Carolina Tocantins[1], Johannes Poppe[1] and Gregor Grass[1#] - Rapid Microscopic Detection of *Bacillus anthracis* by Fluorescent Receptor Binding Proteins of Bacteriophages. *Microorganisms* 2020, 8, 934

Chapter 6:

Peter Braun[1*], Nadja Rupprich[1*], Diana Neif[1] and Gregor Grass[1#] - Enzyme-Linked Phage Receptor Binding Protein Assays (ELPRA) Enable Identification of *Bacillus anthracis* Colonies. *Viruses* 2021, 13, 1462

Chapter 7:

Peter Braun[1], Wolfgang Beyer[3], Matthias Hanczaruk[4], Julia M. Riehm[4], Markus Antwerpen[1], Christian Otterbein[5], Jacqueline Oesterheld[1] and Gregor Grass[1#] - Reoccurring Bovine Anthrax in Germany on the Same Pasture After 12 Years. *Journal of Clinical Microbiology*, accepted

* Authors contributed equally

[#] Corresponding authors

[1] Bundeswehr Institute of Microbiology (IMB), Germany

[2] Bavarian Natural History Collections, Botanische Staatssammlung München, Germany

[3] Department of Livestock Infectiology and Environmental Hygiene, Institute of Animal Science, University of Hohenheim, Germany

[4] Bavarian Health and Food Safety Authority, Germany

[5] Local Veterinarian Unit, District Rosenheim, Germany

Contributions to publications and manuscripts presented in this thesis

Chapter 2:

Conceptualization: D.T., M.A., P.B. and G.G.; investigation: M.K. and P.B.; methodology: M.K., P.B., M.A., and G.G.; formal analysis and validation: M.A. and G.G.; resources: D.T., M.A., and G.G.; data curation: P.B., M.K., D.T., M.A., and G.G.; writing—original draft preparation: P.B., M.A., and G.G.; writing— review and editing: P.B., M.K., D.T., M.A., and G.G.; visualization: P.B., M.K., and G.G.; supervision and project administration: M.A. and G.G.; funding acquisition: M.A. and G.G.

Chapter 3:

P.B., F.Z., G.G. and K.S. designed the study and interpreted the results. M.W. contributed the bioinformatics analysis. I.S., F.Z., K.A. and S.M. performed FISH experiments. P.B. and I.S. performed digital PCR experiments. G.G., P.B., F.Z. and K.S. wrote the first draft manuscript and all authors edited the manuscript.

Chapter 4:

Conceptualization, G.G. and P.B.; investigation, P.B., M.D.-T.N. and M.C.W.; methodology, M.D.-T.N. and P.B.; formal analysis and validation, P.B., M.D.-T.N. and G.G.; resources, G.G. and M.C.W.; data curation, P.B., M.D.-T.N. and M.C.W.; writing—original draft preparation, G.G. and P.B.; writing—review and editing, P.B., M.D.-T.N., M.C.W. and G.G.; visualization, M.D.-T.N., P.B. and G.G.; supervision and project administration, G.G. and P.B.; funding acquisition, G.G.

Chapter 5:

Conceptualization, G.G.; investigation, P.B., I.W., L.B., L.R., A.C.J., C.T. and J.P.; methodology, P.B. and G.G.; formal analysis and validation, P.B., I.W., L.B., L.R. and G.G.; resources, G.G.; data curation, P.B., I.W., L.B., L.R. and G.G.; writing—original draft preparation, P.B. and G.G.; writing—review and editing, P.B., I.W., L.B., L.R., A.C.J., C.T., J.P. and G.G.; visualization, I.W., L.R., P.B. and G.G.; supervision and project administration, P.B. and G.G.; funding acquisition, G.G.

Chapter 6:

Conceptualization, G.G. and P.B.; methodology, G.G and P.B.; validation, G.G. and P.B.; formal analysis, G.G.; investigation, N.R. and D.N.; resources, G.G.; data curation, G.G. and P.B.; writing—original draft preparation, G.G. and P.B.; writing—review and editing, G.G, P.B., N.R. and D.N.; visualization, G.G., N.R. and P.B.; supervision, G.G.; project administration, G.G.

Chapter 7:

Conceptualization, G.G., W.B. and P.B.; methodology, P.B., G.G. W.B., M.A., J.O., C.O. and J.M.R; validation, G.G. and P.B.; formal analysis, G.G. and P.B.; investigation, P.B., M.H., M.A. and J.O.; resources, G.G.; data curation, G.G. and P.B.; writing—original draft preparation, G.G. and P.B.; writing—review and editing, G.G., P.B., W.B. and J.M.R.; visualization, G.G. and P.B.; supervision, G.G.; project administration, G.G.

Zusammenfassung

Das Bakterium *Bacillus anthracis* ist ein Gram-positiver Endosporenbildner und der Erreger der Zoonose Milzbrand. Aufgrund der hohen Virulenz und weil die Sporen in der Umwelt sehr stabil sowie leicht zu kultivieren sind, gilt *B. anthracis* als der Erreger mit dem höchsten Potenzial, als biologischer Kampfstoff oder für bioterroristische Zwecke missbraucht zu werden. Dieses Potential wurde 2001 bei den Briefanschlägen in den USA auf tragische Weise demonstriert. Im Falle eines Milzbrandausbruchs bei Nutz- oder Wildtieren, vor allem aber beim Menschen, sind zwei Aspekte von besonderer Bedeutung und Dringlichkeit, um Gegenmaßnahmen wie Therapie oder Dekontamination betroffener Gebiete einzuleiten: Die eindeutige und schnelle Identifizierung von *B. anthracis* sowie die Aufklärung der Ursachen des Ausbruchs. Aufgrund des fulminanten Verlaufs von Milzbrandinfektionen sind schnelle und zuverlässige Nachweismethoden für *B. anthracis* zwingend erforderlich um ein Überleben der Infizierten zu gewährleisten. Jedoch kann es wegen der engen genetischen Verwandtschaft zwischen *B. anthracis* und anderen Mitgliedern der *Bacillus cereus sensu lato*-(*s.l.*)-Gruppe (wie *Bacillus cereus* oder *Bacillus thuringiensis*) zu einer falschen oder fragwürdigen Identifizierung kommen. So galten beispielsweise die 16S rRNA Gene, die üblicherweise zur Typisierung von Bakterien verwendet werden, bisher als ungeeignet für die Differenzierung von *B. anthracis* von anderen Mitgliedern der *B. cereus s.l.* Gruppe, da die Sequenzunterschiede *B. anthracis* nicht differenzieren. In dieser Arbeit wurde mit einer Kombination aus *in-situ-, in-vitro*- und *in-silico* Methoden ein bisher unbekanntes 16S rRNA Allel in *B. anthracis* beschrieben, in allen verfügbaren Genomsequenzen nachgewiesen und quantifiziert. Neben neuen Erkenntnissen über die Häufigkeit und die genomische Verteilung dieses 16S-BA-Allels sowie die Architektur ganzer rRNA-Operons, ermöglichte diese *B. anthracis* spezifische Variation zum ersten Mal die Entwicklung neuer 16S-basierter Diagnostika, wie etwa eines

FISH-Tests. Die neu entwickelte 16S rRNA SNP (RT)-PCR, mit der eine Detektion auf DNA- und Transkript-Ebene möglich ist, erwies sich im Vergleich zu den getesteten, etablierten PCR-Assays als überdurchschnittlich spezifisch und sensitiv. Da PCR, der Goldstandart für die Detektion von *B. anthracis*, allein für eine zweifelsfreie Erregeridentifizierung nicht ausreicht, sind alternative, Nukleinsäure-unabhängige Methoden zur Bestätigung der PCR-Ergebnisse erforderlich. Diese Methoden sollten vergleichbar empfindlich, spezifisch und schnell wie der PCR-Nachweis sein. Für andere Erreger haben sich Detektionsmethoden, die auf Rezeptorbindeproteine (RBPs) hochspezifischer Bakteriophagen (Phagen) basieren, als geeignet erwiesen, diese Kriterien zu erfüllen. Obwohl es mehrere hochspezifische Phagen gibt, wurde bisher aber kein solcher Ansatz für *B. anthracis* entwickelt. Daher wurden in dieser Arbeit drei RBPs von *B. anthracis*-spezifischen (Pro)phagen identifiziert und experimentell auf ihre Spezifität gegenüber *B. anthracis* sowie auf ihre Rezeptorverfügbarkeit in verschiedenen Wachstumsphasen von *B. anthracis* getestet. Auf dieser Basis wurden anschließend eine Reihe neuer Methoden zum schnellen Nachweis von *B. anthracis* entwickelt. Mittels Fusionen aus RBPs mit dem Fluoreszenzprotein mCherry wurden RBP-basierte, fluoreszierende Biosensoren produziert die, zusammen mit einem neuen 16S FISH Assay, die ersten zuverlässigen mikroskopischen Nachweisverfahren für *B. anthracis* darstellen. Zusammen mit ebenfalls selbst-konstruierten, enzymbasierten RBP-Biosensoren, die für die Entwicklung der neuen ELPRA-Tests verwendet wurden, können diese RBP-Assays zum Nachweis intakter *B. anthracis*-Zellen und als Nukleinsäure-unabhängige Ansätze zur Bestätigung von PCR-Ergebnissen eingesetzt werden. Ist der Erreger einmal identifiziert, muss für die Untersuchung der Ausbruchsursache, also ob es sich um einen natürlichen Ausbruch oder eine absichtliche Freisetzung des Erregers handelt, die genaue und flächendeckende natürliche Phylogeographie des Erregers vorliegen. Damit kann der Genotyp des Ausbruchstammes mit denen der im betroffenen Gebiet natürlich vorkommenden Stämme abgeglichen werden. Für Zentraleuropa konnte diese natürliche

Phylogeographie von *B. anthracis* bisher noch nicht bestätigt werden. Für diesen Zweck wurden in dieser Arbeit aus einer historische *B. anthracis* Probe aus dem Jahr 1878 Nukleinsäuren extrahiert und damit das älteste historische *B. anthracis* Genom charakterisiert, welches der sogenannten B.Br.CNEVA Gruppe zugeordnet werden konnte. Diese Ergebnisse unterstützen die Annahme, dass die B.Br.CNEVA Gruppe einen Teil des autochthonen Genotyps des Erregers für Mitteleuropa darstellt. Aus bioforensischer Sicht kann daher bei einem künftigen Ausbruch, der durch einen *B. anthracis* Stamm aus der B.Br.CNEVA-Gruppe verursacht wird, davon ausgegangen werden, dass es sich wahrscheinlich um eine natürliche Infektion handelt. Sollte im Gegensatz dazu die Isolierung eines *B. anthracis* Stamms aus einer Verwandschaftsgruppe außereuropäischen Ursprungs sorgfältiger untersucht werden, da dies auf eine absichtliche Freisetzung des Erregers hindeuten könnte. So gab beispielsweise der jüngste Milzbrandausbruch in Südbayern keinen Anlass zur Sorge, da er ebenfalls durch einen B.Br.CNEVA-Stamm verursacht wurde, der eng mit dem historischen Stamm von 1878 verwandt ist. Bei diesem Ausbruch konnten außerdem die in dieser Arbeit entwickelten Nachweismethoden an echten klinischen Proben und Umweltproben erfolgreich getestet werden. Es ist wahrscheinlich, dass diese neuen, spezifischen Detektionsmethoden, zusammen mit neuen phylogeographischen Erkenntnissen aus historischen Proben, die moderne Milzbrand-Diagnostik und -Ausbruchsuntersuchung auf ein neues, fortschrittlicheres Niveau heben werden.

Summary

The bacterium *Bacillus anthracis* is a Gram-positive endospore former and the causative agent of the zoonotic disease anthrax. Due to its high virulence and because the spores are very stable in the environment and easy to culture, *B. anthracis* is considered to be the pathogen with one of the highest potentials to be misused as a biological warfare agent or for bioterroristic purposes. This potential was clearly demonstrated in the 2001 letter attacks in the United States. In the event of an anthrax outbreak in livestock or wildlife, but especially in humans, two things are of particular importance and urgency to initiate countermeasures such as therapy or decontamination of affected areas: The unambiguous and rapid identification of *B. anthracis* and the elucidation of the causes of the outbreak. Due to the fulminant course of anthrax infections, rapid and reliable detection methods for *B. anthracis* are crucial to ensure survival of infected individuals. However, because of the close genetic relationship between *B. anthracis* and other members of the *Bacillus cereus sensu lato* (*s.l.)* group (such as *Bacillus cereus* or *Bacillus thuringiensis*), mis- or questionable identification sometimes occurs. For example, due to presumed sequence identity, the 16S rRNA genes commonly used to type bacteria were previously considered unsuitable for differentiating *B. anthracis* from other members of the *B. cereus s.l.* group. In this work, a previously unknown 16S rRNA allele in *B. anthracis* was described using a combination of *in situ, in vitro*, and *in silico* methods. This 16S-BA-allele could be detected and quantified in all available genome sequences. In addition to new insights into the abundance and genomic arrangement of the 16S-BA-allele as well as total rRNA operons, this *B. anthracis*-specific variation enabled for the first time the development of new 16S-based diagnostics, such as FISH. The newly developed 16S rRNA SNP (RT)-PCR, which allows detection on DNA- and transcript-level, proved to have superior specificity and sensitivity compared to most established PCR assays. Since PCR, the gold standard for *B. anthracis* detection, alone is not sufficient for unequivocal

pathogen identification, alternative, nucleic acid-independent methods are needed to confirm PCR results. These methods should be comparably sensitive, specific, and rapid as PCR detection. For other pathogens, detection methods based on receptor binding proteins (RBPs) of highly specific phages have been shown to meet these criteria. However, although several highly specific phages exist, no such approach has yet been developed for *B. anthracis*. Therefore, in this work, three RBPs of *B. anthracis*-specific (pro)phages were identified and experimentally tested for their specificity towards *B. anthracis* as well as for their receptor availability in different growth phases of *B. anthracis*. On this basis, a set of new methods for the rapid detection of *B. anthracis* was developed. Using fusions of RBPs with the fluorescent protein mCherry, RBP-based biosensors were produced which, together with the new 16S FISH assay, represent the first reliable microscopic detection methods for *B. anthracis*. Together with the enzyme-based RBP biosensors used to develop the new ELPRA assays, these RBP assays can be used as nucleic acid-independent approaches to confirm PCR results and to detect intact *B. anthracis* cells. Once the pathogen is identified, in order to investigate the cause of the outbreak, i.e. whether it is a natural outbreak or a deliberate release of the pathogen, the exact and area-wide natural phylogeography of the pathogen must be available so that the genotype of the outbreak strain can be matched with the strains naturally occurring in the affected area. For Central Europe, this natural phylogeography of *B. anthracis* has not yet been confirmed. For this purpose, nucleic acids were extracted in this work from a historical anthrax sample from 1878, characterizing the oldest historical *B. anthracis* genome that could be assigned to the B.Br. CNEVA group. These results support the hypothesis that the B.Br.CNEVA group represents part of the autochthonous genotype of the pathogen for Central Europe. From a bioforensic point of view, therefore, a future outbreak caused by a *B. anthracis* strain from the B.Br.CNEVA group can be assumed to be a natural infection, whereas the isolation of a *B. anthracis* strain from a canSNP group of non-European origin should be investigated more carefully, as this could indicate a deliberate release of the

pathogen. For example, the recent anthrax outbreak in southern Bavaria was not a cause for concern as it was also caused by a B.Br.CNEVA strain closely related to the historical strain of 1878. In this outbreak, moreover, the detection methods developed in this work were successfully tested on authentic clinical and environmental samples. These new, specific detection methods, along with new phylogeographic insights from historical samples, will bring modern anthrax outbreak investigation to a new level.

1. Introduction

1.1. *Bacillus anthracis* – a pathogen with history

Bacillus anthracis, the causative agent of anthrax, is a large (1 by 5 - 8 µm), rod-shaped Gram-positive bacterium which is non-hemolytic, non-motile and forms endospores (Figure 1-1) under adverse environmental conditions (Turnbull 2008). The formation of spores from the vegetative stage of bacilli was first described by Ferdinand J. Cohn in 1874. Just two years later, Robert Koch elucidated the life- and infection-cycle of *B. anthracis* in his seminal work "Die Ätiologie der Milzbrand-Krankheit". Herein, Koch delineated that the bacterium forms spores as a permanent form, from which vegetative cells develop and, if in a suitable host, the disease occurs. Koch thus refuted Casimir Davaine's thesis that anthrax is caused only by the rod-shaped vegetative form of the bacteria (Sternbach 2003).

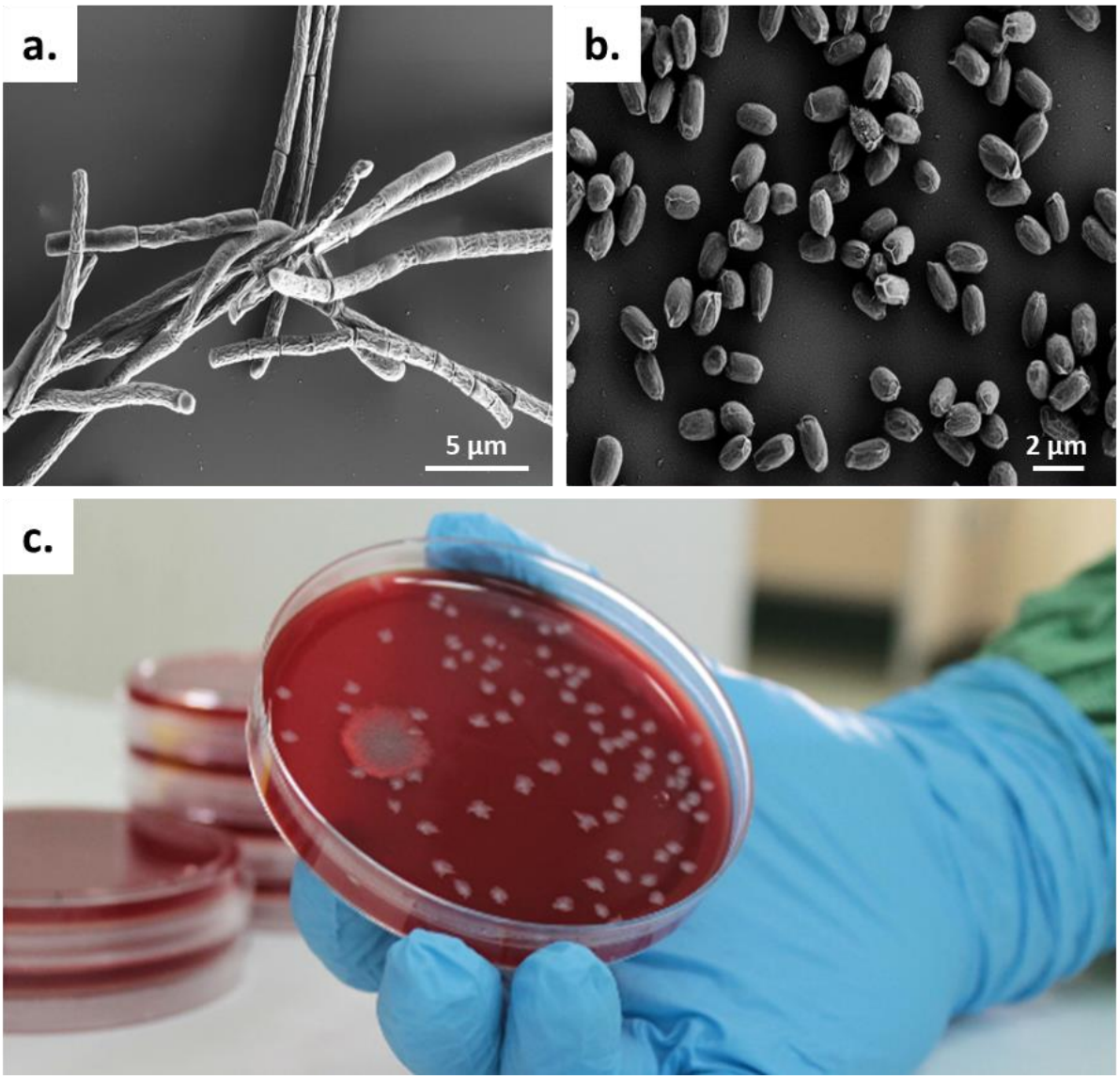

Figure 1-1: Cells, endospores and colonies of *B. anthracis*. Electron micrograph of a.) *B. anthracis* cells growing in chains and of b.) purified *B. anthracis* spores. c.) Whitish, non-hemolytic colonies of *B. anthracis* derived from an environmental sample grown on a blood agar plate show the typical "medusa head" morphology (next to a flat-growing, hemolytic colony of the closely related *Bacillus mycoides*).

Mankind has been plagued by anthrax since the dawn of history. Indications of this go back thousands of years and can already be found in records of ancient Greece, where the name "anthrax" was coined by Hippocrates (Schwartz 2009). Anthrax mainly affects grazing animals such as cattle, sheep and horses and was one of the leading causes of

death in livestock, especially from the seventeenth to the nineteenth century. Because of this, anthrax became the main research topic of Robert Koch and his colleagues and was therefore the primary focus of early modern microbiology (Schwartz 2009; Zasada 2020). While the primary hosts are herbivores, humans, like all mammals, are also susceptible but require higher doses of infection for the disease to manifest (Turnbull 2008). The most frequent form in humans is cutaneous anthrax, which accounts for more than 95% of all anthrax cases. Here, the inert spores are thought to enter human skin through micro-lesions after exposure to, for example, infectious animal tissue (hides or meat), and to germinate in host macrophages after uptake leading ultimately to dissemination and infection. The term anthrax, Greek for charcoal, is derived from the black anthrax carbuncles of skin necrosis that, along with local edema, are the characteristic manifestations of cutaneous anthrax (Turnbull 2008). Historically, infections of this relatively mild form (< 20% mortality rate if untreated; <1 with antibiotic therapy) typically occurred in tanneries or wool-processing plants where workers were exposed to contaminated hides. Rarely, but with a higher mortality rate of more than 50% (even with treatment) due to the high likelihood of lymphatic or hematogenous spread, gastrointestinal anthrax occurs as a result of ingesting (undercooked) meat from infected animals (Missiakas and Schneewind 2005; Turnbull 2008). The gastrointestinal form is associated with enzootic regions in rural and less developed areas where people live in close proximity to livestock and where veterinary surveillance is inadequate (Turnbull 2008). It is estimated that in Africa, Central Asia, and South Asia, up to ten human cases of cutaneous and gastrointestinal anthrax occur after the slaughter of a single infected animal (Turnbull 2008). In contrast, in most European countries and other industrialized regions, an average of only one human case of cutaneous and gastrointestinal anthrax can be observed per ten infected animal carcasses (Turnbull 2008).

In addition to natural enzootic and zoonotic manifestations, a new form, injectional anthrax, has manifested in Europe in the last 20 years, in which heroin users were infected by batches of heroin supposedly contaminated with *B. anthracis* endospores (Hanczaruk et al. 2014). The fourth and most severe form of anthrax is pulmonary anthrax, which, after inhalation of *B. anthracis* spores, leads to systemic infection and death with nearly 100% case-fatality rate if untreated. Even with early antibiotic therapy, the mortality rate is approximately 45% (Turnbull 2008).

1.2. Biological warfare and bioterrorism

Due to its virulence and because the endospores of *B. anthracis* are very stable in the environment and easy to culture, *B. anthracis* is considered the pathogen with the highest potential to be misused as a biological warfare agent or for bioterrorist purposes. The bacterium is therefore listed as a Category A pathogen by the Center for Disease Control and Prevention (CDC, United States of America). This potential was demonstrated in the anthrax attacks in 2001 (Amerithrax), when letters filled with fine powder that consisted of *B. anthracis* endospores were sent to several addressees in the United States. The attacks led to 11 cases of cutaneous anthrax and 11 cases of pulmonary anthrax from which five individuals died as a result of the infection (Inglesby et al. 2002; Fowler and Shafazand 2011). According to the FBI, the total financial burden caused by the Amerithrax events exceeded 1 billion US-Dollars mainly due to immense decontamination efforts (Lengel 2005). In 1972, decades before the anthrax letter attacks, the "Convention on the Prohibition of the Development, Production and Stockpiling of Bacteriological (Biological) and Toxin Weapons and on their Destruction" was adopted by the United Nations. This was a political response to nefarious research, production and use of biological weapons during World War I and II as well as during early Cold War periods despite the Geneva

Protocol that prohibited the use of biological (and chemical) weapons (Barras and Greub 2014). For example, the infamous "Baron von Rosen espionage incident" occurred in 1917, in which sugar cubes allegedly laced with the anthrax agent were used to sabotage Allied horse-powered war support (Redmond et al. 1998; Antwerpen et al. 2017). At the height of the Cold War (1979), an incident occurred at a vaccine-production facility and suspected bioweapons factory in which large quantities of anthrax endospores escaped because of air-filter problems and spread by wind over urban areas of the city of Sverdlovsk (now Yekatarinburg). This officially resulted in 66 deaths in the city (Sahl and Keim 2016). Later conducted genomic analyses of tissue samples from infected individuals revealed that the outbreak strain was neither genetically modified nor were there any indications of an improved pathogenic potential but the genome represented a genotype that occurs naturally in Russia (Sahl and Keim 2016).

1.3. Genetics and Pathophysiology

B. anthracis possesses a single circular chromosome with 5.3 million base pairs and an AT content of approximately 65%, which classifies the Firmicute bacterium as a low GC organism (Ravel et al. 2008). Its pathogenic potential is associated with the presence of two virulence plasmids. Plasmid pXO2 (96 kb) harbors approximately 80 genes including the *capBCADE* operon that encodes enzymes enabling the synthesis of a poly-D-glutamic acid capsule (Figure 1-2) that allows *B. anthracis* to evade opsonization and phagocytosis by macrophages during host infection (Moayeri et al. 2015). The “toxin” plasmid pXO1 (182 kb) encodes 140 genes including three genes for the exotoxin proteins lethal factor (*lef*, LF), edema factor (*cya,* EF), and protective antigen (*pagA*, PA). PA, LF, and EF alone do not have a toxic effect on the host, only the combination of the three leads to the formation of two different AB toxins. PA binds to host cell surface receptors and is

cleavage-activated by host-proteases that leads to the formation of an oligomer that is able to bind LF and EF. After endocytosis of this AB-toxin complex (PA-LF and PA-EF, respectively) and acidification of the endosome, the thus acid-activated PA-pore allows translocation of edema and lethal factor into the cytosol. Edema factor is a calmodulin-binding adenylate cyclase that interferes with intracellular signaling, inhibits the immune response, and leads to edema formation by perturbing water homeostasis (Figure 1-3). The lethal factor, on the other hand, is a four-domain zinc protease that binds specifically to MAPK (mitogen-activated protein kinase). The recognition sequence for downstream kinases is excised and signal transduction is inhibited, resulting in apoptosis and cell lysis (Koehler 2009; Okinaka et al. 1999; Pilo and Frey 2011; Moayeri et al. 2015). The expression of both toxins and capsule genes is mainly regulated by the pleiotropic repressor AtxA. The *atxA* gene located on pXO1 is activated and expressed at elevated CO_2 levels and 37°C inside the host body (Levy et al. 2014).

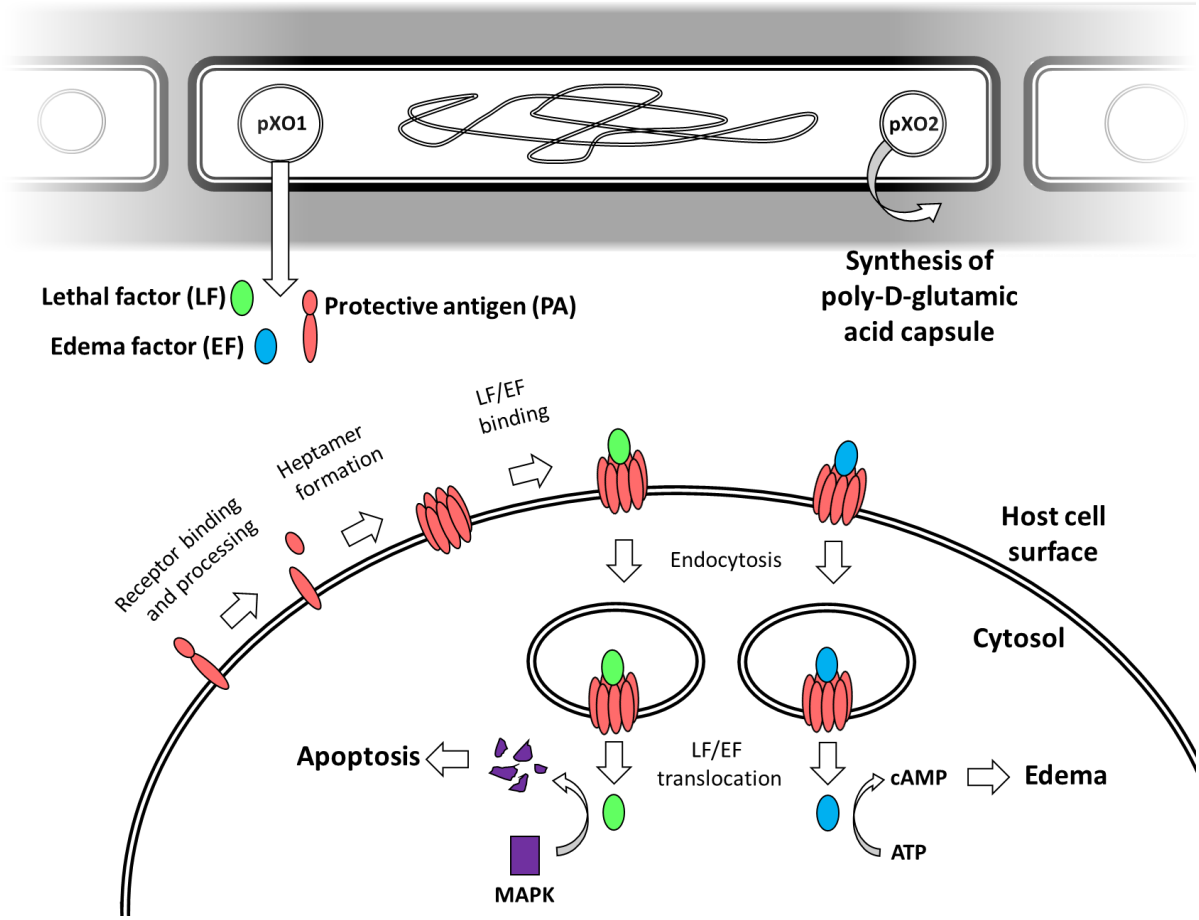

Figure 1-2: Major virulence factors of *B. anthracis*. The upper part of the figure shows encapsulated *B. anthracis* cells, while in the lower part a simplified host cell is depicted. Genes encoding enzymes for the synthesis of the poly-D-glutamic acid capsule (gray shading), which protects the bacteria from the host immune system, are located on virulence plasmid pXO2. Plasmid pXO1 harbors the toxin genes that encode the lethal factor (LF), the edema factor (EF) and the protective antigen (PA). Full length PA initially binds to a host cell receptor and, after cleavage by host proteases, forms heptamers that enable binding of EF or LF. After endocytosis of the complex, the effectors (EF or LF) are translocated by low pH-activated PA into the cytosol of the host cell. LF affects cell signaling by cleavage of MAPK (mitogen-activated protein kinase) leading ultimately to apoptosis and cell lysis. EF is an adenylate cyclase and evokes edema formation by perturbing water homeostasis.

1.4. Phylogeography and Bioforensics

B. anthracis is a very clonal organism with little or no horizontal gene transfer and low intraspecies diversity at the genomic level. Its evolution is probably restricted to the limited reproductive phases of 20-40 generations during host infection, while the resulting spores can remain dormant in the environment for years (Keim et al. 2004). When *B. anthracis* isolates from different parts of the world were compared, only a small amount of genetic variation accumulated since its probable first appearance as a pathogen about 3,000 - 6,000 years ago (Van Ert et al. 2007). However, deeper analysis of numerous genomic data revealed that *B. anthracis* strains can be divided into distinct phylogenetic groups. For each of these groups, a specific suite of phylogenetically meaningful nucleotide bases was set as references, and served as so-called canonical single nucleotide polymorphisms (canSNPs). These canSNP may show either of two states, ancestral (equal to the base in the ancestral reference genome) or derived (evolved base). On the basis of these canSNPs, *B. anthracis* strains can be classified into one of the three major branches A (A.Br.), B (B.Br.), and C (C.Br.), which can be divided into thirteen classical canSNP groups (e.g., B.Br.CNEVA) that reflect the global phylogenetic relationships among strains (Van Ert et al. 2007; Marston et al. 2011) (Figure 1-3).

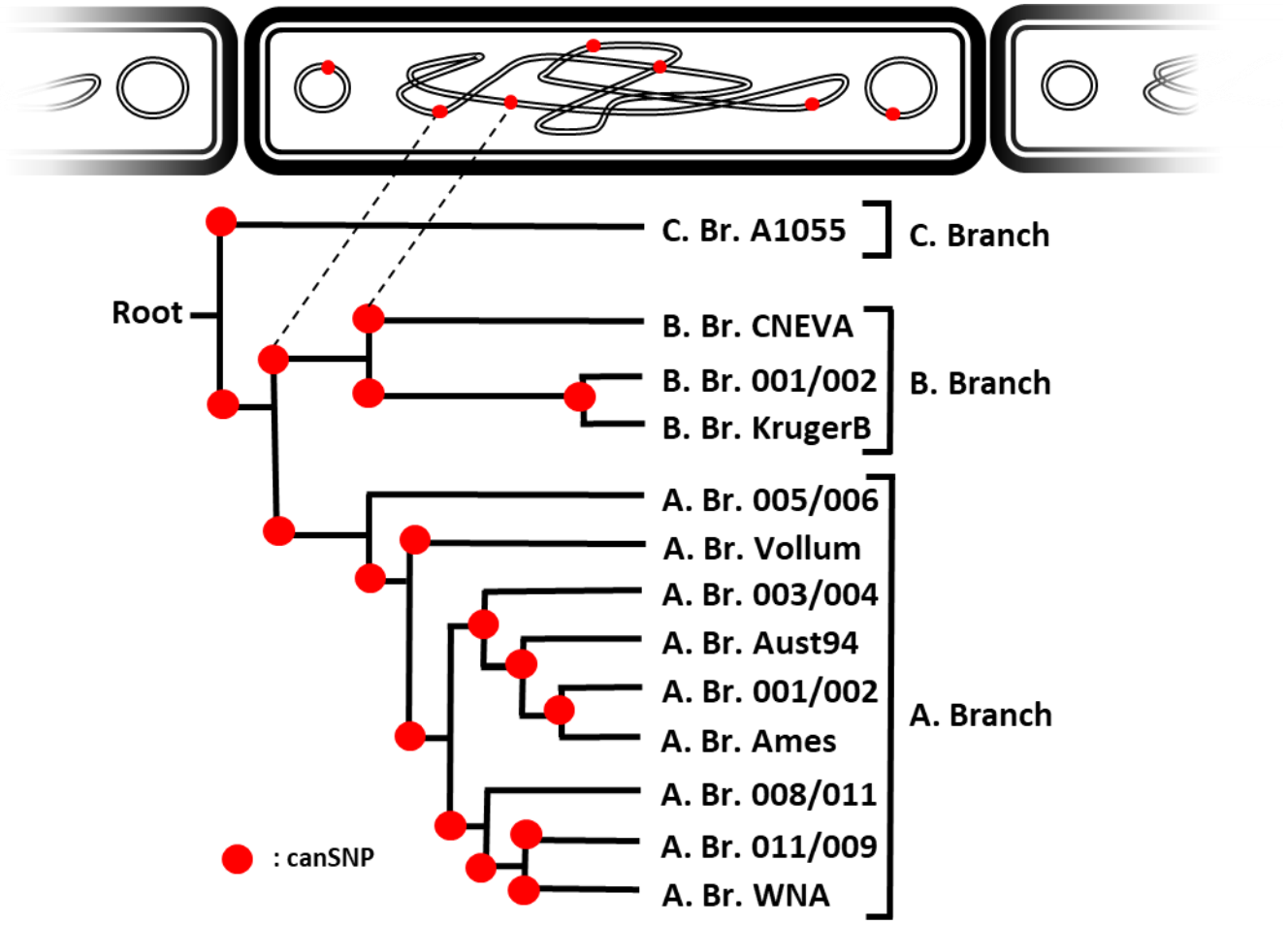

Figure 1-3: Canonical single nucleotide polymorphism (canSNP) analysis. The bioforensic tool of is often used in epidemiological investigations to initially classify new *B. anthracis* strains into previously established, phylogenetically related groups. The upper part of the figure shows simplified *B. anthracis* cells growing in chains. The virulence plasmids pXO1 and pXO2 (circles) and the chromosome (twisted circle) are indicated and labeled with fictitious phylogenetically relevant canSNP positions (red dots). Below that, starting from the phylogenetic origin (last common ancestor, Root), the canonical 13 branches of the three main lineages A, B and C of *B. anthracis* are indicated.

This typing system is widely used for phylogeographical and epidemiological investigations of outbreaks as well as for trace-back analyses in bioforensics and was used, for example, in the 2001 Amerithrax case to determine the origin of the *B. anthracis* isolate (A.Br.Ames) that was misused for the attacks (Hoffmaster et al. 2002; P. Keim et al. 2004).

In order to be able to quickly identify the origin in the event of an anthrax outbreak and to thus clarify whether it is a natural outbreak (i.e. caused by endospores from the

environment) or an act of intentional or unintentional release of the pathogen, precise phylogeographic reference-data for *B. anthracis* must be available. As a basis, the corresponding naturally occurring (autochthonous) genotype(s) for each region must be known to estimate whether an outbreak is likely natural or not. For example, an anthrax outbreak in Kruger National Park in South Africa, would not provide circumstantial evidence of intentional release of the pathogen if the infections were caused by a *B. anthracis* strain of the B. branch B.Br.KrugerB group (Smith et al. 2000). Strains from this group belong to the autochthonous *B. anthracis* population. In contrast, a strain from the A. branch A.Br.Ames group, which includes, among others, the strain from the 2001 letter postings, would provide strong circumstantial evidence for intentional spread in Kruger National Park.

To obtain information on the autochthonous, phyologenetic groups of *B. anthracis* in countries where anthrax is very rare, such as Germany, it is necessary to resort to the few existing live isolates from strain collections. However, these strains have since been repeatedly cultured and have very likely accumulated genetic changes over time making them unsuitable for the reconstruction of the natural phylogeography of *B. anthracis*. On the other hand, well-documented historic specimen would constitute a precious source for bioforensics by providing pivotal genetic information about the autochthonous phylogenetic groups present in the area to which the specimen can be assigned. Unfortunately, such specimens are rare and typically not readily available.

1.5. The *Bacillus cereus sensu lato* group

Taxonomically, *B. anthracis* belongs to the *Bacillus cereus sensu lato* (*s. l.*) group of very closely related organisms. Besides *B. anthracis* and its closest relatives *B. cereus sensu stricto* (*s.s.*) and *B. thuringiensis*, the group includes species such as *B. mycoides*, *B. pseudomycoides* and *B. weihenstephanensis* as well as a variety of less well-

characterized species (Helgason et al. 2004; Zwick et al. 2012). Both DNA sequence analysis of 16S rRNA genes and multi-locus sequence typing (MLST) show very low genetic diversity among the different species, which is why discrimination is often difficult (Cherif et al. 2003; Priest et al. 2004; Rasko et al. 2005). Thus, from a genetic point of view, the members of the *B. cereus s.l.* group can be considered a single species with distinct phenotypes, mainly due to the presence of mobile genetic elements such as plasmids (Jensen et al. 2003). In addition to the virulence plasmids in *B. anthracis*, the genes for insect toxin synthesis in *B. thuringiensis* as well as a variety of endotoxins (e.g. cereulid) in *B. cereus s.s.* are also plasmid-encoded (Ehling-Schulz et al. 2019) and are the only traits that distinguish *B. cereus s.s.* from *B. thuringiensis.* The main genetic feature that distinguishes *B. anthracis* from *B. cereus s.s* is a nonsense mutation in the gene encoding the pleiotropic regulator PlcR that controls the expression of genes for virulence factors associated with foodborne illness in *B. cereus s.s.*, such as diarrheal or emetic toxins (Paul Keim et al. 2009; Zwick et al. 2012). On the other hand, strains of *B. cereus s.s.* have been described containing two virulence plasmids exceedingly similar to pXO1 and pXO2 of *B. anthracis*. These strains were found to cause anthrax-like disease in great apes (Okinaka et al. 2006; Klee et al. 2010) and favor the argument of the members of the *B. cereus s.l.* group to be a single species and clearly show the problematic situation in correct species identification and accurate differentiation within this bacterial group.

1.6. Identification of *B. anthracis* and diagnostics of anthrax

Although differentiation from close relatives of the *B. cereus s.l.* group can be challenging, rapid and specific detection of *B. anthracis* is critical for subsequent therapy and thus, patient survival due to the often fulminant course of anthrax infections. To date, numerous attempts have been made to correctly identify *B. anthracis* and thereby specifically detect anthrax infections (Kozel et al. 2004; Irenge and Gala 2012; Morel et al. 2012; Kolton et

al. 2017; Rohde et al. 2020; Zasada 2020; Cox et al. 2015; Easterday et al. 2005; Dugan et al. 2012).

As for most pathogens, diagnostic realtime PCR is the gold standard for detection of *B. anthracis*. Due to the high genetic similarity between *B. anthracis* and the other members of the *B. cereus s.l.* group even detection of virulence genes encoded on the two *B. anthracis* plasmids pXO1 and pXO2 is not of sufficient specificity, as some *B. cereus* and *B. thuringiensis* strains possess pXO1- or pXO2-like plasmids (Turnbull et al. 1992; Klee et al. 2010; Antonation et al. 2016; Okinaka et al. 2006). Although the presence of virulence genes might be important from a medical point of view, high confidence of *B. anthracis* identification is only achieved in combination with unique chromosomal targets. Among the numerous chromosomal targets commonly used for PCR detection, only a few are truly specific for *B. anthracis* (Ågren et al. 2013). These markers include genes located on prophages, e.g., *dhp61* (Antwerpen et al. 2008) or *PL3* (Ellerbrok et al. 2002). The chromosome of *B. anthracis* contains four putative prophages, named LambdaBa01, 02, 03 and 04, which account for about 2.8% of the *B. anthracis* genome. In no other member of the *B. cereus s.l.* group all four prophages have been detected to date. Notably, according to current knowledge, these prophages are no longer functional, i.e., no longer capable of producing virions (Read et al. 2003; Sozhamannan et al. 2006; Gillis and Mahillon 2014).

Alternative PCR-approaches for *B. anthracis* identification employ interrogations at SNP positions in the *B. anthracis* genome for instance, in the *plcR* (Easterday et al. 2005) or *gyrA* (Hurtle et al. 2004) genes. However, all these targets are present in a single-copy on the *B. anthracis* genome. This principally reduces the diagnostic sensitivities of such assays compared to targeting multi-copy elements (e.g. Klee et al. 2006) such as 16S rRNA genes and transcripts, which are commonly used as convenient multi-copy targets in many species in a variety of detection methods like realtime PCR, fluorescence in situ

hybridization (FISH) or sequencing. However, DNA sequences of the 16S rRNA genes were considered unsuitable for unambiguous distinction of *B. anthracis* from its closest relatives due to the lack of specific sequence variations (Candelon et al. 2004; Ash et al. 1991). Recently, Sanger sequencing of the *B. anthracis* rRNA genes and careful inspections of DNA-sequencing-electropherograms revealed a single SNP present in a minor fraction of only the *B. anthracis* 16S rRNA gene copies, which the authors proposed to be unique for *B. anthracis* (Hakovirta et al. 2016). Unfortunately, the authors did not further explore this possibility. If this sequence variation was truly species specific, it could be used for multi-copy target based *B. anthracis* detection.

In addition to PCR, matrix-assisted laser desorption ionization time-of-flight mass spectrometry (MALDI-TOF MS) can be used to identify *B. anthracis* (Pauker et al. 2018). While commonly used for pathogen identification in well-equipped diagnostic laboratories, this method is highly dependent on the reproducibility of the microorganism's "fingerprint" and the generated peptide databases. A prerequisite for the method is currently still a pure culture, which significantly extends the time horizon required for this approach. Moreover, the choice of culture conditions is also a critical factor for the reproducibility of results and therefore for correct species identification.

Antibody-based assays are also widely used for pathogen detection. To date, numerous assays have been developed to detect toxins, spores and vegetative cells of *B. anthracis*. These include, e.g., fluorescence microscopy based detection (De et al. 2002), lateral flow- (Wang et al. 2014) and flow-cytometry-assays (Zahavy et al. 2012) and surface plasmon resonance (SPR) based methods (Wang et al. 2017). Notably, however, antibody-based methods for *B. anthracis* detection usually lack sufficient sensitivity and specificity (Irenge and Gala 2012).

In addition, classical microbiological methods can be used for identification of pathogens e.g. by their specific colony morphology. When cultured on blood agar plates *B. anthracis*

can be distinguished from a variety of other Bacilli since the ensuing medusa-head shaped colonies lack hemolysis (Figure 1-1 C). Additionally, negative staining using ink can be used to test microscopically for the presence of a capsule (Turnbull 2008). Both methods, however, are not species specific and therefore cannot be used to correctly identify *B. anthracis*.

Another culture-based method for *B. anthracis* identification, which has been in use for centuries, is bacteriophage sensitivity testing using highly specific phages such as phage γ (Gamma). Quickly after the virus was discovered by Brown & Cherry in 1955, the γ phage plaque assay has become a standard tool for anthrax diagnostics especially in less well-equipped laboratories (Brown and Cherry 1955). Phage γ belongs to the family Siphoviridae as it features an icosahedral head as well as a long non-contractile tail (Abshire et al. 2005). It has a high host specificity of 96% (Kolton et al. 2017). Of 700 non-*B. anthracis* strains recently tested (both bacilli and strains outside the genus *Bacillus)*, 29 were infected by phage y (Kolton et al. 2017). In addition to phage γ, Tectiviruses have been isolated with even higher specificity for *B. anthracis.* Tectiviridae is a species-poor family of tail-less phages that possess an internal lipid membrane (Gillis and Mahillon 2014). In 1974, phage AP50t was isolated from soil, which was found to exclusively infect *B. anthracis* (Nagy 1974). Later a lytic mutant of AP50t named AP50c that, compared to temperate wildtype AP50t, was found to form clear plaques and was able to infect 111 of 115 *B. anthracis* strains but none of the 100 *B. cereus s.l.* strains tested (Sozhamannan et al. 2008). In 2010, Schuch et al. isolated another *B. anthracis* specific member of the Tectivirdae family from the gut of the earthworm *Eisenia fetida*. The phage Wip1 (Worm Intestinal Phage 1) has an equally narrow host range as phage AP50c (Schuch et al. 2010).

Phage sensitivity assays using highly specific phages are easy to perform, cost-effective and do not require any special laboratory equipment. However, the bacterium to be tested

must be alive and in pure culture and results can usually be obtained only after a few days. An approach to speed up phage sensitivity assays is to use genetically modified reporter phages. Compared to the plaque assay using wildtype phages, reporter phages enable rapid detection of the target organism by generating a measurable signal, such as bioluminescence or color change, through the production of a reporter molecule (i.e., a protein from a recombinant gene) during host infection. Such phages have been developed for the detection of, e.g. *Yersinia pestis*, *Listeria monocytogenes* and *B. anthracis* (Schofield et al. 2013; Schofield et al. 2009; Meile, Sarbach, et al. 2020). Schofield et al. generated a recombinant Wβ::*luxAB* phage from the wildtype Wβ phage, a very close relative of the phage γ. Incubation of the reporter phage with a *B. anthracis* containing sample and the addition of a luminogenic substrate, leads to LuxAB-mediated, quantifiable emission of light. Although faster than conventional culture based approaches, reporter phages still rely on living cells and, as for most reporter phage based systems, on a pure culture. In contrast, using phage receptor binding proteins (RBP) instead of whole phages diminishes the dependence on pure culture, provides even faster results and opens up the possibility to detect inactivated bacteria (Meile et al. 2020). RBPs are typically responsible for successful adhesion of the phage to a potential host. Previously, RBPs have not yet been used for the detection of *B. anthracis* but served as a versatile tool for detection of other pathogens such as *Shigella flexneri* (Kunstmann et al. 2018), *Salmonella enterica* subsp. I ser. Typhimurium (Denyes et al. 2017), *Listeria monocytogenes* (Sumrall et al. 2020) or *Burkholderia pseudomallei* (Muangsombut et al. 2021).

1.7. Scope of the thesis

In case of an anthrax outbreak in livestock or wildlife, but especially in humans, two aspects are of particular importance and urgency to initiate appropriate countermeasures such as antibiotic therapy of infected individuals, area-wide testing, quarantine or exit restrictions and disinfection of affected areas:

i) The unequivocal and rapid identification of *B. anthracis*
and
ii) the educated assessment of the probability for an exclusion or confirmation of an intentional release of the pathogen as the underlying cause of the outbreak

For i) rapid and reliable detection methods for *B. anthracis* are mandatory. The method of choice here is diagnostic realtime PCR targeting specific single-copy genes such as *dhp61* or *Pl3*. However, these markers principally have limited detection sensitivity compared to multi-copy markers such as 16S rRNA genes.

Therefore, the aim of this work was to validate the previously identified SNP (Hakovirta et al. 2016) in some of the 16S rRNA genes of *B. anthracis* for its specificity and distribution among different *B. anthracis* strains and thus, the potential for using this variation as a convenient multi-copy target for *B. anthracis* detection in realtime PCR or FISH assays.

Because PCR alone is not sufficient for unequivocal pathogen identification, alternative methods are needed to confirm PCR results. These methods must be comparably sensitive, specific and fast as PCR. For other pathogens, detection methods based on RBPs of highly specific phages have proven to meet these criteria (Dunne and Loessner 2019). Although several highly specific phages exist, no such approach has yet been developed for *B. anthracis*. The aim of this work was therefore to identify RBPs of known phages and use them to establish and validate novel methods for rapid, sensitive and

specific protein-based detection of this notorious pathogen and thus improve anthrax diagnostics after natural outbreaks or in the event of a bioterroristic attack.

Once the pathogen has been identified, in order to investigate the cause of the outbreak (ii) the exact and area-wide natural phylogeography of the pathogen must be available so that the genotype of the strain causing the outbreak can be matched with those naturally occurring in the affected area. For Central Europe, the natural phylogeography of *B. anthracis* has not yet been confirmed due to lack of outbreaks and blanket vaccination of livestock. Therefore, the goal of this work was to determine the autochthonous genotype of the pathogen for this region based on genetic analysis of historical samples. The ensuing phylogenetic base-knowledge can then be anticipated to facilitate the assessment of the most probable phylogeographic origin of a pathogen associated with an unexpected future outbreak in Central Europe and thus improve anthrax bioforensics.

1.8. References of Introduction

Abshire, T. G., J. E. Brown, and J. W. Ezzell. 2005. “Production and Validation of the Use of Gamma Phage for Identification of *Bacillus anthracis*.” *J Clin Microbiol* 43 (9): 4780–88. https://doi.org/10.1128/jcm.43.9.4780-4788.2005.

Ågren, J., R. A. Hamidjaja, T. Hansen, R. Ruuls, S. Thierry, H. Vigre, I. Janse, et al. 2013. “In Silico and in Vitro Evaluation of PCR-Based Assays for the Detection of *Bacillus anthracis* Chromosomal Signature Sequences.” *Virulence* 4 (8): 671–85. https://doi.org/10.4161/viru.26288.

Antonation, K. S., K. Grutzmacher, S. Dupke, P. Mabon, F. Zimmermann, F. Lankester, T. Peller, et al. 2016. “*Bacillus cereus* biovar *anthracis* Causing Anthrax in Sub-Saharan Africa-Chromosomal Monophyly and Broad Geographic Distribution.” *PLoS Negl Trop Dis* 10 (9): e0004923. https://doi.org/10.1371/journal.pntd.0004923 PNTD-D-16-00714 [pii].

Antwerpen, M. H., J. W. Sahl, D. Birdsell, T. Pearson, M. J. Pearce, C. Redmond, H. Meyer, and P. S. Keim. 2017. “Unexpected Relations of Historical Anthrax Strain.” *MBio* 8 (2). https://doi.org/10.1128/mBio.00440-17.

Antwerpen, M. H., P. Zimmermann, K. Bewley, D. Frangoulidis, and H. Meyer. 2008. “Real-Time PCR System Targeting a Chromosomal Marker Specific for *Bacillus anthracis*.” *Mol Cell Probes* 22 (5–6): 313–15. https://doi.org/S0890-8508(08)00041-8 [pii] 10.1016/j.mcp.2008.06.001.

Ash, C., J. A. Farrow, M. Dorsch, E. Stackebrandt, and M. D. Collins. 1991. “Comparative Analysis of *Bacillus anthracis*, *Bacillus cereus*, and Related Species on the Basis of Reverse Transcriptase Sequencing of 16S rRNA.” *Int J Syst Bacteriol* 41 (3): 343–46. https://doi.org/10.1099/00207713-41-3-343.

Barras, V., and G. Greub. 2014. “History of Biological Warfare and Bioterrorism.” *Clin Microbiol Infect* 20 (6): 497–502. https://doi.org/10.1111/1469-0691.12706.

Brown, E. R., and W. B. Cherry. 1955. “Specific Identification of *Bacillus anthracis* by Means of a Variant Bacteriophage.” *J Infect Dis* 96 (1): 34–39.

Candelon, B., K. Guilloux, S. D. Ehrlich, and A. Sorokin. 2004. “Two Distinct Types of rRNA Operons in the *Bacillus cereus* Group.” *Microbiology* 150 (Pt 3): 601–11. https://doi.org/10.1099/mic.0.26870-0.

Cherif, A., S. Borin, A. Rizzi, H. Ouzari, A. Boudabous, and D. Daffonchio. 2003. “*Bacillus anthracis* Diverges from Related Clades of the *Bacillus cereus* Group in 16S-23S

Ribosomal DNA Intergenic Transcribed Spacers Containing tRNA Genes." *Appl Environ Microbiol* 69 (1): 33–40. https://doi.org/10.1128/aem.69.1.33-40.2003.

Cox, C. R., K. R. Jensen, R. R. Mondesire, and K. J. Voorhees. 2015. "Rapid Detection of *Bacillus anthracis* by Gamma Phage Amplification and Lateral Flow Immunochromatography." *J Microbiol Methods* 118 (November): 51–56. https://doi.org/10.1016/j.mimet.2015.08.011 S0167-7012(15)30044-0 [pii].

De, B. K., S. L. Bragg, G. N. Sanden, K. E. Wilson, L. A. Diem, C. K. Marston, A. R. Hoffmaster, et al. 2002. "A Two-Component Direct Fluorescent-Antibody Assay for Rapid Identification of *Bacillus anthracis*." *Emerg Infect Dis* 8 (10): 1060–65. https://doi.org/10.3201/eid0810.020392.

Denyes, J. M., M. Dunne, S. Steiner, M. Mittelviefhaus, A. Weiss, H. Schmidt, J. Klumpp, and M. J. Loessner. 2017. "Modified Bacteriophage S16 Long Tail Fiber Proteins for Rapid and Specific Immobilization and Detection of *Salmonella* Cells." *Appl Environ Microbiol* 83 (12). https://doi.org/10.1128/aem.00277-17.

Dugan, L., J. Bearinger, A. Hinckley, C. Strout, and B. Souza. 2012. "Detection of *Bacillus anthracis* from Spores and Cells by Loop-Mediated Isothermal Amplification without Sample Preparation." *J Microbiol Methods* 90 (3): 280–84. https://doi.org/S0167-7012(12)00211-4 [pii] 10.1016/j.mimet.2012.05.022.

Dunne, M., and M. J. Loessner. 2019. "Modified Bacteriophage Tail Fiber Proteins for Labeling, Immobilization, Capture, and Detection of Bacteria." *Methods Mol Biol* 1918: 67–86. https://doi.org/10.1007/978-1-4939-9000-9_6.

Easterday, W. R., M. N. Van Ert, S. Zanecki, and P. Keim. 2005. "Specific Detection of *Bacillus anthracis* Using a TaqMan Mismatch Amplification Mutation Assay." *Biotechniques* 38 (5): 731–35. https://doi.org/05385ST03 [pii].

Ehling-Schulz, M., D. Lereclus, and T. M. Koehler. 2019. "The *Bacillus cereus* Group: *Bacillus* Species with Pathogenic Potential." *Microbiol Spectr* 7 (3). https://doi.org/10.1128/microbiolspec.GPP3-0032-2018.

Ellerbrok, H., H. Nattermann, M. Ozel, L. Beutin, B. Appel, and G. Pauli. 2002. "Rapid and Sensitive Identification of Pathogenic and Apathogenic *Bacillus anthracis* by Real-Time PCR." *FEMS Microbiol Lett* 214 (1): 51–59. https://doi.org/S0378109702008376 [pii].

Fowler, R. A., and S. Shafazand. 2011. "Anthrax Bioterrorism: Prevention, Diagnosis and Management Strategies." *J Bioterr Biodef* 2 (107): doi:10.4172/2157-2526.1000107.

Gillis, A., and J. Mahillon. 2014. “Phages Preying on *Bacillus anthracis, Bacillus aereus*, and *Bacillus thuringiensis*: Past, Present and Future.” *Viruses* 6 (7): 2623–72. https://doi.org/10.3390/v6072623 v6072623 [pii].

Hakovirta, J. R., S. Prezioso, D. Hodge, S. P. Pillai, and L. M. Weigel. 2016. “Identification and Analysis of Informative Single Nucleotide Polymorphisms in 16S rRNA Gene Sequences of the *Bacillus cereus* Group.” *J Clin Microbiol*, August. https://doi.org/JCM.01267-16 [pii] 10.1128/JCM.01267-16.

Hanczaruk, M., U. Reischl, T. Holzmann, D. Frangoulidis, D. M. Wagner, P. S. Keim, M. H. Antwerpen, H. Meyer, and G. Grass. 2014. “Injectional Anthrax in Heroin Users, Europe, 2000-2012.” *Emerg Infect Dis* 20 (2): 322–23. https://doi.org/10.3201/eid2002.120921.

Helgason, E., N. J. Tourasse, R. Meisal, D. A. Caugant, and A. B. Kolsto. 2004. “Multilocus Sequence Typing Scheme for Bacteria of the *Bacillus cereus* Group.” *Appl Environ Microbiol* 70 (1): 191–201.

Hoffmaster, A. R., C. C. Fitzgerald, E. Ribot, L. W. Mayer, and T. Popovic. 2002. “Molecular Subtyping of *Bacillus anthracis* and the 2001 Bioterrorism-Associated Anthrax Outbreak, United States.” *Emerg Infect Dis* 8 (10): 1111–16. https://doi.org/10.3201/eid0810.020394.

Hurtle, W., E. Bode, D. A. Kulesh, R. S. Kaplan, J. Garrison, D. Bridge, M. House, M. S. Frye, B. Loveless, and D. Norwood. 2004. “Detection of the *Bacillus anthracis GyrA* Gene by Using a Minor Groove Binder Probe.” *J Clin Microbiol* 42 (1): 179–85. https://doi.org/10.1128/jcm.42.1.179-185.2004.

Inglesby, T. V., T. O’Toole, D. A. Henderson, J. G. Bartlett, M. S. Ascher, E. Eitzen, A. M. Friedlander, et al. 2002. “Anthrax as a Biological Weapon, 2002: Updated Recommendations for Management.” *JAMA* 287 (17): 2236–52. https://doi.org/jst20007 [pii].

Irenge, Léonid M., and Jean-Luc Gala. 2012. “Rapid Detection Methods for *Bacillus anthracis* in Environmental Samples: A Review.” *Applied Microbiology and Biotechnology* 93 (4): 1411–22. https://doi.org/10.1007/s00253-011-3845-7.

Jensen, G. B., B. M. Hansen, J. Eilenberg, and J. Mahillon. 2003. “The Hidden Lifestyles of *Bacillus cereus* and Relatives.” *Environ Microbiol* 5 (8): 631–40. https://doi.org/461 [pii].

Keim, P., M. N. Van Ert, T. Pearson, A. J. Vogler, L. Y. Huynh, and D. M. Wagner. 2004. “Anthrax Molecular Epidemiology and Forensics: Using the Appropriate Marker for Different Evolutionary Scales.” *Infect Genet Evol* 4 (3): 205–13. https://doi.org/10.1016/j.meegid.2004.02.005 S1567134804000346 [pii].

Keim, Paul, Jeffrey M. Gruendike, Alexandra M. Klevytska, James M. Schupp, Jean Challacombe, and Richard Okinaka. 2009. “The Genome and Variation of *Bacillus anthracis*.” *Molecular Aspects of Medicine* 30 (6): 397–405. https://doi.org/10.1016/j.mam.2009.08.005.

Klee, S. R., E. B. Brzuszkiewicz, H. Nattermann, H. Bruggemann, S. Dupke, A. Wollherr, T. Franz, et al. 2010. “The Genome of a *Bacillus* Isolate Causing Anthrax in Chimpanzees Combines Chromosomal Properties of *B. cereus* with *B. anthracis* Virulence Plasmids.” *PLoS One* 5 (7): e10986. https://doi.org/10.1371/journal.pone.0010986.

Klee, S. R., H. Nattermann, S. Becker, M. Urban-Schriefer, T. Franz, D. Jacob, and B. Appel. 2006. “Evaluation of Different Methods to Discriminate *Bacillus anthracis* from Other Bacteria of the *Bacillus cereus* Group.” *J Appl Microbiol* 100 (4): 673–81. https://doi.org/10.1111/j.1365-2672.2006.02809.x.

Koehler, T. M. 2009. “*Bacillus anthracis* Physiology and Genetics.” *Mol Aspects Med* 30 (6): 386–96. https://doi.org/S0098-2997(09)00052-1 [pii] 10.1016/j.mam.2009.07.004.

Kolton, C. B., N. L. Podnecky, S. V. Shadomy, J. E. Gee, and A. R. Hoffmaster. 2017. “*Bacillus anthracis* Gamma Phage Lysis among Soil Bacteria: An Update on Test Specificity.” *BMC Res Notes* 10 (1): 598. https://doi.org/10.1186/s13104-017-2919-8.

Kozel, T. R., W. J. Murphy, S. Brandt, B. R. Blazar, J. A. Lovchik, P. Thorkildson, A. Percival, and C. R. Lyons. 2004. “mAbs to *Bacillus anthracis* Capsular Antigen for Immunoprotection in Anthrax and Detection of Antigenemia.” *Proc Natl Acad Sci U S A* 101 (14): 5042–47. https://doi.org/10.1073/pnas.0401351101.

Kunstmann, S., T. Scheidt, S. Buchwald, A. Helm, L. A. Mulard, A. Fruth, and S. Barbirz. 2018. “Bacteriophage Sf6 Tailspike Protein for Detection of *Shigella flexneri* Pathogens.” *Viruses* 10 (8). https://doi.org/10.3390/v10080431.

Lengel, Allan. 2005. “Little Progress In FBI Probe of Anthrax Attacks.” *The Washington Post*, September 16, 2005.

Levy, H., I. Glinert, S. Weiss, E. Bar-David, A. Sittner, J. Schlomovitz, Z. Altboum, and D. Kobiler. 2014. “The Central Nervous System as Target of *Bacillus anthracis* Toxin Independent Virulence in Rabbits and Guinea Pigs.” *PLoS One* 9 (11): e112319. https://doi.org/10.1371/journal.pone.0112319 PONE-D-14-29592 [pii].

Marston, C. K., C. A. Allen, J. Beaudry, E. P. Price, S. R. Wolken, T. Pearson, P. Keim, and A. R. Hoffmaster. 2011. “Molecular Epidemiology of Anthrax Cases Associated with Recreational Use of Animal Hides and Yarn in the United States.” *PLoS One*

6 (12): e28274. https://doi.org/10.1371/journal.pone.0028274 PONE-D-11-08570 [pii].

Meile, Susanne, Samuel Kilcher, Martin J. Loessner, and Matthew Dunne. 2020. “Reporter Phage-Based Detection of Bacterial Pathogens: Design Guidelines and Recent Developments.” *Viruses* 12 (9): 944. https://doi.org/10.3390/v12090944.

Meile, Susanne, Anne Sarbach, Jiemin Du, Markus Schuppler, Carmen Saez, Martin J. Loessner, and Samuel Kilcher. 2020. “Engineered Reporter Phages for Rapid Bioluminescence-Based Detection and Differentiation of Viable *Listeria* Cells.” Edited by Karyn N. Johnson. *Applied and Environmental Microbiology* 86 (11). https://doi.org/10.1128/AEM.00442-20.

Missiakas, D. M., and O. Schneewind. 2005. “*Bacillus Anthracis* and the Pathogenesis of Anthrax.” *Infectious Diseases: Biological Weapons Defense: Infectious Diseases and Counterterrorism* Edited by: L. E. Lindler, F. J. Lebeda, and G. W. Korch, Humana Press Inc., Totowa, NJ: 79–97.

Moayeri, M., S. H. Leppla, C. Vrentas, A. Pomerantsev, and S. Liu. 2015. “Anthrax Pathogenesis.” *Annu Rev Microbiol*, July. https://doi.org/10.1146/annurev-micro-091014-104523.

Morel, N., H. Volland, J. Dano, P. Lamourette, P. Sylvestre, M. Mock, and C. Creminon. 2012. “Fast and Sensitive Setection of *Bacillus anthracis* Spores by Immunoassay.” *Appl Environ Microbiol* 78 (18): 6491–98. https://doi.org/AEM.01282-12 [pii] 10.1128/AEM.01282-12.

Muangsombut, V., P. Withatanung, N. Chantratita, S. Chareonsudjai, J. Lim, E. E. Galyov, O. Ottiwet, et al. 2021. “Development of a Bacteriophage Tail Fiber-Based Latex Agglutination Assay for Rapid Clinical Screening of *Burkholderia pseudomallei*.” *Appl Environ Microbiol*, April. https://doi.org/10.1128/aem.03019-20.

Nagy, E. 1974. “A Highly Specific Phage Attacking *Bacillus anthracis* Strain Sterne.” *Acta Microbiol Acad Sci Hung* 21 (3–4): 257–63.

Okinaka, R. T., K. Cloud, O. Hampton, A. R. Hoffmaster, K. K. Hill, P. Keim, T. M. Koehler, et al. 1999. “Sequence and Organization of pxO1, the Large *Bacillus anthracis* Plasmid Harboring the Anthrax Toxin Genes.” *J Bacteriol* 181 (20): 6509–15.

Okinaka, Richard, Talima Pearson, and Paul Keim. 2006. “Anthrax, but Not *Bacillus anthracis*?” *PLoS Pathogens* 2 (11): e122. https://doi.org/10.1371/journal.ppat.0020122.

Pauker, V. I., B. R. Thoma, G. Grass, P. Bleichert, M. Hanczaruk, L. Zoller, and S. Zange. 2018. “Improved Discrimination of *Bacillus anthracis* from Closely Related Species in the *Bacillus cereus sensu lato* Group Based on Matrix-Assisted Laser Desorption

Ionization-Time of Flight Mass Spectrometry." *J Clin Microbiol* 56 (5). https://doi.org/10.1128/jcm.01900-17.

Pilo, P., and J. Frey. 2011. "*Bacillus anthracis*: Molecular Taxonomy, Population Genetics, Phylogeny and Patho-Evolution." *Infect Genet Evol*, May. https://doi.org/S1567-1348(11)00201-2 [pii] 10.1016/j.meegid.2011.05.013.

Priest, F. G., M. Barker, L. W. Baillie, E. C. Holmes, and M. C. Maiden. 2004. "Population Structure and Evolution of the *Bacillus cereus* Group." *J Bacteriol* 186 (23): 7959–70. https://doi.org/186/23/7959 [pii] 10.1128/JB.186.23.7959-7970.2004.

Rasko, D. A., M. R. Altherr, C. S. Han, and J. Ravel. 2005. "Genomics of the *Bacillus cereus* Group of Organisms." *FEMS Microbiol Rev* 29 (2): 303–29. https://doi.org/S0168-6445(05)00003-3 [pii] 10.1016/j.femsre.2004.12.005.

Ravel, J., L. Jiang, S. T. Stanley, M. R. Wilson, R. S. Decker, T. D. Read, P. Worsham, et al. 2008. "The Complete Genome Sequence of *Bacillus Anthracis* Ames 'Ancestor.'" *Journal of Bacteriology* 191 (1): 445–46. https://doi.org/10.1128/jb.01347-08.

Read, T. D., S. N. Peterson, N. Tourasse, L. W. Baillie, I. T. Paulsen, K. E. Nelson, H. Tettelin, et al. 2003. "The Genome Sequence of *Bacillus anthracis* Ames and Comparison to Closely Related Bacteria." *Nature* 423 (6935): 81–86. https://doi.org/10.1038/nature01586.

Redmond, C., M. J. Pearce, R. J. Manchee, and B. P. Berdal. 1998. "Deadly Relic of the Great War." *Nature* 393 (6687): 747–48. https://doi.org/10.1038/31612.

Rohde, A., S. Papp, P. Feige, R. Grunow, and O. Kaspari. 2020. "Development of a Novel Selective Agar for the Isolation and Detection of *Bacillus anthracis*." *J Appl Microbiol*, February. https://doi.org/10.1111/jam.14615.

Sahl, J., and P. Keim. 2016. "NASP: An Accurate, Rapid Method for the Identification of SNPs in WGS Datasets That Supports Flexible Input and Output Formats."

Schofield, D. A., I. J. Molineux, and C. Westwater. 2009. "Diagnostic Bioluminescent Phage for Detection of *Yersinia pestis*." *J Clin Microbiol* 47 (12): 3887–94. https://doi.org/10.1128/jcm.01533-09.

Schofield, D. A., N. J. Sharp, J. Vandamm, I. J. Molineux, K. A. Spreng, C. Rajanna, C. Westwater, and G. C. Stewart. 2013. "*Bacillus anthracis* Diagnostic Detection and Rapid Antibiotic Susceptibility Determination Using 'bioluminescent' Reporter Phage." *J Microbiol Methods* 95 (2): 156–61. https://doi.org/S0167-7012(13)00276-5 [pii] 10.1016/j.mimet.2013.08.013.

Schuch, R., A. J. Pelzek, S. Kan, and V. A. Fischetti. 2010. "Prevalence of *Bacillus anthracis*-like Organisms and Bacteriophages in the Intestinal Tract of the

Earthworm *Eisenia fetida*." *Appl Environ Microbiol* 76 (7): 2286–94. https://doi.org/AEM.02518-09 [pii] 10.1128/AEM.02518-09.

Schwartz, Maxime. 2009. "Dr. Jekyll and Mr. Hyde: A Short History of Anthrax." *Molecular Aspects of Medicine* 30 (6): 347–55. https://doi.org/10.1016/j.mam.2009.06.004.

Smith, K. L., V. DeVos, H. Bryden, L. B. Price, M. E. Hugh-Jones, and P. Keim. 2000. "*Bacillus anthracis* Diversity in Kruger National Park." *J Clin Microbiol* 38 (10): 3780–84.

Sozhamannan, S., M. D. Chute, F. D. McAfee, D. E. Fouts, A. Akmal, D. R. Galloway, A. Mateczun, L. W. Baillie, and T. D. Read. 2006. "The *Bacillus anthracis* Chromosome Contains Four Conserved, Excision-Proficient, Putative Prophages." *BMC Microbiol* 6: 34. https://doi.org/1471-2180-6-34 [pii] 10.1186/1471-2180-6-34.

Sozhamannan, S., M. McKinstry, S. M. Lentz, M. Jalasvuori, F. McAfee, A. Smith, J. Dabbs, et al. 2008. "Molecular Characterization of a Variant of *Bacillus anthracis*-Specific Phage AP50 with Improved Bacteriolytic Activity." *Appl Environ Microbiol* 74 (21): 6792–96. https://doi.org/10.1128/aem.01124-08.

Sternbach, G. 2003. "The History of Anthrax." *J Emerg Med* 24 (4): 463–67. https://doi.org/S0736467903000799 [pii].

Sumrall, E. T., C. Rohrig, M. Hupfeld, L. Selvakumar, J. Du, M. Dunne, M. Schmelcher, Y. Shen, and M. J. Loessner. 2020. "Glycotyping and Specific Separation of *Listeria monocytogenes* with a Novel Bacteriophage Protein Toolkit." *Appl Environ Microbiol*, May. https://doi.org/10.1128/aem.00612-20.

Turnbull, P. C. 2008. *World Health Organization. Anthrax in Humans and Animals*. Geneva (CH): WHO Press.

Turnbull, P. C. B., R. A. Hutson, Mandy J. Ward, Marie N. Jones, C. P. Quinn, N. J. Finnie, C. J. Duggleby, J. M. Kramer, and J. Melling. 1992. "*Bacillus anthracis* but Not Always Anthrax." *Journal of Applied Bacteriology* 72 (1): 21–28. https://doi.org/10.1111/j.1365-2672.1992.tb04876.x.

Van Ert, M. N., W. R. Easterday, L. Y. Huynh, R. T. Okinaka, M. E. Hugh-Jones, J. Ravel, S. R. Zanecki, et al. 2007. "Global Genetic Population Structure of *Bacillus anthracis*." *PLoS One* 2 (5): e461. https://doi.org/10.1371/journal.pone.0000461.

Wang, D. B., B. Tian, Z. P. Zhang, X. Y. Wang, J. Fleming, L. J. Bi, R. F. Yang, and X. E. Zhang. 2014. "Detection of *Bacillus anthracis* Spores by Super-Paramagnetic Lateral-Flow Immunoassays." *Biosens Bioelectron*, September. https://doi.org/S0956-5663(14)00754-4 [pii] 10.1016/j.bios.2014.09.067.

Wang, S., W. Li, K. Chang, J. Liu, Q. Guo, H. Sun, M. Jiang, H. Zhang, J. Chen, and J. Hu. 2017. "Localized Surface Plasmon Resonance-Based Abscisic Acid Biosensor

Using Aptamer-Functionalized Gold Nanoparticles." *PLoS ONE* 12 (9): e0185530. https://doi.org/10.1371/journal.pone.0185530.

Zahavy, E., R. Ber, D. Gur, H. Abramovich, E. Freeman, S. Maoz, and S. Yitzhaki. 2012. "Application of Nanoparticles for the Detection and Sorting of Pathogenic Bacteria by Flow-Cytometry." *Adv Exp Med Biol* 733: 23–36. https://doi.org/10.1007/978-94-007-2555-3_3.

Zasada, A. A. 2020. "Detection and Identification of *Bacillus anthracis*: From Conventional to Molecular Microbiology Methods." *Microorganisms* 8 (1). https://doi.org/10.3390/microorganisms8010125.

Zwick, M. E., S. J. Joseph, X. Didelot, P. E. Chen, K. A. Bishop-Lilly, A. C. Stewart, K. Willner, et al. 2012. "Genomic Characterization of the *Bacillus cereus sensu lato* Species: Backdrop to the Evolution of *Bacillus anthracis*." *Genome Res*, July. https://doi.org/gr.134437.111 [pii] 10.1101/gr.134437.111.

2. A rare glimpse into the past of the anthrax pathogen *Bacillus anthracis*

microorganisms

MDPI

Article

A Rare Glimpse into the Past of the Anthrax Pathogen *Bacillus anthracis*

Peter Braun [1], Mandy Knüpfer [1], Markus Antwerpen [1], Dagmar Triebel [2], and Gregor Grass [1,*]

[1] Bundeswehr Institute of Microbiology (IMB), 80937 Munich, Germany; peter3braun@bundeswehr.org (P.B.); mandyknuepfer@bundeswehr.org (M.K.); markusantwerpen@bundeswehr.org (M.A.)

[2] Bavarian Natural History Collections (SNSB—Botanische Staatssammlung München), 80638 Munich, Germany; triebel@snsb.de

* Correspondence: gregorgrass@bundeswehr.org; Tel.: +49-992692-3981

Received: 28 January 2020; Accepted: 19 February 2020; Published: 21 February 2020

Abstract: The bacterium *Bacillus anthracis* is the causative agent of the zoonotic disease anthrax. While genomics of extant *B. anthracis* isolates established in-depth phylogenomic relationships, there is scarce information on the historic genomics of the pathogen. Here, we characterized the oldest documented *B. anthracis* specimen. The inactive 142-year-old material originated from a bovine diseased in Chemnitz (Germany) in 1878 and is contemporary with the seminal studies of Robert Koch on *B. anthracis*. A specifically developed isolation method yielded high-quality DNA from this specimen for genomic sequencing. The bacterial chromosome featuring 242 unique base-characters placed it into a major phylogenetic clade of *B. anthracis* (B.Branch CNEVA), which is typical for central Europe today. Our results support the notion that the CNEVA-clade represents part of the indigenous genetic lineage of *B. anthracis* in this part of Europe. This work emphasizes the value of historic specimens as precious resources for reconstructing the past phylogeny of the anthrax pathogen.

Keywords: anthrax; *Bacillus anthracis*; historic specimen; genome-sequencing; phylogeny

1. Introduction

For notorious pathogens such as *Yersinia pestis* (plague) or *Mycobacterium tuberculosis* (tuberculosis), there is ample information on the historic phylogeography of the pathogens from human remains. For instance, the oldest molecular evidence for historic plague from Sweden is 4900 years old [1]. In contrast, for *Bacillus anthracis*, the bacterium causing the zoonotic disease anthrax, our knowledge on its historic phylogeny hardly reaches back more than a hundred years. Though Louis Pasteur performed his famous public anthrax vaccination experiment in 1881, the Collection de l'Institut Pasteur (CIP) only initiated the collection of bacterial strains in 1892 [2]. These strains, however, have been cultured ever since, and thus likely have accumulated recent genetic changes. Conversely, dead specimens or bacteria from human remains are evolutionary inert.

Anthrax has plagued humans and both wild and domestic animals for hundreds—possibly many thousands-of years [3]. Even today, the pathogen is rampant in numerous countries on all continents except Antarctica [4]. Only a few countries have managed, through governmental and institutional vaccination campaigns, disease reporting and safe cadaver disposal programs to all but eradicate anthrax outbreaks today. Even Germany, which has seen very limited minor animal outbreaks recently in 2009, 2012, and 2014 [5], had been stricken by the disease only a century ago. From 1912 to 1932 (no data for 1926), 2518 people became infected, of which 431 died. Within the same time period, about 90,000 domestic animals fell from the disease [6]. Within that time occurred the infamous "Baron von Rosen espionage incident" involving sugar lumps allegedly laced with the

anthrax pathogen aimed at sabotaging allied horse-powered war-support-lines in 1917 [7,8]. While there is a large number of live historical *B. anthracis* isolates in culture, the oldest one mentioned in literature is from approx. 1890 [9] but lacks associated metadata. Thus, its origin remains elusive. Finally, *B. anthracis* has recently been isolated from excavation sites at the permafrost zone of northern Russia [10]. If these isolates, however, indeed originated from thousands-of-years-old cadavers devoid of any vegetative episodes of germinating spores and re-sporulating bacteria remains debatable. Also, it cannot be excluded that spores from younger outbreaks have contaminated deeper, older soil horizons. Nevertheless, with large permafrost areas thawing, we might see reemerging anthrax in high latitudes [10].

Historic, fixed specimens of *B. anthracis* on glass slides have attracted surprisingly little interest as valuable means for expanding our knowledge on the anthrax pathogen diversity. Published works comprise information from relatively young samples only: a couple of years old from Jordan [11], up to 30 years old from Zambia [12], or about 35-year-old paraffin-embedded samples from the former Soviet Union [13].

Thus, to date, there is no described bona fide historical genome of *B. anthracis*. In this report, we characterized the oldest documented *B. anthracis* genome from a 142-year-old historic microscopic slide.

2. Materials and Methods

2.1. B. anthracis *Strains, Growth Conditions, and Extraction of DNA from Inactivated Culture Material*

All strains (chromosomes) used in this study are listed in Supplementary Table S1. *B. anthracis* cultures from our strain collections were cultivated in our biosafety level 3 laboratory on blood agar and then chemically inactivated before further use [14]. DNA was isolated using MasterPure™ Gram Positive DNA Purification kit (Lucigen, Middleton, WI, USA) and DNA concentrations were quantified using the Qubit dsDNA HS Assay Kit (Thermo Fisher Scientific, Dreieich, Germany) according to the manufacturers' protocols. DNA preparations were stored at −20 °C until further use.

2.2. Microscopic Evaluation of the Historical B. anthracis *Specimen*

The original glass slide featuring a *B. anthracis* blood smear was carefully unwrapped from cover envelopes and examined by phase contrast microscopy (630-fold magnification) using a Leica DMi8 inverted light microscope (Leica Microsystems, Wetzlar, Germany).

2.3. DNA Extraction from the Historical B. anthracis *Blood Smear*

All manipulations related to sample Chemnitz 1878 (M-0290509 published in 1879 as no. 700 of the exsiccatae series [15]) were conducted in a laboratory not previously utilized to handle *B. anthracis* DNA in order to avoid contamination. A section of the blood smear was carefully removed using a sterile swab (Copan Nylon Floq Swab, Hain Life Science, Nehren, Germany) moistened with 100 μL of sterile phosphate-buffered saline by slowly rotating the swab and sampling the surface in a zig-zag-like movement. The swab was air-dried for 15 min under a laminar air flow. The swab head was then cut off and placed into a 2-mL microcentrifuge tube. DNA was extracted using MasterPure™ Gram Positive DNA Purification kit (Lucigen, Middleton, WI, USA), using a modified protocol. Briefly, 150 μL of TE buffer containing 1250 U of Ready-Lyse lysozyme solution was added directly onto the swab head and incubated at 37 °C for 60 min. To this, 1 μL of proteinase K (50 μg/μL) diluted into 150 μL of Gram-positive lysis solution was added. The tube was then incubated at 65 °C for 15 min at 900 rpm, briefly vortexed every 5 min. After placing the sample on ice for 5 min, the liquid and the swab head were transferred to a QIAshredder spin column (Qiagen, Hilden, Germany) and centrifuged at 14,000 rpm for 2 min. The swab head was discarded and 175 μL of 'MPC' Protein Precipitation Reagent was added to the flow-through. After vortexing, the debris was pelleted by centrifugation at 4 °C for 10 min at 14,000 rpm in a microcentrifuge. The supernatant was transferred to a clean microcentrifuge tube. To this, 5 μL of Roti-Pink (Carl Roth, Karlsruhe, Germany), 10 μL of glycogen solution (5 mg/mL, Carl Roth, Karlsruhe, Germany), and 500 μL of isopropanol (Carl Roth,

Karlsruhe, Germany) was added and gently mixed by inverting the tube 30–40 times. DNA was pelleted by centrifugation at 4 °C for 10 min at 14,000 rpm in a microcentrifuge. The DNA pellet was washed twice with 200 µL 70% ethanol. After removing all of the residual ethanol, the DNA was resuspended in 50 µL TE buffer and stored at −20 °C until further use.

2.4. Whole Genome Sequencing and Data Analysis—Single Nucleotide Polymorphism Calling

From total DNA, an Illumina-compatible library was prepared (NEBNext® Ultra™ II DNA Library Prep Kit, NEB, Frankfurt am Main, Germany) and sequenced on a MiSeq instrument (Illumina, San Diego, CA, USA) using MiSeq V3-chemistry. High-quality paired-end reads were assembled de novo using an in-house script based on SPAdes assembler [16] and Pilon [17] for correcting genome-assembly. In order to exclude age-related DNA-sequencing artifacts and to avoid incorrect conclusions, the genome sequence was curated manually as follows: First, obtained scaffolds (software BWA-SW [18]) were mapped to *B. anthracis* strain BF-1, a close genetic neighbor. Regions not covered by any reads were excluded from the consensus sequence. Second, BWA-mem was used to remap reads to the ordered contigs. Third, for eliminating ambiguous base positions, mpileup (software-package SAMtools [19]) was used with standard parameters. All ambiguous positions (n = 9326; i.e., 0.17% of the chromosome) were masked with "N" in the corresponding consensus-fasta-file. This final curated sequence was used for further comparative analyses. All data generated and analyzed during this study are included in this published article, its supplementary information files, or are publicly available in the NCBI Sequence Read Archive (SRA) repository (Bioproject PRJNA309927).

For multiple chromosome-wide SNP-comparison of *B. anthracis*, the Parsnp tool (Harvest Suite) was used [20]. For this, representative *B. anthracis* chromosomes from public databases (supplementary Table S1) and newly sequenced chromosomes Chemnitz 1878, Tyrol 3520 and 6282 were aligned (Parsnp parameters -c -e -u -C 1000) using *B. anthracis* Ames Ancestor reference chromosome (NC_007530) as phylogenetic outgroup.

Called SNPs were extracted into a multi-isolate-vcf file using the HarvestTools (version 1.0) from the same software suite [20]. To enhance data quality, closely adjacent SNPs with a distance of less than 10 bp as well as positions harboring undefined nucleotides ("N") were removed. This curated vcf-file was used as an input file in the HarvestTools to compile a FASTA-file comprising the concatenated SNPs of the investigated chromosome set as multiple-sequence alignment.

This concatenated sequence information was used to infer and analyze a maximum likelihood tree-based phylogeny in MEGA 7 [21,22]. SNPs found within the analyzed *B. anthracis* chromosomes are summarized in supplementary Table S2. A minimum spanning tree was computed in BioNumerics 6.6 (Applied Maths, Sint-Martens-Latem, Belgium) from the vcf SNP-file (in binary format) as input and manually edited for style.

3. Results and Discussion

3.1. Characterization of a Glass Slide Specimen Labeled B. anthracis *from 1878.*

The 142-year-old microscopic slide featured an infected blood specimen from the Bavarian Natural History Collections SNSB—*Botanische Staatssammlung München* (Germany). It was rediscovered during an inventory in 2018. The slide envelope was orderly labeled, providing information on the responsible veterinarian and the time and geographic location of the diseased bovine from which the blood smear was taken (Figure 1a). A veterinarian named Dr. O. E. R. Zimmermann prepared the smear from infected bovine blood on a glass slide in 1878 (Figure 1b), only two years after Robert Koch started systematic research on *B. anthracis*. Careful microscopic documentation of the specimen indicated rod-like structures among likely dried-up bovine blood cells and even possible nascent spores, supporting the claim *B. anthracis* was indeed possibly present (Figure 1c).

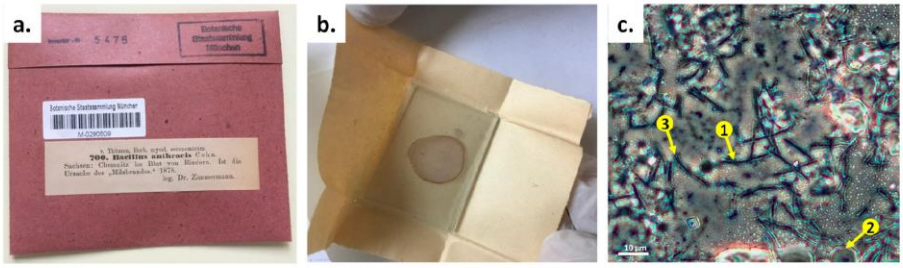

Figure 1. Initial characterization of a *B. anthracis* specimen from 1878. (**a**) The specimen with original label (translated from German: "Saxonia: Chemnitz in the blood of bovines. It is the source of 'anthrax'"). (**b**) Unpacking of the specimen, which was a glass slide paper-wrapped without any further glass cover. The red color from blood cells can still be identified. (**c**) Microscopic (phase-contrast) examination of the specimen. Arrow #1 indicates rod-like structures, likely *B. anthracis* cells; arrow #2 indicates possible bovine blood cells; and arrow #3 indicates structures that resemble nascent endospores.

3.2. DNA Isolation from Specimen Chemnitz 1878 and Genome Sequencing Yielded a B. anthracis *Genome Typical for Central Europe*

Using an improved swab-based extraction method specifically developed for this need, we were able to isolate DNA from the historic specimen. Unexpectedly, the quality and quantity of the extracted DNA was sufficient for PCR and subsequent whole-genome sequencing. Thus, 2 × 21,106,786 reads were generated. Of the six Gb obtained, only about 2% (117,288,692 bases) were *B. anthracis*. The remaining 98% reads were of other bacterial (e.g., *Cutibacterium* sp.), bovine, or human (6,590,587 reads; 31%) origin. The latter likely reflecting repeated contact with museum staff during the last 100+ years of storage, because the slide was not glass-covered.

Genomic in silico analysis revealed that the chromosomal *B. anthracis* PCR-marker *dhp61* was present as well as both virulence plasmids pXO1 and pXO2. Canonical SNP-typing phylogenetically placed the historic genome, which we named Chemnitz 1878, within the B.Br.CNEVA clade of *B. anthracis* [23]. Next, we inferred the phylogenetic placement of the Chemnitz 1878 chromosome within the B.Br.CNEVA clade of *B. anthracis* (Figure 2a).

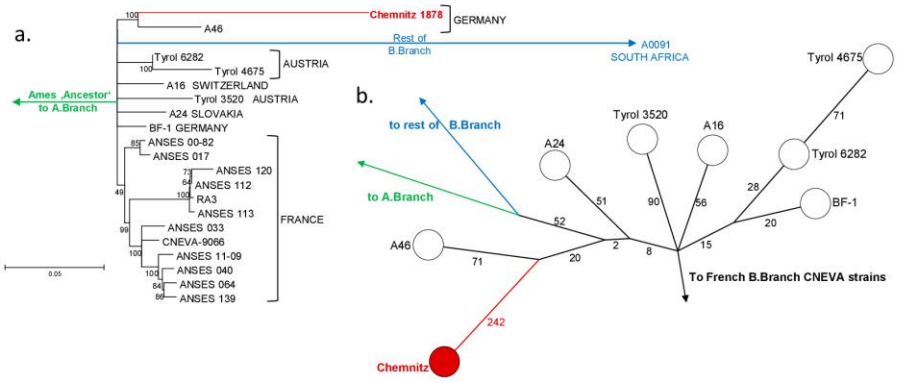

Figure 2. Phylogenetic placement of *B. anthracis* specimen Chemnitz 1878. (**a**) Rooted maximum likelihood tree derived from chromosomal Single Nucleotide Polymorphisms of Chemnitz 1878 and representative relatives (2450 chromosomal SNPs in total; bootstrap confidence-values based on 500 permutations). Isolate names and countries of origin are indicated at branch termini. The tree is rooted to the *B. anthracis* reference strain Ames 'Ancestor', which belongs to the A.Br.Ames clade. (**b**)

Minimum spanning tree based on chromosomal SNPs showing strain Chemnitz 1878 alongside its closest relatives. Numbers next to branch-lines indicate SNPs separating nodes or strains.

The closest living relative was strain A46, isolated from a pig near Stuttgart (Germany), with a distance of 313 SNPs, though a more distant relative, cattle isolate BF-1 from Bavaria, was at 307 SNPs distance (Figure 2b). Isolates from central Europe (Austria, Switzerland, and Slovakia) were grouped to the same lineage). From these, strain Tyrol 4675 featured the most SNP differences to strain Chemnitz 1878 (386 SNPs; Figure 2b). B.Br.CNEVA strains from France grouped phylogenetically further away, forming several distinct sub-clusters within CNEVA canSNP group (Figure 2a). Notably, with new B.Br.CNEVA-genomes now available, there is a significant polytomy right at the base of the B.Br.CNEVA lineage (Figure 2a), contrary to what was reported before based on more limited information [9].

While German *B. anthracis* strain collections feature a broad diversity of eight out of the twelve original *B. anthracis* canSNP-groups [23], recent data suggests B-branch isolates constituting the autochthonous population of the anthrax pathogen in countries from central [9] and northern [24] Europe, as well as from northwestern Asia (Russian Federation) [10]. Thus, from a bioforensics point of view, the isolation of a B.Br.CNEVA-type *B. anthracis* strain from a future outbreak would raise fewer concerns than would an isolate from a canSNP-group typical for a non-European origin.

4. Conclusions

This work emphasizes that historic specimen slides in mycological collections of herbaria, museums, and alike may constitute invaluable sources for reconstructing the historic phylogeny of the anthrax pathogen in countries in which the disease is all but eradicated today. Making this approach more broadly known would likely also avoid such mishaps (from a scientific point of view) as the one at the Chrysler Herbarium at Rutgers University in 2016 (https://news.illinois.edu/view/6367/350255). During a digitization project of historical samples, a 121-year-old specimen, an envelope labeled *B. anthracis*, was unearthed. Unfortunately, the envelope's content had been destroyed years before without further characterization.

Supplementary Materials: The following are available online at www.mdpi.com/xxx/s1: Table S1: Genome sequences accession numbers of newly sequenced and additional *B. anthracis* strains from publicly available databases; Table S2: Chromosome-wide binary SNP matrix of all analyzed *B. anthracis* chromosomes.

Author contributions: Conceptualization: D.T., M.A., and G.G.; investigation: M.K. and P.B.; methodology: M.K., P.B., M.A., and G.G.; formal analysis and validation: M.A. and G.G.; resources: D.T., M.A., and G.G.; data curation: P.B., M.K., D.T., M.A., and G.G.; writing—original draft preparation: M.K., M.A., and G.G.; writing—review and editing: P.B., M.K., D.T., M.A., and G.G.; visualization: P.B., M.K., and G.G.; supervision and project administration: M.A. and G.G.; funding acquisition: M.A. and G.G. All authors have read and agreed to the published version of the manuscript.

Funding: This research was funded by funds from the Medical Biological Defense Research Program of the Bundeswehr Joint Medical Service.

Acknowledgments: The authors thank Franz Allerberger, Austrian Agency for Health and Food Safety (Vienna, Austria) for the gift of Austrian *B. anthracis* strains. Thanks are due to Mathias Walter for support in bioinformatics analysis and script development; we also thank Linda Dobrzykowski and Josua Zinner for technical assistance and Ursula Rambold for identifying the historic anthrax material during a herbarium inventory.

Conflicts of Interest: The authors declare no conflict of interest. Opinions, interpretations, conclusions, and recommendations are those of the authors and are not necessarily endorsed by any governmental agency, department or other institutions. The funders had no role in the design of the study; in the collection, analyses, or interpretation of data; in the writing of the manuscript, or in the decision to publish the results.

References

1. Rascovan, N.; Sjogren, K.G.; Kristiansen, K.; Nielsen, R.; Willerslev, E.; Desnues, C.; Rasmussen, S. Emergence and spread of basal lineages of *Yersinia pestis* during the Neolithic decline. *Cell* **2019**, *176*, 295–305.
2. Bennett, R.J.; Baker, K.S. Looking backward to move forward: The utility of sequencing historical bacterial genomes. *J Clin. Microbiol* **2019**, *57*, doi:10.1128/JCM.00100-19.
3. Dirckx, J.H. Virgil on anthrax. *Am. J. Dermatopathol.* **1981**, *3*, 191–195.
4. World Health Organization. *Anthrax in Humans and Animals*, 4th ed.; WHO Press: Geneva, Switzerland, 2008.
5. Elschner, M.C.; Busch, A.; Schliephake, A.; Gaede, W.; Zuchantke, E.; Tomaso, H. High-quality genome sequence of *Bacillus anthracis* strain 14RA5914 isolated during an outbreak in Germany in 2014. *Genome Announc.* **2017**, *5*, doi:10.1128/genomeA.01002-17.
6. Hunziker, S. Über gewerblichen Milzbrand. Ph.D. Thesis, University of Basel, Switzerland, Grob & Zürcher (Amriswil), 1939; 44 pages.
7. Redmond, C.; Pearce, M.J.; Manchee, R.J.; Berdal, B.P. Deadly relic of the Great War. *Nature* **1998**, *393*, 747–748.
8. Antwerpen, M.H.; Sahl, J.W.; Birdsell, D.; Pearson, T.; Pearce, M.J.; Redmond, C.; Meyer, H.; Keim, P.S. Unexpected relations of historical anthrax strain. *MBio* **2017**, *8*, doi:10.1128/mBio.00440-17.
9. Vergnaud, G.; Girault, G.; Thierry, S.; Pourcel, C.; Madani, N.; Blouin, Y. Comparison of French and worldwide *Bacillus anthracis* strains favors a recent, post-Columbian origin of the predominant North-American clade. *PLoS ONE* **2016**, *11*, e0146216.
10. Timofeev, V.; Bahtejeva, I.; Mironova, R.; Titareva, G.; Lev, I.; Christiany, D.; Borzilov, A.; Bogun, A.; Vergnaud, G. Insights from *Bacillus anthracis* strains isolated from permafrost in the tundra zone of Russia. *PLoS ONE* **2019**, *14*, e0209140.
11. Aqel, A.A.; Hailat, E.; Serrecchia, L.; Aqel, S.; Campese, E.; Vicari, N.; Fasanella, A. Molecular characterization of the circulating *Bacillus anthracis* in Jordan. *Trop. Anim. Health Prod.* **2015**, *47*, 1621–1624.
12. Fasanella, A.; Serrecchia, L.; Chiaverini, A.; Garofolo, G.; Muuka, G.M.; Mwambazi, L. Use of canonical single nucleotide polymorphism (canSNPs) to characterize *Bacillus anthracis* outbreak strains in Zambia between 1990 and 2014. *PeerJ* **2018**, *6*, e5270.
13. Sahl, J.W.; Pearson, T.; Okinaka, R.; Schupp, J.M.; Gillece, J.D.; Heaton, H.; Birdsell, D.; Hepp, C.; Fofanov, V.; Noseda, R.; et al. A *Bacillus anthracis* genome sequence from the Sverdlovsk 1979 autopsy specimens. *MBio* **2016**, *7*, e01501–e01516.
14. Braun, P.; Grass, G.; Aceti, A.; Serrecchia, L.; Affuso, A.; Marino, L.; Grimaldi, S.; Pagano, S.; Hanczaruk, M.; Georgi, E.; et al. Microevolution of anthrax from a young ancestor (M.A.Y.A.) suggests a soil-borne life cycle of *Bacillus anthracis*. *PLoS ONE* **2015**, *10*, e0135346.
15. Thümen, F. *Herbarium Mycologicum Oeconomicum*: [die für Land-, Forst- und Hauswirthschaft, den Gartenbau und die Industrie schädlichen resp. nützlichen Pilze in getrockneten Exemplaren]; Fasc. 14, no. 651-700; Thümen, F von: Vienna, Austria, 1879 ; IndExs Exsiccatae ID 307188034.
16. Bankevich, A.; Nurk, S.; Antipov, D.; Gurevich, A.A.; Dvorkin, M.; Kulikov, A.S.; Lesin, V.M.; Nikolenko, S.I.; Pham, S.; Prjibelski, A.D.; et al. SPAdes: A new genome assembly algorithm and its applications to single-cell sequencing. *J. Comput. Biol.* **2012**, *19*, 455–477.
17. Walker, B.J.; Abeel, T.; Shea, T.; Priest, M.; Abouelliel, A.; Sakthikumar, S.; Cuomo, C.A.; Zeng, Q.; Wortman, J.; Young, S.K.; et al. Pilon: An integrated tool for comprehensive microbial variant detection and genome assembly improvement. *PLoS ONE* **2014**, *9*, e112963.
18. Li, H.; Durbin, R. Fast and accurate long-read alignment with Burrows-Wheeler transform. *Bioinformatics* **2010**, *26*, 589–595.
19. Li, H.; Handsaker, B.; Wysoker, A.; Fennell, T.; Ruan, J.; Homer, N.; Marth, G.; Abecasis, G.; Durbin, R. The sequence alignment/map format and SAMtools. *Bioinformatics* **2009**, *25*, 2078–2079.
20. Treangen, T.J.; Ondov, B.D.; Koren, S.; Phillippy, A.M. The Harvest suite for rapid core-genome alignment and visualization of thousands of intraspecific microbial genomes. *Genome Biol.* **2014**, *15*, 524.
21. Tamura, K.; Nei, M. Estimation of the number of nucleotide substitutions in the control region of mitochondrial DNA in humans and chimpanzees. *Mol. Biol. Evol.* **1993**, *10*, 512–526.
22. Kumar, S.; Stecher, G.; Tamura, K. MEGA7: Molecular Evolutionary Genetics Analysis version 7.0 for bigger datasets. *Mol. Biol. Evol.* **2016**, *33*, 1870–1874.

23. Van Ert, M.N.; Easterday, W.R.; Huynh, L.Y.; Okinaka, R.T.; Hugh-Jones, M.E.; Ravel, J.; Zanecki, S.R.; Pearson, T.; Simonson, T.S.; U'Ren, J.M.; et al. Global genetic population structure of *Bacillus anthracis*. *PLoS ONE* **2007**, *2*, e461.
24. Lienemann, T.; Beyer, W.; Pelkola, K.; Rossow, H.; Rehn, A.; Antwerpen, M.; Grass, G. Genotyping and phylogenetic placement of *Bacillus anthracis* isolates from Finland, a country with rare anthrax cases. *BMC Microbiol.* **2018**, *18*, 102.

3. In-depth analysis of Bacillus anthracis 16S rRNA genes and transcripts reveals intra- and intergenomic diversity and facilitates anthrax detection

AMERICAN SOCIETY FOR MICROBIOLOGY | mSystems®

RESEARCH ARTICLE

In-Depth Analysis of *Bacillus anthracis* 16S rRNA Genes and Transcripts Reveals Intra- and Intergenomic Diversity and Facilitates Anthrax Detection

Peter Braun,[a] Fee Zimmermann,[a] Mathias C. Walter,[a] Sonja Mantel,[a] Karin Aistleitner,† Inga Stürz,[a] Gregor Grass,[a] Kilian Stoecker[a]

[a]Bundeswehr Institute of Microbiology, Munich, Germany

Gregor Grass and Kilian Stoecker contributed equally.

ABSTRACT Analysis of 16S rRNA (rRNA) genes provides a central means of taxonomic classification of bacterial species. Based on presumed sequence identity among species of the *Bacillus cereus sensu lato* group, the 16S rRNA genes of *B. anthracis* have been considered unsuitable for diagnosis of the anthrax pathogen. With the recent identification of a single nucleotide polymorphism in some 16S rRNA gene copies, specific identification of *B. anthracis* becomes feasible. Here, we designed and evaluated a set of *in situ*, *in vitro*, and *in silico* assays to assess the unknown 16S state of *B. anthracis* from different perspectives. Using a combination of digital PCR, fluorescence *in situ* hybridization, long-read genome sequencing, and bioinformatics, we were able to detect and quantify a unique 16S rRNA gene allele of *B. anthracis* (16S-BA-allele). This allele was found in all available *B. anthracis* genomes and may facilitate differentiation of the pathogen from any close relative. Bioinformatics analysis of 959 *B. anthracis* SRA data sets inferred that abundances and genomic arrangements of the 16S-BA-allele and the entire rRNA operon copy numbers differ considerably between strains. Expression ratios of 16S-BA-alleles were proportional to the respective genomic allele copy numbers. The findings and experimental tools presented here provide detailed insights into the intra- and intergenomic diversity of 16S rRNA genes and may pave the way for improved identification of *B. anthracis* and other pathogens with diverse rRNA operons.

IMPORTANCE For severe infectious diseases, precise pathogen detection is crucial for antibiotic therapy and patient survival. Identification of *Bacillus anthracis*, the causative agent of the zoonosis anthrax, can be challenging when querying specific nucleotide sequences such as in small subunit rRNA (16S rRNA) genes, which are commonly used for typing of bacteria. This study analyzed on a broad genomic scale a cryptic and hitherto underappreciated allelic variant of the bacterium's 16S rRNA genes and their transcripts using a set of *in situ*, *in vitro*, and *in silico* assays and found significant intra- and intergenomic heterogeneity in the distribution of the allele and overall rRNA operon copy numbers. This allelic variation was uniquely species specific, which enabled sensitive pathogen detection on both DNA and transcript levels. The methodology used here is likely also applicable to other pathogens that are otherwise difficult to discriminate from their less harmful relatives.

KEYWORDS 16S rRNA, *Bacillus anthracis*, fluorescence *in situ* hybridization, anthrax, digital PCR, genomics, pathogen detection

Anthrax, caused by the spore-forming bacterium *Bacillus anthracis*, is a disease of animals but can also affect humans either through contact with infected animals

Editor Pedro H. Oliveira, Génomique Métabolique, Genoscope, Institut Francois Jacob, CEA, CNRS, Université Paris-Saclay

Address correspondence to Gregor Grass, gregor_grass@hotmail.com.

The authors declare no conflict of interest.

†Deceased 31 March 2019.

Received 17 November 2021
Accepted 20 December 2021
Published 25 January 2022

and their products or as a consequence of deliberate acts of bioterrorism (1, 2). Because of its high pathogenicity, rapid, sensitive, and unambiguous identification of the pathogen is vital. However, diagnostic differentiation of *B. anthracis* from its closest relatives of the *Bacillus cereus sensu lato* group is challenging. Phenotypic properties are not species specific, and nearly identical derivatives of the anthrax virulence plasmids can also be found in related bacilli (2).

In spite of earlier work (3), rRNA gene sequences have not been deemed discriminatory for unambiguous distinction of *B. anthracis* from its closest relatives due to the lack of specific sequence variations. Recent analysis of 16S rRNA gene alleles of *B. anthracis* and relatives, however, revealed an unexpected SNP (single-nucleotide polymorphism) at position 1110 (position 1139 in reference 4; 1110 according to the *B. anthracis* strain Ames ancestor, NC_007530) in some of the 16S rRNA gene copies (4). This SNP has previously been missed, most likely because it is present only in some of the eleven 16S rRNA gene copies (4). Despite the high abundance of more than 1,000 publicly available short-read genomic data sets and more than 260 genome assemblies, reliable information about sequence variations within *B. anthracis* rRNA operons is still scarce due to the limitations of short-read whole-genome sequencing (WGS) and subsequent reference mapping to detect sequence variations in paralogous, multicopy genes. Producing high-quality genomes, e.g., through hybrid assemblies of long- and short-read approaches, would help bridge this gap.

In this study, we validated a species-discriminatory SNP within the 16S rRNA genes of *B. anthracis* using a set of different *in situ*, *in vitro*, and *in silico* approaches on both genomic and transcript levels. Through this work, we established new diagnostic tools for *B. anthracis*, including a fluorescence *in situ* hybridization (FISH) assay and a digital PCR (dPCR) test for both genomic and transcript identification and quantification. While these new tools do not replace existing diagnostic approaches for identification of *B. anthracis*, they are a valuable addition to the toolbox for its detection and characterization. Finally, we expanded our analysis on all short-read *B. anthracis* data sets available in the NCBI Short Read Archive (SRA) and calculated the rRNA operon copy numbers and allele frequencies using a coverage ratio-based bioinformatics approach.

RESULTS

An SNP in transcripts of 16S rRNA genes enables specific microscopic detection of *B. anthracis* by FISH. Triggered by earlier data on a unique SNP position in some copies of the 16S rRNA gene of *B. anthracis* (guanine-to-adenine transition at position 1110) (4), we aimed at developing a new FISH assay for the identification of *B. anthracis*. Previous work has introduced a probe set for the FISH-based identification of *B. anthracis* (5). Evaluation of the probe sequences revealed, however, that they are unsuitable for unambiguous *B. anthracis* identification due to unspecific probe binding (6). Thus, we designed a FISH probe for discriminating *B. anthracis* from all of its close relatives targeting this specific SNP in 16S rRNA genes (probe BA_SNP_Cy3). Additionally, we developed probe BC_SNP_FAM, which binds to 16S rRNA sequence found in all *B. cereus sensu lato* strains, including *B. anthracis* (see Table S2 in the supplemental material). No other bacterial or archaeal 16S rRNA gene in the SILVA database had a full match for both of the newly designed probes (accessed 1 March 2021). To increase signal intensity and stringency (7), we incorporated two locked nucleic acids (LNA) in probe BA_SNP_Cy3 and one LNA in probe BC_SNP_FAM. Optimum formamide concentrations in the hybridization buffer of this FISH assay were titrated and finally set at 30% (vol/vol) formamide for species differentiation (Fig. S1).

For assay validation, the 16S rRNA probes were tested against a broad panel of *B. cereus sensu lato* strains, including *B. cereus* biovar *anthracis* (Table S1). The FISH assay allowed differentiation of *B. anthracis* from all other *B. cereus sensu lato* group members. *B. anthracis* cells displayed red fluorescence Cy3 signals after hybridization of the specific 16S rRNA variation at position 1110 and green fluorescence 6-carboxyfluorescein (FAM) signals resulting from hybridization to the divergent 16S rRNA featuring no

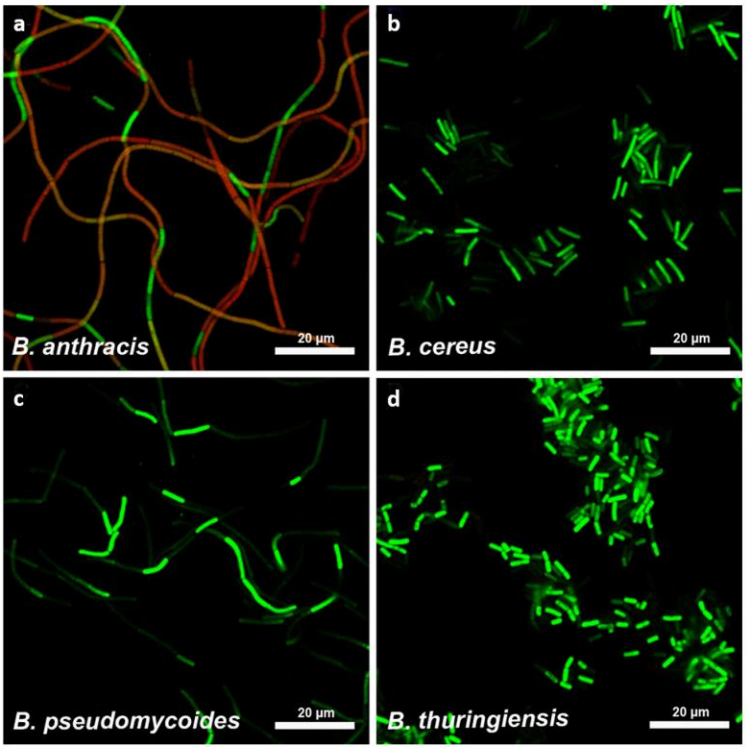

FIG 1 FISH-based microscopic differentiation of *B. anthracis* from other *B. cereus sensu lato* group species. Representative images for *B. anthracis* (a; strain Bangladesh 28/01) *B. cereus* (b; strain ATCC 6464), *B. pseudomycoides* (c; strain WS 3119), and *B. thuringiensis* (d; strain WS 2614) are shown as overlay images of red (probe BA_SNP_Cy3/568 nm) and green (fluorescent channels probe BC_SNP_FAM/520 nm).

B. anthracis-specific SNP (Fig. 1). No red Cy3-signals were detected in any of the non-*B. anthracis B. cereus sensu lato* group strains.

While we found Cy3 FISH signals for all *B. anthracis* strains, we discovered broad variations in Cy3 fluorescence signal intensities for different cells of the same and between different *B. anthracis* strains. Even for cells of the same chain, there were individual cells showing almost uniquely either the Cy3 or the FAM signal, resulting in a mosaic-like pattern (Fig. 1). Total fluorescence intensities varied between different *B. anthracis* strains from very strong Cy3 signals to the extreme cases of *B. anthracis* strains ATCC 4229 Pasteur, SA20, and A3783, for which Cy3 signals were very weak (for signal intensities see Table S1). These findings strongly indicate that the 16S rRNA of *B. anthracis* can be used for microscopy-based specific pathogen detection. Notably, variations in fluorescence intensities suggest differences in the rRNA expression level. As these differences might be caused by a gene dose effect, we decided to analyze the genomic distribution of the *B. anthracis*-specific SNP in 16S rRNA genes.

Genomic analysis of *B. anthracis* genomes reveals variations in 16S-BA-allele frequencies. We correlated FISH results with the abundance of 16S rRNA gene copies harboring the *B. anthracis*-specific SNP within different *B. anthracis* genomes. Despite the significant number of *B. anthracis* genomes published, the vast majority of sequences have been generated using short-read sequencing with subsequent mapping to the reference genome (Ames Ancestor; GenBank accession no. NC_007530 [8]). Due to multiple copies of the rRNA operons, conventional short-read sequencing and mapping approaches do not allow for reliable detection of allele variations. During *de novo* assembly of short reads, nearly identical regions like rRNA operons are collapsed into

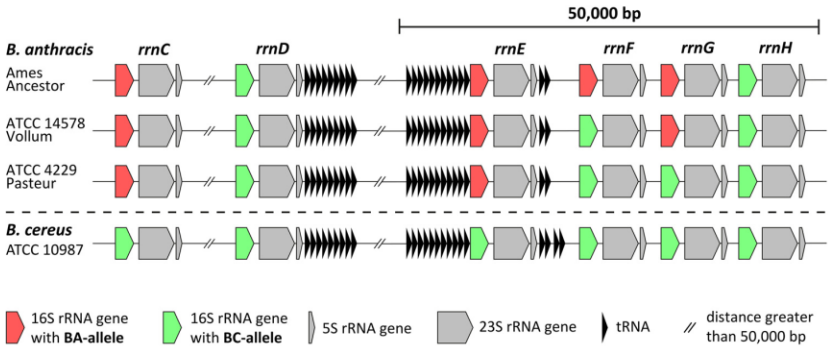

FIG 2 Schematic illustration of the genomic organization of rRNA operons and distribution of 16S alleles in *B. anthracis*. Depicted are the 16S, 23S, and 5S ribosomal subunits and tRNA genes from operons *rrnC* to *-H* in strains Ames Ancestor, ATCC 14578 Vollum, ATCC 4229 Pasteur, and *B. cereus* ATCC 10987. The 16S rRNA genes are either displayed in red for 16S-BA-alleles or in green for 16S-BC-alleles. Not shown are operons *rrnA*, *-B*, *-I*, *-J*, and *-K* exclusively carrying the 16S-BC allele in any strain. Distances are not to scale.

one contig representing only a consensus sequence missing any minor allele variations. Thus, potential differences in allele frequencies can easily be missed. Because of mapping to the reference genome, consensus sequences always feature 16S rRNA allele distribution identical to that of the reference. Hence, there is a need for high-quality genomes generated by hybrid assemblies using long- and short-read sequences for obtaining insights into the real distribution and diversity of 16S rRNA alleles in *B. anthracis* genomes.

To start meeting this need, we analyzed and compared the 16S gene sequences and locations in all available high-quality genomes of *B. anthracis* (accessed at the end of 2020) that are based on long-read sequencing and *de novo* assembly. Figure 2 shows a schematic illustration of the genomic organization of rRNA operons, including 16S, 23S, and 5S ribosomal subunits as well as tRNA genes from operons *rrnC* to *-H* (outlying operons A, B, I, J, and K are not shown) of representative strains for different 16S rRNA genotypes (Ames Ancestor, NC_007530 [8]; ATCC 14578 Vollum [in-house sequenced; this work; Table S3]; ATCC 4229 Pasteur, NZ_CP009476 [9]) and closely related *B. cereus* strain ATCC 10987, NC_003909 (10).

We found that all 16S rRNA gene copies featuring the *B. anthracis*-specific SNP have 100% sequence identity, representing a distinct allele. For simplification, copies featuring this guanine-to-adenine transition at position 1110 were termed 16S-BA-(*B. anthracis*)-alleles, while all other variants lacking this transition were designated 16S-BC-(*B. cereus sensu lato*)-alleles.

The three *B. anthracis* strains, Ames Ancestor, ATCC 14578 Vollum, and ATCC 4229 Pasteur, harbored different 16S-BA/BC-allele frequencies, with 4/7, 3/8, and 2/9 copies, respectively (Fig. 2). No 16S-BA-alleles were found in *B. cereus* ATCC 10987 or any other non-*B. anthracis* strain. In all three *B. anthracis* strains, rRNA operons *rrnA*, *-B*, *-D*, *-H*, *-I*, *-J*, and *-K* carried 16S-BC-alleles, while for *rrnC* and *rrnE* exclusively the 16S-BA-allele was identified. Only two rRNA operons, *rrnF* and *rrnG*, were found to be variable, with strain Ames Ancestor harboring two 16S-BA-alleles and strain ATCC 4229 Pasteur only the BC-alleles for *rrnF* and *rrnG*. Strain ATCC 14578 Vollum exhibited an intermediate state with a 16S-BA-allele in *rrnG* and a BC-allele in *rrnF* (Fig. 2). Thus, it is possible that these differences in 16S rRNA allele distributions caused the observed variations in *B. anthracis*-specific FISH signals (Fig. 1) by gene dose-mediated differences in rRNA transcription levels.

A tetraplex dPCR assay enables the absolute quantification of species-specific 16S rRNA gene allele numbers in *B. anthracis*. To verify this finding and to quantify the ratios of each allele in a diverse panel of *B. anthracis* strains, we designed and tested a hydrolysis probe-based digital PCR (dPCR) assay (Fig. 3a). This assay utilized

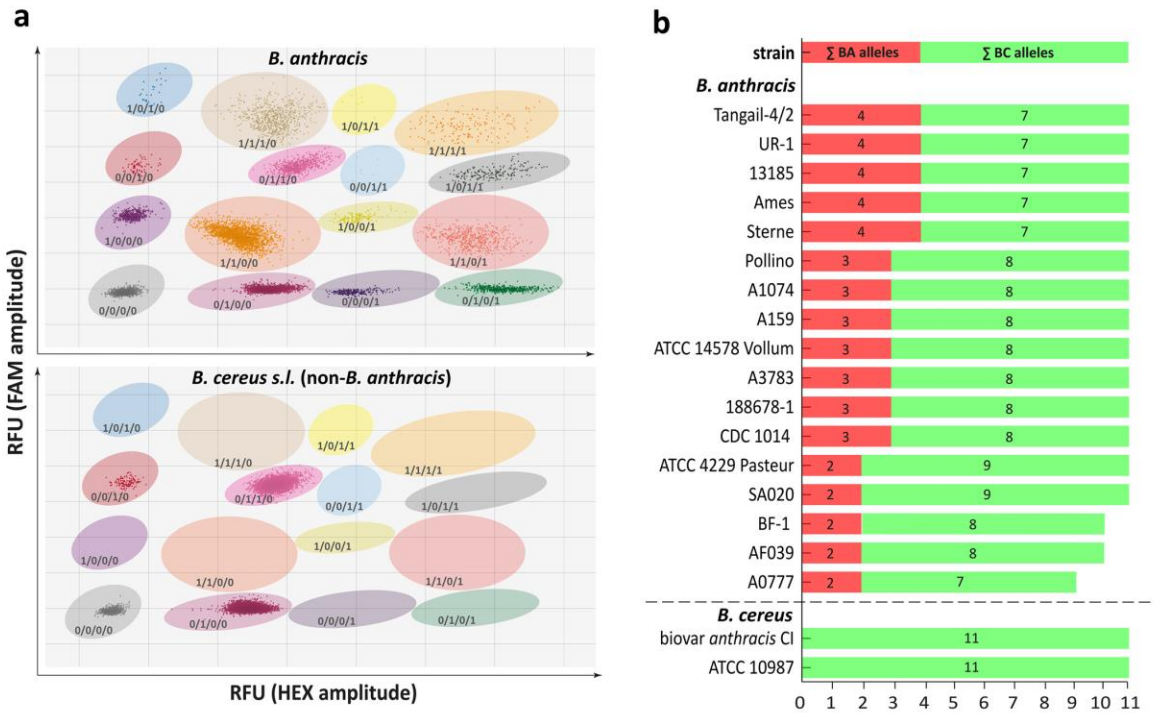

FIG 3 Detection and quantification of 16S rRNA gene alleles in *B. anthracis* and *B. cereus sensu lato* strains. (a) Typical results of a tetraplex dPCR assay using *B. anthracis* template DNA (upper) and DNA of a non-*B. anthracis* member of the *B. cereus sensu lato* group (lower). With each dot representing a droplet plotted according to its FAM signal amplitude (RFU, relative fluorescence units) on the *y* axis and HEX signal amplitude on the *x* axis, a total of 16 (for *B. anthracis*, upper) or 4 (non-*B. anthracis* members of the *B. cereus sensu lato* group, lower) clusters (defined by shaded areas) can be assigned to a certain dPCR marker combination of *gyrA* (FAM high signal), *PL3* (HEX high signal), 16S-BA-allele (FAM low signal), and 16S-BC-allele (HEX low signal). Each cluster is labeled with 1 (positive for respective marker) or 0 (negative for respective marker) according to its marker combination (*gyrA*/*PL3*/16S-BA-allele/16S-BC-allele). Since both the *PL3* gene and the 16S-BA-allele are exclusively found in *B. anthracis*, the 16S-BA- and 16S-BC-allele copy numbers can be calculated from the positive droplets of single-copy genes (*PL3* and *gyrA*) and multicopy 16S rRNA genes. All dPCR patterns lacking both the *PL3* gene and the 16S-BA-allele clusters represent DNA of a non-*B. anthracis* member of the *B. cereus sensu lato* group. (b) Copy numbers for 16S-BA- and 16S-BC-alleles for all *B. anthracis* strains and *B. cereus* biovar *anthracis* CI tested.

hexachlorofluorescein (HEX) (green) and FAM (blue) fluorescent dye-labeled allele-specific probes for the 16S-BC-allele and -BA-allele, respectively, with both probes targeting SNP 1110 of the 16S rRNA genes (Table S2). In parallel, a previously published second hydrolysis probe-based PCR assay using HEX dye was adopted for dPCR. This assay targets the *B. anthracis*-specific chromosomal *PL3* gene (11). Finally, a pan-*B. cereus sensu lato* hydrolysis probe-based PCR assay on the *gyrA* (gyrase gene) marker using FAM dye was designed, facilitating the detection and quantification of *B. cereus sensu lato* species (including *B. anthracis*) chromosomes. In these dPCR assays, the *PL3* and *gyrA* dPCR tests served as internal controls (for *B. anthracis* and *B. cereus sensu lato*, respectively), each positive for *B. anthracis* genomic DNA versus negative for *PL3* and positive for *gyrA* using genomic DNA of other members of the *B. cereus sensu lato* group.

These four assays were combined into a single tetraplex dPCR assay. To achieve the required signal separation of the four individual dPCR reactions (on our dPCR analysis instrument featuring only two channels, FAM and HEX), we deliberately altered the signal output levels by titrating concentrations of probes labeled with the same dye (Fig. 3a). Thus, the *PL3* marker assay was tuned to produce high HEX signals versus low HEX signals coming from 16S-BC-alleles. Likewise, the *gyrA* marker assay was set to produce high FAM signals versus low FAM signals originating from 16S-BA-alleles. Since both *PL3* and *gyrA* are single-copy genes located on the chromosome of *B. anthracis*,

these markers should result in very similar quantitative outputs when individual *B. anthracis* DNA samples are analyzed. Therefore, these markers served as internal quantification controls in this work.

A typical analysis output of this tetraplex dPCR assay is exemplified in Fig. 3a. In a two-dimensional plot (FAM signal amplitude on the *y* axis and HEX signal amplitude on the *x* axis) of such tetraplex dPCR data, one can discriminate a specific fluorescence pattern after dPCR, representing 16 clusters (when *B. anthracis* DNA was used as a template). Each of the droplets within a cluster contained a certain target combination of *gyrA*, *PL3*, 16S-BA-allele, and/or 16S-BC-allele (for example, *gyrA*$^+$/*PL3*$^+$/16S-BC-allele$^+$/16S-BA-allele$^+$ or *gyrA*$^-$/*PL3*$^-$/16S-BC-allele$^-$/16S-BA-allele$^-$). Using template DNA originating from a non-*B. anthracis* member of the *B. cereus sensu lato* group (i.e., not harboring any 16S-BA allele) resulted in the expected formation of only four droplet clusters, i.e., lacking all signals of *B. anthracis*-specific clusters containing combinations of the *PL3* marker or the 16S-BA-allele (Fig. 3a).

Testing the assay on the reference strains Ames, ATCC 14578 Vollum, and ATCC 4229 Pasteur, we found four, three, and two 16S-BA-alleles, respectively, and eleven 16S rRNA total copies per cell in all three strains. This agreed with the values determined by genomic analysis and, therefore, validated the dPCR assay being able to accurately quantify 16S rRNA alleles in *B. anthracis*.

Using the validated tetraplex dPCR assay, we analyzed the same strain panel as that tested by FISH (Table S1). Similar to FISH, there was no signal for 16S-BA-alleles in the 32 non-*B. anthracis* strains of the *B. cereus sensu lato* group. This panel included *B. cereus* biovar *anthracis*, which can cause anthrax-like disease due to the presence of both virulence plasmids. Its chromosomal background is closer to *B. cereus*, and, as expected, no 16-S-BA-allele signal was detected. However, all of the 17 *B. anthracis* strains harbored at least two (up to four) copies of the 16S-BA-allele per cell (Fig. 3b). The majority of *B. anthracis* strains exhibited the genotype 4/7 or 3/8 (16S-BA/BC-alleles; six and seven strains, respectively). These predominant genotypes, together with genotype 2/9 (strain ATCC 4229 Pasteur and strain SA020), were all found to harbor 11 rRNA operons in total, which agrees with previously determined numbers of rRNA operons in these strains. Conversely, strains A182 and BF-1 harbored only ten 16S gene copies in total (genotype 2/8). Notably, strain A0777 exhibited just nine rRNA copies, two of which contained the *B. anthracis*-specific SNP (genotype 2/7).

16S-BA-allele frequencies and total rRNA operon copy numbers vary between different *B. anthracis* strains. To further confirm dPCR results and to exclude underestimation by dPCR as a possible cause of the unexpectedly low number of total rRNA operons in strains A182, BF-1, and A0777, we conducted a combination of long- and short-read sequencing on these and 32 additional *B. anthracis* strains (Table S1). A mean read length of about 15 kb generated by Nanopore sequencing combined with Illumina 2 × 300 bp paired-end sequencing allowed for the precise assembly of complete genomes, including correct positioning of rRNA operons on the chromosome. Coverage values of more than 200-fold enabled the accurate quantification of SNPs; therefore, genotypes based on 16S-BA/BC-allele distribution could be reliably determined. The results matched those obtained from dPCR, confirming the accuracy and reliability of the tetraplex assay. We found that strain A0777 lacked rRNA operons *rrnG* and *rrnH*. rRNA operon *rrnG* was not present in strains AF039, SA020, and BF-1. The genome regions downstream of the missing rRNA operons and upstream of the next rRNA operon were also absent.

To extend our analysis of 16S rRNA allelic states to more *B. anthracis* strains, we expanded our investigation on all publicly available short-read sequence data for *B. anthracis* generated using Illumina sequencing technology. Starting from our newly generated high-quality hybrid assemblies, we developed a *k*-mer- and coverage ratio-based tool to calculate the rRNA operon copy numbers and allele frequencies from all SRA data sets published until the end of 2020. These numbers of rRNA operons and 16S-BA-alleles (from short-read data sets) were identical to the long-read data of the same genomes (Data Set S1). After this method validation, we analyzed 986 SRA

TABLE 1 16S rRNA genotypes obtained from *k*-mer-based SRA analysis[a]

16S-BA-allele	No. (%) of strains	No. of rRNA operon copies per genome	16S rRNA genotype (16S-BA-alleles/BC-alleles)	No. (%) of strains
1	3 (0.31)	9	1/8	1 (0.10)
		10	1/9	2 (0.21)
2	221 (23.0)	9	2/7	28 (2.92)
		10	2/8	116 (12.10)
		11	2/9	77 (8.03)
3	560 (58.39)	9	3/6	3 (0.31)
		10	3/7	39 (4.10)
		11	3/8	518 (54.01)
4	164 (17.10)	9	4/5	3 (0.31)
		10	4/6	32 (3.34)
		11	4/7	129 (13.45)
5	11 (1.15)	11	5/6	11 (1.15)

[a]Numbers of 16S-BA-alleles, overall rRNA operon numbers, and 16S rRNA genotypes resulting from these values are listed with their respective frequencies.

Illumina sequenced data sets for 16S rRNA operon and BA/BC-allele distribution. After assembly and filtering, 959 genomes remained for a detailed comparison. The majority (n = 735, 76.64%) contained 11 rRNA operons, 189 genomes (19.71%) harbored 10 rRNA operons, and only 35 genomes (3.65%) contained 9 rRNA operons (Table 1). This ratio is comparable to that found in our initial strain set tested with FISH and dPCR (11 copies, 82.35%; 10 copies, 11.76%; 9 copies, 5.88%). Of these 959 genomes, the 16S-BA-allele distributions showed that 23.04% had 2, 58.39% had 3 and 17.10% had 4 copies (Table 1). As with the rRNA operon copy numbers, this distribution correlated with the 16S-BA-allele distribution in our strain set analyzed by dPCR and WGS (2, 29.41%; 3, 41.17%; 4, 29.41%). Notably, a few strains were calculated to possess 1 (0.31%) or 5 (1.15%) 16S-BA-alleles. The overall diversity of 16S rRNA genotypes (BA alleles/BC alleles) was higher than that in our initial strain set (genotypes 4/7, 3/8, and 2/9). Additional major genotypes (frequency, >5) obtained from SRA analysis comprised 16S-BA-/BC-allele ratios of 2/8 and 2/7 and minor genotypes were 5/6, 4/6, 4/5, 3/7, 3/6, 1/9, and 1/8, each with frequencies of <5.

Interestingly, 10 of the genomes that were calculated to possess five BA alleles are from the same originating lab and were sequenced with a 100 bp single-end technique only (Data Set S1). Thus, without genomic context it is hardly possible to validate the presence of a fifth 16S-BA-allele from single-end short reads. The same applies to the only other strain (BC038/2000031523) sequenced with 2 × 100 bp paired-end reads and a mean insert size of 520 bp. Along with three strains putatively containing a single 16S-BA-allele only, strains with five BA-alleles should be resequenced using long-read technology for validation.

Finally, we tested to which degree 16S rRNA genotypes fit the phylogenetic placement of strains. For this, we correlated established phylogeny of *B. anthracis* based on a number of canonical SNPs (12) with the distribution of 16S-BA-alleles within 10 major canonical SNP groups of the three branches, A, B, and C, of *B. anthracis*. Figure S2 shows that there is limited correlation. Notably, B-branch featured a small set of genotypes besides the major 2/8 type. The few C-branch strains all had the 3/7 genotype. A-branch (comprising the majority of isolates) was the most diverse, dominantly showing the 2/9 genotype (with the exception of canSNP group Ames, 4/7). Although the 16S rRNA genotypes did not follow the established phylogeny of *B. anthracis*, the newly developed tools (tetraplex dPCR and *k*-mer-based SRA analysis) might still be harnessed as an alternative typing system for *B. anthracis* strains.

Expression of 16S-BA-alleles is proportional to gene copy number. Various ratios of 16S-BA/BC-alleles constitute possible explanations for differences in FISH signals of cells of diverse *B. anthracis* strains (Fig. 1). Indeed, we found a significant correlation between 16S-BA/BC-allele ratios in sequenced genomes and mean intensities of the

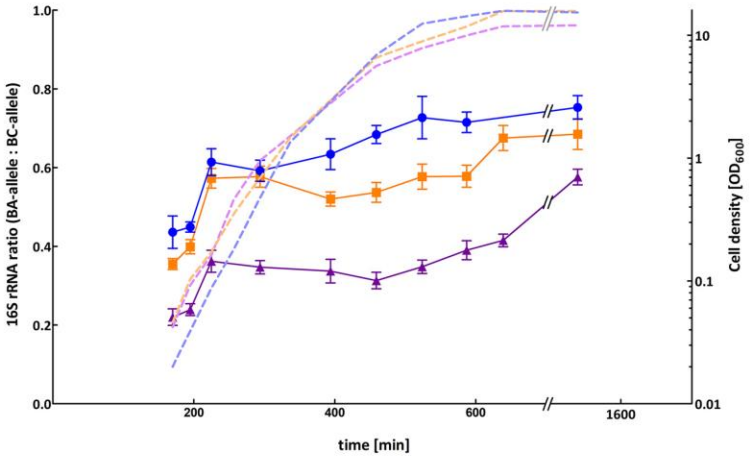

FIG 4 Expression ratios of 16S-BA- and -BC-alleles in three different *B. anthracis* strains at different growth phases. Expression level ratios of 16S-BA-alleles relative to 16S-BC-alleles were calculated from absolute target concentrations obtained by RT-dPCR. Values were plotted against time points of each sample taken during growth from early exponential to stationary phase for *B. anthracis* Sterne (blue), CDC1014 (orange), and Pasteur ATCC 4229 (purple) representing three major 16S rRNA genotypes (BA/BC), 4/7, 3/8, and 2/9, respectively. Error bars indicate the Poisson 95% confidence intervals for each copy number ratio. Dotted lines depict cell densities over time.

Cy3 FISH signals targeting the16S-BA-allele (tested with the cor.test function in R, Pearson's $r = 0.61$, $P = 0.009$), confirming this assumption.

To investigate whether the 16S-BA-alleles are differentially expressed throughout different growth phases of *B. anthracis*, we quantified 16S rRNA from growth experiments (Fig. 4). For this, culture samples of *B. anthracis* strains Sterne, CDC1014, and Pasteur ATCC 4229, representing three major 16S-BA/BC-allele genotypes, 4/7, 3/8, and 2/9, respectively, were taken for total RNA extraction at several time points during lag, log, and stationary growth phase. To compare rRNA levels with FISH signals, we also took parallel samples from six of these time points for FISH analysis. By a one-step reverse transcription duplex dPCR, the two 16S allele targets were interrogated for the expression ratios of the 16S-BA- to 16S-BC-alleles. *B. anthracis* RNA yielded four clusters of droplets in two-dimensional analysis plots, namely, 16S-BC-allele-/16S-BA-allele$^-$, 16S-BC-allele$^+$/16S-BA-allele$^-$, 16S-BC-allele$^-$/16S-BA-allele$^+$, and 16S-BC-allele$^+$/16S-BA-allele$^+$ (compare Fig. 3). RNA of other *B. cereus sensu lato* strains produced only two cluster types lacking 16S-BC-allele$^-$/16S-BA-allele$^+$ and 16S-BC-allele$^+$/16S-BA-allele$^+$. Absolute quantification of the two initial target concentrations of 16S-BA-alleles/BC-alleles in samples from growth cultures made it possible to determine their ratios representing the expression levels of the 16S-BA-alleles relative to those of 16S-BC-alleles (Fig. 4). Notably, 16S-BA/BC-allele rRNA ratios varied during growth and showed similar expression patterns in all three tested *B. anthracis* strains. Starting from a relatively low 16S-BA/BC-allele ratio in early log phase, the fraction of 16S-BA-allele expression increased in early log phase and decreased in mid-log phase with a final increase toward the stationary phase. While shifts in 16S-BA/BC-allele expression patterns in these strains were similar, differences were observed in numerical expression ratios. *B. anthracis* Sterne showed the highest 16S-BA/BC-allele expression ratio, ranging from 0.44 (early exponential phase) up to 0.75 (stationary phase), compared to CDC1014 with 0.36 to 0.69 and Pasteur ATCC 4229 with 0.22 to 0.58, which was found to have the lowest 16S-BA-allele expression in all growth phases. The largest differences in expression levels between all strains were observed in late log phase (Fig. 4). The observed diverging levels of 16S-BA-allele expression in the three tested strains can easily be explained by the different numbers of 16S-BA-allele copies per genome (2, 3, or 4). Nevertheless, the proportion of 16S-BA-allele rRNA in late

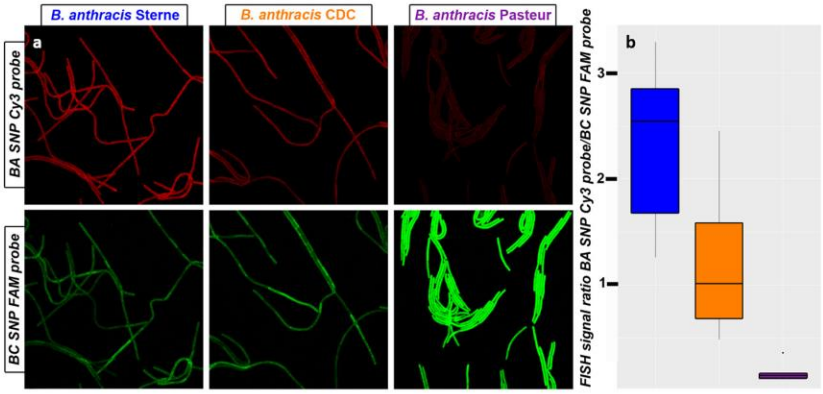

FIG 5 FISH of *B. anthracis* strains harboring different numbers of 16S-BA-alleles. (a) Representative FISH images showing signal intensities of *B. anthracis* strains with diverging genomic 16S (BA/BC) allele profiles Sterne (4/7), CDC1014 (3/8), and Pasteur ATCC 4229 (2/9). Samples were taken and processed after 460 min of continuous growth. (b) Boxplot of BA_SNP_Cy3 and BC_SNP_FAM FISH signal ratios across all sampled time points for *B. anthracis* Sterne (blue), CDC1014 (orange), and Pasteur ATCC 4229 (purple).

exponential *B. anthracis* cells is quite disproportionate. If all rRNA operons were transcribed at a constant and equal rate, one would expect a ratio of 0.22 (Pasteur 2/9), 0.38 (CDC3/8), and 0.57 (Sterne 4/7). Instead, we measured ratios that correlate to a 1.57 (Pasteur)-, 1.46 (CDC)-, and 1.09 (Sterne)-fold 16S-BA-allele overrepresentation on average throughout all growth phases and up to 2.59 (Pasteur)-, 1.83 (CDC)-, and 1.32 (Sterne)-fold in stationary phase.

The shift toward elevated expression of the 16S-BA-allele genes over time was not significantly reflected in FISH signal intensities, possibly due to the general decrease of FISH signals over time. However, if cells were sampled and fixed at identical time points, 16S-BA/BC-allele ratios were always highest for *B. anthracis* Sterne and lowest for *B. anthracis* Pasteur, which reflects their 16S-BA/BC-allele ratios on the genomic and transcript levels (Fig. 5). Also, sampled across all time points, 16S-BA/BC-allele FISH signal ratios correlated well with allele distributions in the three different strains (analysis of variance in R, $P = 0.0002$) (Fig. 5).

DISCUSSION

Using a combination of newly developed *in situ*, *in vitro*, and *in silico* approaches, we unraveled the elusive heterogeneity of 16S rRNA genes in the biothreat agent *B. anthracis*. Results consistently delineate the organism's intragenomic diversity of 16S rRNA genes, their differential expression across growth phases, and their intergenomic heterogeneity in publicly available and newly sequenced genomes. Intragenomic microdiversity within 16S rRNA genes has long been known from other species (13, 14) and was found to increase with higher copy numbers of rRNA operons (15). Thus, the species-wide intra- and intergenomic microdiversity related to SNP 1110 in 9 to 11 copies of the 16S rRNA gene of *B. anthracis* is not totally unsurprising (3, 4). Whereas some such polymorphic sites are associated with a distinct phenotypic trait (e.g., stress resistance) (16, 17), the functional assignment for the majority of these sequence variations (including those in *B. anthracis* 16S rRNA genes) remains elusive.

Although discovered before using Sanger sequencing (4), the specific SNP in the 16S rRNA genes of *B. anthracis* was disregarded despite the availability of numerous published genomes. Generally, sequence variations in multicopy genes such as 16S rRNA genes can hardly be detected when relying on conventional short-read WGS and subsequent reference mapping (18), which was used to generate the majority of publicly available *B. anthracis* whole-genome sequences. SNP calling in different rRNA operons or other paralogous genes gives ambiguous results, since assemblers tend to

interpret low-frequency sequence variations as sequencing errors and correct them prior to assembly (19). Even if detected, distances of the SNP to unique flanking regions up- and downstream of the multicopy gene may be >1,000 bases and, thus, are larger than typical library fragment sizes of 500 to 800 bases. In such cases, chromosomal locations of SNPs cannot be reconstructed. Instead, all rRNA gene-related reads are assembled into one contig with diverse fringes (20). The average read length of Nanopore sequencing is typically larger than 5 kb and therefore can cover complete rRNA operons. Thus, any unique SNP occurring in a single or a few rRNA gene alleles can be precisely allocated to a specific chromosome position, especially when combined with short-read sequencing and hybrid assembly as used here. Therefore, the challenges described above will become rather minor for future genomic analysis of *B. anthracis*. Such work is facilitated by the additional 33 complete high-quality genomes we have contributed here. These genomes cover all three major phylogenetic lineages (canSNP groups), all bona fide 16S-BA-allele frequencies (2, 3, and 4), and all known rRNA operon copy numbers.

On the *B. anthracis* chromosome, the 16S rRNA operons *rrnE*, *-F*, *-G*, and *-H* are located in close proximity to each other, with only 15.8, 8.5, and 5.2 kb, respectively, between them (forming a genomic region with a high density of four 16S rRNA operons within less than 50 kb). Conversely, the other 16S rRNA genes are rather dispersed, with distances greater than 50 kb between them. The 16S-BA-allele is present in operons *rrnC* and *rrnE* in all strains analyzed with long-read WGS, while *rrnF* and *rrnG* seem to be variable. Since the four operons *rrnE*, *-F*, *-G*, and *-H* are relatively close to each other in the *B. anthracis* chromosome, homologous recombination and gene duplications might be the reason for this allelic variation. Compared to all other 16S rRNA alleles on the *B. anthracis* genome, the 16S rRNA copies in this region (*rrnE* to *rrnH*) seem to differ from each other only in SNP position 1110. This finding promotes the explanation that the 16S rRNA copies in this region of high rRNA operon density are subject to an increased recombination rate between alleles with and without *B. anthracis*-specific SNP 1110. This notion is also supported by the fact that only operons *rrnG* and *-H* seem to be affected by deletion events in all strains analyzed by long-read WGS. The alternative explanation, horizontal gene transfer of a divergent allele, seems unlikely. We were unable to identify any 16S rRNA gene in public databases matching the 16S-BA-allele outside *B. anthracis*.

Recombination and deletion events in 16S rRNA operons of *B. anthracis* do occur. These events were experimentally shown in a study on bacitracin resistance. Two deletion events, DelFG and DelGH, were described that caused elimination of gene clusters between rRNA operons *rrnF*, *-G*, and *-H* (18). These DelFG and DelGH events describe a possible origin of *B. anthracis* strains with 10 16S rRNA gene copies, i.e., 21% of all strains (Table 1). Random gene duplication and gene elimination by recombination also might explain another observation: the newly defined 16S rRNA genotypes did not convincingly reflect the established *B. anthracis* phylogeny (Fig. S2). Instead, some 16S rRNA genotypes seem to be dominant yet not exclusive in separate branches, e.g., 2/8 copies in B-branch or 3/8 in A-branch (Fig. S1).

The recognition of intra- and intergenomic 16S rRNA allele diversity in *B. anthracis* opens possibilities to harness unique SNPs in 16S rRNA gene alleles and their transcripts. This finding strongly highlights the great potential of such genomic variations for both identification of *B. anthracis* and for diagnostics of anthrax disease. This approach is probably also applicable to other pathogens that are otherwise difficult to discriminate from their less notorious relatives.

MATERIALS AND METHODS

Cultivation of bacteria. The cultivation of the virulent *B. anthracis* strains was performed in a biosafety level 3 laboratory (BSL3) (see Table S1 in the supplemental material). All *Bacillus* strains were cultivated overnight on Columbia blood agar plates (containing 5% sheep blood; Becton, Dickinson, Heidelberg, Germany) at 37°C.

For isolation of DNA, a 1-μl loop of colonies was transferred to a 2-ml screwcap microcentrifuge tube, inactivated with 2% terralin PAA (Schülke & Mayr GmbH, Norderstedt, Germany) for 30 min, and washed three times with phosphate-buffered saline (PBS) as described previously (21).

For FISH, 50-ml centrifuge tubes containing 5 ml of tryptic soy broth (TSB; Merck KGaA, Darmstadt, Germany) were inoculated with one colony from an overnight culture (described above) and incubated at 37°C with shaking at 150 rpm. After 4 h of growth, bacteria were pelleted by centrifugation at 5,000 × *g* for 10 min, washed with PBS, and fixated with 3 ml 4% (vol/vol) formaldehyde for 1 h at ambient temperature. After fixation, cells were washed three times with PBS, resuspended in a 1:1 mixture of absolute ethanol and PBS, and stored at −20°C until further use. To ensure sterility, 1/10 of the inactivated material was incubated in thioglycolate medium (Merck KGaA, Darmstadt, Germany) for 7 days without growth before material was taken out of the BSL3 laboratory.

For growth-phase analysis, 1 ml of overnight cultures of attenuated *B. anthracis* (Sterne, CDC1014, and ATCC 4229 Pasteur) in TSB was used to inoculate 100 ml of fresh TSB in 1-liter baffled flasks and incubated at 37°C with shaking at 100 rpm. Every 30 min, turbidity was measured as the optical density at 600 nm (OD_{600}), and 1-ml samples were taken for FISH and RNA isolation, respectively. After pelleting by centrifugation, samples for RNA isolation were resuspended and inactivated using 2% terralin PAA for 30 min and washed three times with PBS. FISH samples were treated as described above.

Design of primers and probes. Primers and probes were designed using Geneious 10.1.3 (Biomatters, Auckland, New Zealand), and numerous probe variations were tested to identify the best combination and number of locked nucleic acids for differentiation of *B. anthracis* and the other *B. cereus sensu lato* group species based on the SNP (position 1110) detected previously (4). The final probes for FISH included 2 and 1 locked nucleic acid, while dPCR probes contained 5 and 6 for the *B. anthracis* (BA) and the *B. cereus sensu lato* (BC) probe, respectively (Table S2). For sequences of positive (EUB338 [22]) and negative (nonEUB [23]) control probes for FISH, see Table S2. Primers as well as probes labeled with 6-carboxyfluorescein (FAM), hexachlorofluorescein (HEX), indocarbocyanine (Cy3), and indodicarbocyanine (Cy5) were purchased commercially (TIB Molbiol, Berlin, Germany).

To determine the ideal formamide concentration for the FISH hybridization buffer, the fluorescence signals of probe BA_SNP_Cy3 and probe BC_SNP_FAM were assessed with *B. anthracis* Sterne and *B. cereus* ATCC 10987 at different formamide concentrations (0, 10, 20, 25, 30, 35, 40, 45, and 50% FA concentration in the hybridization buffer) as described elsewhere (24). Hybridization at 30% formamide was determined to be ideal for differentiation of *B. anthracis* and *B. cereus sensu lato* group (Fig. S1).

FISH and image processing. FISH was carried out as described elsewhere (24). A positive-control probe targeting eubacteria (EUB338 [22]) and a nonsense probe targeting no known bacterial species (nonEUB [23]) as a control for unspecific probe binding were included in each hybridization experiment. Briefly, 2 μl of fixed cells was spotted on Teflon-coated slides (Marienfeld, Lauda-Königshofen, Germany) and dried at 46°C. The cells then were permeabilized using 10 ml of 15 mg/ml lysozyme (no. 62970; Merck KGaA, Darmstadt, Germany) per well at 46°C for 12 min. After dehydration in an ascending ethanol series (50, 80, and 96% [vol/vol] ethanol), cells were covered with 10 μl hybridization buffer (0.9 M NaCl, 20 mM Tris-HCl [pH 8.0], 0.01% SDS, 30% formamide) with probes at a concentration of 10 μM and incubated in a humid chamber in the dark at 46°C for 1.5 h. Slides were washed in 50 ml prewarmed washing buffer (0.1 M NaCl, 20 mM Tris-HCl [pH 8.0], 5 mM EDTA [pH 8.0]) for 10 min at 48°C in a water bath. Finally, slides were dipped in ice-cold double-distilled water and carefully dried with compressed air. For each strain, FISH was performed in duplicate and two pictures were taken per well, so that the resulting fluorescence intensity was the mean of four images. To increase accuracy in the growth curve assay, five pictures were taken per well, so that the resulting fluorescence intensity was the mean of 10 images. All images were recorded with a confocal laser-scanning microscope (LSM 710; Zeiss, Jena, Germany). Excitations for FAM, Cy3, and Cy5 were at 490, 560, and 630 nm, respectively. Emission was measured within the following ranges: FAM, 493 to 552 nm; Cy3, 561 to 630 nm; and Cy5, 638 to 724 nm. Images were processed with Daime (25), using the area of the EUB signal as a mask to measure average fluorescence intensity for BA_SNP_Cy3 and BC_SNP_FAM. The EUB images were segmented and unspecific fluorescence excluded with default threshold settings, and this object layer was transferred to BA_SNP_Cy3 and BC_SNP_FAM images.

Isolation of nucleic acids. DNA isolation from inactivated cells was carried out using a MasterPure Gram-positive DNA purification kit (Lucigen, Middleton, WI, USA) according to the manufacturer's protocol. DNA samples were quantified using the Qubit dsDNA HS assay kit protocol (Thermo Scientific, Dreieich, Germany). For RNA isolation from inactivated cells, an RNeasy Protect bacterial minikit (Qiagen, Hilden, Germany) was used according to the supplier's protocol for enzymatic lysis and proteinase K digestion of bacteria. To eliminate residual DNA, RNA samples were purified twice using an RNeasy MinElute cleanup kit (Qiagen, Hilden, Germany) and quantified using the Qubit RNA HS assay kit protocol (Thermo Scientific, Dreieich, Germany). The absence of DNA in the final RNA preparation was verified by conducting PCR on marker *dhp61* (26) with negative results.

Tetraplex droplet dPCR assay for quantification of 16S rRNA gene alleles. Digital PCR (dPCR) allows for absolute quantification of DNA or RNA template concentrations (27). For 16S rRNA gene analysis, the 20-μl dPCR predroplet mix consisted of 10 μl dPCR supermix for probes (Bio-Rad Laboratories, Munich, Germany), 1 μl 20× 16S SNP primer mix (final concentrations, 900 nM), 0.6 μl of 20× mix of 16S SNP BC probe (final concentration, 150 nM), 0.6 μl of 20× mix of 16SSNP BA probe (final concentration, 150 nM), 0.9 μl of 20× PL3 primer-probe mix (final concentrations, probe, 225 nM; primers, 810 nM), 1.5 μl of GyrA 20× primer-probe mix (final concentrations, probe, 375 nM; primers, 1,350 nM), 4.4 μl of nuclease-free water (Qiagen, Hilden, Germany), and 1 μl of template DNA freshly diluted to a concentration of 0.05 ng/μl. To ensure independent segregation of the 16S rRNA gene copies from the bacterial chromosome and the reference genes into droplets, template DNA was digested (no cut sites within 16S rRNA genes) prior to dPCR by BsiWI-HF, BsrGI-HF, and HindIII-HF (New England Biolabs GmbH, Frankfurt am Main, Germany) in 1× Cutsmart buffer (New England Biolabs GmbH, Frankfurt am Main, Germany)

for 60 min, and then the enzymes were heat inactivated at 80°C for 20 min according to the manufacturer's protocol.

Partitioning of the reaction mixture into up to 20,000 individual droplets was achieved using a QX200 dPCR droplet generator (Bio-Rad Laboratories, Munich, Germany). A two-step PCR was performed on a Mastercycler Pro instrument (Eppendorf, Wesseling-Berzdorf, Germany) with the following settings: one DNA polymerase activation step at 95°C for 10 min was followed by 40 cycles of denaturation at 94°C for 30 s and annealing/extension at 58°C for 1 min. Final enzyme inactivation was performed at 98°C for 10 min before the samples were cooled down and held at 4°C. All steps were carried out with a temperature ramp rate of 2°C/s. After completion, droplets were analyzed using the QX100 droplet reader (Bio-Rad), and absolute concentrations for each target were quantified using Poisson statistics as implemented in the Quantasoft Pro Software (Bio-Rad Laboratories, Munich, Germany).

The absolute concentrations of *PL3* and *gyrA* were compared. To ensure assay integrity, samples with a deviation range greater than 10% within the two markers were excluded and had to be repeated. If deviation was below 10%, both targets were set as a reference with a copy number of one. The software then automatically takes the mean concentration of both references to calculate the copy numbers of BC and BA alleles. According to the recommendations provided previously (28), all samples with copy numbers between 0.35 and 0.65 deviations from an integer number or with a confidence interval greater than 1 were excluded from analysis and were repeated. All valid runs were rounded to the next integer number.

Duplex one-step reverse transcription dPCR to compare expression levels of 16S BC- and 16S-BA-allele. The 20 μl reverse transcription-dPCR reaction mixture consisted of 5 μl one-step RT-dPCR advanced supermix for probes (Bio-Rad, Laboratories, Munich, Germany), 2 μl of reverse transcriptase (final concentration, 20 U/μl; Bio-Rad), 0.6 μl of dithiothreitol (DTT) (final concentration, 10 nM; Bio-Rad Laboratories, Munich, Germany), 1.5 μl 20$\times$ 16S SNP primer mix (final concentration, 1,350 nM), 1.5 μl of 20$\times$ mix of 16S SNP BC probe (final concentration, 375 nM), 1.5 μl of 20$\times$ mix of 16S SNP BA probe (final concentration, 375 nM), 6.9 μl of nuclease-free water (Qiagen, Hilden, Germany), and 1 μl of template RNA. Reverse transcription was achieved within droplets prior to dPCR. Partitioning of the reaction mixture into up to 20,000 droplets was carried out using a QX200 dPCR droplet generator (Bio-Rad Laboratories), and PCR was performed on a Mastercycler Pro (Eppendorf, Wesseling-Berzdorf, Germany) with the following settings. The initial reverse transcription step was performed at 48°C for 60 min. An enzyme activation step at 95°C was carried out for 10 min, followed by 40 cycles of a two-step program of denaturation at 94°C for 30 s and annealing/extension at 58°C for 1 min. Final enzyme inactivation was performed at 98°C for 10 min before the samples were cooled down and held at 4°C. All steps were carried out with a temperature ramp rate of 2°C/s. After completion, droplets were analyzed using the QX100 droplet reader (Bio-Rad Laboratories, Munich, Germany), and results were quantified with the Quantasoft Pro Software (Bio-Rad Laboratories).

Library preparation, sequencing, and assembly of genomes. The libraries for the Illumina sequencing were prepared using the NEBNext Ultra II FS DNA library prep kit for Illumina (New England BioLabs GmbH, Frankfurt am Main, Germany) according to the protocol for large fragment sizes of >550 bp but with a minimal fragmentation time of only 30 s. Afterwards, libraries were pooled equimolarly and sequenced on an Illumina MiSeq device (Illumina Inc., San Diego, CA) using the MiSeq reagent kit v3 (2 $\times$ 300 bp).

The libraries for the nanopore sequencing were prepared using the ligation sequencing kit SQK-LSK109 (Oxford Nanopore Technologies, Oxford, UK) combined with the Native Barcoding Expansion EXP-NBD104 and sequenced as one pool on a MinION flowcell FLO-MIN106D (type R9.4.1; Oxford Nanopore Technologies, Oxford, UK) for 48 h. Basecalling and demultiplexing were done separately using Guppy v3.2.10 (Oxford Nanopore Technologies, Oxford, UK) with the high-accuracy basecalling model. Quality (≥10) and length (≥1,000 bp) filtering was done using Filtlong version 0.2.0 (https://github.com/rrwick/Filtlong).

Hybrid assemblies were constructed in two stages. First, nanopore reads were assembled using Flye version 2.7 (29) with default parameters and two iterations of polishing. Second, Illumina reads were assembled together with the nanopore raw reads and the nanopore assembly as trusted contigs using SPAdes version 3.14 (30) with parameters "-k 55,77,99,113,127 -careful." Afterwards, the assembled contigs were reverse complemented, if necessary, and rotated to the same start sequence as strain Ames Ancestor. Finally, the contigs were polished once more using Pilon version 1.23 (31).

Bioinformatics analyses. For the long-read assemblies, ribosomal operons were annotated using barrnap version 0.9 (https://github.com/tseemann/barrnap). SNP alleles were searched using USEARCH version 11 (32) and the 16S SNP BA/BC probe sequences (Table S2) as an oligonucleotide sequence database. To investigate the frequency and distribution of the alleles of 16S rRNA genes in the *B. anthracis* species comprehensively, we downloaded all available short-read Illumina data sets (at the end of 2020) from the NCBI Sequence Read Archive (33). These data sets were then assembled using SPAdes v1.14 (30) with parameters "-k 55,77,99,113,127 -careful." The contigs of the resulting assemblies were extended using tadpole from the BBTools package (34) and with parameters "el=1000 er=1000 mode=extend." Afterwards, blastn (35) with parameters "-evalue 1e-10 -word_size 9" was used to align the 23S rRNA sequence against each extended contig end. For each assembly, the number of contigs ending with a 23S rRNA fragment were counted, and CanSNPer (36) was used to determine the canonical SNPs and likely position in the CanSNP tree. In a next step, kmercountexact from the BBTools package was used with the parameters "fastadump=f mincount=2 *k*=16" to count all *k*-mers of size 16 from error-corrected reads. From these *k*-mers, the frequencies of the two allelic *k*-mers (sequences of 16 nucleotides used for the dPCR probes) were extracted. kmercountexact also reports a *k*-mer-based coverage

estimation of the sequenced reads, which is used to filter the assemblies by coverage (minimum of 20×), number of contigs (maximum of 200), number of potential rRNAs (>8), and success of CanSNPer prediction. For each remaining assembly, the number of rRNAs carrying the SNP of the 16S BA allele was estimated by determining the ratio of the allelic *k*-mers multiplied by the total number of rRNAs, rounded to a whole number. To validate this estimation, we applied the same algorithm to every assembly where both short and long reads and/or dPCR results were available and compared the estimated number of BA alleles to the counted number in the long-read assembly or to the measured number from the dPCR experiments. They were consistent across different sequencing coverages, total number of rRNA operons, and known BA allele frequencies.

Data availability. All genomic data generated or analyzed prior to or during this study can be accessed via the NCBI BioProject number PRJNA695105. Individual accession numbers are listed in Tables S3 and Data Set S1.

SUPPLEMENTAL MATERIAL

Supplemental material is available online only.

DATA SET S1, XLSX file, 0.2 MB.

FIG S1, TIF file, 0.2 MB.

FIG S2, TIF file, 0.1 MB.

TABLE S1, XLSX file, 0.01 MB.

TABLE S2, XLSX file, 0.01 MB.

TABLE S3, XLSX file, 0.01 MB.

ACKNOWLEDGMENTS

We thank Linda Dobrzykowski and Josua Zinner for technical assistance. For providing bacterial strains, we are grateful to Fabian Leendertz, Silke Klee, and Roland Grunow (RKI), Wolfgang Beyer (University of Hohenheim), and Paul Keim (Northern Arizona University). We also thank Olfert Landt and his team at TIB Molbiol (Berlin) for technical support in designing LNA-based probes.

This study was supported by funds from the German Federal Ministry of Defense (Sonderforschungsprojekt 36Z1-S-431618 and STAN 48-2009-23).

The research described here is part of the Medical Biological Defense Research Program of the Bundeswehr Joint Medical Service. Opinions, interpretations, conclusions, and recommendations are those of the authors and are not necessarily endorsed by any governmental agency, department, or other institutions.

P.B., F.Z., G.G., and K.S. designed the study and interpreted the results. M.W. contributed the bioinformatics analysis. I.S., F.Z., K.A., and S.M. performed FISH experiments. P.B. and I.S. performed digital PCR experiments. G.G., P.B., F.Z., and K.S. wrote the first draft manuscript, and all authors edited the manuscript. The authors dedicate this work to our dear late colleague Karin Aistleitner, who left us too soon and unexpectedly.

We declare no competing interests.

REFERENCES

1. Takahashi H, Keim P, Kaufmann AF, Keys C, Smith KL, Taniguchi K, Inouye S, Kurata T. 2004. *Bacillus anthracis* incident, Kameido, Tokyo, 1993. Emerg Infect Dis 10:117–120. https://doi.org/10.3201/eid1001.030238.
2. Turnbull PC (ed). 2008. Anthrax in humans and animals, 4th edition. WHO Press, Geneva, Switzerland.
3. Candelon B, Guilloux K, Ehrlich SD, Sorokin A. 2004. Two distinct types of rRNA operons in the *Bacillus cereus* group. Microbiology (Reading) 150:601–611. https://doi.org/10.1099/mic.0.26870-0.
4. Hakovirta JR, Prezioso S, Hodge D, Pillai SP, Weigel LM. 2016. Identification and analysis of informative single nucleotide polymorphisms in 16S rRNA gene sequences of the *Bacillus cereus* group. J Clin Microbiol 54:2749–2756. https://doi.org/10.1128/JCM.01267-16.
5. Weerasekara MLMAW, Ryuda N, Miyamoto H, Okumura T, Ueno D, Inoue K, Someya T. 2013. Double-color fluorescence in situ hybridization (FISH) for the detection of *Bacillus anthracis* spores in environmental samples with a novel permeabilization protocol. J Microbiol Methods 93:177–184. https://doi.org/10.1016/j.mimet.2013.03.007.
6. Quast C, Pruesse E, Yilmaz P, Gerken J, Schweer T, Yarza P, Peplies J, Glöckner FO. 2013. The SILVA ribosomal RNA gene database project: improved data processing and web-based tools. Nucleic Acids Res 41:D590–D596. https://doi.org/10.1093/nar/gks1219.
7. Koshkin AA, Singh SK, Nielsen P, Rajwanshi VK, Kumar R, Meldgaard M, Olsen CE, Wengel J. 1998. LNA (locked nucleic acids): synthesis of the adenine, cytosine, guanine, 5-methylcytosine, thymine and uracil bicyclonucleoside monomers, oligomerisation, and unprecedented nucleic acid recognition. Tetrahedron 54:3607–3630. https://doi.org/10.1016/S0040-4020(98)00094-5.
8. Ravel J, Jiang L, Stanley ST, Wilson MR, Decker RS, Read TD, Worsham P, Keim PS, Salzberg SL, Fraser-Liggett CM, Rasko DA. 2009. The complete genome sequence of *Bacillus anthracis* Ames "Ancestor." J Bacteriol 191:445–446. https://doi.org/10.1128/JB.01347-08.
9. Johnson SL, Daligault HE, Davenport KW, Jaissle J, Frey KG, Ladner JT, Broomall SM, Bishop-Lilly KA, Bruce DC, Gibbons HS, Coyne SR, Lo C-C, Meincke L, Munk AC, Koroleva GI, Rosenzweig CN, Palacios GF, Redden CL, Minogue TD, Chain PS. 2015. Complete genome sequences for 35 biothreat assay-relevant bacillus species. Genome Announc 3:e01501-15. https://doi.org/10.1128/genomeA.00151-15.
10. Rasko DA, Altherr MR, Han CS, Ravel J. 2005. Genomics of the *Bacillus cereus* group of organisms. FEMS Microbiol Rev 29:303–329. https://doi.org/10.1016/j.femsre.2004.12.005.

11. Ellerbrok H, Nattermann H, Ozel M, Beutin L, Appel B, Pauli G. 2002. Rapid and sensitive identification of pathogenic and apathogenic *Bacillus anthracis* by real-time PCR. FEMS Microbiol Lett 214:51–59. https://doi.org/10.1111/j.1574-6968.2002.tb11324.x.
12. Van Ert MN, Easterday WR, Huynh LY, Okinaka RT, Hugh-Jones ME, Ravel J, Zanecki SR, Pearson T, Simonson TS, U'Ren JM, Kachur SM, Leadem-Dougherty RR, Rhoton SD, Zinser G, Farlow J, Coker PR, Smith KL, Wang B, Kenefic LJ, Fraser-Liggett CM, Wagner DM, Keim P. 2007. Global genetic population structure of *Bacillus anthracis*. PLoS One 2:e461. https://doi.org/10.1371/journal.pone.0000461.
13. Cilia V, Lafay B, Christen R. 1996. Sequence heterogeneities among 16S ribosomal RNA sequences, and their effect on phylogenetic analyses at the species level. Mol Biol Evol 13:451–461. https://doi.org/10.1093/oxfordjournals.molbev.a025606.
14. Acinas SG, Marcelino LA, Klepac-Ceraj V, Polz MF. 2004. Divergence and redundancy of 16S rRNA sequences in genomes with multiple *rrn* operons. J Bacteriol 186:2629–2635. https://doi.org/10.1128/JB.186.9.2629-2635.2004.
15. Větrovský T, Baldrian P. 2013. The variability of the 16S rRNA gene in bacterial genomes and its consequences for bacterial community analyses. PLoS One 8:e57923. https://doi.org/10.1371/journal.pone.0057923.
16. Werner G, Bartel M, Wellinghausen N, Essig A, Klare I, Witte W, Poppert S. 2007. Detection of mutations conferring resistance to linezolid in *Enterococcus* spp. by fluorescence in situ hybridization. J Clin Microbiol 45:3421–3423. https://doi.org/10.1128/JCM.00179-07.
17. Kurylo CM, Parks MM, Juette MF, Zinshteyn B, Altman RB, Thibado JK, Vincent CT, Blanchard SC. 2018. Endogenous rRNA sequence variation can regulate stress response gene expression and phenotype. Cell Rep 25:236–248. https://doi.org/10.1016/j.celrep.2018.08.093.
18. Furuta Y, Harima H, Ito E, Maruyama F, Ohnishi N, Osaki K, Ogawa H, Squarre D, Hang'ombe BM, Higashi H. 2018. Loss of bacitracin resistance due to a large genomic deletion among *Bacillus anthracis* strains. mSystems 3:e00182-18. https://doi.org/10.1128/mSystems.00182-18.
19. Heydari M, Miclotte G, Demeester P, Van de Peer Y, Fostier J. 2017. Evaluation of the impact of Illumina error correction tools on de novo genome assembly. BMC Bioinformatics 18:374. https://doi.org/10.1186/s12859-017-1784-8.
20. Salzberg SL, Phillippy AM, Zimin A, Puiu D, Magoc T, Koren S, Treangen TJ, Schatz MC, Delcher AL, Roberts M, Marçais G, Pop M, Yorke JA. 2012. GAGE: a critical evaluation of genome assemblies and assembly algorithms. Genome Res 22:557–567. https://doi.org/10.1101/gr.131383.111.
21. Braun P, Grass G, Aceti A, Serrecchia L, Affuso A, Marino L, Grimaldi S, Pagano S, Hanczaruk M, Georgi E, Northoff B, Schöler A, Schloter M, Antwerpen M, Fasanella A. 2015. Microevolution of anthrax from a young ancestor (M.A.Y.A.) suggests a soil-borne life cycle of *Bacillus anthracis*. PLoS One 10:e0135346. https://doi.org/10.1371/journal.pone.0135346.
22. Stahl DA, Flesher B, Mansfield HR, Montgomery L. 1988. Use of phylogenetically based hybridization probes for studies of ruminal microbial ecology. Appl Environ Microbiol 54:1079–1084. https://doi.org/10.1128/aem.54.5.1079-1084.1988.
23. Manz W, Amann R, Ludwig W, Wagner M, Schleifer K-H. 1992. Phylogenetic oligodeoxynucleotide probes for the major subclasses of proteobacteria: problems and solutions. Syst Appl Microbiol 15:593–600. https://doi.org/10.1016/S0723-2020(11)80121-9.
24. Daims H, Stoecker K, Wagner M. 2005. Fluorescence in situ hybridization for the detection of prokaryotes, p 213–239. *In* Osborn AM, Smith CJ (ed), Advanced methods in molecular microbial ecology. Bio-Garland, Abingdon, United Kingdom.
25. Daims H, Lücker S, Wagner M. 2006. Daime, a novel image analysis program for microbial ecology and biofilm research. Environ Microbiol 8:200–213. https://doi.org/10.1111/j.1462-2920.2005.00880.x.
26. Antwerpen MH, Zimmermann P, Bewley K, Frangoulidis D, Meyer H. 2008. Real-time PCR system targeting a chromosomal marker specific for *Bacillus anthracis*. Mol Cell Probes 22:313–315. https://doi.org/10.1016/j.mcp.2008.06.001.
27. Kuypers J, Jerome KR. 2017. Applications of digital PCR for clinical microbiology. J Clin Microbiol 55:1621–1628. https://doi.org/10.1128/JCM.00211-17.
28. Bell AD, Usher CL, McCarroll SA. 2018. Analyzing copy number variation with droplet digital PCR. Methods Mol Biol 1768:143–160. https://doi.org/10.1007/978-1-4939-7778-9_9.
29. Kolmogorov M, Yuan J, Lin Y, Pevzner PA. 2019. Assembly of long, error-prone reads using repeat graphs. Nat Biotechnol 37:540–546. https://doi.org/10.1038/s41587-019-0072-8.
30. Bankevich A, Nurk S, Antipov D, Gurevich AA, Dvorkin M, Kulikov AS, Lesin VM, Nikolenko SI, Pham S, Prjibelski AD, Pyshkin AV, Sirotkin AV, Vyahhi N, Tesler G, Alekseyev MA, Pevzner PA. 2012. SPAdes: a new genome assembly algorithm and its applications to single-cell sequencing. J Comput Biol 19:455–477. https://doi.org/10.1089/cmb.2012.0021.
31. Walker BJ, Abeel T, Shea T, Priest M, Abouelliel A, Sakthikumar S, Cuomo CA, Zeng Q, Wortman J, Young SK, Earl AM. 2014. Pilon: an integrated tool for comprehensive microbial variant detection and genome assembly improvement. PLoS One 9:e112963. https://doi.org/10.1371/journal.pone.0112963.
32. Edgar RC. 2010. Search and clustering orders of magnitude faster than BLAST. Bioinformatics 26:2460–2461. https://doi.org/10.1093/bioinformatics/btq461.
33. Leinonen R, Sugawara H, Shumway M, International Nucleotide Sequence Database Collaboration. 2011. The sequence read archive. Nucleic Acids Res 39:D19–D21. https://doi.org/10.1093/nar/gkq1019.
34. Bushnell B, Rood J, Singer E. 2017. BBMerge–accurate paired shotgun read merging via overlap. PLoS One 12:e0185056. https://doi.org/10.1371/journal.pone.0185056.
35. Altschul SF, Madden TL, Schäffer AA, Zhang J, Zhang Z, Miller W, Lipman DJ. 1997. Gapped BLAST and PSI-BLAST: a new generation of protein database search programs. Nucleic Acids Res 25:3389–3402. https://doi.org/10.1093/nar/25.17.3389.
36. Lärkeryd A, Myrtennäs K, Karlsson E, Dwibedi CK, Forsman M, Larsson P, Johansson A, Sjödin A. 2014. CanSNPer: a hierarchical genotype classifier of clonal pathogens. Bioinformatics 30:1762–1764. https://doi.org/10.1093/bioinformatics/btu113.

4. Ultrasensitive detection of *Bacillus anthracis* by real-time PCR targeting a polymorphism in multi-copy 16S rRNA genes and their transcripts

International Journal of
Molecular Sciences

MDPI

Article

Ultrasensitive Detection of *Bacillus anthracis* by Real-Time PCR Targeting a Polymorphism in Multi-Copy 16S rRNA Genes and Their Transcripts

Peter Braun, Martin Duy-Thanh Nguyen, Mathias C. Walter and Gregor Grass *

Bundeswehr Institute of Microbiology (IMB), 80937 Munich, Germany; peter3braun@bundeswehr.org (P.B.); martin2nguyen@bundeswehr.org (M.D.-T.N.); mathias1walter@bundeswehr.org (M.C.W.)
* Correspondence: gregorgrass@bundeswehr.org; Tel.: +49-992692-3981

Abstract: The anthrax pathogen *Bacillus anthracis* poses a significant threat to human health. Identification of *B. anthracis* is challenging because of the bacterium's close genetic relationship to other *Bacillus cereus* group species. Thus, molecular detection is founded on species-specific PCR targeting single-copy genes. Here, we validated a previously recognized multi-copy target, a species-specific single nucleotide polymorphism (SNP) present in 2–5 copies in every *B. anthracis* genome analyzed. For this, a hydrolysis probe-based real-time PCR assay was developed and rigorously tested. The assay was specific as only *B. anthracis* DNA yielded positive results, was linear over 9 $\log_{10}$ units, and was sensitive with a limit of detection (LoD) of 2.9 copies/reaction. Though not exhibiting a lower LoD than established single-copy PCR targets (*dhp61* or *PL3*), the higher copy number of the *B. anthracis*–specific 16S rRNA gene alleles afforded $\leq$2 unit lower threshold (Ct) values. To push the detection limit even further, the assay was adapted for reverse transcription PCR on 16S rRNA transcripts. This RT-PCR assay was also linear over 9 $\log_{10}$ units and was sensitive with an LoD of 6.3 copies/reaction. In a dilution series of experiments, the 16S RT-PCR assay achieved a thousand-fold higher sensitivity than the DNA-targeting assays. For molecular diagnostics, we recommend a real-time RT-PCR assay variant in which both DNA and RNA serve as templates (thus, no requirement for DNase treatment). This can at least provide results equaling the DNA-based implementation if no RNA is present but is superior even at the lowest residual rRNA concentrations.

Keywords: anthrax; *Bacillus anthracis*; 16S rRNA; detection; identification; real-time PCR; RT-PCR

Citation: Braun, P.; Nguyen, M.D.-T.; Walter, M.C.; Grass, G. Ultrasensitive Detection of *Bacillus anthracis* by Real-Time PCR Targeting a Polymorphism in Multi-Copy 16S rRNA Genes and Their Transcripts. *Int. J. Mol. Sci.* **2021**, *22*, 12224. https://doi.org/10.3390/ijms222212224

Academic Editors: Amelia Casamassimi, Alfredo Ciccodicola and Monica Rienzo

Received: 14 October 2021
Accepted: 10 November 2021
Published: 12 November 2021

1. Introduction

Within the genus *Bacillus*, the notorious anthrax pathogen *Bacillus anthracis* poses the greatest risk for humans, mammal livestock, and wildlife [1]. Other *Bacillus* spp. such *as B. cereus* or *B. thuringiensis*, which are typical soil bacteria, may also have pathogenic traits related to food poisoning, infections in immunocompromised persons, or production of insecticides [2]. Yet, only obligatory pathogenic *B. anthracis* (and a few *B. anthracis*-like bacilli) features a unique suite of pathogenicity factors rendering the endospore-forming bacterium a first-rate biothreat agent. These factors are encoded on two plasmids called pXO1 and pXO2. Plasmid pXO1 encodes the anthrax toxin genes producing the lethal toxin (gene products of *pagA* and *lef*) and edema toxin (gene products of *pagA* and *cya*) [1]. These toxins damage host cells on various levels [3]. Plasmid pXO2 harbors the capsule genes endowing the pathogen with a poly-glutamyl capsule which helps evade host immune response [1,4]. Phylogenetically, *B. anthracis* belongs to the very closely related *Bacillus cereus sensu lato* group. Besides the better-known species *B. cereus sensu stricto*, *B. anthracis*, or *B. thuringiensis*, the group also comprises several other familiar species such as *B. weihenstephanensis*, *B. mycoides*, *B. cytotoxicus*, and a variety of lesser-characterized members [5].

In the past, the high degree of genetic relatedness to several *B. cereus s.l.* strains has rendered molecular diagnostics of *B. anthracis* challenging (e.g., by polymerase chain reaction assays, PCR). One would think it should be straightforward to identify *B. anthracis* by detecting genetic marker genes (typically *pagA*, *lef*, *cya*, *capB*, or *capC*) [6–8] on one or both of its virulence plasmids. Identifying these genes comprising constituents of toxin or capsule biosynthesis (*cap*-genes), however, only verifies the presence of these plasmids. This is relevant because several *B. cereus s.l.* isolates are documented to possess very similar virulence plasmids, but not necessarily all of these belong to the species *B. anthracis*. Further, there are *B. anthracis* strains that lack one or both virulence plasmids. Species-specific molecular identification of *B. anthracis* is achieved by targeting a small number of validated chromosomal targets. These targets comprise sections of genes such as *dhp61* (*BA_5345*; [9]), *PL3* (*BA_5358*; [6]), or mutations characterized as single nucleotide polymorphisms (SNPs), e.g., in the *rpoB* [7] or the *plcR* [10] gene. A comprehensive overview of suitable and less ideal specific markers for *B. anthracis* has been provided previously [11]. Notwithstanding, the advantage of assaying for pXO1 or pXO2 markers over chromosomal ones is that the plasmid markers occur as multi-copy genes (since the virulence plasmids are present in more than one copy per cell) [12]. Large-scale genomic sequencing revealed that in *B. anthracis* plasmids, pXO1 and pXO2 (with their respective PCR-marker genes) are present on average in 3.86 and 2.29 copies, respectively [13]. Conversely, no multi-copy chromosomal marker has been employed for *B. anthracis* detection thus far.

Likewise, ribosomal RNA (particularly 16S rRNA) has not yet been routinely used for identification and detection of *B. anthracis* even though rRNA molecules are generally the most abundant ribonucleic acid entities in cells constituting up to approximately 80% of total RNA [14]. In fact, copies of 16S rRNA transcripts per cell as constituents of ribosomes number in many thousands (e.g., in *E. coli*, the number of ribosomes per cell ranges from 8×10^3 at a doubling time of 100 min to 7.3×10^4 at a doubling time of 20 min) [15]. Even in stationary culture, a single *E. coli* bacterium contains about 6.5×10^3 copies of ribosomes [16]. Phylogenetically closer to *B. anthracis* than *E. coli* is *Bacillus licheniformis*. For this bacillus, the average number of ribosomes per cell was calculated at 1.25×10^4, 3.44×10^4, or 9.2×10^4 in cultures growing at 37 °C with doubling times of 120, 60, and 35 min, respectively [17]. While these numbers are well in agreement, somewhat lower numbers of 9×10^3 ribosomes have been determined for exponentially growing cells of *Bacillus subtilis* [18]. While unexplored for *B. anthracis*, bacterial detection using rRNA genes and transcripts has been successfully harnessed to challenge previous limits of detection (LoD) for other pathogens [19–21].

In this study, we introduce a species-specific multi-copy chromosomal PCR marker of *B. anthracis*. This marker is represented by a unique SNP within a variable number of loci of the multi-copy 16S rRNA gene in this organism. Though the 16S rRNA gene sequences feature a very high degree of identity among the *B. cereus s.l.* group species [22], this SNP has previously been identified as unique and present in all publicly available *B. anthracis* genomic data [23–25]. Since all 16S rRNA gene copies harboring the SNP have 100% sequence identity, this specific sequence variation represents a distinct 16S rRNA gene allele named 16S-BA-allele. For simplification, all other 16S rRNA gene alleles lacking the sequence variation were named 16S-BC-allele. The relative abundance of these 16S-BA- and -BC-alleles were recently quantified in 959 *B. anthracis* isolates [25]. Here, we also harnessed this SNP to develop a *B. anthracis* specific reverse transcription (RT) real-time PCR assay. This approach brings the multi-copy marker concept for *B. anthracis* up to a new level owing to the excess numbers of ribosomes (and thus 16S rRNA moieties) in relation to chromosomes within a *B. anthracis* cell.

2. Results

2.1. Set-Up and Optimization of a New 16S rRNA Gene Allele-Specific PCR Assay

The "16S SNP BA probe" for hybridization to the *B. anthracis* specific sequence variation in 16S-BA-alleles in the *B. anthracis* genome was designed so that the SNP position was

located centrally. In order to increase the fidelity of this probe, six locked nucleic acid (LNA) bases were introduced (Table 1). Similarly, five LNA positions were added to the alternative "16S SNP BC probe", recognizing the non-*B. anthracis* specific 16S-BC-alleles of *B. anthracis* (Table 1). The 16S SNP BA probe was verified in silico against the NCBI database to be highly specific for *B. anthracis*, i.e., all *B. anthracis* genomes showed a 100% match, and only genomes of a few other bacterial isolates exhibited identical sequences. Among these was, e.g., a small number of *Sphingomonas* spp. Others, such as a few genomes annotated as *Staphylococus aureus*, had the same one-base-pair mismatch at the SNP-position (relative to *B. anthracis*) and were thus identical to other *B. cereus s.l.* genomes, hybridizing perfectly against the alternative "16S SNP BC probe" (Figure S1).

Table 1. Primers and probes.

Oligonucleotide	Sequence (5′-3′)
16S SNP F *	CGAGCGCAACCCTTGA
16S SNP R *	CAGTCACCTTAGAGTGCCC
16S SNP BA probe	6FAM-CTT+AGTT+A+C+C+AT+CATT–BHQ1
16S SNP BC probe	HEX-CTT+AGTT+G+C+C+ATCATT–BHQ1
Dark 16S SNP BC probe	CTT+AGTT+G+C+C+ATCATT-C3-spacer **

Locked nucleic acids are designated by prepositioned (+); 6FAM—6-Fluorescein phosphoramidite; HEX—Hexachloro-fluorescein; BHQ1—Black Hole Quencher-1. * The expected amplicon length of the PCR reaction is 57 bp. ** blocked with a C3-spacer in 3′-position. Hairpin Tm: Primer 16S SNP R: 37.7, else: none; self-dimer Tm: Primer 16S SNP F: 11.5, else: none.

Initially, the 16S SNP BC probe, which deviates only by the one central SNP base from the 16S SNP BA probe, also carried a fluorescent dye/quencher pair. However, since this probe was found to be not entirely specific for recognizing 16S rRNA fragments of *B. cereus s.l.* members, we decided to additionally design this SNP-competing probe as a fluorescently "dark" probe in order to reduce costs of synthesis (Table 1). Thus, the 16S rRNA SNP-PCR may be considered a pseudo-duplex assay (see below for details). All PCR runs were performed with both probes, typically with the 6FAM-labeled 16S SNP BA probe and the dark 16S SNP BC probe.

In silico analysis against the NCBI nt database confirmed that the PCR amplification primers 16S SNP F and 16S SNP R (Table 1) were not species-specific for *B. anthracis*. Indeed, besides DNA from other members of the *B. cereus s.l.* group, these primers would also amplify genome sequences of various other bacteria, such as *Paenibacillus* spp., or the reverse primer would bind to sequences of *Alkalihalobacillus clausii* or *Bacillus licheniformis*, among others. This ambiguity is not surprising for primers hybridizing against 16S rRNA gene sequences. Conversely, the pivotal factor for the detection assay introduced here is that only the 16S SNP BA probe hybridizes without any mismatch against 16S-BA-allele in *B. anthracis* (Figure S1). Thus, the specificity of the PCR assay is uniquely and entirely governed by the LNA-enhanced 16S SNP BA probe.

The 16S rRNA SNP-PCR was robust for deviations from the optimum annealing temperature (62 °C; Table S1). Additionally, primer (Table S2), probe (Table S3), and $MgCl_2$ (Table S4) concentrations and pipetting errors (Table S5) were tolerated quite well. Intra- and inter-assay (Tables S6 and S7) variability was determined with positive, weakly positive, and negative template DNA. The average PCR variations were at 0.0–1.1% (intra-assay) and 1.1–1.2% (inter-assay), respectively (Tables S6 and S7), indicating high precision of the PCR. Melt point analysis of the 16S-BA-allele PCR product vs. the 16S-BC-allele PCR product (Figure S2) indicated specific amplification of each allele fragment.

2.2. Competitive Amplification-Inhibition of the 16S-BA-Allele Fragment-PCR by Excess of the Alternative 16S-BC-Allele

Though the new 16S rRNA SNP-PCR assay was tested very robust and precise, we wondered to which degree the assay would be inhibited by large excesses of the alternative 16S-BC-allele fragment featuring a single mismatch at the SNP located centrally

in the hybridizing 16S-BA-allele-specific PCR probe (Figure S1). For testing this, we first evaluated which probe ratio (16S rRNA SNP BA vs. BC probe) would yield the lowest residual fluorescence values (in the 6FAM-channel of the 16S-BA-allele-specific probe) when providing only 16S-BC-allele containing DNA as PCR template. In these tests, the concentration of the 16S-BA-allele-specific probe was kept constant at 0.25 µM. The resulting 6FAM-fluorescence values were very low compared to regular amplification (Table S8), signals were weakly linearly increasing, and no Ct values were detected. The lowest fluorescence, barely above the negative control level, was recorded at a ratio of 0.25/0.75 µM (16S rRNA SNP-BA probe/-BC probe). Thus, this ratio was used for all following tests.

Next, a constant 100 template copies of the 16S-BA-allele fragment per reaction were titrated against increasing copy numbers of the alternative 16S-BC–allele fragment. Figure S3 and Table S9 show that an excess of 16S-BC-allele to BA-allele fragments of 10^6, 10^5, 10^4, or 10^3 to 1 (Table S9; assay #1–4) inhibits detection of the 16S-BA-allele fragment. This is because there was neither any *bona fide* sigmoidal PCR amplification nor were there any fluorescence signals with values meaningfully above the 16S-BC-allele-only controls (assays #11 and #12). Starting with 7.5×10^4 copies of competing 16S-BC-alleles (vs. 100 16S-BA-allele copies, i.e., 750 to 1; assay #5), both a regular Ct value was provided, and fluorescence started to markedly increase above the base level. At a ratio of 500 to 1 (16S-BC- to BA-alleles), *B. anthracis* detection became possible (assays #6 vs. #12; #7). Latest at a surplus of equal or less than 100 to 1 (assay #8), detection of 16S-BA-allele among BC-alleles was robustly possible. Thus, at the very least, a single copy of 16S-BA-allele can be detected in the presence of 100 BC-alleles.

2.3. Sensitivity and Specificity of the 16S rRNA SNP-PCR Assay

Similar to earlier work [26], we sought to harness the specificity of SNP-interrogation without assaying the alternative SNP state (i.e., the 16S-BC-allele here). Because detecting the 16S-BC-allele was not of interest for the assay at hand, the respective labeled 16S SNP BC probe was replaced by an unlabeled, fluorescently "dark" probe (i.e., a BA allele SNP-competitor probe; Table 1). In effect, primers would still amplify both alleles; however, the fluorescent probe for the 16S-BA-allele would be outcompeted by the dark probe on 16S-BC-allele targets, and the fluorescent 16S rRNA BA SNP probe would only generate signals in the presence of cognate 16S-BA-allele sequences. Thus, this approach using a dark competing probe would diminish the inadvertent generation of unspecific fluorescence generated by mishybridization of 16S rRNA BA SNP probes to 16S-BC-allele sequences.

To formally validate the sensitivity of the 16S rRNA SNP-PCR assay, a panel of 14 different *B. anthracis* DNAs was employed. These *B. anthracis* strains represent all major branches A, B, and C [27], including prominent sub-branches [28] of the global *B. anthracis* phylogeny (Table S10). All DNAs produced positive PCR results. Similarly, we tested a "specificity panel" of potentially cross-reacting organisms (Table S11). This panel included 13 DNAs of non-*anthracis B. cereus s.l.* strains. Additionally included were DNAs of common animal host organisms such as cattle, goat, sheep, and human. Neither of these DNAs yielded any positive PCR results. Finally, DNAs of organisms relevant for differential diagnostics and other prominent microbial pathogens were also assayed by the new *B. anthracis* specific 16S rRNA SNP-PCR (Table S12). Again, none of these DNAs resulted in false-positive PCR results. Of note, *Sphingomonas zeae* JM-791 [29] harboring 16S rRNA genes 100% identical in the region of the 16S SNP BA probe but different in the primer binding sites yielded negative PCR results. These results clearly indicated that the new PCR is both sensitive and specific for *B. anthracis*.

2.4. Linear Dynamic Range, Efficiency, and Limit of Detection of the B. anthracis Specific 16S rRNA SNP-PCR Assay

The linear dynamic range of the new PCR was determined based on measurements of serial DNA dilutions using recombinant 16S-BA-allele fragments or genomic DNA of *B. anthracis* Ames, respectively, as templates (Figure 1). Linearity was observed over a

range from 10^1 to 10^9 copies per reaction for cloned template DNA (Figure 1A; Table S13). In nine out of nine PCR replicates, positive signals were obtained down to 10^1 copies per reaction. At 10^0, two out of nine reactions were negative, thus defining the lower limit of the linear dynamic range. The coefficient of determination (R^2) was calculated as >0.999. From the slope of the linear regression, the efficacy of the PCR was derived as 2.0 (which is 100.1% of the theoretical optimum). Thus, the 16S rRNA SNP-PCR assay performed very well over a wide 9 $\log_{10}$ concentration range of template DNA.

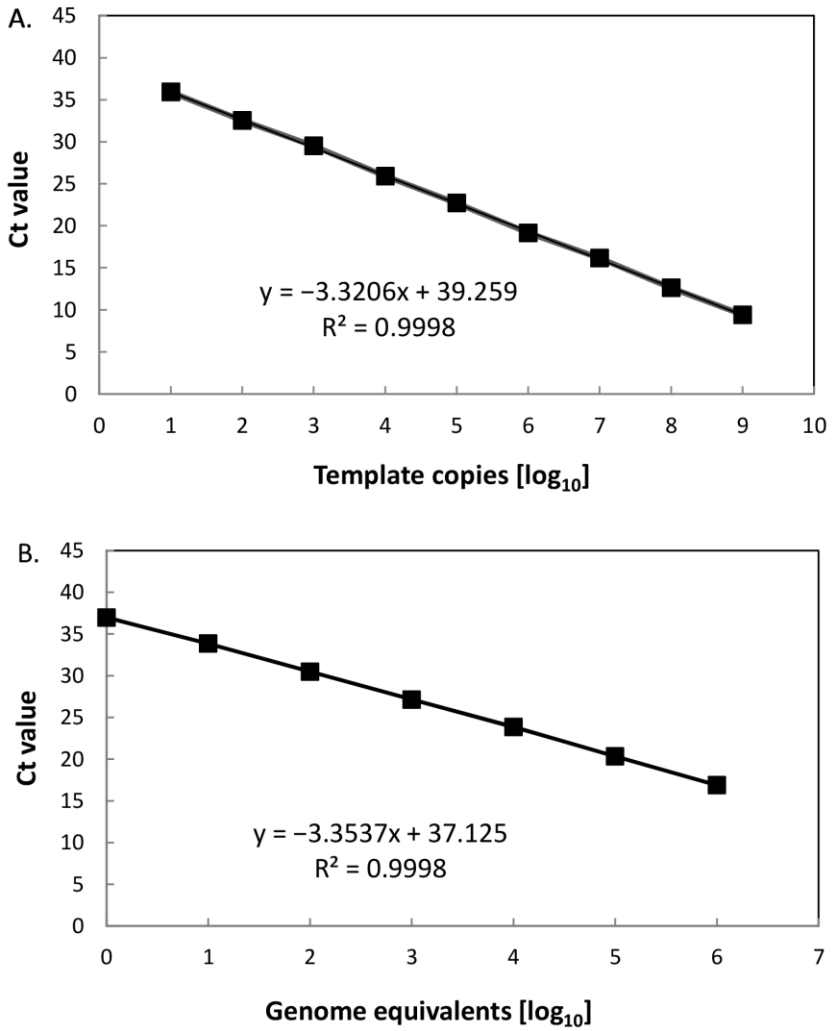

Figure 1. Linearity of the 16S rRNA SNP-PCR. Serial dilutions of DNA of (**A**) a fragment comprising the 16S-BA-allele or (**B**) *B. anthracis* strain Ames were serially diluted 1:10, PCR-tested, and template copies (**A**) or genome equivalents (**B**) plotted against Ct values. Indicated in the graphs are the slopes of the linear regressions and the coefficients of determination (R^2). Individual data points represent average values from $n = 3 \times 3$ PCR-tests.

The *B. anthracis* Ames genome harbors four copies of the 16S-BA-allele and seven copies of the BC-allele. Linear range parameters were very similar to that of cloned 16S-BA-allele DNA fragment (Figure 1B; Table S13). Because of the upper concentration limit of our *B. anthracis* Ames DNA preparations, the highest value in the linear range was 10^6 genome copies. Thus, here the linear range covered target concentrations from 10^0 to 10^6 copies per reaction. R^2 was determined as >0.999 and the efficacy of the PCR as 1.99 (which is 98.7% of the theoretical optimum). This indicated that the 16S rRNA SNP PCR assay yielded very similar results in these experiments, whether recombinant target DNA or authentic *B. anthracis* DNA was used as templates. Note, though, a single *B. anthracis* Ames genome carries four copies of the 16S-BA-allele. This explains why all PCRs yielded positive signals with DNA template at 10^0 copies (genome equivalents), whereas PCRs using single copy recombinant template did not.

Next, we determined the LoD for the 16S rRNA SNP-PCR assay by probit analysis (Figure 2; numerical data in Table S14). The assay had a limit of detection of 2.9 copies per reaction. This calculates to about 0.6 copies/µL with a probability of success of 95% with a confidence interval of 2.4–4.5 copies/assay.

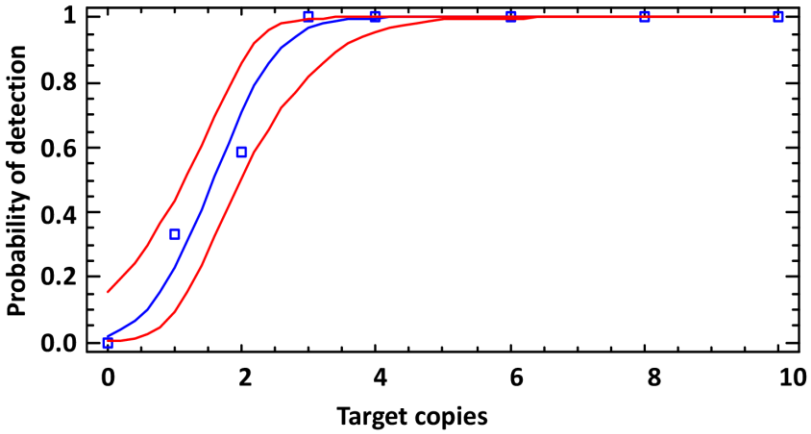

Figure 2. Limit of detection (LoD) of the 16S rRNA SNP-PCR (analytical sensitivity). DNA fragments comprising the 16S-BA-allele were diluted to the indicated copies per reaction (numerical data in Table S14) and subjected to real-time PCR (12 replicates for each data point). Probit analysis (plot of fitted model) was performed to determine the LoD by fitting template copies against the cumulative fractions of positive PCR observations (blue squares and line) and used for calculating the lower and upper 95% confidence limits (red lines).

2.5. Comparison of the New 16S rRNA SNP-PCR Assay with Existing PCR Assays

In order to further assess the performance of the 16S rRNA SNP-PCR assay, we compared it with other established PCR assays for *B. anthracis* identification currently used in our laboratory. These assays target the single-copy genes *dhp61* [9] or *PL3* [6] that have been individually validated before and compared to other commonly used *B. anthracis* PCRs [11]. Using $\log_{10}$ dilutions of *B. anthracis* Ames DNA, the 16S rRNA SNP-PCR exhibited markedly, at least three units, lower Ct values (27.9 ± 0.4; 31.7 ± 0.1; 35.4 ± 0.7) than *dhp61* (32.1 ± 0.0; 35.4 ± 0.6; 38.9 ± 1.5) or *PL3* (31.8 ± 0.2; 36.1 ± 0.7; >40) at 1000, 100, or 10 genome equivalents, respectively (Figure 3). *B. cereus* DNA did not result in amplification by any PCR assay. This result strongly suggested that the multi-copy 16S rRNA SNP-PCR assay performs competitively when compared back-to-back with established PCR assays for the detection of *B. anthracis*.

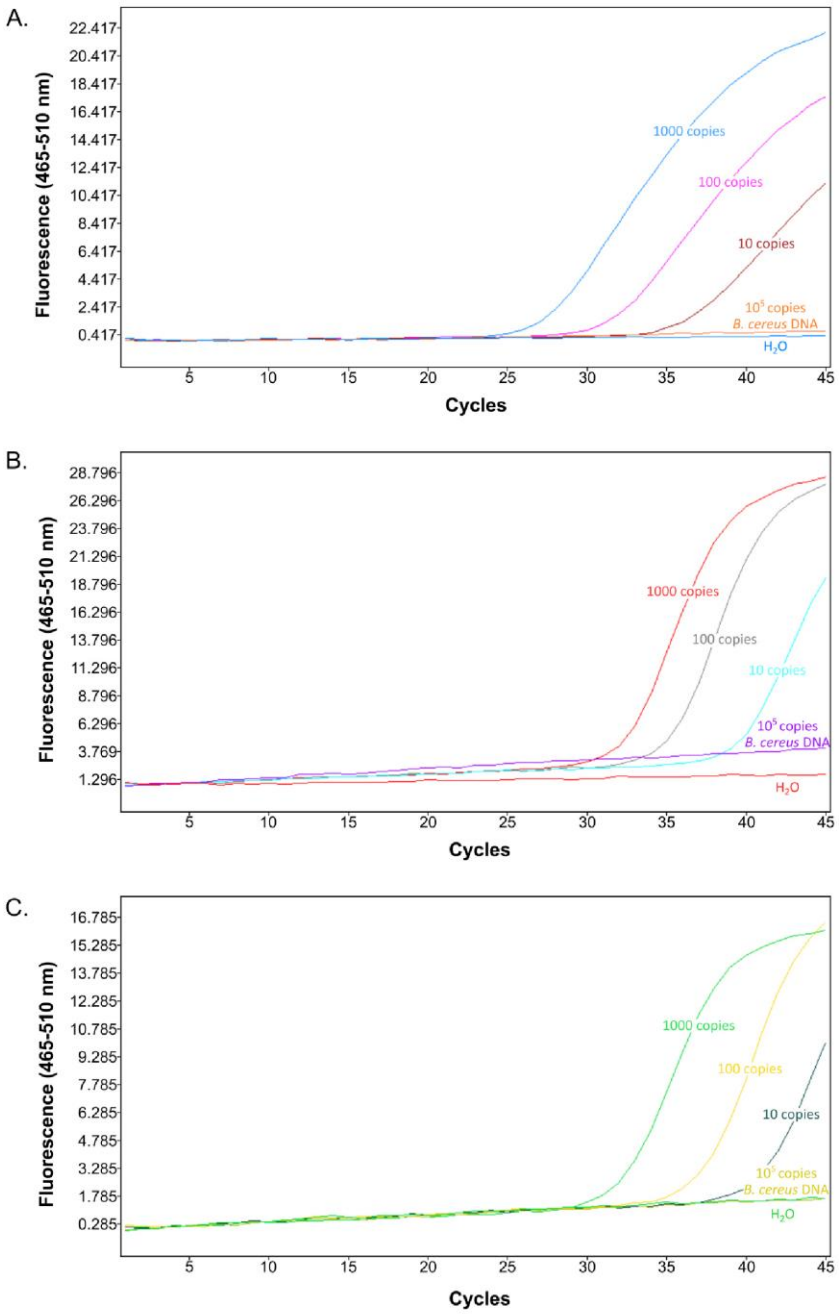

Figure 3. Comparison of the new 16S rRNA SNP-PCR assay with existing PCR assays. Different quantities of *B. anthracis* Ames template DNA (1000, 100, or 10 genome equivalents per reaction), non-target DNA (10^5 templates of *B. cereus* DNA), or water (negative) control were subjected to real-time PCR using the new 16S rRNA SNP assay (**A**), published *dhp61* gene assay [9] (**B**) or published *PL3* gene assay [6] (**C**). Representative amplification curves (from $n = 3$ with similar results) are shown.

2.6. Challenge of the New 16S rRNA SNP-PCR Assay with Samples from a Ring Trial

Along this line of reasoning, we next challenged the 16S rRNA SNP-PCR assay with samples from a previous ring trial for *B. anthracis* nucleic acid detection [30]. Again, the test was performed in comparison with the established PCR assays for *B. anthracis* identification, *dhp61* [9], and *PL3* [6]. Each of the assays was able to correctly identify the two positives out of four samples (Figure S4). Similar to evaluating known concentrations (Figure 3), the 16S rRNA SNP-PCR assay performed the best. It yielded the lowest Ct values (Figure S4), about two units lower than that of *dhp61* or *PL3* PCR. The 16S rRNA SNP-PCR assay may thus be ideally suited for this kind of analysis in which low target DNA quantities can be expected.

2.7. Challenge of the New 16S rRNA SNP-PCR Assay with Total DNA from Spiked Soil Samples

Since the 16S rRNA SNP-PCR assay performed well thus far, even in the presence of *E. coli* and human (Figure S4) or competing *B. cereus* (Figure S3) DNA, we evaluated to what extent the assay would be able to detect target DNA in spiked soil samples. These samples were spiked with cells of *E. coli* and *F. tularensis* and cells or endospores of *B. anthracis* and/or *B. thuringiensis* and were subjected to DNA purification. As above, the 16S rRNA SNP-PCR assay was conducted in comparison with the established PCR assays for *B. anthracis* identification *dhp61* [9] and *PL3* [6]. Figure S5 shows the PCR amplification curves. Samples #1, #2, and #4 were samples spiked with *B. anthracis*; sample #3 only contained *E. coli* and *B. thuringiensis*. Sample #4 had a large excess of *B. thuringiensis* over *B. anthracis* (a factor of 10^4). The 16S rRNA SNP-PCR assay detected *B. anthracis* in samples #1 and #2 but not in #4. Conversely, *dhp61* or *PL3* assays detected all three positive samples. The failure to detect *B. anthracis* by the 16S rRNA SNP-PCR assay in sample #4 is in line with our initial tests using massive excess of *B. cereus* DNA competing with *B. anthracis* detection (Figure S3; Table S9). Notably, the 16S rRNA SNP-PCR exhibited markedly, about three units, lower Ct values (23.6 ± 0.7 or 16.4 ± 0.0) than *dhp61* (26.2 ± 0.1 or 19.9 ± 0.1) or *PL3* (25.7 ± 0.0 or 19.5 ± 0.1) for samples #1 and #2, respectively. This result confirmed our preceding findings that the 16S rRNA SNP-PCR assay can reach a lower detection limit than the established assay as long as there is no large excess of other *B. cereus s.l.* DNA competing for amplification primers.

2.8. The New 16S rRNA SNP-PCR Assay also Functions as an RT-PCR Assay

We reasoned that the real-time 16S rRNA SNP-PCR assay targeting *B. anthracis* DNA might be converted into an RT-PCR assay targeting RNA in the form of 16S-BA-allele transcripts that harbor the *B. anthracis*-specific SNP. In order to test this, cells of *B. anthracis* Sterne or *B. cereus* 10987 were grown to exponential growth phase, inactivated, and total nucleic acids (including genomic DNA) were isolated alongside parallel preparations of DNA only. The one-step RT-PCR reaction was thus run with a mixture of genomic DNA and RNA, which can both be targeted by the assay. For comparison, the above-validated 16S rRNA real-time SNP-PCR was conducted in parallel with genomic DNA as the only template (no RT-reaction). When using identical samples, RT-PCR reactions (with templates consisting of total RNA and DNA) resulted in intensely lower Ct values than without reverse transcription (since only genomic DNA served as a template; Figure 4). Notably, differences in Ct values (RT-PCR vs. PCR) were in the range between 9 and 10 units. This translates to an about 1000-fold improvement using RT-PCR over DNA-only PCR. This result indicated that the 16S rRNA SNP-PCR assay functions both for DNA- and RNA-based (RT) PCR.

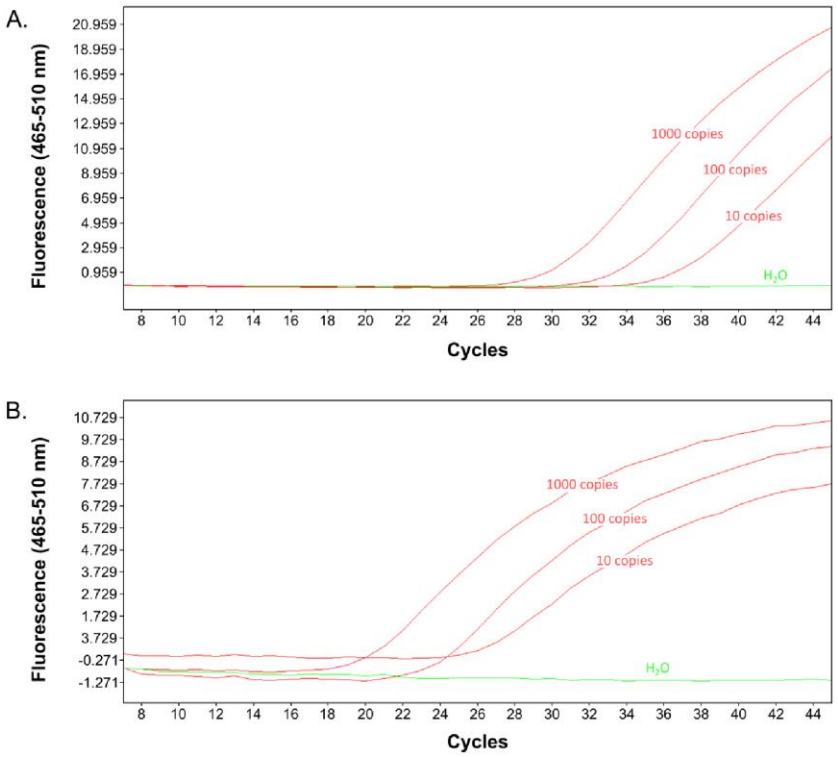

Figure 4. Comparison of the 16S rRNA SNP-PCR assay (DNA-only) with the RT-16S rRNA SNP-PCR assay (DNA+RNA). Total DNA or total DNA+RNA isolated from exponentially growing cells of *B. anthracis* or *B. cereus*, respectively, were used for PCR amplification of 16S-BA-allele DNA (**A**) or additionally after reverse transcription of 16S rRNA (ribosomal RNA) (**B**). Representative amplification curves (from $n = 3$ with similar results) are shown.

2.9. Linear Dynamic Range, Efficiency, and Limit of Detection of the B. anthracis 16S rRNA SNP RT-PCR Assay

To further characterize the RT-PCR, we determined the linear dynamic range and determined the LoD (Probit) of the 16S rRNA SNP RT-PCR using total RNA/DNA of *B. anthracis* Sterne (similar to DNA-only templates, see above). The RT-PCR was linear over a range from 10^0 to 10^8 template rRNA+DNA per reaction (Figure 5A; Table S15). The coefficient of determination (R^2) was 0.9982, and the efficacy of the RT-PCR was 1.92 (which is 92.3% of the theoretical optimum). Thus, the 16S rRNA SNP RT-PCR assay performed well over a wide 9 $\log_{10}$ concentration range of template RNA+DNA (higher template numbers than 1.5×10^8 were not tested).

The LoD for the 16S rRNA SNP RT-PCR assay as determined by probit analysis (Figure 5B; numerical data in Table S16) was 6.3 copies per reaction. This calculates to about 1.3 copies/µL with a probability of success of 95% with a confidence interval of 5.0–8.9 copies/assay. Thus, the RT-PCR reaction performed similarly well as the PCR reaction. Mindful of the about 3 $\log_{10}$ units higher number of 16S rRNAs in cells than genomes, detection of *B. anthracis* with the rRNA-directed RT-PCR is superior to the respective real-time PCR assay and all other *B. anthracis* PCR assays tested.

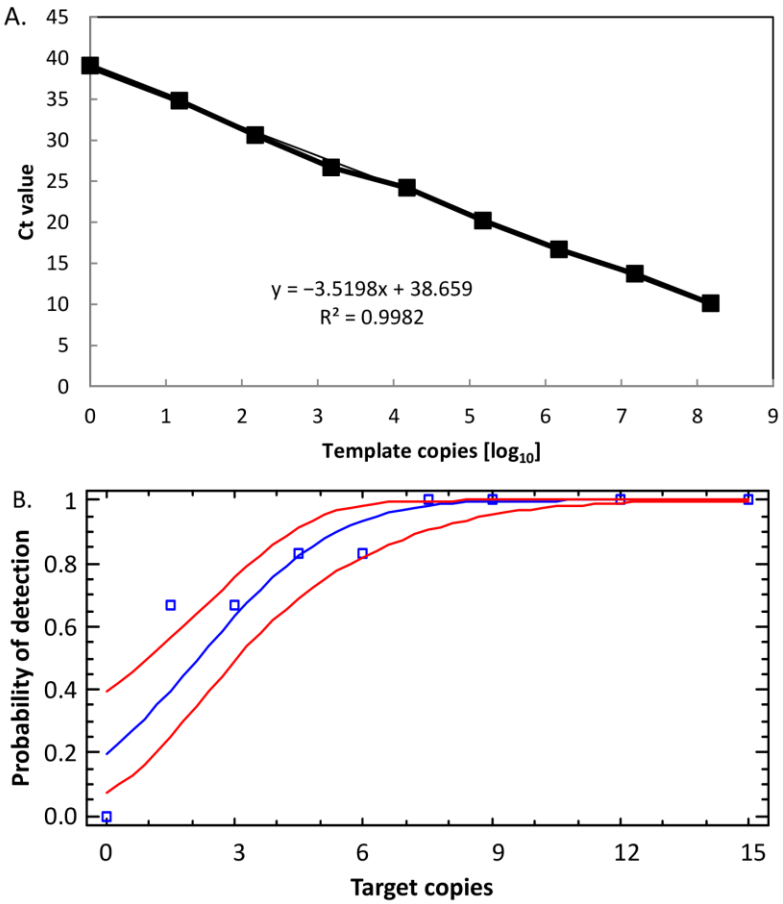

Figure 5. Linearity and LoD of the 16S rRNA SNP RT-PCR. Serial dilutions of RNA (with DNA) of *B. anthracis* strain Sterne were serially diluted 1:10, RT-PCR-tested and template copies plotted against Ct values (**A**). Indicated in the graph is the slope of the linear regression and the coefficients of determination (R^2). Individual data points represent average values from $n = 3 \times 3$ PCR-tests. Analytical sensitivity of the 16S rRNA SNP RT-PCR was determined by diluting samples from (**A**) to the indicated copies per reaction (numerical data in Table S16) and subjected to RT-PCR (12 replicates for each data point). To determine the LoD, probit analysis (plot of fitted model, blue squares, and line) was performed (as in Figure 2), and the lower and upper 95% confidence limits (red lines) were determined (**B**).

3. Materials and Methods

3.1. Bacterial Culture, Inactivation, and DNA Samples for Quality Assessment

B. anthracis strains and other Bacilli were cultivated at 37 °C on tryptic soy agar plates (TSA, Merck KGaA, Darmstadt, Germany). Bacteria comprising the negative panel (Table S1) were grown on appropriate agar media (with 10% CO_2 atmosphere where required) at 37 °C until colonies emerged. Risk group 3 (RG-3) *B. anthracis* strains were cultivated in the biosafety level 3 (BSL-3) facilities at the Bundeswehr Institute of Microbiology (IMB) and then chemically inactivated by resuspending a loop of colony material in aqueous peracetic acid solution (4% (*v/v*) Terralin PAA, Schülke & Mayr GmbH, Norderstedt, Germany) before further use [31]. RG-2 strains of endospore formers were inactivated

likewise. All other bacterial cultures were inactivated by 70% (*v*/*v*) ethanol. Ring trial *B. anthracis* DNA samples published in [30] were obtained from Instant (Düsseldorf, Germany).

3.2. Isolation of DNA, RNA, and Nucleic Acid Quantification

Bacterial DNA and RNA were isolated using MasterPure™ Gram Positive DNA Purification kit (Lucigen, Middleton, WI, USA). For RNA (+DNA) isolation, RNase treatment was omitted. DNA and RNA concentrations were quantified using the Qubit dsDNA HS Assay or RNA HS Assay kits (ThermoFisher Scientific, Darmstadt, Germany) according to the manufacturer's protocols. DNA and RNA (+DNA) preparations were stored at −20 °C and −80 °C, respectively, until further use.

3.3. Design and in Silico Bioinformatic Analysis of Primer and Probe DNA Sequences

All relevant DNA sequence data for oligonucleotide design were retrieved from public databases (NCBI). Primer and probe DNA oligonucleotides [25] were designed with Geneious Prime (version 2021.1.1; Biomatters, Auckland, New Zealand). In silico specificity analysis was performed by probing each primer and probing nucleotide sequences against the NCBI nt databases using BLASTN for short input sequences (Primer BLAST) [32]. The two amplification oligonucleotide primers target a consensus region within the 16S rRNA genes on the chromosome of *B. cereus s.l.* species (Table 1), including *B. anthracis*. The two oligonucleotide probes (Table 1) feature the centrally located discriminatory SNP (pos. 1110 in *B. anthracis* strain Ames Ancestor, NC_007530) [23,24]. These probes thus either match the allele unique for *B. anthracis* (named 16S-BA-allele; with an adenine, A at the SNP position) or the general 16S-BC-allele (guanine, G at the SNP position), respectively (the two alleles are depicted in Figure S1). Due to placement and length restrictions related to another non-discriminatory SNP (pos. 1119), each probe was amended with locked nucleic acids (LNA). LNA are modified nucleic acids in which the sugar is conformationally locked. This rigidity causes exceptional hybridization affinity through stable duplexes with DNA and RNA [33], eventually improving mismatch discrimination in SNP genotyping studies. Similar to unmodified ssDNA probes, the LNA-containing probes (Table 1) are susceptible to 5′-nuclease attack during PCR. LNA probes as well as primers were purchased from TIB MolBiol (Berlin, Germany).

3.4. Real-Time and Reverse Transcription PCR Conditions

All (pseudo) duplex real-time PCR amplifications were performed in reaction mixtures of a final volume of 20 µL containing 2 µL LightCycler® FastStart DNA Master HybProbe mix (Roche Diagnostics, Mannheim, Germany), 5 mM $MgCl_2$, 0.5 µM of each primer, 0.25 µM of 16S SNP BA probe, 0.75 µM of (dark) 16S SNP BC probe, and various quantities of template DNA template. All reactions were performed on a LightCycler 480 real-time PCR system fitted with color compensation (Roche Diagnostics, Mannheim, Germany). The optimized amplification conditions were 95 °C for 10 min, and then 45 consecutive cycles of first 15 s at 95 °C and then 20 s at 62 °C, followed by 20 s at 72 °C.

Reverse transcription PCR reaction mixtures contained 7.4 µL LightCycler® 480 RNA Master Hydrolysis Probes mix, 1.3 µL Activator, 1 µL Enhancer (Roche Diagnostics, Mannheim, Germany), 0.5 µM of each primer, 0.25 µM of 16S SNP BA probe, 0.75 µM of (Dark) 16S SNP BC probe, a variable volume of RNA and/or DNA template. Finally, nuclease-free water (Qiagen, Hilden, Germany) was added to a final volume of 20 µL. Using the LightCycler 480 real-time PCR system (Roche Diagnostics, Mannheim, Germany), reverse transcription was performed at 63 °C for 3 min followed by an activation step at 95 °C for 30 s and 45 cycles of 95 °C for 15 s, 62 °C for 20 s and 72 °C for 1 s.

A fluorescent signal 10-fold higher than the standard deviation of the mean baseline emission was counted as a positive detection. Samples were tested in triplicate (unless noted otherwise) and data recorded as Cycle thresholds (Ct) with Ct defined as the PCR cycle at which the fluorescent intensity raised above the threshold [34].

3.5. Droplet Digital PCR (ddPCR) and Reverse Transcription (RT) ddPCR

All DNA and RNA templates used for real-time and reverse transcription PCR were quantified by ddPCR and RT ddPCR, respectively. A 20 µL ddPCR reaction mixture consisted of 10 µL ddPCR Supermix for Probes (Bio-Rad Laboratories, Munich, Germany), 0.9 µM of each primer, 0.15 µM of each probe, and 5 µL of template DNA. RT-ddPCR reaction mixtures comprised of 5 µL One-Step RT-ddPCR Advanced Supermix for Probes (Bio-Rad, Munich, Germany), 2 µL of Reverse Transcriptase (Bio-Rad, Munich, Germany; final concentration 20 U/µL), 0.6 µL of DTT (Bio-Rad, Munich, Germany; final concentration 10 nM), 0.9 µM of each primer, 0.15 µM of each probe, and 5 µL of template RNA. Droplets were generated using a QX200 ddPCR droplet generator (Bio-Rad, Munich, Germany). PCR amplification for both assays was performed on the Mastercycler Gradient (Eppendorf, Hamburg, Germany) with the following conditions.

Initial reverse transcription was carried out at 48 °C for 60 min (only for RT-ddPCR). Enzyme activation at 95 °C for 10 min was followed by 40 cycles of denaturation at 94 °C for 30 s and annealing/extension at 58 °C for 1 min. Before the samples were cooled to 4 °C, a final enzyme inactivation was carried out at 98 °C for 10 min. The cooling and heating ramp rate was set to 2 °C/s for all steps. After PCR runs, droplets were analyzed using the QX100 Droplet Reader (Bio-Rad, Munich, Germany), and absolute target concentrations of each sample were calculated using Quantasoft Pro Software (Bio-Rad, Munich, Germany).

3.6. Generation of PCR Positive Controls from Reference Plasmids Harboring 16S-BA- or BC-Allele Fragments

Though we generally used genomic DNA from *B. cereus* or *B. anthracis*, respectively, for PCR testing and validation, generic positive control reference plasmids for either allele, the *B. anthracis*-specific 16S-BA-allele or the *B. cereus*-specific 16S-BC-allele were constructed. For this, a PCR-amplicon was generated from *B. anthracis* Ames DNA with primers 16S SNP F and 16S SNP R using Platinum™ Taq DNA Polymerase High Fidelity (ThermoFisher Scientific, Darmstadt, Germany). This DNA comprises a mixture of both alleles in a ratio of 4 to 7 [25]. The PCR-amplicon was analyzed on agarose gel electrophoresis, a band of the expected size (57 bp) cut from the gel and gel-purified using QIAquick Gel Extraction kit (QIAGEN, Hilden Germany). PCR products were ligated into pCR2.1 TOPO vector (ThermoFisher Scientific, Darmstadt, Germany) using TOPO TA Cloning kit (Thermo Scientific, Darmstadt, Germany) and transformed into One Shot TOP10 chemically competent cells (ThermoFisher Scientific, Darmstadt, Germany) according to the manufacturer's protocol. Several recombinant plasmids isolated from different clones were sequenced (Eurofins Genomics Germany, Ebersberg, Germany) in order to obtain plasmids harboring either the 16S-BA-allele or the 16S-BC-allele. From these plasmids, PCR products were generated using primers M13 F and M13 R, which contained the target region for the 16S rRNA SNP-PCR with either the 16S-BA- or BC-allele. After purification with QIAquick PCR purification kit (QIAGEN, Hilden Germany), PCR products were quantified using digital PCR and diluted as required.

3.7. Determination of the Specificity (Inclusivity/Exclusivity) of the B. anthracis 16S rRNA Allele Assay

PCR specificity for the 16S rRNA SNP assay was assessed by verifying the amplification of DNA containing or lacking respective markers. "Inclusivity" was evaluated by (exponential) amplification above threshold levels obtained with template DNA comprising the markers' sequences. Vice versa, "exclusivity" was confirmed by lack of amplification of genomic DNA from *B. cereus s.l.* strains reported to lack the particular 16S-BA-allele but also may harbor the alternative 16S-BC-allele or include no-template negative controls (NTC). Positive PCR results were further analyzed via agarose gel electrophoresis, demonstrating a single band with a molecular weight corresponding to the predicted size of the 16S rRNA SNP-PCR amplicon (note: this cannot differentiate between the two alternative SNP states in the 16S rRNA gene alleles).

3.8. Dynamic Linear Range, PCR Efficiency, and Limit of Detection

The dynamic linearity of the PCR assay was determined over a 9 $\log_{10}$ concentration range for DNA (real-time PCR) and RNA (RT-PCR) templates. Each dilution was assayed 6-fold, and analysis for linearity and PCR-efficiency (E) was performed from the plot of the Ct's versus the logarithm of the target concentrations [35]. The sensitivity of the PCR assay was expressed as the limit of detection (LoD) of 16S rRNA SNP genome or transcript copies. LoD was formally defined as the concentration permitting detection of the analyte at least 95% of the time. For this, DNA fragments comprising the 16S rRNA SNP were diluted to between 10 and 0 copies per reaction, subjected to real-time PCR with 12 replicates for each dilution step. Probit analysis (plot of the fitted model) was performed [36] using StatGraphics Centurion XVI.I (16.1.11; Statgraphics Technologies, The Plains, VA, USA) to determine the LoD by fitting template copies against the cumulative fractions of positive PCR observations and used for calculating the lower and upper 95% confidence limits. The LoD of the 16S rRNA SNP RT-PCR was determined likewise using samples with 0–15 rRNA copies per reaction (12 replicates for each dilution step).

4. Discussion

The use of SNPs as reliable markers for the identification of *B. anthracis* among its closest relatives of the *B. cereus* group is not a novel approach. This has previously been achieved with high specificity and sensitivity for nucleotide position 640 in the *plcR* gene [10] or at position 1050 in the *purA* gene [26], and diverse assays were thoroughly evaluated in [11]. Likewise, ribosomal gene sequences and intergenic transcribed spacers (ITS) between 16S and 23S rRNA genes have also been employed for *B. anthracis* identification in the past [37–40]. However, while these authors focused on the specific identification of *B. anthracis*, they neglected the potential of developing a sensitive assay making use of the multi-copy nature of their targets. An interesting exception is a study on fluorescent DNA-heteroduplex detection of *B. anthracis* [41]. Herein detection was preceded by general PCR-amplification of a fragment of the 16S rRNA gene region of *B. cereus s.l.* group strains containing a presumably specific SNP (pos. 980). This SNP, however, is neither specific for *B. anthracis* nor for the *B. cereus s.l.* group [24]. Anyway, Merrill et al. succeeded in establishing a LoD for their PCR of approximately 0.05 pg of purified *B. anthracis* genomic DNA (which can be calculated to represent 10–20 cell equivalents per reaction) [41]. This is higher than the LoD of about 1–2 cell equivalents per reaction found in our study. More importantly, Merrill et al. also took the effort to determine the detection limit of their presumably specific SNP in mixtures of 16S rRNA gene amplicons from *B. anthracis* and *B. cereus* [41]. The authors observed a detection limit of 1 out of 50 for *B. anthracis* DNA mixed with *B. cereus* DNA. They explained this limit as narrowed by methodological constraints and from competitive hybridization dynamics during probe annealing [41]. This finding can be compared with our results. The PCR assay developed here was able to detect at least one *B. anthracis* 16S-BA-allele target among 100 BC-allele targets (Figure S3 and Table S9). At higher alternative (16S-BC-allele) concentrations, these templates will outcompete the 16S-BA-allele for primer binding. Thus, the higher the fraction of 16S-BC-allele, the lower the relative amplification of 16S-BA-allele resulting in increasingly non-exponential amplification of the latter. In contrast, for a SNP in the DNA target *plcR* used for the differentiation of *B. anthracis* from *B. cereus*, a 20,000-fold excess of the alternate *B. cereus* allele did not preclude the detection of the *B. anthracis* allele [42]. With *B. cereus* spore counts in soils spanning a wide range of from 1×10^1 to 2.5×10^4 CFU per g soil [43], the *plcR* SNP-PCR should be able to detect *B. anthracis* in practically any sample. Here, the new 16S rRNA SNP-PCR on DNA as target molecule would fall short with only covering up to medium *B. cereus*-loaded soils. However, when targeting ribosomal RNA, the sensitivity (LoD) of the 16S rRNA SNP RT-PCR would be at least three orders of magnitude increased. Then, it should be possible to challenge the LoD values achieved by the *plcR* SNP-PCR (25 fg DNA or about 5 genome equivalents) [42].

A potential limitation of the multi-copy nature of the 16S-BA-allele may be the variable abundance of this allele in different *B. anthracis* strains. Previously, we could show that most *B. anthracis* strains harbor 3 (58.39%) 16S-BA-alleles. There are, however, also a number of isolates only possessing 2 (23.04%), 4 (17.10%), 5 (1.15%), and a single one with only 1 (0.31%) 16S-BA-alleles [25]. Thus, in most cases, this multi-copy gene allele can be harnessed nevertheless. A more typical multi-copy marker for detection of bacterial biothreat agents (and of other pathogens) constitute insertion sequence (IS) elements, which are widespread mobile genetic entities. For instance, in *Brucella* spp. *IS711* occurs in multiple genomic copies, and thus, the detection of this *IS711* is very sensitive. *B. melitensis* and *B. suis* contain seven complete copies, *B. abortus* carries six complete and one truncated *IS711* copies, *B. ovis*, *B. ceti*, and *B. pinnipedialis* even more than 20 copies [44]. Consequently, the lowest concentration of *Brucella* sp. DNA that could be detected was about ten times lower for *IS711* than, e.g., for single-copy genes *bcsp31* (*Brucella* cell surface 31 kDa protein) or *per* (perosamine synthetase), respectively [45]. Similarly, in *Coxiella burnetii*, the detection sensitivity of specific *IS1111* was compared to that of the single-copy *icd* gene (isocitrate dehydrogenase) [46]. While both PCRs for *icd* and *IS1111* had similar LoDs of 10.38 and 6.51, respectively, the sensitivity of *IS1111* was still superior because of its multiple-copy nature. Between 7 and 110 copies of this mobile element were found in various *C. burnetii* isolates [46].

The differences in threshold values (ΔCt = 9.96 $\pm$ 0.65) of identical samples obtained from (RT)-PCR using 16S-BA-allele DNA-only vs. 16S-BA-alleleDNA+RNA is enormous. There is an approximate factor of about 1000 ($2^{9.96}$) times more templates in the DNA+RNA sample than in the DNA-only sample. This factor favorably agrees with the numbers of genome copies and 16S rRNA transcripts in cells [17,18]. Similar to the work at hand, earlier work employed a combination of a DNA multi-copy marker and sensitive detection of rRNA transcript targets in *Mycobacterium ulcerans* [20]. The authors determined an LoD of six copies of the 16S rRNA transcript target sequence. For comparison, an LoD of two target copies of the high-copy insertion sequence element *IS2404*, which is present in 50–100 copies in different *M. ulcerans* strains, was calculated from parallel experiments [20]. Ribosomal RNA detection was also utilized for *Mycobacterium leprae* diagnosis by the same research team. Here, an LoD of three *M. leprae* target copies was achieved for a novel 16S rRNA RT-PCR assay; the same value as determined for the *M. leprae* specific multi-copy repetitive DNA target assayed in parallel [21]. At first glance, these values do not especially speak in favor of querying for 16S rRNA transcripts; however, one has to consider the high numbers of these molecules per cell in comparison to DNA markers (including the high-copy ones). Thus, the chance of capturing one of the more abundant rRNA molecules should be higher than that of the more limited DNA molecules. Indeed, this idea was explored, e.g., for *Escherichia coli*, *Enterococcus faecalis*, *Staphylococcus aureus*, *Clostridium perfringens*, and *Pseudomonas aeruginosa* by [19]. Comparative quantitative detection of these bacteria by RT-PCR (16S rRNA) vs. PCR (16S rRNA genes) revealed that the rRNA-detecting assay was from 64- to 1024-fold more sensitive than the one detecting DNA. Similarly, work on pathogenic spirochete *Leptospira* spp. found that 16S rRNA-based assays were at least 100-fold more sensitive than a DNA-based approach [47]. These authors also found that Leptospiral 16S rRNA molecules remain appreciably stable in blood. From this insight, the authors then highlighted the potential use of 16S RNA targets for the diagnosis of early infection. Nevertheless, potential limitations of this approach were also noted. Efficacy of the required reverse transcription reaction has to be considered, RNA molecules are notoriously less stable than other biomarkers, and their cellular abundance (and as a consequence, their detection) can be expected to be variable [47]. Finally, though not required for qualitative detection, absolute quantification of microbial cells based solely on enumeration of RNA molecules is complicated because of these variations in transcript numbers depending, e.g., on the growth phase [47]. However, the cell numbers determined by RT-PCR were similar when compared alongside standard methods such as cell counts, PCR, or fluorescence in situ hybridization (FISH) [48]. Yet, in certain instances, there might

be an additional advantage of performing PCR on rRNA directly (via RT-PCR) instead of targeting DNA (including DNA of rRNA genes). Because DNA is more stable than RNA, DNA may originate from both live and dead bacterial cells. In contrast, rRNA molecules may be considered to be more closely associated with viable bacteria [49]. Though this might also be possible with the new PCR assays introduced in the work at hand, we chose to combine DNA and rRNA detection in a single test tube for the sake of simplicity (no troublesome DNase treatment of purified RNA required) and depth of detection.

5. Conclusions

In this work, we designed and validated a new PCR-based detection assay for the biothreat agent *B. anthracis*. This assay can be run as a real-time PCR with solely DNA as a template or as an RT-real-time version using both cellular nucleic acid pools (DNA and RNA) as a template. This assay was found to be highly species specific, yielding no false positives, and was sensitive with a LoD of about 0.6 copies/µL (DNA-only) and about 1.3 copies/µL (DNA+RNA). With the high abundance of 16S rRNA moieties in cells, this assay can be expected to facilitate the detection of *B. anthracis* by PCR. While standard PCR assays are well established for the identification of *B. anthracis* from pure culture, the exceptional sensitivity of the new 16S rRNA-based assay might excel in clinical and public health laboratories when detection of minute residues of the pathogen is required.

Supplementary Materials: The following are available online: https://www.mdpi.com/article/10.3390/ijms222212224/s1.

Author Contributions: Conceptualization, G.G. and P.B.; investigation, P.B., M.D.-T.N. and M.C.W.; methodology, M.D.-T.N. and P.B.; formal analysis and validation, P.B., M.D.-T.N. and G.G.; resources, G.G. and M.C.W.; data curation, P.B., M.D.-T.N. and M.C.W.; writing—original draft preparation, G.G. and P.B.; writing—review and editing, P.B., M.D.-T.N., M.C.W. and G.G.; visualization, M.D.-T.N., P.B. and G.G.; supervision and project administration, G.G. and P.B.; funding acquisition, G.G. All authors have read and agreed to the published version of the manuscript.

Funding: This research was funded by funds from the Medical Biological Defense Research Program of the Bundeswehr Joint Medical Service.

Institutional Review Board Statement: Not applicable.

Informed Consent Statement: Not applicable.

Data Availability Statement: Not applicable.

Acknowledgments: The authors thank Mandy Knüper (Bundeswehr Institute of Microbiology) for support with probit-analysis and the gift of DNA from spiked soil samples, Stefanie Gläser (Justus-Liebig-University Gießen, Germany), Erwin Märtlbauer (Ludwig-Maximilians-University, Munich, Germany) and Monika-Ehling Schultz (University of Veterinary Medicine, Vienna, Austria) for several *B. cereus* strains, as well as Paul Keim (Northern Arizona University, Flagstaff, AZ, USA) and Wolfgang Beyer (Hohenheim University, Stuttgart, Germany) for the gift of *B. anthracis* strains/DNA. Thanks are due to Rahime Terzioglu for technical assistance and Olfert Landt (TIB Molbiol, Berlin) for support in LNA-probe design.

Conflicts of Interest: The authors declare no conflict of interest. Opinions, interpretations, conclusions, and recommendations are those of the authors and are not necessarily endorsed by any governmental agency, department, or other institutions. The funders had no role in the design of the study; in the collection, analyses, or interpretation of data; in the writing of the manuscript, or in the decision to publish the results.

References

1. Turnbull, P.C.; World Health Organization. *Anthrax in Humans and Animals*; Turnbull, P., Ed.; WHO Press: Geneva, Switzerland, 2008.
2. Ehling-Schulz, M.; Lereclus, D.; Koehler, T.M. The *Bacillus cereus* group: *Bacillus* species with pathogenic potential. *Microbiol. Spectr.* **2019**, 7. [CrossRef]
3. Mock, M.; Fouet, A. Anthrax. *Annu. Rev. Microbiol.* **2001**, *55*, 647–671. [CrossRef] [PubMed]

4. Jelacic, T.M.; Chabot, D.J.; Bozue, J.A.; Tobery, S.A.; West, M.W.; Moody, K.; Yang, D.; Oppenheim, J.J.; Friedlander, A.M. Exposure to *Bacillus anthracis* capsule results in suppression of human monocyte-derived dendritic cells. *Infect. Immun.* **2014**, *82*, 3405–3416. [CrossRef] [PubMed]
5. Patino-Navarrete, R.; Sanchis, V. Evolutionary processes and environmental factors underlying the genetic diversity and lifestyles of *Bacillus cereus* group bacteria. *Res. Microbiol.* **2017**, *168*, 309–318. [CrossRef]
6. Wielinga, P.R.; Hamidjaja, R.A.; Ågren, J.; Knutsson, R.; Segerman, B.; Fricker, M.; Ehling-Schulz, M.; de Groot, A.; Burton, J.; Brooks, T.; et al. A multiplex real-time PCR for identifying and differentiating *B. anthracis* virulent types. *Int. J. Food Microbiol.* **2011**, *145*, S137–S144. [CrossRef] [PubMed]
7. Ellerbrok, H.; Nattermann, H.; Ozel, M.; Beutin, L.; Appel, B.; Pauli, G. Rapid and sensitive identification of pathogenic and apathogenic *Bacillus anthracis* by real-time PCR. *FEMS Microbiol. Lett.* **2002**, *214*, 51–59. [CrossRef]
8. Ramisse, V.; Patra, G.; Garrigue, H.; Guesdon, J.L.; Mock, M. Identification and characterization of *Bacillus anthracis* by multiplex PCR analysis of sequences on plasmids pXO1 and pXO2 and chromosomal DNA. *FEMS Microbiol. Lett.* **1996**, *145*, 9–16. [CrossRef]
9. Antwerpen, M.H.; Zimmermann, P.; Bewley, K.; Frangoulidis, D.; Meyer, H. Real-time PCR system targeting a chromosomal marker specific for *Bacillus anthracis*. *Mol. Cell. Probes* **2008**, *22*, 313–315. [CrossRef]
10. Easterday, W.R.; Van Ert, M.N.; Simonson, T.S.; Wagner, D.M.; Kenefic, L.J.; Allender, C.J.; Keim, P. Use of single nucleotide polymorphisms in the *plcR* gene for specific identification of *Bacillus anthracis*. *J. Clin. Microbiol.* **2005**, *43*, 1995–1997. [CrossRef]
11. Ågren, J.; Hamidjaja, R.A.; Hansen, T.; Ruuls, R.; Thierry, S.; Vigre, H.; Janse, I.; Sundström, A.; Segerman, B.; Koene, M.; et al. In silico and in vitro evaluation of PCR-based assays for the detection of *Bacillus anthracis* chromosomal signature sequences. *Virulence* **2013**, *4*, 671–685. [CrossRef]
12. Straub, T.; Baird, C.; Bartholomew, R.A.; Colburn, H.; Seiner, D.; Victry, K.; Zhang, L.; Bruckner-Lea, C.J. Estimated copy number of *Bacillus anthracis* plasmids pXO1 and pXO2 using digital PCR. *J. Microbiol. Methods* **2013**, *92*, 9–10. [CrossRef]
13. Pena-Gonzalez, A.; Rodriguez-R, L.; Marston, C.K.; Gee, J.E.; Gulvik, C.A.; Kolton, C.B.; Saile, E.; Frace, M.; Hoffmaster, A.R.; Konstantinidis, K.T. Genomic characterization and copy number variation of *Bacillus anthracis* plasmids pXO1 and pXO2 in a historical collection of 412 strains. *mSystems* **2018**, *3*, e00065-18. [CrossRef]
14. Hansen, M.C.; Nielsen, A.K.; Molin, S.; Hammer, K.; Kilstrup, M. Changes in rRNA levels during stress invalidates results from mRNA blotting: Fluorescence in situ rRNA hybridization permits renormalization for estimation of cellular mRNA levels. *J. Bacteriol.* **2001**, *183*, 4747–4751. [CrossRef]
15. Bremer, H.; Dennis, P.P. Modulation of chemical composition and other parameters of the cell at different exponential growth rates. *EcoSal Plus* **2008**, *3*. [CrossRef] [PubMed]
16. Wiśniewski, J.R.; Rakus, D. Multi-enzyme digestion FASP and the 'Total Protein Approach'-based absolute quantification of the *Escherichia coli* proteome. *J. Proteom.* **2014**, *109*, 322–331. [CrossRef] [PubMed]
17. van Dijk-Salkinoja, M.S.; Planta, R.J. Rate of ribosome production in *Bacillus licheniformis*. *J. Bacteriol.* **1971**, *105*, 20–27. [CrossRef] [PubMed]
18. Barrera, A.; Pan, T. Interaction of the *Bacillus subtilis* RNase P with the 30S ribosomal subunit. *RNA* **2004**, *10*, 482–492. [CrossRef]
19. Matsuda, K.; Tsuji, H.; Asahara, T.; Kado, Y.; Nomoto, K. Sensitive quantitative detection of commensal bacteria by rRNA-targeted reverse transcription-PCR. *Appl. Environ. Microbiol.* **2007**, *73*, 32–39. [CrossRef]
20. Beissner, M.; Symank, D.; Phillips, R.O.; Amoako, Y.A.; Awua-Boateng, N.Y.; Sarfo, F.S.; Jansson, M.; Huber, K.L.; Herbinger, K.H.; Battke, F.; et al. Detection of viable *Mycobacterium ulcerans* in clinical samples by a novel combined 16S rRNA reverse transcriptase/IS2404 real-time qPCR assay. *PLoS Negl. Trop. Dis.* **2012**, *6*, e1756. [CrossRef]
21. Beissner, M.; Woestemeier, A.; Saar, M.; Badziklou, K.; Maman, I.; Amedifou, C.; Wagner, M.; Wiedemann, F.X.; Amekuse, K.; Kobara, B.; et al. Development of a combined RLEP/16S rRNA (RT) qPCR assay for the detection of viable *M. leprae* from nasal swab samples. *BMC Infect. Dis.* **2019**, *19*, 753. [CrossRef]
22. Ash, C.; Farrow, J.A.; Dorsch, M.; Stackebrandt, E.; Collins, M.D. Comparative analysis of *Bacillus anthracis*, *Bacillus cereus*, and related species on the basis of reverse transcriptase sequencing of 16S rRNA. *Int. J. Syst. Bacteriol.* **1991**, *41*, 343–346. [CrossRef] [PubMed]
23. Candelon, B.; Guilloux, K.; Ehrlich, S.D.; Sorokin, A. Two distinct types of rRNA operons in the *Bacillus cereus* group. *Microbiology* **2004**, *150 Pt 3*, 601–611. [CrossRef]
24. Hakovirta, J.R.; Prezioso, S.; Hodge, D.; Pillai, S.P.; Weigel, L.M. Identification and analysis of informative single nucleotide polymorphisms in 16S rRNA gene sequences of the *Bacillus cereus* group. *J. Clin. Microbiol.* **2016**, *54*, 2749–2756. [CrossRef] [PubMed]
25. Braun, P.; Zimmermann, F.; Walter, M.C.; Mantel, S.; Aistleitner, K.; Stürz, I.; Grass, G.; Stoecker, K. In-depth analysis of *Bacillus anthracis* 16S rRNA genes and transcripts reveals intra- and intergenomic diversity and facilitates anthrax detection. *bioRxiv* **2021**. [CrossRef]
26. Irenge, L.M.; Durant, J.F.; Tomaso, H.; Pilo, P.; Olsen, J.S.; Ramisse, V.; Mahillon, J.; Gala, J.L. Development and validation of a real-time quantitative PCR assay for rapid identification of *Bacillus anthracis* in environmental samples. *Appl. Microbiol. Biotechnol.* **2010**, *88*, 1179–1192. [CrossRef] [PubMed]
27. Sahl, J.W.; Pearson, T.; Okinaka, R.; Schupp, J.M.; Gillece, J.D.; Heaton, H.; Birdsell, D.; Hepp, C.; Fofanov, V.; Noseda, R.; et al. A *Bacillus anthracis* genome sequence from the Sverdlovsk 1979 autopsy specimens. *mBio* **2016**, *7*, e01501-16. [CrossRef]

28. Antwerpen, M.; Beyer, W.; Bassy, O.; Ortega-García, M.V.; Cabria-Ramos, J.C.; Grass, G.; Wölfel, R. Phylogenetic placement of isolates within the Trans-Eurasian clade A.Br.008/009 of *Bacillus anthracis*. *Microorganisms* **2019**, *7*, 689. [CrossRef]
29. Kämpfer, P.; Busse, H.J.; McInroy, J.A.; Glaeser, S.P. *Sphingomonas zeae* sp. nov., isolated from the stem of *Zea mays*. *Int. J. Syst. Evol. Microbiol.* **2015**, *65*, 2542–2548. [CrossRef]
30. Reischl, U.; Ehrenschwender, M.; Hiergeist, A.; Maaß, M.; Baier, M.; Frangoulidis, D.; Grass, G.; von Buttlar, H.; Scholz, H.; Fingerle, V.; et al. Bacterial and fungal genome detection PCR/NAT: Comprehensive discussion of the June 2018 distribution for external quality assessment of nucleic acid-based protocols in diagnostic medical microbiology by INSTAND e.V., GMS Z Forder Qualitatssich. *Med. Lab.* **2019**, *10*, 1869–4241.
31. Braun, P.; Grass, G.; Aceti, A.; Serrecchia, L.; Affuso, A.; Marino, L.; Grimaldi, S.; Pagano, S.; Hanczaruk, M.; Georgi, E.; et al. Microevolution of anthrax from a young ancestor (M.A.Y.A.) suggests a soil-borne life cycle of *Bacillus anthracis*. *PLoS ONE* **2015**, *10*, e0135346.
32. Altschul, S.F.; Gish, W.; Miller, W.; Myers, E.W.; Lipman, D.J. Basic local alignment search tool. *J. Mol. Biol.* **1990**, *215*, 403–410. [CrossRef]
33. Koshkin, A.A.; Singh, S.K.; Nielsen, P.; Rajwanshi, V.K.; Kumar, R.; Meldgaard, M.; Olsen, C.E.; Wengel, J. LNA (Locked Nucleic Acids): Synthesis of the adenine, cytosine, guanine, 5-methylcytosine, thymine and uracil bicyclonucleoside monomers, oligomerisation, and unprecedented nucleic acid recognition. *Tetrahedron* **1998**, *54*, 3607–3630. [CrossRef]
34. Perelle, S.; Dilasser, F.; Grout, J.; Fach, P. Detection by 5′-nuclease PCR of Shiga-toxin producing *Escherichia coli* O26, O55, O91, O103, O111, O113, O145 and O157:H7, associated with the world's most frequent clinical cases. *Mol. Cell. Probes* **2004**, *18*, 185–192. [CrossRef] [PubMed]
35. Stolovitzky, G.; Cecchi, G. Efficiency of DNA replication in the polymerase chain reaction. *Proc. Natl. Acad. Sci. USA* **1996**, *93*, 12947–12952. [CrossRef]
36. Forootan, A.; Sjöback, R.; Björkman, J.; Sjögreen, B.; Linz, L.; Kubista, M. Methods to determine limit of detection and limit of quantification in quantitative real-time PCR (qPCR). *Biomol. Detect. Quantif.* **2017**, *12*, 1–6. [CrossRef]
37. Nübel, U.; Schmidt, P.M.; Reiß, E.; Bier, F.; Beyer, W.; Naumann, D. Oligonucleotide microarray for identification of *Bacillus anthracis* based on intergenic transcribed spacers in ribosomal DNA. *FEMS Microbiol. Lett.* **2004**, *240*, 215–223. [CrossRef]
38. Daffonchio, D.; Raddadi, N.; Merabishvili, M.; Cherif, A.; Carmagnola, L.; Brusetti, L.; Rizzi, A.; Chanishvili, N.; Visca, P.; Sharp, R.; et al. Strategy for identification of *Bacillus cereus* and *Bacillus thuringiensis* strains closely related to *Bacillus anthracis*. *Appl. Environ. Microbiol.* **2006**, *72*, 1295–1301. [CrossRef]
39. Cherif, A.; Borin, S.; Rizzi, A.; Ouzari, H.; Boudabous, A.; Daffonchio, D. *Bacillus anthracis* diverges from related clades of the *Bacillus cereus* group in 16S-23S ribosomal DNA intergenic transcribed spacers containing tRNA genes. *Appl. Environ. Microbiol.* **2003**, *69*, 33–40. [CrossRef]
40. Hadjinicolaou, A.V.; Demetriou, V.L.; Hezka, J.; Beyer, W.; Hadfield, T.L.; Kostrikis, L.G. Use of molecular beacons and multi-allelic real-time PCR for detection of and discrimination between virulent *Bacillus anthracis* and other *Bacillus* isolates. *J. Microbiol. Methods* **2009**, *78*, 45–53. [CrossRef]
41. Merrill, L.; Richardson, J.; Kuske, C.R.; Dunbar, J. Fluorescent heteroduplex assay for monitoring *Bacillus anthracis* and close relatives in environmental samples. *Appl. Environ. Microbiol.* **2003**, *69*, 3317–3326. [CrossRef]
42. Easterday, W.R.; Van Ert, M.N.; Zanecki, S.; Keim, P. Specific detection of *Bacillus anthracis* using a TaqMan mismatch amplification mutation assay. *Biotechniques* **2005**, *38*, 731–735. [CrossRef]
43. Altayar, M.; Sutherland, A.D. *Bacillus cereus* is common in the environment but emetic toxin producing isolates are rare. *J. Appl. Microbiol.* **2006**, *100*, 7–14. [CrossRef] [PubMed]
44. Mancilla, M.; Ulloa, M.; López-Goñi, I.; Moriyón, I.; María Zárraga, A. Identification of new IS711 insertion sites in *Brucella abortus* field isolates. *BMC Microbiol.* **2011**, *11*, 176. [CrossRef] [PubMed]
45. Bounaadja, L.; Albert, D.; Chénais, B.; Hénault, S.; Zygmunt, M.S.; Poliak, S.; Garin-Bastuji, B. Real-time PCR for identification of *Brucella* spp.: A comparative study of *IS711*, *bcsp31* and *per* target genes. *Veter- Microbiol.* **2009**, *137*, 156–164. [CrossRef]
46. Klee, S.R.; Tyczka, J.; Ellerbrok, H.; Franz, T.; Linke, S.; Baljer, G.; Appel, B. Highly sensitive real-time PCR for specific detection and quantification of *Coxiella burnetii*. *BMC Microbiol.* **2006**, *6*, 2. [CrossRef]
47. Backstedt, B.T.; Buyuktanir, O.; Lindow, J.; Wunder, E.A., Jr.; Reis, M.G.; Usmani-Brown, S.; Ledizet, M.; Ko, A.; Pal, U. Efficient detection of pathogenic Leptospires using 16S ribosomal RNA. *PLoS ONE* **2015**, *10*, e0128913. [CrossRef] [PubMed]
48. Kubota, H.; Tsuji, H.; Matsuda, K.; Kurakawa, T.; Asahara, T.; Nomoto, K. Detection of human intestinal catalase-negative, Gram-positive cocci by rRNA-targeted reverse transcription-PCR. *Appl. Environ. Microbiol.* **2010**, *76*, 5440–5451. [CrossRef] [PubMed]
49. Tsuji, H.; Matsuda, K.; Nomoto, K. Counting the countless: Bacterial quantification by targeting rRNA molecules to explore the human gut microbiota in health and disease. *Front. Microbiol.* **2018**, *9*, 1417. [CrossRef] [PubMed]

5. Rapid microscopic detection of *Bacillus anthracis* by fluorescent receptor binding proteins of bacteriophages

microorganisms

MDPI

Article

Rapid Microscopic Detection of *Bacillus anthracis* by Fluorescent Receptor Binding Proteins of Bacteriophages

Peter Braun, Immanuel Wolfschläger, Leonie Reetz, Lilia Bachstein, Ana Clara Jacinto, Carolina Tocantins, Johannes Poppe and Gregor Grass *

Dept. Bacteriology and Toxinology, Bundeswehr Institute of Microbiology (IMB), 80937 Munich, Germany; peter3braun@bundeswehr.org (P.B.); tgs_wolfschlaegeri@yahoo.de (I.W.); reetz.leonie@outlook.de (L.R.); lilia.bachstein@gmx.de (L.B.); aclarajacinto@gmail.com (A.C.J.); carolina.tocantins.23.3@gmail.com (C.T.); poppe.johannes0@hm.edu (J.P.)

* Correspondence: gregorgrass@bundeswehr.org; Tel.: +49-992692-3981

Received: 29 May 2020; Accepted: 19 June 2020; Published: 21 June 2020

Abstract: *Bacillus anthracis*, the etiological agent of anthrax disease, is typically diagnosed by immunological and molecular methods such as polymerase chain reaction (PCR). Alternatively, mass spectrometry techniques may aid in confirming the presence of the pathogen or its toxins. However, because of the close genetic relationship between *B. anthracis* and other members of the *Bacillus cereus sensu lato* group (such *as Bacillus cereus* or *Bacillus thuringiensis*) mis- or questionable identification occurs frequently. Also, bacteriophages such as phage gamma (which is highly specific for *B. anthracis*) have been in use for anthrax diagnostics for many decades. Here we employed host cell-specific receptor binding proteins (RBP) of (pro)-phages, also known as tail or head fibers, to develop a microscopy-based approach for the facile, rapid and unambiguous detection of *B. anthracis* cells. For this, the genes of (putative) RBP from *Bacillus* phages gamma, Wip1, AP50c and from lambdoid prophage 03 located on the chromosome of *B. anthracis* were selected. Respective phage genes were heterologously expressed in *Escherichia coli* and purified as fusions with fluorescent proteins. *B. anthracis* cells incubated with either of the reporter fusion proteins were successfully surface-labeled. Binding specificity was confirmed as RBP fusion proteins did not bind to most isolates of a panel of other *B. cereus s.l.* species or to more distantly related bacteria. Remarkably, RBP fusions detected encapsulated *B. anthracis* cells, thus RBP were able to penetrate the poly-γ-D-glutamate capsule of *B. anthracis*. From these results we anticipate this RBP-reporter assay may be useful for rapid confirmative identification of *B. anthracis*.

Keywords: anthrax; *Bacillus anthracis*; bacteriophage; receptor binding protein; reporter fusions; detection assay

1. Introduction

Bacillus anthracis causing the zoonotic infectious disease anthrax in mammals and humans phylogenetically belongs to the *Bacillus cereus sensu lato* group of very closely related Firmicutes bacteria. The group comprises several familiar species, including *Bacillus cereus sensu stricto*, *Bacillus thuringiensis*, *Bacillus weihenstephanensis*, *Bacillus mycoides* and a variety of lesser characterized members [1]. Classical, culture-based techniques and classification upon phenotypic traits such as susceptibility against penicillin or lack of hemolysis are ambiguous and often fail to reliably differentiate *B. anthracis* from its close relatives. When comparing the 16S rRNA gene sequences, a very high degree of agreement can be observed among these species [2], thus far essentially disfavoring assays for species identification targeting these genetic elements. Similar challenges arise when using techniques such as multi locus

sequence typing on members of the *B. cereus s.l.* group. In fact, most species of this group should be regarded as a single species [1]. However, some species carry characteristic virulence plasmids on which the genetic information for certain toxins is encoded. These include megaplasmid pCER270 for production of cereulide toxin in a clade of *B. cereus sensu stricto* strains [3] or plasmid pXO1 encoding a three-partite AB toxin from *B. anthracis* better known as lethal and edema toxin, respectively [4]. These phenotypic characteristics facilitate clinical differentiation, but do not always constitute reliable criteria for rapid identification of individual species. For example, virulence plasmids typical for *B. anthracis* (pXO1 and pXO2) can also be found in certain *B. cereus* isolates [1].

The crucial need for species identification without necessitating live bacteria is typically met by applying molecular methods such as polymerase chain reaction (PCR). For the identification of the tier 1 agent *B. anthracis*, chromosomal markers such as *PL3* [5], *dhp61* (BA5345) [6] or a nonsense mutation within the *plcR*-gene are frequently interrogated for [7]. Plasmids pXO1 and pXO2 are identified by virulence factor genes *pagA*, *lef*, *cya*, *capB* or *capC*, respectively [5,8,9]. In addition, immunological tests have been established which, due to their sensitivities to specific proteins, can not only detect antibodies after infection but also the pathogen's antigens in the host blood such as the poly-γ-D-glutamic acids forming the bacterial capsule [10] or the toxin-subunit protective antigen (PA) during acute infection [11]. However, the challenge of species-specificity remains. Finally, a newer approach, matrix-assisted laser desorption ionization-time of flight mass spectrometry (MALDI-TOF MS), has proven successful because it facilitates rapid identification of difficult-to-identify pathogens such as *B. anthracis* [12].

In contrast to these assays which strongly rely on financial investments in equipment and consumables, the application of the classical bacteriophage (phage) plaque assay is both resource saving and easy to perform. As phages are viruses that only infect target bacteria, some phages have a very narrow host range accepting just a single species or even only a few strains within a species [13,14]. A number of virulent bacteriophages have been described in the literature that infect and multiply in *B. anthracis*. The most *B. anthracis*-specific phages can be assigned to the families Siphorviridae [15,16] and Tectiviridae [17,18] and always feature double-stranded DNA (dsDNA) as their genetic material. Brown et al. (1955) discovered the γ (gamma) phage which is a Siphovirus [16]. Phage γ has been introduced as a standard for plaque assay identification of *B. anthracis* [19–21], even though newer work has found a number of additional non-*B.-anthracis* strains susceptible to the phage [15]. Another *B. anthracis* specific phage named Wip1 (worm intestinal phage 1) is from the Tectiviridae family [18]. This phage was first isolated from the earthworm *Eisenia fetida* [18]. Schuch et al. (2010) compared Wip1 and γ phages for their host specificities towards *B. anthracis* and *B. cereus s. s.* strains. Remarkably, phage Wip1 achieved higher specificity than the γ phage [18,22]. Another Tectivirus phage that is very specific for *B. anthracis* is called AP50c [17]. This lytic phage was derived from temperate parental phage AP50t isolated from soil [23] and is genomically very similar to phage Wip1 but not identical [18]. Genome sequencing has revealed that the genome of *B. anthracis* contains four (inactive) prophages which have been named LambdaBa01-04 [24]. The presence of these prophages in a genome is also very specific for *B. anthracis*. This is especially true for LambdaBa01, 03 and 04 which were only found in strains of this species but not in close relatives of the *B. cereus s.l.* group [24].

The particular host specificity of phages is usually determined by receptor binding proteins (RBP) which enable the phage to recognize and bind to cell wall structures of the host bacterium [13,25]. In the above-mentioned specific "anthrax" phages, these receptor binding proteins (RBP) comprise the so-called tail (Siphorviridae) or head (Tectiviridae) fibers [25]. The RBP of phages Wip1 and γ were already provisionally characterized by in silico analysis and subsequent experimentation [18,26] but not yet the RBP of phage AP50c or of prophage LambdaBa03. The structural make-up of the typically homotrimeric RBP is similar in many phages [27,28]. RBP feature two critical domains: at the *N*-terminus, the RBP is anchored to the phage (head or tail) while the recognition and binding domain is located at the C-terminus of the protein. This binding domain can either confer narrow or broad specificity. The corresponding surface structures of the bacteria (i.e., the receptors), which are responsible

for recognition and adsorption of the phage or its RBP can be quite different, including such diverse entities as polysaccharides, teichoic acids, structural or capsule proteins [27,28]. Davison et al. (2005) showed that for the binding of the γ phage, the receptor protein GamR of *B. anthracis* is essential [29]. The RBP of γ phage was identified as the product of the *gp14* gene on the phage genome [26]. For phage Wip1 the receptor of *B. anthracis* has not yet been unambiguously identified but it has been proposed from earlier work that the surface layer protein Sap (surface array protein) is involved in binding by the RBP either directly or indirectly [18]. The CsaB protein, a cell-surface anchoring protein, was found to be required for phage AP50c adsorption [30]. Because Sap is anchored by CsaB, Sap is the likely receptor for the *B. anthracis* specific phage AP50c [31], yet no indication of the RBP involved was given. From these previous works we further characterized *Bacillus* (pro)-phage RBP and developed tools to be used in routine DNA-independent, fluorescence microscopic rapid identification of the highly pathogenic bacterium *B. anthracis*.

2. Materials and Methods

2.1. Bacterial Culture and Inactivation

Unless specified differently, *B. anthracis* strains and other Bacilli were cultivated at 37 °C on tryptic soy agar plates (TSA, Merck KGaA, Darmstadt, Germany) or in 250 mL baffled flasks containing 50 mL tryptic soy broth (TSB, Merck KGaA) with shaking at 110 rpm. All risk group 3 (RG-3) *B. anthracis* strains were grown in the biosafety level 3 (BSL-3) laboratory at the Bundeswehr Institute of Microbiology (IMB) and then chemically inactivated before further use [32]. Inactivation of RG 2 strains for subsequent RBP reporter tests was carried out by pelleting 1 mL of a bacterial culture at 5000× *g* for 3 min and resuspending the cell pellet in aqueous peracetic acid solution (2% Terralin PAA, Schülke & Mayr GmbH, Norderstedt, Germany) or 4% paraformaldehyde (Merck KGaA) and incubating at room temperature for 30 or 60 min, respectively. For heat inactivation another sample was resuspended in PBS and incubated at 98 °C for 30 min (with heated lid cover). After inactivation, all samples were washed twice with PBS. For cultivation of encapsulated *B. anthracis* cells, a fresh colony from a TSA plate was used to inoculate 5 mL of Luria Bertani (LB) broth (Merck KGaA) containing 0.8% $NaHCO_3$ in cell culture flaks (Nunc EasYFlask 25 cm^2; ThermoFisher Scientific, Darmstadt, Germany) followed by incubation with 10% CO_2 atmosphere at 37 °C for 4 h or overnight. *Escherichia coli* cultures were grown in LB broth or on Luria Bertani (LB)-agar (Merck KGaA) with 20 µg/mL of gentamycin and 100 µg/mL carbenicillin (Carl Roth, Karlsruhe, Germany) where required.

2.2. Spore Preparation

Sporulation and subsequent spore purification of *B. anthracis* and other Bacilli was done as previously described [33] with slight modifications. A colony of a fresh overnight culture of *B. anthracis* (or other Bacilli) was used to inoculate 50 mL sporulation medium containing 0.8% nutrient broth (Merck KGaA) amended with 0.05 mM $MnCl_2$, 0.7 mM $CaCl_2$ and 1.0 mM $MgCl_2$ [34] in 500 mL baffled flasks. After incubation at 37 °C and 110 rpm shaking for 72 h, Tween 80 was added to a final concentration of 3% and the culture incubated for another 24 h. The culture was transferred to a 50 mL centrifugation tube and harvested by centrifugation at 2000× *g* and 20 °C for 10 min. The supernatant was discarded and the pellet washed twice with 25 mL 3% Tween 80 and further incubated on a rotary shaker at 150 rpm for 24 h. Purity of spore suspensions was checked by phase contrast microscopy and spores were harvested by centrifugation (2000× *g* and 20 °C for 10 min) when purity was above 95% (fewer than 5% vegetative cells present). If purity was less than 95%, spores were washed again with 25 mL 3% Tween 80 and incubated for another 24 h until purity was sufficient. Finally, the spore pellet was resuspended in 3 mL ice-cold ultrapure H_2O and stored at 4 °C until further use. Spore preparations reached concentrations of up to 10^9 spores per mL.

2.3. Isolation of DNA

DNA from Bacilli and bacteriophages was isolated using MasterPure™ Gram Positive DNA Purification kit (Lucigen, Middleton, WI, USA) and DNA concentrations quantified using the Qubit dsDNA HS Assay Kit (ThermoFisher Scientific) according to the manufacturers' protocols. DNA preparations were stored at −20 °C until further use.

2.4. Cloning of RBP-Fusion Constructs

For construction of genetic *RBP-mCherry*-fusions, first the *mCherry* open reading frame from plasmid mCherry-pBAD (mCherry-pBAD was a gift from Davidson, Shaner and Tsien, University of California at San Diego, La Jolla, CA, USA; Addgene plasmid #54630 (company, Watertown, MA, USA; http://n2t.net/addgene:54630; RRID:Addgene_54630; [35]) was PCR amplified creating overhangs containing restriction sites for Esp3I for cloning into pASG-IBA105 expression plasmid downstream of the *twin-strep-tag* epitope sequence. Primer overhangs also introduced recognition sites for restriction enzymes SalI, EcoRI and BsrGI as well as XhoI, PstI and BsiWI upstream and downstream of the *mCherry* gene, respectively, for subsequent insertion of RBP genes. Primer sequences are listed in Table 1. One-step Esp3I digestion and ligation was carried out using StarGate Direct transfer cloning System (IBA GmbH, Göttingen, Germany) as described in the manufacturer's protocol and plasmids were transformed into NEB Turbo cells (New England Biolabs GmbH, Frankfurt am Main, Germany). Clones were confirmed by Sanger sequencing (Eurofins Genomics Germany GmbH, Ebersberg, Germany) of their recombinant pASG-mCherry plasmids using primers flanking the insert. Next, for generation of *mCherry-RBP* fusions, respective RBP genes were PCR amplified from purified DNA generating XhoI and BsiWI overhangs and were digested with XhoI and BsiWI alongside pASG-mCherry. After ligation of the fragments, constructs were transformed and plasmid sequences of clones checked as described above.

Table 1. Primers used for cloning.

Oligonucleotide	Sequence (5′–3′)
BA4079 forward	AAACTCGAGATGAGTTCTTTTTCATTTAATGGGGAAC
BA4079 reverse	AAACGTACGTCTGTATCTCTCCCTATAACTGATTGTTG
BA4079λ03$_{\Delta 1\text{-}120}$ forward	AAACTCGAGATGAGTTCTTTTTCATTTAATGGGGAAC
gp14 forward	AAACTCGAGTTGGGGAAACTTAGTTTTACTTTTAATAATATTAG
gp14 reverse	AAACGTACGTCTATATCTCTCCCTATAACTGATTGTTGC
p23 forward	AAACTCGAGATGGGACTTAAGAAACCTGCGG
p23 reverse	AAACGTACGTTCATAAGCAACCCACGGTTG
p23+p24 reverse	AAACGTACGCATTCCTCCTAGTAATATATCGTTAATTGCAC
p28 forward	AAACTCGAGATGGGACTGAAAAAACCTAGCGG
p28 reverse	AAACGTACGGAATGGTTTTTCCGCTTCCTCTTTTAC
p28+p29 reverse	AAACGTACGCATTCCTCCTAATAGAATATCGTTAATTGTAC
mCherry forward	AGCGCGTCTCCAATGGTCGACGGTGAATTCGGCTGTACA GTTAGTAAAGGAGAAGAAAATAACATGGC
mCherry reverse	AGCGCGTCTCCTCCCCGTACGGCCCTGCAGACCCTCGAG TTTGTATAGTTCATCCATGCCACCAG

Restriction endonuclease recognition sites are underscored.

2.5. Expression and Purification of Strep-Tagged mCherry-RBP Fusion Reporters

The pASG-mCherry::RBP plasmids were transformed into *E. coli* ArcticExpress cells (Agilent Technologies Inc., Waldbronn, Germany). Single colonies harboring recombinant plasmids with fusion constructs were used to inoculate 5 mL of LB medium with gentamycin and carbenicillin in a 50 mL centrifugation tube. After overnight incubation at 37 °C with shaking at 150 rpm, 400 µL of the culture were added to a 1000 mL baffled flask containing 200 mL prewarmed LB medium and incubated at 30 °C with shaking at 110 rpm until the optical density (OD_{600}) of the culture reached 0.6–0.8. Temperature was decreased to 12 °C and gene expression derepressed with a final concentration of 0.2 ng/mL anhydrotetracycline (AHT; IBA GmbH, Göttingen, Germany) for 24 h. The culture was harvested

by centrifugation and the cell pellet resuspended in 50 mL lysis buffer containing 100 mM Tris-HCl, pH 8.0, 1 mM EDTA, 150 mM NaCl, 40 µg/mL lysozyme and 1% Halt Protease-Inhibitor Cocktail, EDTA-free (ThermoFisher Scientific). Mechanical lysis was carried out using a French press system (Emulsiflex-C3; Avestin Europe GmbH, Mannheim, Germany) and lysate was then centrifuged at 10,000× *g*, at 4 °C for 10 min and filtered through a 0.45 µm pore size syringe filter.

For subsequent affinity chromatography using the Äkta pure system (GE Healthcare Life Science, Munich, Germany), the cleared lysate was loaded onto 1 mL Streptactin XT columns (IBA GmbH, Göttingen, Germany), washed with 20 mL buffer W (100 mM Tris-HCl, pH 8.0, 1 mM EDTA, 150 mM NaCl) and the protein was eluted with buffer BXT (buffer W containing 50 mM biotin). After dialysis against a 1000-fold volume of HEPES buffer (50 mM HEPES, 50 mM NaCl, 5 mM EDTA, pH 7.5) using SnakeSkin 10K MWCO dialysis membrane (ThermoFisher Scientific), protein concentrations were measured with Pierce BCA Protein Assay Kit (ThermoFisher Scientific). Next, Amicon Ultra 15 Centrifugal Filters 10K MWCO (Merck KGaA) were used to adjust protein concentrations to 1 mg/mL and protein aliquots were directly stored at −80 °C until further use or first amended with 50% glycerol (final concentration) as cryo-protectant and kept at −20 °C for testing in RBP-fusion reporter assays.

2.6. SDS-PAGE and Western Blot

Protein samples were mixed with 10× NuPAGE Sample Reducing Agent (ThermoFisher Scientific) and 4× NuPAGE LDS Sample Buffer (ThermoFisher Scientific), denatured at 95 °C for 5 min and applied to a polyacrylamide gel (Novex NuPAGE 4–12% Bis-Tris protein-gel, 1.0 mm, 10-well; ThermoFisher Scientific) using a mini gel tank (ThermoFisher Scientific). SDS-PAGE was performed at 200 V for 60 min with MOPS running buffer (ThermoFisher Scientific). Then the proteins were transferred onto a 0.45 µm pore size nitrocellulose membrane (ThermoFisher Scientific) at 30 V for 75 min via semidry blotting (Novex Semi-Dry Blotter, ThermoFisher Scientific) in NuPAGE transfer buffer. Pierce Reversible Protein Stain Kit (ThermoFisher Scientific) was used to stain whole blotted protein before detection of Strep-tagged proteins, which was carried out using Strep-MAB-Classic (HRP conjugate, IBA GmbH) based chemiluminescence detection and Clarity Western ECL substrate (Bio-Rad Laboratories, Munich, Germany) according to the manufacturers' protocols. A ChemiDoc MP imaging system (Bio-Rad Laboratories) and image Lab 5.2 software (Bio-Rad Laboratories) were used for documentation.

2.7. RBP Testing for Binding to Host Cells

An overnight culture of *B. anthracis* or other Bacilli was used to inoculate 50 mL of fresh TSB in a 250 mL baffled shaking flask to an optical density (OD_{600}) of 0.05 and the culture was incubated at 37 °C and 110 rpm. For growth phase experiments starting from spores, 10^7 spores were used to inoculate 50 mL of brain heart infusion (BHI, Merck KGaA) broth containing 10% fetal bovine serum (Merck KGaA). At different time points, OD_{600} was measured and a sample taken equivalent to 100 µL of an OD_{600} of 1 (for non-germinated spores as inoculum a volume of 1 mL of the inoculated culture was used as first sample at T_0). Treatment was the same for inactivated or encapsulated *B. anthracis* cells. Samples were pelleted by centrifugation at 5000× *g* for 2 min in 1.5 mL centrifugation tubes, resuspended in 100 µL of Ringer-HEPES buffer (50 mM HEPES, 1.5 mM $CaCl_2$, 1.5 mM KCl, 100 mM NaCl, 0.6 mM $NaHCO_3$, pH 7.4) and mixed with 5 µg of purified RBP fusions. After 5 min incubation at room temperature, cells were washed once with Ringer-HEPES (5000× *g* for 2 min) and 3 µL were transferred into a well of a chamber slide with lid (µ-slide 8 Well, Ibidi GmbH, Martinsried, Germany). When encapsulated cells were tested, samples were mixed with an equal volume of ink prior to transfer to the chamber slide. For proper microscopic analysis of cells, suspensions were covered with a 1 mm thick agar-agar pad serving as a coverslip (1% molten agar-agar solidified between two microscopy slides). Samples were analyzed for cells emitting mCherry signal (extinction: 587 nm, emission: 610 nm) from bound RBP fusions using Axio Observer Z1 700 Confocal Laser Scanning Microscope (Carl Zeiss, Oberkochen, Germany).

3. Results

3.1. Cloning of Phage RBP Genes and Production of Recombinant RBP-Fusion Reporters in E. coli

When initiating this work we performed sequence similarity database searches in order to identify relatives of RBP from phages γ (protein Gp14) and Wip1 (P23) [36] and did protein sequence alignments in order to identify possible RBP of phage AP50c (Figure S1). We recognized that a hypothetical protein, BA4079, very similar to RBPγ was encoded on the *B. anthracis* chromosome located within previously identified prophage LambdaBa03 [24]. Protein alignment of BA4079 with RBPγ (Gp14) revealed amino acid (aa) identities of 83.0% (similarity 89.0%) across the entire length (500 aa) of the alignment (Figure S1). These values increased to 95.2% and 98.4% when only the *C*-terminal section of the proteins, comprising a continuous stretch without gaps of 374 aa were reanalyzed. The second information gained from this database search relevant for the study at hand, was that there is not any (hypothetical) protein encoded on the genome of phage AP50c that has significant similarity to the one identified from phage Wip1. However, we recognized a corresponding (hypothetical) polypeptide to Wip1 P24 in phage AP50c. P24 from phage Wip1 was found to be required for RBP_{Wip} (P23) activity [18]. The respective gene encoding the hypothetical AP50c protein P29 is located directly downstream of a gene for yet another hypothetical protein, P28, without any relatives in the database. When P28 (phage AP50c) was aligned with P23 (phage Wip1) the identity score was low, only 32 out of 151 aa (21.2%) with a similarity of 36.4% but featuring 52 gap positions (Figure S1). Remarkably, the first seven aa residues of both polypeptides (MGLKKPS) were a perfect match. Thus, by genomic position and the short identical stretch to P23, we selected putative protein P28 to be further studied as RBP candidate of phage AP50c.

As a basis of a versatile expression plasmid for production of fluorescent reporter fusions, a plasmid chassis was constructed. For this, the PCR-amplified gene of mCherry was cloned in *E. coli* using expression vector pASG-IBA105, which contains a *twin-strep-tag*–encoding sequence (*tst*), resulting in pASG-mCherry. The previously identified RBP genes from phages Gamma and Wip1, as well as putative RBP genes from phage AP50c and prophage λ03 were PCR-amplified from genomic DNA and inserted in-frame downstream to the fluorescent protein gene in vector pASG-mCherry, to yield a set of plasmids of the following composition; pASG::*tst*::*mCherry*::$RBP_{\gamma/Wip/AP50/\lambda03}$. In case of constructs harboring RBP from phages Wip1 and AP50c the gene downstream of the RBP gene on the phage genome was cloned as a transcriptional fusion to the RBP gene. This is because in a previous study the necessity of this adventitious protein for RBP function has been demonstrated [18]. Thus, if not stated otherwise for $RBP_{Wip/AP50}$ the term RBP comprises two polypeptides in our study (P23+P24 for phage Wip1 and P28+P29 for phage AP50c). Nevertheless, we also included production of P23 or P28, respectively, alone in plasmids pASG::*tst*::*mCherry*::$P23_{Wip}$/$P28_{AP50}$. Also, we included 5′-truncated versions of the $RBP_{\lambda03}$ gene. Aiming at improving solubility of the corresponding protein, coding regions of the following peptides were cloned as well: $RBP_{\lambda03\Delta1\text{-}120}$, $RBP_{\lambda03\Delta1\text{-}139}$, $RBP_{\lambda03\Delta1\text{-}316}$, $RBP_{\lambda03\Delta1\text{-}342}$. All fusion proteins were produced in *E. coli* ArcticExpress, as other *E. coli* expression strains tested were found to produce insoluble proteins mostly incorporated into inclusion bodies. Sizes of fusion proteins purified by affinity chromatography were confirmed by Western blotting as shown in Figure 1 and Figure S2.

Protein yield of RBPγ was low, most of the protein was found as insoluble inclusion bodies. Proteins could also be obtained for $RBP_{\lambda03\Delta\ 1\text{-}139}$, $RBP_{\lambda03\Delta1\text{-}316}$, and $RBP_{\lambda03\Delta1\text{-}342}$ (Figure S2) as well as for P23 and P28 alone. Truncated $RBP_{\lambda03\Delta1\text{-}120}$ was soluble and gave higher protein yields than full-length $RBP_{\lambda03}$ (Figure 1). A minor degradation signal was detected for this $RBP_{\lambda03\Delta1\text{-}120}$ by protein staining (Figure 1a). This byproduct lacked a TST epitope because it was not visible after TST detection (Figure 1b). A faint smaller-sized degradation product of $RBP_{\lambda03\Delta1\text{-}120}$ featuring the TST was observed by Western blotting (Figure 1b). More prominently degraded TST-labeled RBP reporters were detected for $RBP_{\lambda03}$ and RBPγ (Figure 1b).

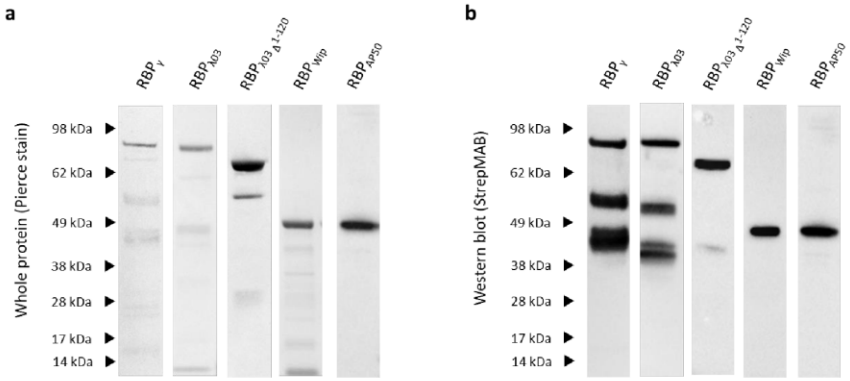

Figure 1. Western blot of heterologously produced RBP-fusion reporter proteins. Affinity purified proteins were subjected to SDS-PAGE, stained (Pierce stain) after transfer onto a nitrocellulose membrane (**a**) and the TST epitope detected using a HRP-conjugated TST-antibody (StrepMAB) (**b**). Expected sizes of RBP mCherry reporters: RBP_{γ} 88 kDa, $RBP_{\lambda 03}$ 88 kDa, $RBP_{\lambda 03\Delta 1\text{-}120}$ 74 kDa, RBP_{Wip} 44 kDa, RBP_{AP50} 46 kDa. Letters indicate the size-positions of the protein size marker (SeeBlue Plus2 prestained, ThermoFisher Scientific, Darmstadt, Germany).

3.2. (Pro)-Phage RBP Bind to Bacillus anthracis Cells

The RBP fusion proteins were next tested for their abilities to bind to *B. anthracis* cells, especially with regard to putative RBP_{AP50} P28(+P29), as the RBP of phage AP50c has not been identified thus far. A second emphasis was on putative $RBP_{\lambda 03}$ and its truncated derivatives. For testing of RBP binding, 2–3 h old vegetative cultures of *B. anthracis* CDC 1014 were used. The $RBP_{\lambda 03}$ reporter showed binding to *B. anthracis* as microscopically detectable fluorescence and cell surfaces were visibly labeled (Figure 2). Of the deliberately truncated $RBP_{\lambda 03}$ only $RBP_{\lambda 03\Delta 1\text{-}120}$ was able to bind to cells (Figure 2). Binding to cell surfaces of this truncated $RBP_{\lambda 03\Delta 1\text{-}120}$ was stronger than that of the full-length parent $RBP_{\lambda 03}$ (Figure 2). Related RBPγ reporter also yielded signals, however, similar to full length $RBP_{\lambda 03}$ most of the protein was found in insoluble inclusion bodies. Thus, further testing of low-yield RBPγ and $RBP_{\lambda 03}$ as well as of non-binding derivatives $RBP_{\lambda 03\Delta 1\text{-}139}$, $RBP_{\lambda 03\Delta 1\text{-}316}$ and $RBP_{\lambda 03\Delta 1\text{-}342}$ was abandoned in favor of the other RBP reporters including $RBP_{\lambda 03\Delta 1\text{-}120}$.

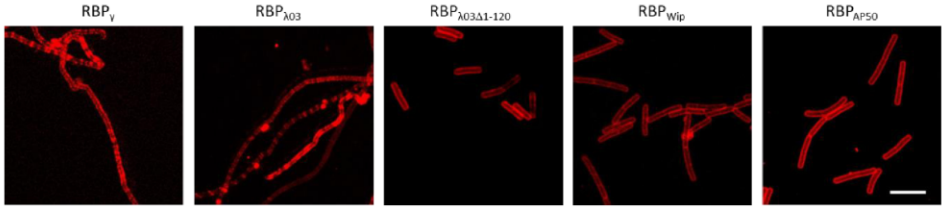

Figure 2. Representative fluorescent microscopy detection of *B. anthracis* cells using RBP reporters. Cultures of *B. anthracis* CDC 1014 were grown for 2–3 h, washed with HEPES-Ringer-buffer, mixed with RBP, washed again to remove unbound RBP and subjected to fluorescence microscopy. Shown are mCherry-RBP reporters of phage Gamma (RBP_{γ}), prophage LambdaBa03 ($RBP_{\lambda 03\Delta}$ and truncated $RBP_{\lambda 03\Delta 1\text{-}120}$), phage Wip1 ($RBP_{Wip}$) and phage AP50 ($RBP_{AP50}$). Scale bar: 10 µm.

Fluorescent labeling of *B. anthracis* cells was also achieved for RBP_{AP50} P28(+P29) (Figure 2), which supported our initial hypothesis that P28(+P29) is the actual RBP of phage AP50c. When AP50c P28 was tested by itself (and also when Wip1 P23 was tested by itself) only a very weak binding signal was observed (Figure S3) and thus, P28 and P23 alone were also abandoned for further testing. These results suggest P29 playing a pivotal role for proper function of P28 as RBP. Also, Figure 2

supports our hypothesis that locus *BA4079* of prophage Lambda03 encodes for a RBP ($RBP_{\lambda 03}$) and that its truncated derivative $RBP_{\lambda 03;\ \Delta 1\text{-}120}$ functions as a *B. anthracis* reporter.

3.3. Binding of (Pro)-Phage RBP to B. anthracis Cells Is Growth Phase Dependent

During the initial RBP reporter binding experiments we observed that RBP fusion proteins exhibited variations in their binding patterns. We reasoned this is most likely dependent on the host's growth phase since we did not use synchronized *B. anthracis* cultures in initial binding experiments. In particular, $RBP_{\lambda 03\Delta 1\text{-}120}$ fusion proteins showed declining binding signals on cell surfaces of *B. anthracis* CDC 1014 or Sterne the longer cultures grew (Figures 2 and 3). To investigate this observation in more detail, growth experiments were carried out for *B. anthracis* CDC 1014 or Sterne cultures starting from spores. Since spores need time to germinate, differences in RBP binding patterns should occur as a function of cultivation time. RBP binding was monitored from culture samples taken at intervals of typically 30 min during a period of 0 to 8 h including a final 24 h sample.

From the micrographs depicted in Figure 3 (time point T_0 min), it can be seen that none of the RBP fusion reporters of (pro)-phages AP50c, LambdaBa03 or Wip1 showed any detectable fluorescence signals when tested on non-germinated spores. It is thus likely that RBP do not bind to spores under the conditions tested. This finding was corroborated by incubating these RBP reporters with spores of *B. anthracis* Sterne and *B. cereus* strains 10987 and 4342 as well as *B. thuringiensis* 10792.

Conversely, all RBP reporters produced significant fluorescent signals on cell surfaces of germinated *B. anthracis* spores at the latest after 120 min, with the $RBP_{\lambda 03;\ \Delta 1\text{-}120}$ fusion being the only one that already showed binding after 90 min. The $RBP_{\lambda 03\Delta 1\text{-}120}$ reporter reached maximum binding signal after 120 min, whereupon the signal remained strong, decreasing after 180 min and was no longer detectable after 240 min. However, this complete lack of binding in later growth phases did not occur in each growth experiment conducted. If, for example, vegetative cells of an overnight culture were inoculated instead of spores, the signal was also retained in later phases and even after 24 h, which was certainly due to the unsynchronized cell division.

For the RBP_{AP50} reporter, the first fluorescence signal on germinating spores was detected after 120 min, which continuously intensified and reached its peak after about 180 to 240 min, whereupon it remained constant for several hours and only became slightly weaker between 8 and 24 h.

A similar fluorescence signal pattern was observed when RBP_{Wip} was tested. The strongest binding signal was scored 180 to 240 min after germination was initiated. In the further course the signal became significantly weaker between 8 and 24 h (Figure 3) and featured incompletely distributed, patchy fluorescence signals on the cell surfaces (e.g., RBP_{Wip} at 480 min; also compare Figure 2). This "tiger stripes" pattern also appeared yet more weakly on ageing cells labeled with RBP_{AP50} or $RBP_{\lambda 03\Delta 1\text{-}120}$, respectively.

In order to show the temporal RBP binding pattern on *B. anthracis* cells in a semi-quantitative manner, we next correlated RBP reporter signal strength with *B. anthracis* growth phases during growth experiments (growth curves). Analysis showed that all three RBP reporters feature maximum binding to host cells via fluorescence during logarithmic growth phase of *B. anthracis* cultures (Figure 4). The earliest response exhibited the $RBP_{\lambda 03\Delta 1\text{-}120}$ reporter from early to mid-logarithmic growth phase (Figure 4), the latest, RBP_{Wip}, peaking near the end of logarithmic growth (Figure 4). In contrast, the RBP_{AP50} reporter yielded measurable signals from the mid-logarithmic growth phase, climaxing at late logarithmic-phase to early stationary phase yet remained clearly detectable until the end of the experiments (Figure 4). Thus, it appears that the RBP_{AP50} reporter was the most versatile for this RBP recognized cells in the widest range of growth phases, except spores and freshly germinated spores (<2 h) (compare Figure 3, e.g., RBP_{Wip} at 480 min).

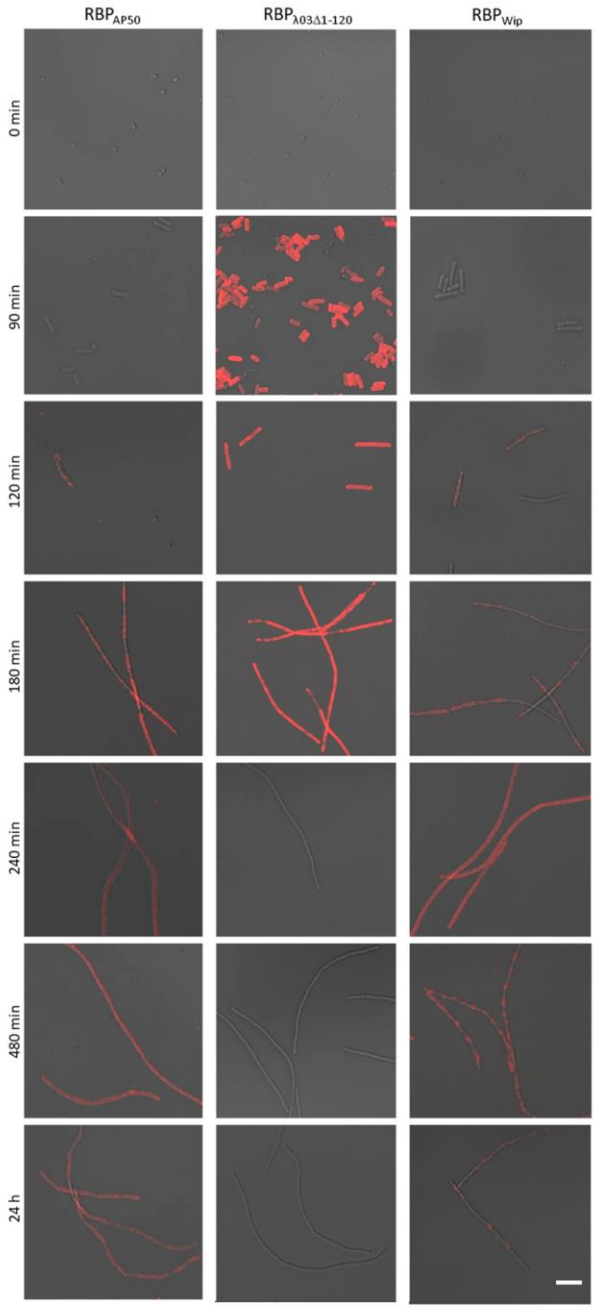

Figure 3. Binding of red-fluorescent RBP reporters to *B. anthracis* cells at different time points during culture growth phases. Tested were germinating *B. anthracis* Sterne spores over a period of 24 h. Representative time points are shown for binding of the three reporters RBP$_{AP50}$, RBP$_{\lambda03\Delta1\text{-}120}$ and RBP$_{Wip}$ recorded in merged light and fluorescence channels. Scale bar: 10 μm.

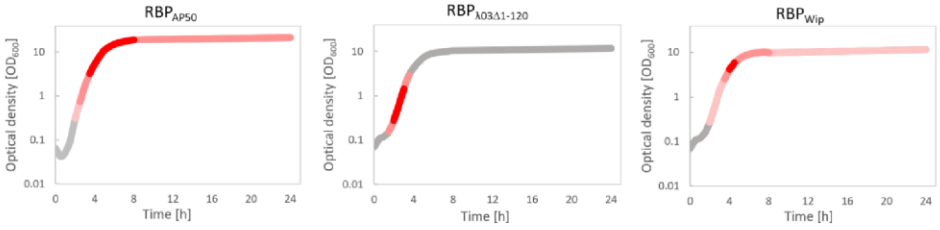

Figure 4. Binding of RBP reporters to *B. anthracis* cells varies between RBP of different phages but yields strongest signals during logarithmic growth phase of host cells. Growth experiments were started from germinating *B. anthracis* Sterne spores and the growth phase was derived from recordings in optical cell densities at 600 nm (OD_{600}). Binding strengths of reporters RBP$_{AP50}$, RBP$_{\lambda 03\Delta 1\text{-}120}$ or RBP$_{Wip}$ are indicated by colored sections of the growth curves: grey = no binding, light red = weak RBP binding, i.e., either only sporadic binding and/or binding to only a few areas of the cell surface. red: distinct RBP binding (easily recognizable binding to the majority of all cells). dark red = very strong RBP binding ((almost) all cells exhibit very intense fluorescence signals).

Next, we compared these results with that of not-synchronized cultures featuring cells of different growth phases. In contrast to that of synchronized cultures, the results here were quite erratic, as would be expected. Some patterns, however, emerged. Binding of the RBP$_{Wip}$ reporter was maximum at the start of the cultures and after 3 to 5 h. RBP$_{\lambda 03\Delta 1\text{-}120}$ recognized cells best between 1 and 2.5 h. Binding of RBP$_{AP50}$ was most constant; weaker signals were obtained only around 3 h, 7 h and after 24 h. In contrast to synchronized cultures, weak fluorescence signals could be obtained at any time using any of the three RBP reporters on non-synchronized cultures.

3.4. Inactivated Cells of B. anthracis Can Be Labeled With (Pro)-Phage RBP Reporters

Often times it is not possible to work with live cultures of *B. anthracis* e.g., in field laboratory settings lacking required equipment or in the absence of a fluorescence microscope in BSL-3 facilities. Also, mindful of laboratory work safety, we were curious whether it was possible to use the RBP reporters on inactivated *B. anthracis* cells. To test this, we evaluated different in-house validated *B. anthracis* inactivation regimens for suitability of subsequent RBP reporter binding on inactivated cells of *B. anthracis* strains Sterne or CDC1014. Cultures were inactivated either by heat, formaldehyde or peracetic acid.

Cells inactivated by heat yielded strong fluorescence signals upon binding of the RBP$_{AP50}$ and RBP$_{\lambda 03\Delta 1\text{-}120}$ reporters similar to fluorescence levels of non-inactivated cells. Conversely, heat-inactivated cells were only poorly labeled by the RBP$_{Wip}$ reporter (Figure 5). Similarly, formaldehyde-inactivation did not prevent the binding of the RBP$_{AP50}$ and RBP$_{\lambda 03\Delta 1\text{-}120}$ reporters but the RBP$_{Wip}$ reporter did not bind. In contrast, inactivation with peracetic acid yielded fluorescence signals for all three RBP reporters upon binding to inactivated cells, however, of lower intensities than the controls (Figure 5). Nevertheless, this line of experiments made possible the further use of inactivated *B. anthracis* cells and of inactivated cells of other pathogenic Bacilli.

Thus, we then tested binding of the RBP reporters on inactivated cells of fully virulent *B. anthracis* isolates of risk group 3 (RG 3) from our collection. These strains were of diverse phylogenetic composition from all three major branches A, B and C [37]. RBP reporter binding was done on overnight cultures and on fresh, 4 h old cultures inoculated thereof. Cultures of RG 2 strains were inoculated under the same conditions as controls as some of these strains have been used for the experiments described above. All RG 3 strains were successfully labeled by the three RBP reporters yet with different signal strengths (Table 2).

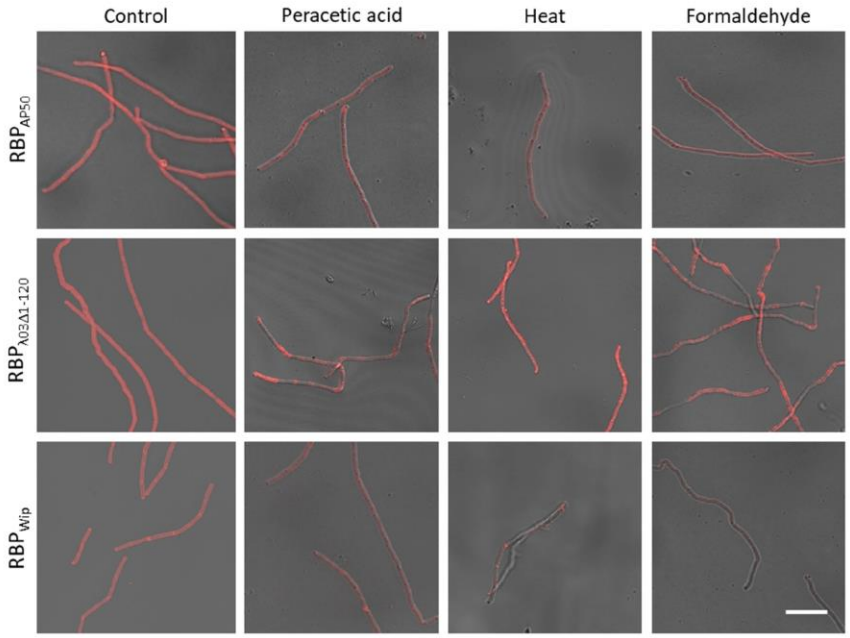

Figure 5. Binding of RBP reporters to inactivated cells of *B. anthracis* CDC1014. Cells were either inactivated by heat, formaldehyde or peracetic acid treatment. Inactivated cells or live control cells (from the same culture) were incubated with RBP reporters (RBP$_{AP50}$, RBP$_{\lambda03\Delta1\text{-}120}$ or RBP$_{Wip}$) and subjected to fluorescence microscopy. Representative micrographs recorded as merged light and fluorescence channels are shown. Scale bar: 10 μm.

Table 2. Labeling of RG-3 *B. anthracis* cells with RBP reporters [1].

Cultures of Peracetic Acid-Inactivated *B. anthracis* Strains RG-3 (RG-2)	Phylogenetic Group	RBP$_{AP50}$	RBP$_{\lambda03\Delta1\text{-}120}$	RBP$_{Wip}$
(CDC 1014)	A.Br.WNA	+++	+++	+++
(Sterne 34F2)	A.Br.001/002	+++	+++	+++
Vollum	A.Br.Vollum	++	+++	++
188678-1	A.Br.Aust94	+++	+++	+++
Ames	A.Br.Ames	+++	+++	+++
A0777	A.Br.WNA	++	+++	+++
BF-1	B.Br.CNEVA	++	+++	++
SA020	B.Br.Kruger	++	+++	++
A1074	C.Br.	+	++	+

[1] Cultures were tested for binding of RBP reporters after 4 h of growth and overnight culture with similar results. (+): weak RBP binding, i.e., either only sporadic binding and/or binding to only a few areas of the cell surface; (++): distinct RBP binding, i.e., easily detectable binding to the majority of cells; (+++): very distinct RBP binding, i.e., almost all or all cells with very intense fluorescence signal.

Most strains yielded strong fluorescent signals for any of the three reporters, yet cells of the C-branch isolate A1074 were labeled less efficiently. Also, cells of B-branch strains seemed to be accessible to the three RBP reporters, though binding of RBP$_{\lambda03\Delta1\text{-}120}$ was more efficient than binding of RBP$_{AP50}$ or RBP$_{Wip}$. A similar pattern was observed for A-branch strain Vollum (Table 2).

3.5. Encapsulated Cells of Bacillus anthracis Can Be Labeled with (Pro)-Phage RBP Reporters

When grown in host mammals, *B. anthracis* produces a poly-D-glutamyl capsule for averting the host's immune response. We tested thus to which extend this capsule would hinder penetration and

binding of RBP reporters to *B. anthracis* cells. For this, pXO2 (capsule) positive *B. anthracis* strain Ames and the other six RG-3 strains from Table 2 were grown under capsule inducing conditions, after 4 h of growth in fresh inducing culture, cells were inactivated using peracetic acid and negative-stained with ink. The three RBP reporters were added and samples subjected to fluorescence microscopy. Figure 6 shows that the capsule did not prevent cell labeling by the three RBP reporters. All samples gave strong fluorescence signals, clearly showing binding of the RBP reporters amidst the capsule and the bacterial cell as exemplified by the Ames strain (Figure 6). Even the largest of the three RBP reporters, $RBP_{\lambda 03\Delta 1\text{-}120}$, was able to label encapsulated cells.

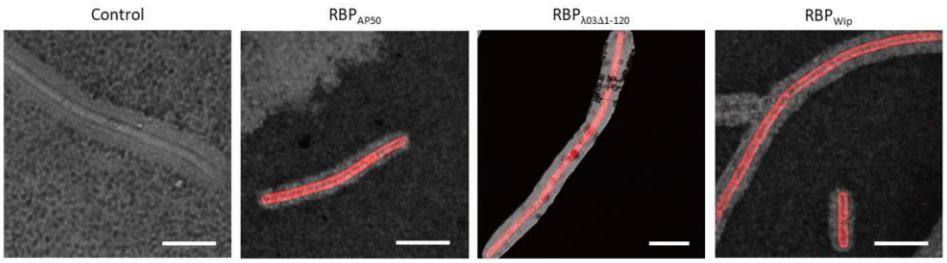

Figure 6. Binding of RBP reporters to encapsulated cells of *B. anthracis*. Fresh cultures of *B. anthracis* strain Ames inoculated from overnight cultures were grown for 4 h under capsule-inducing conditions and then inactivated by peracetic acid treatment. Cells were incubated with RBP reporters (RBP_{AP50}, $RBP_{\lambda 03\Delta 1\text{-}120}$ or RBP_{Wip}) or no RBP (control) and subjected to fluorescence microscopy in the presence of negative-staining ink. Representative micrographs were recorded as merged light and fluorescence channels. Scale bars: 10 μm.

Care had to be taken when adjusting the ink concentration, otherwise capsule visualization by negative staining with black ink eclipsed fluorescence signals noticeably. Notwithstanding this caveat, this line of experiments clearly demonstrated that all three RBP reporters, RBP_{AP50}, $RBP_{\lambda 03\Delta 1\text{-}120}$ and RBP_{Wip} were capable of labeling encapsulated cells of *B. anthracis*.

3.6. Binding of (Pro)-Phage RBP Is Specific to B. anthracis Cells

Next, we determined RBP reporter binding to a panel of *Bacillus* strains closely related to *B. anthracis*. Of 56 non-*anthracis Bacillus* ssp. tested, most (42%) did not bind any of the three RBP reporters at all and a small number (12%), only very weakly (Table 3; Figure 7). Three strains (*B. cereus* 3094, *B. paranthracis* 2002 and *B. weihenstephanensis* B0293) were significantly labeled by the $RBP_{\lambda 03\Delta 1\text{-}120}$ reporter, yet clearly yielding a weaker signal than *B. anthracis* host cells, even distinct from signals of cells of rare *B. anthracis* C-branch strain A1074 (Figure 7). Cells of a single one of these strains (*B. cereus* 3094) was also markedly labeled by RBP_{AP50} and RBP_{Wip} reporters. Again higher fluorescence signals upon RBP reporter binding were observed when *B. anthracis* cells (even the few colored cells of C-branch strain A1074 were more uniformly labeled) were used as positive control hosts (Table 3; Figure 7). Thus, from analysis of Table 3 and mindful of the results depicted in Figure 7 we suggest specificities of the RBP reporters may be as high as 98% (1 false positive out of 56 non-*anthracis* Bacilli) for RBP_{AP50} (*B. cereus* 3093) and RBP_{Wip} (*B. cereus* 2700) or 95% (three false positives out of 56 non-*anthracis* Bacilli) for $RBP_{\lambda 03\Delta 1\text{-}120}$ (*B. cereus* 3094, *B. weihenstephanensis* B0293 and *B. paranthracis* 2002).

Table 3. Labeling of *Bacillus* spp. cells with RBP reporters [1].

Species Strain	RBP_{AP50}	$RBP_{\lambda 03\Delta 1\text{-}120}$	RBP_{Wip}
B. anthracis Sterne 34F2	+++	+++	+++
B. anthracis A1074	+	++	+
B. cereus 3094	+	++	+
B. cereus 2700, 3093	+	−*	+
B. cereus ATCC 706, ATCC 4342 [2], ATCC 10987, DSM 2302, 2832	−	+	−
B. cereus ATCC 312	−	−*	−
B. cereus ATCC 14579, ATCC 2787, ATCC 3301, DSM 345, 288, 1356, 2690, 2698, 2815, 2830, 2856, 2866, 2868, 2892, 2893, 2894, 2895, 2896, 2897, 2899, 2900, 2901, 2902, 2903, 2904, 2905, 3045, 3068, 3080, 3090, 3092, 3095, 3096, 3097, 3098, 3109	−	−	−
B. thuringiensis ATCC 10792, DSM 2046	−	+	+
B. thuringiensis ATCC 336, ATCC 33679	−	−*	−
B. thuringiensis Berliner 1915, sv. Tolworthi	−	−	−
B. paranthracis 2002	−	++	−
B. weihenstephanensis B0293	−	++	−
B. mycoides NCTC 2603, B 732	−	−	−
B. megaterium ATCC 14581, MS941	−	−	−
B. subtilis ATCC 6091	−	−	−

[1] Cultures were tested for binding of RBP reporters after 2 (RBP_{AP50} and RBP_{Wip}) and 4 h ($RBP_{\lambda 03\Delta 1\text{-}120}$) of growth. (−): no RBP binding; (−*) few weakly labeled cells; (+): weak RBP binding, i.e., either only sporadic binding and/or binding to only a few areas of the cell surface; (++): distinct RBP binding, i.e., easily detectable binding to the majority of cells; (+++): very distinct RBP binding, i.e., almost all or all cells with very intense fluorescence signal. [2] is a known host of phage γ [18].

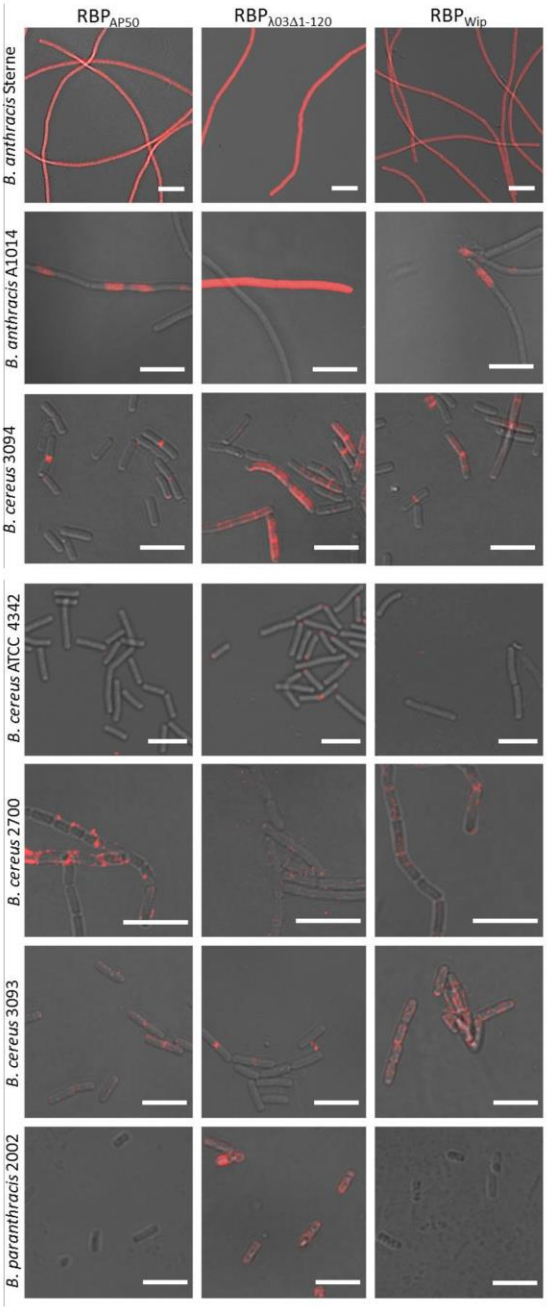

Figure 7. Binding of RBP reporters to cells of non-*anthracis* bacilli. Fresh cultures inoculated from overnight cultures of representative strains from Table 3 were grown for 2 (for labeling with RBP$_{\lambda 03\Delta 1\text{-}120}$) or 4 h (for labeling with RBP$_{AP50}$ or RBP$_{Wip}$), incubated with RBP reporters (RBP$_{AP50}$, RBP$_{\lambda 03\Delta 1\text{-}120}$ or RBP$_{Wip}$) and subjected to fluorescence microscopy. Representative micrographs were recorded as merged light and red fluorescence channel. Cells of *B. anthracis* Sterne and A1014 served as genuine positive examples. Scale bars: 10 µm.

4. Discussion

The confirmatory specific identification of *B. anthracis* is often achieved by means of antigen–antibody interaction, be it in the form of enzyme-linked immunosorbent assays (ELISA) [38], lateral flow assays [39,40] or by the use of fluorescently labeled antibodies in microscopy [41] (further alternative detection techniques for *B. anthracis* are reviewed in a contribution to the special issue "An Update on Anthrax" of Microorganisms [42]). The direct fluorescent-antibody (DFA) assay [41] may be seen as being related to the study at hand insofar as both methods take advantage of fluorescence reporters for detecting presumptive *B. anthracis* cultures and thus helping confirming the identity of this notorious biothreat agent. In contrast to RBP fused to fluorescent protein for visual labeling of target cells, recognition via DFA was achieved using two fluorescent dye-labeled monoclonal antibodies, one specifically directed to the galactose/*N*-acetylglucosamine polysaccharide cell wall antigen, the other one recognizing the capsule antigen. Only when these two antibody reporters were combined, the DFA assay reached high specificity. Of 230 *B. anthracis* isolates tested 227 were positive (99% specificity) and 56 of 56 non-*anthracis Bacillus* strains were found to be negative. This DFA assay is fast, taking less than 1 h for completion [41], thus requiring only moderately more time than the RBP reporter assay described here (see graphical abstract for a visualization of the timescale of the assay).

The use of RBP (and other phage-derived proteins) for detection and identification of bacteria is not a new methodology; its utility has been extensively reviewed [13,43,44]. Depending on the specificities of utilized phage proteins, RBP can even be used for the identification and separation of different isolates of the same species according to different O-antigens on the surface of *Listeria monocytogenes* cells [45]. The situation might be viewed as similar to the situation of *B. anthracis* within the *B. cereus s.l.* group of bacteria. Taking into account the very close genetic relationship of *B. anthracis* to *B. cereus*, *B. anthracis* may also be considered a subspecies within the *B. cereus s.l.* group [46]. Thus, our RBP reporters would detect a subspecies as well, in this case *B. anthracis*.

In contrast to the canonical *B. anthracis* typing phage γ [21], phage Wip1 showed no binding to cells of an untypical strain of *B. cereus* (strain ATCC 4342) [18,22]. This result correlates with our findings regarding lack of recognition of RBP_{Wip} to cells of this *B. cereus* isolate. Kan et al. (2013) in their infection and adsorption tests showed affinity of the Wip1 phage for the *B. cereus* CDC 2000032805 strain [47], which is also a host for the γ phage [18]. Since this *B. cereus* CDC 2000032805 strain was not available to us, RBP reporter binding to this strain could not be tested and thus we were not able to assess if RBP_{Wip} (or RBP_{AP50}) would merely show marginal binding as did a small group of the other Bacilli tested (Table 3) or whether this untypical host would be recognized as efficiently as *B. anthracis*. However, recognition of phage Wip1 RBP proteins P23(+P24) to cells of strain CDC2000032805 was shown previously as a patchy fluorescence pattern [18]. Thus, strain CDC2000032805 must be added to list of *B. cereus s.l.* strains able to be partly recognized by RBP_{Wip}.

Phage AP50c infected 111 of 115 tested *B. anthracis* strains (~97%) except for e.g., a Sap mutant of Sterne strain and none of 100 *B. cereus sensu lato* strains [17]. Remarkably, in the same study two out of three different Vollum derivatives also were insensitive to phage AP50c. With today's knowledge on the receptor of phage AP50 [31], these are derivatives that have likely lost their S-layers. Later, two additional *B. cereus* strains were found to be sensitive to phage AP50c, *B. cereus* RS438 (CDC2000032805) and *B. cereus* RS756 (better known as E33L ZK; Zebra Killer [48]), with efficiencies of plating reduced by about one third compared to a *B. anthracis* Sterne derivative host. Two additional strains (*B. thuringiensis* serovar *pulsiensis* BGSC 4CC1 and *B. thuringiensis* serovar *monterrey* BGSC 4AJ1) allowed adsorption of the phage but not propagation. In contrast, *B. cereus* ATCC 4342 sensitive to phage γ, was insensitive to phage AP50c [31]. In the same study, Sap was identified as likely receptor of phage AP50 [31]. This finding was supported by a parallel study in which by analysis of mutants that failed to support AP50 propagation, the CsaB protein was found to be required for phage AP50 host recognition and adsorption. CsaB is required for cell-surface anchoring of the S-layer and thus including Sap [30]. Our and earlier observations [18] of "tiger stripes" binding patterns of RBP reporters (Figure 3) that depend on host cell growth phases support earlier notions [18]. In their thorough characterization of the

phage Wip1 genome and several protein functions, the authors suspected a temporal change in S-layer proteins Sap to EA1 (extractable antigen 1 encoded by the *eag* gene) when cultures of *B. anthracis* exit from logarithmic into stationary phase [49,50] and that this was the underlying reason for diminished binding of RBP P23 in their study [18].

Likely, the Sap protein may also be the reason why *B. cereus* strains 2700, 3093 and 3094 cross-reacted weakly with our AP50 and Wip reporters (Table 3). Some *B. cereus* strains possess Sap proteins that have a high similarity to Sap of *B. anthracis* [31]. Likewise, binding of $RBP_{\lambda 03\Delta 1\text{-}120}$ reporter to several *B. cereus* strains (Table 3) may be based on similarities of their GamR receptor (i.e., the receptor of phage γ and likely also the receptor for $RBP_{\lambda 03}$) with that of *B. anthracis* [29]. Because RBP reporter binding is dependent on the presence of the cognate receptors (Sap or GamR, respectively) on the bacterial host cell surface, recognition is not dependent on the presence or absence of *B. anthracis* virulence plasmids (pXO1 and pXO2). Thus, *B. cereus* strains harboring such plasmids [1] cannot *per se* be expected to be labeled by the RBP reporters. Conversely, the rather weak binding of RBP reporters to cells of rare *B. anthracis* C-branch strain A1074 may be linked to the overall poor growth of this strain in our hands on both solidified and liquid media.

Interestingly, phage Bam35, a Tectivirus of *B. thuringiensis* genomically closely related to phages Wip1 and AP50 does not encode for proteins related to P23 or P28, respectively [51]. Attempts to identify the RBP of this Bam35 phage have thus far been unsuccessful. The protein encoded by a gene occupying the same location on the phage Bam35 genome (P29) as P23/P24 (of phage Wip1) [18] or P28/P29 (of phage AP50) did not bind to host cells, though this protein is very likely positioned on the surface of Bam35 virons [52]. Instead this phage seems to utilize different means of host cell recognition. Experiments with peptidoglycan isolated from Bacilli and *E. coli* demonstrated that *N*-acetyl-muramic acid in the bacterial cell wall is required for binding of phage Bam35 [52]. Thus, even in genomically closely related *Bacillus* Tectivirus phages it is not always that straightforward to identify (i) the phage RBP and (ii) the cellular receptor recognized by this RBP.

Though we abandoned early experiments with phage γ RBP (Gp14) reporters because of protein yield and solubility issues, this protein nevertheless bound to cells of *B. cereus* ATCC 4342 (Figure S4). This result agrees with earlier results on a different host cell wall binding protein, the endolysin PlyG of phage γ [53]. This PlyG is produced from phage-infected cells right before new virions are to be released from the dying host cell. PlyG depolymerizes the peptidoglycan from within after PlyG is transported across the cytoplasmic membrane. However, PlyG can also act from without, digesting the *B. anthracis* cell wall when added to growing cells [53]. The authors found PlyG to be highly specific for *B. anthracis* cells; only two non-B. *anthracis* Bacilli were targeted: strain *B. cereus* RSVF1 (identical to strain 4342 [53]) and *B. cereus* ATCC 10987. These two were among the isolates our $RBP_{\lambda 03\Delta 1\text{-}120}$ reporter recognized weakly (Table 3; Figure 7). Though endolysins are typically investigated for as alternative antimicrobial compounds [54], the terminal cell wall binding domain (CBD) of PlyG was later used for *B. anthracis* detection as a bioprobe [55]. The bioprobe assay was tested for specificity on two *B. anthracis* and 17 *Bacillus* spp. strains, however, atypical *B. cereus* strains such as strain 4342 were not included. Notably, and in concurrence with our results using RBP reporters for detection of *B. anthracis*, PlyG-CDB was able to detect encapsulated cells, however, spores were not detected unless germination was induced first. While this PlyG-CBD detection seemed to be specific, the detection assay took a couple of hours to complete [55]. This PlyG-based detection assay was later further developed by shortening the PlyG-CDB down to 20, 15 or 10 aa residues and by including attached fluorescent Qdots for microscopic analysis. Remarkably, even the shortest derivative was able to bind to *B. anthracis* Sterne cells but not to cells of three other *B. cereus s.l.* strains tested [56]. However, similar to our $RBP_{\lambda 03}$ reporter, cells of *B. cereus* strain 4342 were also labeled. Further, while our new RBP reporter assays take about 10 min to perform from harvesting cell cultures to fluorescence microscopy (see graphical abstract for details), PlyG-Qdots detection took at least 3 h because two 90 min incubation steps are required [56].

In order to accelerate phage-based detection and identification of *B. anthracis* such methods have also seen significant improvements. One is combining phage-amplification in its natural host coupled with phage nucleic acid amplification by PCR [57]. This assay can be expected to be as specific as the classical plaque assay for the oligonucleotide primers used were tested for specificity against a DNA negative panel. A short phage propagation period is followed by signal (DNA) amplification by real time PCR. This approach shortened the total assay time to about 5 h (including 4 h of growth of host and phage) [57]. The host-mediated phage amplification/PCR amplification hybrid identification approach has recently seen methodological improvements. In an improved technique named phage-mediated molecular detection (PMMD) a short incubation period of bacterial host culture (*Staphylococcus aureus* or *B. anthracis*) with a species-specific phage is followed by RNA extraction and reverse transcription PCR (RT-PCR) on specific phage transcripts [58]. The authors thus took advantage of the high number (relative to DNA) of phage RNA molecules produced per infected cell, which can be expected to far exceed the number of nascent phage DNA genomes. Indeed, the concentration of phage RNA after host infection was sufficient for the generation of strong signals. In this assay *B. anthracis* was grown prior to RT-PCR for 3 h without phage followed by an infection phase of about 13 min and RNA-preparation. A further advantage of this technique is that it can be coupled to antibiotic susceptibility testing [58]. Nevertheless, in contrast to the new RBP reporter assay, *B. anthracis* detection by PMMD requires growth of live bacteria not always possible, especially in field settings [59], whereas RBP reporters introduced here, may be also used on inactivated cells if required.

5. Conclusions

In this work, we developed RBP proteins of several (pro)-phages of *B. anthracis* into microscopy-based detection tools. In doing so we identified two new RBP from phage AP50c and chromosomally integrated prophage LambdaBa03. Detection can be achieved within about 10 min when live cells of *B. anthracis* are used, yet the assay also works very well on inactivated and on encapsulated cells. The assay is very specific, especially in the case of the RBP reporters constructed from RBP of phages AP50c and Wip1, while $RBP_{\lambda 03\Delta 1\text{-}120}$ exhibited a slightly broader host range basically following the specificities of their parental phages. Of note, however, our RBP reporter assay is a qualitative rather than a quantitative detection method requiring a fluorescence microscope. Because of its rapidity and specificity we envision this RBP reporter assay to be able to supplant the original phage based plaque-assay for confirmative pathogen identification in laboratories with access to fluorescence microscopy.

Supplementary Materials: The following are available online at http://www.mdpi.com/2076-2607/8/6/934/s1, Figure S1: Protein sequence alignments of RBP and accessory proteins of *Bacillus anthracis* phages Wip1 AP50 and prophage lambdaBa03; Figure S2: Pierce stain of heterologously produced additional or truncated RBP reporter fusions; Figure S3: Binding of different fluorescent RBP reporter fusions to *B. anthracis* cells; Figure S4: Binding of RBPγ reporter to *B. cereus* ATCC4342 cells.

Author Contributions: Conceptualization, G.G.; investigation, P.B., I.W., L.B., L.R., A.C.J., C.T. and J.P.; methodology, P.B. and G.G.; formal analysis and validation, P.B., I.W., L.B., L.R. and G.G.; resources, G.G.; data curation, P.B., I.W., L.B., L.R. and G.G.; writing—original draft preparation, P.B. and G.G.; writing—review and editing, P.B., I.W., L.B., L.R., A.C.J., C.T., J.P. and G.G.; visualization, I.W., L.R., P.B. and G.G.; supervision and project administration, P.B. and G.G.; funding acquisition, G.G. All authors have read and agreed to the published version of the manuscript.

Funding: This research was funded by funds from the Medical Biological Defense Research Program of the Bundeswehr Joint Medical Service.

Acknowledgments: The authors thank Vincent A. Fischetti (Rockefeller University New York, USA) for phage Wip1, Shanmuga Sozhamannan (Defense Biological Product Assurance Office, CBRND-EB, JPEO, Frederick, USA) for phage AP50c, Les Baillie (Cardiff University, UK) for strain *B. cereus* 4342, Erwin Märtlbauer (Ludwig-Maximilians-University Munich, Germany) and Monika-Ehling Schultz (University of Veterinary Medicine, Vienna, Austria) for several *B. cereus* strains, as well as Paul Keim (Northern Arizona University, Flagstaff, USA), Miriam Koene (Wageningen University and Research, Lelystad, Netherlands), Franz Allerberger (Austrian Agency for Health and Food Safety, Vienna, Austria) and Wolfgang Beyer (Hohenheim University, Stuttgart, Germany) for the gift of *B. anthracis* strains. Thanks are due to Linda Dobrzykowski for technical assistance.

Conflicts of Interest: The authors declare no conflict of interest. Opinions, interpretations, conclusions, and recommendations are those of the authors and are not necessarily endorsed by any governmental agency, department or other institutions. The funders had no role in the design of the study; in the collection, analyses, or interpretation of data; in the writing of the manuscript, or in the decision to publish the results.

References

1. Patino-Navarrete, R.; Sanchis, V. Evolutionary processes and environmental factors underlying the genetic diversity and lifestyles of *Bacillus cereus* group bacteria. *Res. Microbiol.* **2017**, *168*, 309–318. [CrossRef] [PubMed]
2. Ash, C.; Farrow, J.A.; Dorsch, M.; Stackebrandt, E.; Collins, M.D. Comparative analysis of *Bacillus anthracis*, *Bacillus cereus*, and related species on the basis of reverse transcriptase sequencing of 16S rRNA. *Int. J. Syst. Bacteriol.* **1991**, *41*, 343–346. [CrossRef] [PubMed]
3. Ehling-Schulz, M.; Fricker, M.; Grallert, H.; Rieck, P.; Wagner, M.; Scherer, S. Cereulide synthetase gene cluster from emetic *Bacillus cereus*: Structure and location on a mega virulence plasmid related to *Bacillus anthracis* toxin plasmid pXO1. *BMC Microbiol.* **2006**, *6*, 20. [CrossRef] [PubMed]
4. Okinaka, R.T.; Cloud, K.; Hampton, O.; Hoffmaster, A.R.; Hill, K.K.; Keim, P.; Koehler, T.M.; Lamke, G.; Kumano, S.; Mahillon, J.; et al. Sequence and organization of pXO1, the large *Bacillus anthracis* plasmid harboring the anthrax toxin genes. *J. Bacteriol.* **1999**, *181*, 6509–6515. [CrossRef] [PubMed]
5. Wielinga, P.R.; Hamidjaja, R.A.; Agren, J.; Knutsson, R.; Segerman, B.; Fricker, M.; Ehling-Schulz, M.; de Groot, A.; Burton, J.; Brooks, T.; et al. A multiplex real-time PCR for identifying and differentiating *B. anthracis* virulent types. *Int. J. Food. Microbiol.* **2011**, *145* (Suppl. 1), S137–S144. [CrossRef] [PubMed]
6. Antwerpen, M.H.; Zimmermann, P.; Bewley, K.; Frangoulidis, D.; Meyer, H. Real-time PCR system targeting a chromosomal marker specific for *Bacillus anthracis*. *Mol. Cell. Probes* **2008**, *22*, 313–315. [CrossRef]
7. Easterday, W.R.; Van Ert, M.N.; Simonson, T.S.; Wagner, D.M.; Kenefic, L.J.; Allender, C.J.; Keim, P. Use of single nucleotide polymorphisms in the *plcR* gene for specific identification of *Bacillus anthracis*. *J. Clin. Microbiol.* **2005**, *43*, 1995–1997. [CrossRef]
8. Ellerbrok, H.; Nattermann, H.; Ozel, M.; Beutin, L.; Appel, B.; Pauli, G. Rapid and sensitive identification of pathogenic and apathogenic *Bacillus anthracis* by real-time PCR. *FEMS Microbiol. Lett.* **2002**, *214*, 51–59. [CrossRef]
9. Ramisse, V.; Patra, G.; Garrigue, H.; Guesdon, J.L.; Mock, M. Identification and characterization of *Bacillus anthracis* by multiplex PCR analysis of sequences on plasmids pXO1 and pXO2 and chromosomal DNA. *FEMS Microbiol. Lett.* **1996**, *145*, 9–16. [CrossRef]
10. Kozel, T.R.; Murphy, W.J.; Brandt, S.; Blazar, B.R.; Lovchik, J.A.; Thorkildson, P.; Percival, A.; Lyons, C.R. mAbs to *Bacillus anthracis* capsular antigen for immunoprotection in anthrax and detection of antigenemia. *Proc. Natl. Acad. Sci. USA* **2004**, *101*, 5042–5047. [CrossRef]
11. Sastry, K.S.R.; Tuteja, U.; Santhosh, P.K.; Lalitha, M.K.; Batra, H.V. Identification of *Bacillus anthracis* by a simple protective antigen-specific mAb dot-ELISA. *J. Med. Microbiol.* **2003**, *52*, 47–49. [CrossRef] [PubMed]
12. Pauker, V.I.; Thoma, B.R.; Grass, G.; Bleichert, P.; Hanczaruk, M.; Zoller, L.; Zange, S. Improved discrimination of *Bacillus anthracis* from closely related species in the *Bacillus cereus sensu lato* group based on Matrix-Assisted Laser Desorption Ionization-Time of Flight mass spectrometry. *J. Clin. Microbiol.* **2018**, *56*, e01900-17. [CrossRef] [PubMed]
13. Dunne, M.; Hupfeld, M.; Klumpp, J.; Loessner, M.J. Molecular basis of bacterial host interactions by Gram-positive targeting bacteriophages. *Viruses* **2018**, *10*, 397. [CrossRef] [PubMed]
14. de Jonge, P.A.; Nobrega, F.L.; Brouns, S.J.J.; Dutilh, B.E. Molecular and evolutionary determinants of bacteriophage host range. *Trends Microbiol.* **2019**, *27*, 51–63. [CrossRef] [PubMed]
15. Kolton, C.B.; Podnecky, N.L.; Shadomy, S.V.; Gee, J.E.; Hoffmaster, A.R. *Bacillus anthracis* gamma phage lysis among soil bacteria: An update on test specificity. *BMC Res. Notes* **2017**, *10*, 598. [CrossRef]
16. Brown, E.R.; Cherry, W.B. Specific identification of *Bacillus anthracis* by means of a variant bacteriophage. *J. Infect. Dis.* **1955**, *96*, 34–39. [CrossRef]
17. Sozhamannan, S.; McKinstry, M.; Lentz, S.M.; Jalasvuori, M.; McAfee, F.; Smith, A.; Dabbs, J.; Ackermann, H.W.; Bamford, J.K.; Mateczun, A.; et al. Molecular characterization of a variant of *Bacillus anthracis*-specific phage AP50 with improved bacteriolytic activity. *Appl. Environ. Microbiol.* **2008**, *74*, 6792–6796. [CrossRef]

18. Kan, S.; Fornelos, N.; Schuch, R.; Fischetti, V.A. Identification of a ligand on the Wip1 bacteriophage highly specific for a receptor on *Bacillus anthracis*. *J. Bacteriol.* **2013**, *195*, 4355–4364. [CrossRef]
19. Turnbull, P.C.; World Health Organization. *Anthrax in Humans and Animals*; Turnbull, P.C.B., Ed.; WHO Press: Geneva, Switzerland, 2008.
20. Abshire, T.G.; Brown, J.E.; Ezzell, J.W. Production and validation of the use of gamma phage for identification of *Bacillus anthracis*. *J. Clin. Microbiol.* **2005**, *43*, 4780–4788. [CrossRef]
21. Popovic, T.; Hoffmaster, A.; Ezzell, J.W.; Abshire, T.G.; Brown, J.E. Validation of methods for confirmatory identification of presumptive isolates of *Bacillus anthracis*. *J. AOAC Int.* **2005**, *88*, 175–177. [CrossRef]
22. Schuch, R.; Pelzek, A.J.; Kan, S.; Fischetti, V.A. Prevalence of *Bacillus anthracis*-like organisms and bacteriophages in the intestinal tract of the earthworm *Eisenia fetida*. *Appl. Environ. Microbiol.* **2010**, *76*, 2286–2294. [CrossRef] [PubMed]
23. Nagy, E. A highly specific phage attacking *Bacillus anthracis* strain Sterne. *Acta Microbiol. Acad. Sci. Hung.* **1974**, *21*, 257–263. [PubMed]
24. Sozhamannan, S.; Chute, M.D.; McAfee, F.D.; Fouts, D.E.; Akmal, A.; Galloway, D.R.; Mateczun, A.; Baillie, L.W.; Read, T.D. The *Bacillus anthracis* chromosome contains four conserved, excision-proficient, putative prophages. *BMC Microbiol.* **2006**, *6*, 34. [CrossRef] [PubMed]
25. Dowah, A.S.A.; Clokie, M.R.J. Review of the nature, diversity and structure of bacteriophage receptor binding proteins that target Gram-positive bacteria. *Biophys. Rev.* **2018**, *10*, 535–542. [CrossRef] [PubMed]
26. Schuch, R.; Fischetti, V.A. Detailed genomic analysis of the Wß and ß phages infecting *Bacillus anthracis*: Implications for evolution of environmental fitness and antibiotic resistance. *J. Bacteriol.* **2006**, *188*, 3037–3051. [CrossRef]
27. Mitraki, A.; Miller, S.; van Raaij, M.J. Review: Conformation and folding of novel beta-structural elements in viral fiber proteins: The triple beta-spiral and triple beta-helix. *J. Struct. Biol.* **2002**, *137*, 236–247. [CrossRef]
28. Simpson, D.J.; Sacher, J.C.; Szymanski, C.M. Development of an assay for the Identification of receptor binding proteins from bacteriophages. *Viruses* **2016**, *8*, 17. [CrossRef]
29. Davison, S.; Couture-Tosi, E.; Candela, T.; Mock, M.; Fouet, A. Identification of the *Bacillus anthracis* (gamma) phage receptor. *J. Bacteriol.* **2005**, *187*, 6742–6749. [CrossRef]
30. Bishop-Lilly, K.A.; Plaut, R.D.; Chen, P.E.; Akmal, A.; Willner, K.M.; Butani, A.; Dorsey, S.; Mokashi, V.; Mateczun, A.J.; Chapman, C.; et al. Whole genome sequencing of phage resistant *Bacillus anthracis* mutants reveals an essential role for cell surface anchoring protein CsaB in phage AP50c adsorption. *Virol. J.* **2012**, *9*, 246. [CrossRef]
31. Plaut, R.D.; Beaber, J.W.; Zemansky, J.; Kaur, A.P.; George, M.; Biswas, B.; Henry, M.; Bishop-Lilly, K.A.; Mokashi, V.; Hannah, R.M.; et al. Genetic evidence for the involvement of the S-layer protein gene sap and the sporulation genes *spo0A*, *spo0B*, and *spo0F* in phage AP50c infection of *Bacillus anthracis*. *J. Bacteriol.* **2014**, *196*, 1143–1154. [CrossRef]
32. Braun, P.; Grass, G.; Aceti, A.; Serrecchia, L.; Affuso, A.; Marino, L.; Grimaldi, S.; Pagano, S.; Hanczaruk, M.; Georgi, E.; et al. Microevolution of anthrax from a young ancestor (M.A.Y.A.) suggests a soil-borne life cycle of *Bacillus anthracis*. *PLoS ONE* **2015**, *10*, e0135346. [CrossRef] [PubMed]
33. Cote, C.K.; Buhr, T.; Bernhards, C.B.; Bohmke, M.D.; Calm, A.M.; Esteban-Trexler, J.S.; Hunter, M.; Katoski, S.E.; Kennihan, N.; Klimko, C.P.; et al. A standard method to inactivate *Bacillus anthracis* spores to sterility via gamma irradiation. *Appl. Environ. Microbiol.* **2018**, *84*, e00106-18. [CrossRef] [PubMed]
34. Malvar, T.; Gawron-Burke, C.; Baum, J.A. Overexpression of *Bacillus thuringiensis* HknA, a histidine protein kinase homology, bypasses early Spo mutations that result in CryIIIA overproduction. *J. Bacteriol.* **1994**, *176*, 4742–4749. [CrossRef] [PubMed]
35. Shaner, N.C.; Campbell, R.E.; Steinbach, P.A.; Giepmans, B.N.; Palmer, A.E.; Tsien, R.Y. Improved monomeric red, orange and yellow fluorescent proteins derived from *Discosoma* sp. red fluorescent protein. *Nat. Biotechnol.* **2004**, *22*, 1567–1572. [CrossRef]
36. Altschul, S.F.; Gish, W.; Miller, W.; Myers, E.W.; Lipman, D.J. Basic local alignment search tool. *J. Mol. Biol.* **1990**, *215*, 403–410. [CrossRef]
37. Van Ert, M.N.; Easterday, W.R.; Huynh, L.Y.; Okinaka, R.T.; Hugh-Jones, M.E.; Ravel, J.; Zanecki, S.R.; Pearson, T.; Simonson, T.S.; U'Ren, J.M.; et al. Global genetic population structure of *Bacillus anthracis*. *PLoS ONE* **2007**, *2*, e461. [CrossRef] [PubMed]

38. Walper, S.A.; Anderson, G.P.; Brozozog Lee, P.A.; Glaven, R.H.; Liu, J.L.; Bernstein, R.D.; Zabetakis, D.; Johnson, L.; Czarnecki, J.M.; Goldman, E.R. Rugged single domain antibody detection elements for *Bacillus anthracis* spores and vegetative cells. *PLoS ONE* **2012**, *7*, e32801. [CrossRef]
39. Ramage, J.G.; Prentice, K.W.; DePalma, L.; Venkateswaran, K.S.; Chivukula, S.; Chapman, C.; Bell, M.; Datta, S.; Singh, A.; Hoffmaster, A.; et al. Comprehensive laboratory evaluation of a highly specific lateral flow assay for the presumptive identification of *Bacillus anthracis* spores in suspicious white powders and environmental samples. *Health Secur.* **2016**, *14*, 351–365. [CrossRef]
40. Kolton, C.B.; Marston, C.K.; Stoddard, R.A.; Cossaboom, C.; Salzer, J.S.; Kozel, T.R.; Gates-Hollingsworth, M.A.; Cleveland, C.A.; Thompson, A.T.; Dalton, M.F.; et al. Detection of *Bacillus anthracis* in animal tissues using InBios active anthrax detect rapid test lateral flow immunoassay. *Lett. Appl. Microbiol.* **2019**, *68*, 480–484. [CrossRef]
41. De, B.K.; Bragg, S.L.; Sanden, G.N.; Wilson, K.E.; Diem, L.A.; Marston, C.K.; Hoffmaster, A.R.; Barnett, G.A.; Weyant, R.S.; Abshire, T.G.; et al. A two-component direct fluorescent-antibody assay for rapid identification of *Bacillus anthracis*. *Emerg. Infect. Dis.* **2002**, *8*, 1060–1065. [CrossRef]
42. Zasada, A.A. Detection and identification of *Bacillus anthracis*: From conventional to molecular microbiology methods. *Microorganisms* **2020**, *8*, 125. [CrossRef] [PubMed]
43. Dams, D.; Brondsted, L.; Drulis-Kawa, Z.; Briers, Y. Engineering of receptor-binding proteins in bacteriophages and phage tail-like bacteriocins. *Biochem. Soc. Trans.* **2019**, *47*, 449–460. [CrossRef] [PubMed]
44. Singh, A.; Arutyunov, D.; Szymanski, C.M.; Evoy, S. Bacteriophage based probes for pathogen detection. *Analyst* **2012**, *137*, 3405–3421. [CrossRef] [PubMed]
45. Sumrall, E.T.; Rohrig, C.; Hupfeld, M.; Selvakumar, L.; Du, J.; Dunne, M.; Schmelcher, M.; Shen, Y.; Loessner, M.J. Glycotyping and specific separation of *Listeria monocytogenes* with a novel bacteriophage protein toolkit. *Appl. Environ. Microbiol.* **2020**. [CrossRef] [PubMed]
46. Carroll, L.M.; Wiedmann, M.; Kovac, J. Proposal of a taxonomic nomenclature for the *Bacillus cereus* group which reconciles genomic definitions of bacterial species with clinical and industrial phenotypes. *MBio* **2020**, *11*, e00034-20. [CrossRef]
47. Marston, C.K.; Gee, J.E.; Popovic, T.; Hoffmaster, A.R. Molecular approaches to identify and differentiate *Bacillus anthracis* from phenotypically similar *Bacillus* species isolates. *BMC Microbiol.* **2006**, *6*, 22. [CrossRef]
48. Han, C.S.; Xie, G.; Challacombe, J.F.; Altherr, M.R.; Bhotika, S.S.; Bruce, D.; Campbell, C.S.; Campbell, M.L.; Chen, J.; Chertkov, O.; et al. Pathogenomic sequence analysis of *Bacillus cereus* and *Bacillus thuringiensis* isolates closely related to *Bacillus anthracis*. *J. Bacteriol.* **2006**, *188*, 3382–3390. [CrossRef]
49. Kern, V.J.; Kern, J.W.; Theriot, J.A.; Schneewind, O.; Missiakas, D. Surface-Layer (S-Layer) proteins Sap and EA1 govern the binding of the S-layer-associated protein BslO at the cell septa of *Bacillus anthracis*. *J. Bacteriol.* **2012**, *194*, 3833–3840. [CrossRef]
50. Mignot, T.; Mesnage, S.; Couture-Tosi, E.; Mock, M.; Fouet, A. Developmental switch of S-layer protein synthesis in *Bacillus anthracis*. *Mol. Microbiol.* **2002**, *43*, 1615–1627. [CrossRef]
51. Berjon-Otero, M.; Lechuga, A.; Mehla, J.; Uetz, P.; Salas, M.; Redrejo-Rodriguez, M. Bam35 tectivirus intraviral interaction map unveils new function and localization of phage ORFan proteins. *J. Virol.* **2017**, *91*, e00870-17. [CrossRef]
52. Gaidelyte, A.; Cvirkaite-Krupovic, V.; Daugelavicius, R.; Bamford, J.K.; Bamford, D.H. The entry mechanism of membrane-containing phage Bam35 infecting *Bacillus thuringiensis*. *J. Bacteriol.* **2006**, *188*, 5925–5934. [CrossRef] [PubMed]
53. Schuch, R.; Nelson, D.; Fischetti, V.A. A bacteriolytic agent that detects and kills *Bacillus anthracis*. *Nature* **2002**, *418*, 884–889. [CrossRef] [PubMed]
54. Schmelcher, M.; Donovan, D.M.; Loessner, M.J. Bacteriophage endolysins as novel antimicrobials. *Future Microbiol.* **2012**, *7*, 1147–1171. [CrossRef] [PubMed]
55. Fujinami, Y.; Hirai, Y.; Sakai, I.; Yoshino, M.; Yasuda, J. Sensitive detection of *Bacillus anthracis* using a binding protein originating from gamma-phage. *Microbiol. Immunol.* **2007**, *51*, 163–169. [CrossRef] [PubMed]
56. Sainathrao, S.; Mohan, K.V.; Atreya, C. Gamma-phage lysin PlyG sequence-based synthetic peptides coupled with Qdot-nanocrystals are useful for developing detection methods for *Bacillus anthracis* by using its surrogates, *B. anthracis*-Sterne and *B. cereus*-4342. *BMC Biotechnol.* **2009**, *9*, 67. [CrossRef]
57. Reiman, R.W.; Atchley, D.H.; Voorhees, K.J. Indirect detection of *Bacillus anthracis* using real-time PCR to detect amplified gamma phage DNA. *J. Microbiol. Methods* **2007**, *68*, 651–653. [CrossRef]

58. Malagon, F.; Estrella, L.A.; Stockelman, M.G.; Hamilton, T.; Teneza-Mora, N.; Biswas, B. Phage-mediated molecular detection (PMMD): A novel rapid method for phage-specific bacterial detection. *Viruses* **2020**, *12*, 435. [CrossRef]
59. Kong, M.; Shin, J.H.; Heu, S.; Park, J.K.; Ryu, S. Lateral flow assay-based bacterial detection using engineered cell wall binding domains of a phage endolysin. *Biosens. Bioelectron.* **2017**, *96*, 173–177. [CrossRef]

6. Enzyme-linked phage receptor binding protein assays (ELPRA) enable identification of *Bacillus anthracis* colonies

viruses

MDPI

Article

Enzyme-Linked Phage Receptor Binding Protein Assays (ELPRA) Enable Identification of *Bacillus anthracis* Colonies

Peter Braun †, Nadja Rupprich †, Diana Neif and Gregor Grass *

Department of Bacteriology and Toxinology, Bundeswehr Institute of Microbiology (IMB), 80937 Munich, Germany; peter3braun@bundeswehr.org (P.B.); nadjarupprich@googlemail.com (N.R.); diananeif@bundeswehr.org (D.N.)

* Correspondence: gregorgrass@bundeswehr.org; Tel.: +49-992692-3981

† Both authors contributed equally to this work.

Abstract: Bacteriophage receptor binding proteins (RBPs) are employed by viruses to recognize specific surface structures on bacterial host cells. Recombinant RBPs have been utilized for detection of several pathogens, typically as fusions with reporter enzymes or fluorescent proteins. Identification of *Bacillus anthracis*, the etiological agent of anthrax, can be difficult because of the bacterium's close relationship with other species of the *Bacillus cereus sensu lato* group. Here, we facilitated the identification of *B. anthracis* using two implementations of enzyme-linked phage receptor binding protein assays (ELPRA). We developed a single-tube centrifugation assay simplifying the rapid analysis of suspect colonies. A second assay enables identification of suspect colonies from mixed overgrown solid (agar) media derived from the complex matrix soil. Thus, these tests identified vegetative cells of *B. anthracis* with little processing time and may support or confirm pathogen detection by molecular methods such as polymerase chain reaction.

Keywords: bacteriophage; receptor binding protein; reporter fusions; enzyme-linked phage protein assay; ELPRA; anthrax; *Bacillus anthracis*

Citation: Braun, P.; Rupprich, N.; Neif, D.; Grass, G. Enzyme-Linked Phage Receptor Binding Protein Assays (ELPRA) Enable Identification of *Bacillus anthracis* Colonies. *Viruses* **2021**, *13*, 1462. https://doi.org/10.3390/v13081462

Academic Editors: Joana Azeredo and Sílvio Santos

Received: 30 June 2021
Accepted: 24 July 2021
Published: 27 July 2021

1. Introduction

Identification of *B. anthracis*, the etiological bacterial agent of anthrax disease of mammals, can be accomplished by bacteriophage (phage) sensitivity testing [1]. Phage-based specific detection of *B. anthracis* cells offers additional avenues for diagnostics of this notorious pathogen. Particularly, this complements nucleic acid-based detection techniques such as polymerase chain reaction (PCR), which is the current gold standard for *B. anthracis* identification [1]. Only a few phages have been found to be specific for *B. anthracis*. These mainly comprise phages Gamma [2,3], Wip1 [4], and AP50c [5]. Among these, phage Gamma is the one most widely used [2,3] and has a long history as a "diagnostic phage" [1,6]. A recent evaluation of its host specificity confirmed the Gamma phage's suitability as its specificity reached 97% when tested against 700 aerobic, spore-forming bacteria, including other members of the closely related *Bacillus cereus sensu lato* group [7].

Host specificity of phages is typically determined by their receptor binding proteins (RBPs), which may be tail fibers or spike proteins. Typically, RBPs specifically recognize protein, teichoic acid, or polysaccharide entities on the host's surface [8]. This interaction is the first step in the phage infection process. Recently, modified RBPs have opened new avenues for labeling, detecting, and capture of host bacterial cells. These phage RBP-based assays are already widely used as versatile tools for pathogen detection [9,10]. Target bacteria include biothreat agents that cause melioidosis (*Burkholderia pseudomallei*) [11], plague (*Yersinia pestis*) [12], or anthrax [13]. For *B. anthracis* phage Gamma, the GamR protein has been previously identified as the phage's host cell receptor [14]. Recently, we have harnessed the Gamma phage RBP (Gp14) as a fluorescent reporter fusion for rapid microscopic detection of *B. anthracis* [13]. While functional, this reporter protein was

difficult to heterologously produce in *Escherichia coli*. We thus resorted to a very similar protein, BA4079 [13], encoded by lambdoid prophage 03 located on the chromosome of *B. anthracis* [15]. BA4079, which acts as a specific *B. anthracis* RBP (named $RBP_{\lambda 03}$), and Gp14 (Gamma) share high amino acid sequence identities (83.0%; 89.0% similarity) with a continuous C-terminal region without gaps of 374 aa featuring 95.2% and 98.4% identity and similarity, respectively. An N-terminally truncated derivative of the BA4079 protein, termed $RBP_{\lambda 03\Delta 1\text{-}120}$, was both highly soluble and bound specifically to *B. anthracis* cells over a broad range of growth phases [13]. As a fusion with mCherry, the fluorescent RBP reporter was used to identify *B. anthracis* cells via fluorescence microscopy. Specificity of $RBP_{\lambda 03\Delta 1\text{-}120}$ toward *B. anthracis* was 95% (one false positive each among *B. cereus*, *B. weihenstephanensis*, and *B. paranthracis*) [13], thus, offering specificity quite similar to the 96–97% of phage Gamma [7].

In this study, we developed two enzyme-linked phage RBP assays (ELPRA) on the basis of the $RBP_{\lambda 03\Delta 1\text{-}120}$ reporter as novel tools for identification of *B. anthracis.* This comprises a colony lift and blot ELPRA utilizing a luminogenic reporter fused to $RBP_{\lambda 03\Delta 1\text{-}120}$, facilitating the detection of *B. anthracis* colonies after pre-enrichment from the complex matrix soil on solidified media. The alternative ELPRA implementation linking the RBP with a peroxidase function enabled rapid, colorimetric identification of live or inactivated colony material of *B. anthracis*.

2. Materials and Methods

2.1. Bacterial Culture, Soil Sample, B. anthracis Enrichment, and Cell Inactivation

Unless specified otherwise, *B. anthracis* Sterne [16] ATCC 4229 Pasteur and *B. cereus sensu lato* strains (Supplementary Materials Table S1) were grown on Columbia blood agar or *B. anthracis* agar [17]. A soil sample was taken from non-*B. anthracis*-contaminated park soil near the institute. *B. anthracis* Sterne was spiked in this soil as spores (generated according to [18], with modifications [13]) and enriched from this sample using a previously developed method [17]. Gamma phage sensitivity was tested by the melted overlay agar method [2]. Colonies of bacilli were chemically inactivated in aqueous peracetic acid solution (4% (*v*/*v*) Terralin PAA; Schülke & Mayr GmbH, Norderstedt, Germany), as described earlier [13].

2.2. DNA Isolation, Polymerase Chain Reaction, 16S rRNA Gene Sequencing, and Sequence Analysis

A bacterial colony grown on blood agar was chemically inactivated and DNA isolated using the MasterPure™ Gram Positive DNA Purification kit (Lucigen, Middleton, WI, USA) as described for Gram-positive bacteria, with minor modifications as described in [19]. DNA concentrations were quantified using the Qubit dsDNA HS Assay Kit (Thermo Fisher Scientific, Dreieich, Germany), according to the supplier's protocol. DNA preparations were stored at −20 °C until further use.

For the identification of *B. anthracis* via PCR, the chromosomal marker *dhp61* was used as described previously [20]. The 16S rRNA gene region of new isolate *B. cereus s.l.* IMB-2021-1 was partially PCR-amplified using primer pairs 27r and 1492r [21] and subjected to DNA Sanger sequencing [21,22] (Eurofins Genomics Germany GmbH, Ebersberg, Germany).

2.3. Fluorescence Microscopy of Bacillus Cells Labeled with mCherry-$RBP_{\lambda 03\Delta 1\text{-}120}$ Reporter

Chemically inactivated cells were labeled with mCherry-$RBP_{\lambda 03\Delta 1\text{-}120}$ reporter protein, as described in [13]. In short, ca. 0.2 µg reporter protein was added to ca. 50 µL cells of an optical density at 600 nm (OD_{600}) of 1 and 1 µL of the mixture was transferred into a well of a chamber slide with lid (µ-slide 8 Well, Ibidi GmbH, Martinsried, Germany). Cell suspensions were covered with a thin agarose pad and samples analyzed for mCherry signal (extinction: 587 nm, emission: 610 nm) using an Axio Observer Z1 700 Confocal Laser Scanning Microscope (Carl Zeiss, Oberkochen, Germany).

2.4. Cloning of a NanoLuc-RBP$_{\lambda 03\Delta 1\text{-}120}$ Reporter Fusion Construct

For construction of an expression plasmid for heterologous production of Twin-StrepTag (TST) tagged fusion protein NanoLuc-RBP$_{\lambda 03\Delta 1\text{-}120}$, the previously generated plasmid pASG-IBA105::*tst*::*mCherry*::*RBP*$_{\lambda 03\Delta 1\text{-}120}$ was used as a basis [13]. Forward and reverse primers, used for amplification of the *NanoLuc* gene from template pNL1.1 (Promega, Walldorf, Germany), contained recognition sites for endonucleases BsrGI and XhoI, respectively (Supplementary Materials Table S2). These endonuclease recognition sites are also present up- and downstream of the *mCherry* gene in plasmid pASG-IBA105::*tst*::*mCherry*::*RBP*$_{\lambda 03\Delta 1\text{-}120}$ [13] and utilized to replace the *mCherry* gene with *NanoLuc*, resulting in plasmid pASG-IBA105::*tst*::*NanoLuc*::*RBP*$_{\lambda 03\Delta 1\text{-}120}$.

2.5. Expression, Purification, and Western Blot Analysis of Strep-Tagged NanoLuc/mCherry-RBP$_{\lambda 03\Delta 1\text{-}120}$ Reporter Fusions

The pASG-IBA105::*tst*::*NanoLuc*::*RBP*$_{\lambda 03\Delta 1\text{-}120}$ and the pASG-IBA105::*tst*::*mCherry*::*RBP*$_{\lambda 03\Delta 1\text{-}120}$ plasmids were transformed into *E. coli* ArcticExpress cells (Agilent Technologies Inc., Waldbronn, Germany). A single colony was used for protein production, as described in [13]. In short, for protein production, an exponentially growing culture at an optical density of 0.6–0.8 (OD_{600}) was cooled down to 12 °C, induced with anhydrotetracycline, and incubation continued for 24 h at 12 °C. Cells were harvested, lysed, and filtered. The filtered lysate was subjected to affinity chromatography (Äkta pure system; GE Healthcare Life Science, Munich, Germany) using a 1 mL Strep-Tactin® XT column (IBA GmbH, Göttingen, Germany). The eluted protein was dialyzed against HEPES buffer (50 mM HEPES, 50 mM NaCl, 5 mM EDTA, pH 7.5), protein concentration measured (Pierce BCA Protein Assay Kit; ThermoFisher Scientific, Darmstadt, Germany), and adjusted to a concentrations of 1 mg protein/mL. Protein aliquots were either kept at −80 °C for long-term storage use or mixed with 50% (*v*/*v*) glycerol (final concentration) as a cryo-protectant and stored at −20 °C for testing in RBP-fusion reporter assays.

SDS-PAGE and Western blot analysis was performed as described in [13]. The polyacrylamide gel (Novex NuPAGE 4–12% Bis-Tris protein-gel; ThermoFisher Scientific, Darmstadt, Germany) was transferred onto a 0.45 µm pore size nitrocellulose membrane (ThermoFisher Scientific, Darmstadt, Germany) and subjected to semi-dry blotting at 30 V for 75 min (Novex Semi-Dry Blotter, ThermoFisher Scientific, Darmstadt, Germany). TST-tagged proteins were detected using Strep-MAB-Classic (HRP antibody conjugate, IBA GmbH, Göttingen, Germany) via chemiluminescence detection (Clarity Western ECL substrate; Bio-Rad Laboratories, Munich, Germany), according to the manufacturers' protocols.

2.6. Horseradish Peroxidase Labeling of mCherry-RBP$_{\lambda 03\Delta 1\text{-}120}$ Fusion Protein

The mCherry-RBP$_{\lambda 03\Delta 1\text{-}120}$ fusion protein was labeled with horseradish peroxidase (HRP) using the EZ-Link™ Plus Activated Peroxidase Kit (ThermoFisher Scientific, Darmstadt, Germany) in carbonate–bicarbonate buffer (pH 9.4), according to the manufacturer's protocol.

2.7. Colony Lift and Blot ELPRA for NanoLuc -RBP$_{\lambda 03\Delta 1\text{-}120}$ Reporter-Mediated Detection and Identification of B. anthracis

Agar plates from enrichment grown overnight were blotted onto hydrophobic nitrocellulose membranes (Carl Roth, Karlsruhe, Germany). For this, membranes were cut into circles fitting into 81 mm diameter plastic petri dishes using a home-made cardboard template. The membrane was labeled with a permanent pen as was the corresponding rim of the petri dish to ensure reconstruction of the relative orientation of plate and membrane. The colony lift method was loosely adapted from [23], the colony blot assay modified from manual protocols "Strep-tag® detection in Western blots" (chapter 2; IBA GmbH, Göttingen, Germany) and "Nano-Glo® HiBiT Blotting System" (chapter 3; Promega, Walldorf, Germany). The colony lift and blot comprised the following steps: a membrane was carefully lowered onto the agar surface and softly pressed so complete contact between

membrane and agar (colonies) was achieved (air bubbles can escape). The membrane was immediately (<10 s) removed using forceps ("lift") and carefully pressed onto a pre-wetted (with blocking buffer, i.e., 3% (*w*/*v*) bovine serum albumin (BSA) in Tris-buffered saline (TBS, pH 7.4) thick Whatman filter paper (Life Technologies, Darmstadt, Germany) with the colony-bearing side down to remove superfluous colony material not yet attached to the membrane. The membrane was carefully lifted and immediately (without drying) submerged into 15 mL blocking buffer (in an unused petri dish) and rocked gently for 30 min in order to block unspecific binding sites on the membrane. The blocking buffer was replaced with 20 mL TBS wash buffer. After about one minute with light agitation, the wash buffer was replaced with 5 mL TBST (TBS with 0.05% (*v*/*v*) Tween 20) containing 0.2 µg NanoLuc-RBP$_{\lambda 03\Delta 1\text{-}120}$ and the petri dish was gently rocked for 10 min to facilitate RBP binding to membrane-attached cells. The membrane (in petri dish) was then washed four times with 15 mL fresh TBST with gentle agitation for about 1 min. In the meantime, 7.5 mL Nano-Glo®-Blotting-Buffer (from Nano-Glo® HiBiT Blotting System, Promega, Walldorf, Germany) was diluted to 1x (from 10x stock) with sterile aqua$_{dest}$. To yield NanoLuc substrate buffer, the 1x blotting buffer was mixed with 15 µL Nano-Glo® Luciferase Assay Substrate (from Nano-Glo® HiBiT Blotting System, Promega, Walldorf, Germany) and poured into a fresh petri dish. The membrane was dipped and completely submerged into NanoLuc substrate buffer from both sides ("blot") and transferred immediately (without drying) onto a transparent plastic foil with the colony-bearing side up. The membrane was covered with a second foil and transferred into a suitable transparent transport container. Luminescence was recorded on a ChemiDoc MP imaging system (Bio-Rad Laboratories, Munich, Germany) with Image Lab 5.2 software (Bio-Rad Laboratories, Munich, Germany) for documentation.

2.8. Rapid Dichotomous Colorimetric ELPRA for Identification of Suspect B. anthracis Colonies

To identify a suspect *B. anthracis* colony, it was lifted with a loop and resuspended into a 1.5 mL reaction tube containing 100 µL PBS. From this, up to 50 µL was transferred to a new tube and 50 µL blocking buffer (3% (*w*/*v*) BSA in phosphate-buffered saline) was added. For two-step, indirect ELPRA, 0.2 µg of mCherry-RBP$_{\lambda 03\Delta 1\text{-}120}$ reporter (fluorescence of mCherry is irrelevant here, any protein featuring a TST can be used) was added and the reaction was either flicked by hand a couple of times or shaken at 600 rpm for 1 min. Next, 1 mL PBST (PBS with 0.05% Tween 20) was added, mixed and centrifuged for 1 min at 10,000× *g*. The pellet was resuspended in 1.5 mL PBST and pelleted by centrifugation at 10,000× *g*. Strep-Tactin® horse radish peroxidase conjugate (IBA GmbH, Göttingen, Germany) was diluted 1:4000 into PBST and 100 µL used to resuspend the cell pellet. The sample was either flicked by hand a couple of times or shaken at 600 rpm for 1 min. One mL PBST was added, mixed and centrifuged for 1 min at 10,000× *g*. The pellet was washed once with 1.5 mL PBST and once with 1.5 mL PBS. Finally, the pellet was resuspended in 50 µL SeramunBlau® slow (containing 3,3′,5,5′-tetramethylbenzidin) peroxidase substrate (Seramun Diagnostica GmbH, Heidesee, Germany). Blue color development was monitored for several minutes and photo-documented (photos were adjusted for contrast and brightness). If necessary, the color reaction was stopped by centrifugation and removal of the cell pellet.

Alternatively, 0.1 µg HRP-conjugated mCherry-RBP$_{\lambda 03\Delta 1\text{-}120}$ reporter was used for one-step ELPRA, replacing separate steps of RBP and HRP addition to colony material. All other incubation and wash steps were the same as described for the two-step ELPRA. All steps were conducted at room temperature. As process controls served *B. anthracis* colony material treated as above but (i) TST-tagged protein, (ii) peroxidase conjugate, or (iii) both were replaced with PBS. Colony material of *B. cereus* served as negative control.

Colony material of any *B. anthracis* strain may be used as positive control when assaying suspect colonies. This assay may be conducted using live or inactivated cells of *B. anthracis* or *B. cereus s.l.* (controls). Complete inactivation of *B. anthracis* cells and spores

was achieved using 4% (*v*/*v*) Terralin PAA [13]. Other means of inactivation may also work for this assay to varying degrees [13].

3. Results

3.1. Production of the Recombinant Luminescence-Reporter NanoLuc-RBP$_{\lambda 03\Delta 1\text{-}120}$

We adapted the colony lift and colony blot techniques for the detection and identification of *B. anthracis* on solidified (agar) media. Initial experiments using our established mCherry-RBP$_{\lambda 03\Delta 1\text{-}120}$ reporter (pASG-IBA105::*tst*::*mCherry*::*RBP$_{\lambda 03\Delta 1\text{-}120}$*) featuring a TST epitope [13] for detection of *B. anthracis* colonies by colony lift and blot assay yielded unsatisfactory results. Discrimination between signal (*B. anthracis* colonies) and background (bacteria-loaded membrane) was poor when using horseradish peroxidase as a reporter. We thus resorted to using the visible light generating reporter protein NanoLuc, a truncated derivative of deep-sea shrimp (*Oplophorus gracilirostris*) luciferase. The heterologously produced NanoLuc-RBP$_{\lambda 03\Delta 1\text{-}120}$ reporter protein was soluble but appeared slightly smaller on SDS-PAGE than the expected molecular weight of 66 KDa, as shown in Supplementary Materials Figure S1. The yield was about 5 mg protein/L culture.

3.2. A Colony Lift and Luminescent Blot-Based ELPRA Using NanoLuc-RBP$_{\lambda 03\Delta 1\text{-}120}$ as Reporter Probe Facilitates Identification of B. anthracis

As a proof of principle for detection of *B. anthracis* colonies, the NanoLuc-RBP$_{\lambda 03\Delta 1\text{-}120}$ reporter served as a luminescence-generating probe. Figure 1A shows the result of detecting colonies of *B. anthracis* in a mixed culture plate with *B. cereus* ATCC10987. All membrane-transferred *B. anthracis* colonies but none of the *B. cereus* colonies showed significant luminescence resulting from the specific binding of NanoLuc-RBP$_{\lambda 03\Delta 1\text{-}120}$ to the *B. anthracis* cells. Starting from the colony lift step, the assay takes about 1.5–2 h until completion.

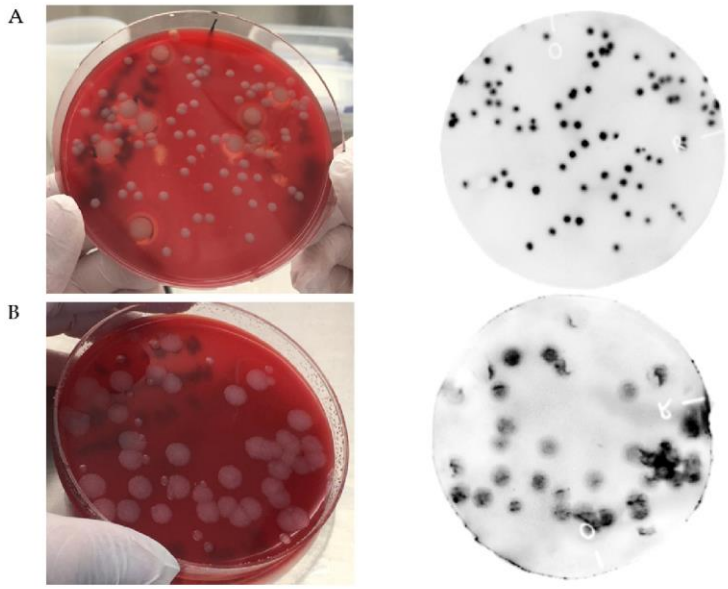

Figure 1. Luminogenic reporter probe NanoLuc-RBP$_{\lambda 03\Delta 1\text{-}120}$ for differentiation of *B. anthracis* from *B. cereus* in a colony lift and blot assay. Cells of *B. anthracis* and *B. cereus* were mixed and plated on solid anthrax blood agar media. (**A**) *B. anthracis* Sterne and *B. cereus* ATCC 10,987 grown overnight at 28 °C; (**B**) *B. anthracis* Sterne and *B. cereus* environmental isolate IMB-4-0-Rott grown for 24 h at 37 °C. Left panels: photos of incubated agar plates; right panels: luminescence signals on nitrocellulose membranes after lift and blot assay from respective agar plate. Markings ("O" and "R) are just for orientation and alignment.

Since differentiation between typical *B. anthracis*- and *B. cereus*-colonies on an erythrocyte-containing agar plate is obvious due to the hemolysis exerted by the bigger *B. cereus* colonies, we next tested the assay against an environmental, non-hemolytic *B. cereus* isolate (strain IMB-4-0-Rott) that forms colonies on anthrax blood agar that look suspiciously similar to *B. anthracis*. To increase the visual confusion, we prolonged the incubation time to 24 h at 37 °C, after which *B. anthracis* formed large colonies resembling that of typical strains of non-hemolytic *B. cereus,* whereas the non-hemolytic *B. cereus* strain formed small colonies (Figure 1B, left panel). Indeed, luminescence probe-based detection identified the correct, i.e., large-sized colonies (Figure 1B, right panel).

3.3. B. anthracis Can Be Detected and Identified from Spiked Soil Sample Preparations Using Colony Lift and Blot Based ELPRA with NanoLuc-RBP$_{\lambda 03\Delta 1\text{-}120}$ as Reporter Probe

Enriching and isolating *B. anthracis* from complex environmental matrices can be challenging. This becomes a nuisance with low *B. anthracis* spore concentrations in soil samples in the presence of a relative high abundance of related bacilli and other spore formers. Therefore, we combined semi-selective enrichment of *B. anthracis* from soil on solid agar medium [17] with the new colony lift and blot assay. For lack of authentic soil-samples contaminated with *B. anthracis*, we spiked *B. anthracis*-free soil samples with spores of *B. anthracis* prior to enrichment. Colonies from overgrown plates were then lifted and blotted. As shown in Figure 2, individual *B. anthracis* colonies can easily be identified on the membrane. The corresponding location on the agar plate can be deducted by comparing the photo of the overgrowing plate (Figure 2, left panel) with the photo of the developed colony bearing membrane (Figure 2, right panel). From there, it should be straight forward to re-streak colony material from this plate area to a fresh plate and to further test arising suspect individual colonies.

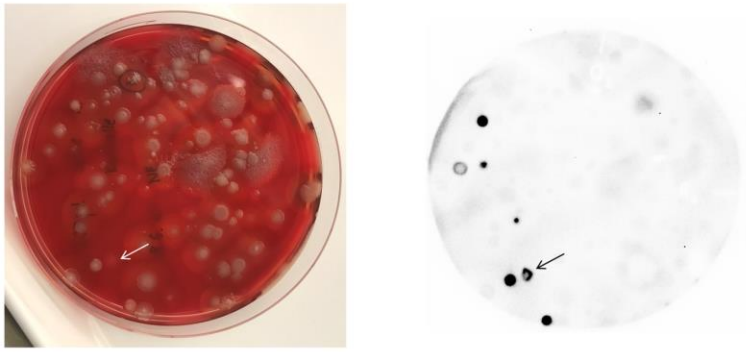

Figure 2. Colony lift and blot assay with luminogenic reporter probe NanoLuc-RBP$_{\lambda 03\Delta 1\text{-}120}$ for identification of *B. anthracis* in a heterogeneous environmental plate culture. A soil sample was spiked with *B. anthracis* spores, subjected to enrichment, plated on *B. anthracis*-agar [17], and assayed by lift and blot ELPRA for *B. anthracis*. Left panel: photo of incubated agar plate; right panel: luminescence signals on nitrocellulose membrane after lift and blot ELPRA from respective agar plate. The colony labeled with an arrow showing untypical colony morphology for *B. anthracis* was selected for further analysis.

We did so for one colony giving rise to signals in Figure 2, (arrow). Its colony morphology resembled *Bacillus mycoides* rather than *B. anthracis*. After subculture on a fresh agar plate, this fuzzy phenotype remained. The isolate was sensitive to Gamma as the phage produced plaques on pour plates [2], but negative for the *B. anthracis* PCR marker *dhp61* [20]. Sequencing of the isolate's partial 16S rRNA gene revealed that this bacterium, which was named IMB-2021-1, had as closest characterized relatives (with identical DNA sequences over 1462 bp in the 16S rRNA gene): *Bacillus toyonensis* strain MCCC 1A00418 (GenBank: KJ812421), *Bacillus toyonensis* strain MCCC 1A01056 (GenBank: KJ812432), and

Bacillus wiedmannii strain SX13.1LB (GenBank: MT052668). Thus, strain IMB-2021-1 very likely represented a new *B. toyonensis* or *B. wiedmannii* strain.

3.4. Suspect B. anthracis Colonies Can Be Identified by ELPRA Using Strep-Tagged-RBP$_{\lambda 03\Delta 1\text{-}120}$ Derivatives as a Dichotomous Colorimetric Reporter

The TST-labeled mCherry-RBP$_{\lambda 03\Delta 1\text{-}120}$ reporter has previously facilitated rapid identification via fluorescent microscopy within a few minutes [13]. In an effort to make this assay more accessible to laboratories lacking sophisticated equipment, we designed a rapid dichotomous ("yes/no") colorimetric test. The mCherry component of the reporter construct does not participate in signal generation but instead serves to enhance solubility of the heterologous protein and facilitates monitoring of protein production and purification. In a test tube, material from a single suspect colony is successively mixed with the reporter RBP harboring a TST epitope, a Strep-Tactin®–horseradish–peroxidase conjugate (Strep-Tactin®-HRP) and chromogenic HRP substrate. Samples containing *B. anthracis* colony material turn blue because the RBP reporter binds to the cell surfaces, the attached TST is recognized and binds to Strep-Tactin®-HRP, which in turn oxidizes the chromogenic substrate. This assay, including wash steps, was optimized for speed and can be completed within <30 min. A representative test is shown in Figure 3A. Clearly, the sample containing *B. anthracis* cell material turned blue, whereas the sample with *B. cereus* remained colorless (as did several process controls). This assay works with both live and peracetic acid inactivated cells (Figure 3B), giving flexibility to perform the assay within or outside BSL-3 containment.

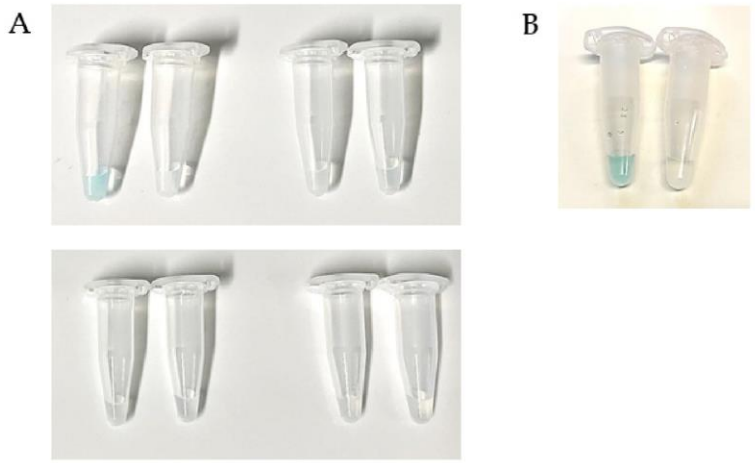

Figure 3. Two-step dichotomous colorimetric centrifugation ELPRA for RBP-dependent identification of *B. anthracis* cells. (**A**) Live colony material (50 µL of ca. 0.5 OD_{600}) of *B. anthracis* Sterne (left sample in each pair) or *B. cereus* ATCC10987 (right sample in each pair) were first labeled with RBP$_{\lambda 03\Delta 1\text{-}120}$ reporter probe (step 1). After several buffer washes, Strep-Tactin®-HRP conjugate was added to cell solutions (step 2). Cells were washed again with buffer and chromogenic substrate was added, which is converted by HRP into a blue dye. From left to right, first row: Complete assay (steps 1 + 2); process control 1 (step 2 only, i.e., no RBP probe); second row: process control 2 (step 1 only, i.e., no Strep-Tactin®-HRP-conjugate); process control 3 (neither step 1 nor step 2). (**B**) Same as (**A**, first pair) but inactivated cell material was used.

3.5. The Dichotomous Colorimetric ELPRA for Identification of B. anthracis Can Be Simplified to a One-Step Assay

Alternative to the two-step ELPRA approach (RBP binding followed by Strep-Tactin®-HRP binding to cells) described above, we also developed a one-step test system. For this, the HRP moiety was directly conjugated to the RBP$_{\lambda 03\Delta 1\text{-}120}$ reporter protein. When

HRP-RBP$_{\lambda 03\Delta 1\text{-}120}$ was tested on inactivated *B. anthracis* Sterne and *B. cereus* ATCC10987 colony material, only *B. anthracis* yielded blue signals (Figure 4A).

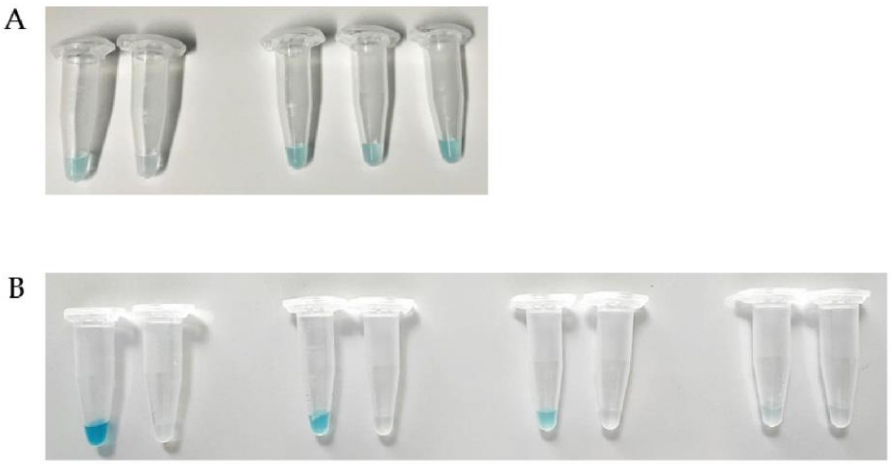

Figure 4. Identification of *B. anthracis* cells by rapid one-step dichotomous colorimetric ELPRA. (**A**) Inactivated colony material (50 µL of ca. 0.5 OD$_{600}$) of *B. anthracis* Sterne, *B. cereus* ATCC10987, *B. cereus s.l.* IMB-2021-1, *B. cereus* CDC2000032805, or *B. cereus* ATCC4342 (from left to right) were labeled in a one-step reaction with Strep-Tactin®XT-HRP-conjugated RBP$_{\lambda 03\Delta 1\text{-}120}$ reporter probe, washed several times with buffer, and chromogenic substrate was added, which was converted by HRP to a blue dye. (**B**) Same as (**A**) but a 1:5 dilution series is shown for *B. anthracis* Sterne and *B. cereus* ATCC10987 using 50 µL of colony material. The second pair of tubes from the left was taken from cell material of an optical density of 1 (OD$_{600}$).

While the one-step ELPRA assay required additional work beforehand and financial investment imposed by the RBP-Strep-Tactin®-HRP conjugation procedure, it further sped up the entire assay process and diminished pipetting steps. As a consequence, three parallel samples (an unknown sample and positive and negative control colony material) can be processed in as little as 20 min until scoring results (blue vs. no color).

Since there are a few *B. cereus s.l.* isolates known to yield false-positive results for binding of RBP$_{\lambda 03\Delta 1\text{-}120}$ [13] and to serve as host for Gamma phage as well [7], we included two of such strains in our testing. Additionally, we included the new isolate *B. cereus s.l.* IMB-2021-1 recovered by the colony lift and blot assay from Figure 2. Inactivated colony material of both *B. cereus* 4342 and CDC2000032805 was recognized by the HRP-RBP$_{\lambda 03\Delta 1\text{-}120}$ reporter, as indicated by blue color development (Figure 4A). Similarly, the new isolate *B. cereus s.l.* IMB-2021-1 was also receptive for the RBP reporter. This finding was corroborated by the Gamma phage assay [2] and fluorescence microscopy using the mCherry-RBP$_{\lambda 03\Delta 1\text{-}120}$ reporter (lacking conjugated HRP; Supplementary Materials Figure S2) vis-à-vis *B. anthracis* in which *B. cereus* 4342 and CDC2000032805 showed at least partially labeled cells. The partial labeling may also explain the lighter blue color of samples containing these isolates compared to cells of *B. anthracis*. Notably, isolate *B. cereus s.l.* IMB-2021-1 cells became fluorescent to the same extent as *B. anthracis* and the labeling reaction in Figure 4A commenced with a similar velocity.

In order to determine cell concentration ranges suitable for one-step dichotomous colorimetric ELPRA, we assayed a 1:5 dilution series of inactivated *B. anthracis* or *B. cereus* cell material. Dilutions were adjusted, so the first 1:5 dilution step samples had optical densities of 1 (OD$_{600}$) (Figure 4B; second pair of tubes). While the 1:125 dilution contained too little cell material to elicit any signal from *B. anthracis* cells, the 1:25 dilution was sufficient to differentiate the *B. anthracis* signal from that of *B. cereus* (no signal). A strong signal developed from the 1:5 (OD 1) sample and the undiluted sample produced a very strong signal. At all these cell densities, *B. cereus* still did not yield any visible signal

(Figure 4B). Notably, the signal from undiluted *B. anthracis* sample arose very rapidly, within a few seconds after addition of chromogenic substrate to the sample. Other signals took a couple minutes to develop. These results indicate that the one-step dichotomous colorimetric ELPRA for identification of *B. anthracis* is both as specific as the Gamma phage assay, largely flexible to the amount of cell material used, and quick to perform.

4. Discussion

Detection and identification of *B. anthracis* faces a variety of challenges. First, vegetative cells and spores may not be readily susceptible to identical analytical techniques. Second, *B. anthracis* is notoriously difficult to differentiate from its closest neighbors of the *B. cereus s.l.* group. The Gold Standard for *B. anthracis* identification still remains PCR targeting species-specific genetic markers such as *dhp61* [20], *PL3* [24], or others, including single nucleotide variations in genes like *plcR* [25]. Less reliable methods than PCR for *B. anthracis* identification are also available that may confirm PCR results or serve as rapid preliminary screening tools for pathogen detection. A common approach, especially in the field or in mobile laboratory settings, is the use of lateral flow assays (LFAs) for their quick and easy application. Unfortunately, LFAs are repeatedly neither very sensitive (in terms of limit of detection) nor highly specific [26,27]. For instance, a well-documented validation of the Tetracore RedLine Alert LFA yielded a sensitivity of >97% for *B. anthracis* with only a single *B. cereus* giving a false-positive result. However, upon closer examination, the panel of organisms tested included only seven *B. cereus* isolates [28]. In contrast, application of $RBP_{\lambda 03\Delta 1\text{-}120}$ for microscopy-based identification of *B. anthracis* has previously shown 95% specificity with only three false-positive *B. cereus s.l.* out of 56 non-*B. anthracis* bacilli. Similarly, another commercial LFA (InBios Active Anthrax Detect Rapid Test) reached 82% specificity [3], however, samples used in that study also included more difficult to test contaminated animal tissues. In contrast to many RBP-based assays [12,13], however, most LFAs are not depending on samples derived from actively growing *B. anthracis* cells. Among the RBPs previously tested for *B. anthracis*, we selected $RBP_{\lambda 03\Delta 1\text{-}120}$ because it is both host-specific and the least affected by the growth phases of its host cells [13]. Notably, for the intended use of screening of fresh growth on agar (colony lift and blot ELPRA) or of colony material (colorimetric ELPRA), growth-phase dependency of the RBP may not need to be a limiting factor. Previously, we have shown that $RBP_{\lambda 03\Delta 1\text{-}120}$ is able to label encapsulated cells of *B. anthracis* [13]. Though we did not explicitly retest this again, we expect the rapid assay introduced here works on encapsulated cells as well. Conversely, some LFAs have limitations, e.g., LFAs for *B. anthracis* detection requiring spores rather than cells as targets may fail to detect vegetative cells [27]. Conversely, ELPRA using $RBP_{\lambda 03\Delta 1\text{-}120}$ does not recognize carefully purified spores (i.e., preparations devoid of dead cells, ghosts, and cell debris) at all [13].

Spectrometric methods require specialized instrumentation and typically highly trained personnel [29,30]. In contrast, the long-established Gamma phage assay has proven to be a useful tool to complement PCR-based *B. anthracis* identification as it is both cheap and does not require specialized equipment or training [1]. With a high specificity of 96–97% toward *B. anthracis* [7], its usefulness is only limited by the duration of the identification procedure, which requires actively growing cells of *B. anthracis* [6]. In this the Gamma phage assay is similar to the ELPRA, but $RBP_{\lambda 03\Delta 1\text{-}120}$ is less restricted to the growth phase [13].

The *B. anthracis*-specific RBPs reported in this and previous work [13] bridge host-specific phage-based identification and ease of application with the speed of the detection assay. Starting from colony material, results can be obtained in just a few minutes using the one-step dichotomous colorimetric assay introduced here. Of course, another limit inherent in the Gamma phage assay carries over to the advanced RBP assay. Specificity remains high (>95%) but does not reach the near 100% certainty of PCR tests [20,24,25].

Colony blot assays for detecting microorganisms have a long history of application. They can help detect colonies of rare target organisms among those of other species isolated

from complex sample matrices, especially when there are no suitable means of prior enrichment. While antibodies or sera are typically recruited for primary detection of the target organism, e.g., [23,31], subsequent enrichment by cultivating colony-bearing membranes can also be used [32]. Alternatively, DNA probes may be employed on lysed target cells if genetic material is assayed, e.g., [33]. A phage-derived RBP, as in the study at hand, has, to the best of our knowledge, not yet been used for the purpose of target bacteria detection by colony blot before.

The newly introduced colony lift and blot ELPRA for *B. anthracis* may not only be useful for the analysis of complex environmental matrices with only minute numbers of contaminating *B. anthracis*. If extant semi-selective growth media overwhelmed by overgrowing bacterial flora are used, positions of positive signals on such agar plates can still be located and subjected to further analysis. Possibly, future progress in further developing *B. anthracis*-specific agar media may ameliorate this issue. Recently, for instance, a new selective agar medium for *B. anthracis* has been introduced [34]. The colony lift and blot ELPRA may be applied in conjunction with this improved agar medium for complex environmental samples bearing only low contamination of *B. anthracis* spores. Alternatively or in combination, the ELPRA could be included as a final step of analysis of more complex spore-enrichment procedures such as the one described in [35]. Herein, very low spore contaminations in soil of only 14 *B. anthracis* spores per g soil could be detected; however, the enrichment procedure took about 3.5 h (excluding cultivation). For the lack of authentic soil samples contaminated with *B. anthracis*, we were not able to compare our colony lift and blot ELPRA against this earlier protocol. Possibly, the colony lift and blot ELPRA may be combined with immunomagnetic enrichment for capturing *B. anthracis* spores [36,37]. Additionally, the colony lift and blot ELPRA for *B. anthracis* may also become a tool for the detection and subsequent isolation of bacteria outside *B. anthracis* that have properties that enabled these host cells to sequester RBPs or even complete phages.

5. Conclusions

This study introduced two new RBP-based identification assays for *B. anthracis*. The colony lift and blot ELPRA can be expected to facilitate *B. anthracis* identification from complex environmental matrices. The rapid colorimetric ELPRA may support PCR-based testing, for example, by pre-screening of suspect colonies for *B. anthracis*. More generally, RBP derivatives provide a valuable extension to the toolbox for pathogen detection and are both relatively easy to produce and to adapt to newly arising diagnostic needs.

Supplementary Materials: The following are available online at https://www.mdpi.com/article/10.3390/v13081462/s1, Figure S1: Western blot of heterologously produced NanoLuc-RBP$_{\lambda 03\Delta 1\text{-}120}$ reporter protein, Figure S2: Binding of mCherry-RBP$_{\lambda 03\Delta 1\text{-}120}$ reporter to cells of cultures of B. anthracis and cross-reacting B. cereus cells, Table S1: Strains used in this work, Table S2: Oligonucleotide primers used for DNA sequencing and cloning in this work.

Author Contributions: Conceptualization, G.G.; methodology, G.G and P.B.; validation, G.G. and P.B.; formal analysis, G.G.; investigation, N.R. and D.N.; resources, G.G.; data curation, G.G. and P.B.; writing—original draft preparation, G.G.; writing—review and editing, G.G, P.B., N.R. and D.N.; visualization, G.G., N.R. and P.B.; supervision, G.G.; project administration, G.G.; funding acquisition, G.G. All authors have read and agreed to the published version of the manuscript.

Funding: This research received funding from the Medical Biological Defense Research Program of the Bundeswehr Joint Medical Service.

Institutional Review Board Statement: Not applicable.

Informed Consent Statement: Not applicable.

Acknowledgments: The authors thank Gabriele Echle and Linda Dobrzykowski for their skillful technical assistance.

Conflicts of Interest: The authors declare no conflict of interest. Opinions, interpretations, conclusions, and recommendations are those of the authors and are not necessarily endorsed by any

governmental agency, department, or other institutions. The funders had no role in the design of the study; in the collection, analyses, or interpretation of data; in the writing of the manuscript, or in the decision to publish the results.

References

1. World Health Organization. *Anthrax in Humans and Animals Fourth Edition*; Turnbull, P., Ed.; WHO Press: Geneva, Switzerland, 2008; p. 285.
2. Abshire, T.G.; Brown, J.E.; Ezzell, J.W. Production and Validation of the Use of Gamma Phage for Identification of Bacillus Anthracis. *J. Clin. Microbiol.* **2005**, *43*, 4780–4788. [CrossRef]
3. Kolton, C.B.; Marston, C.K.; Stoddard, R.A.; Cossaboom, C.; Salzer, J.S.; Kozel, T.R.; Gates-Hollingsworth, M.A.; Cleveland, C.A.; Thompson, A.T.; Dalton, M.F.; et al. Detection of *Bacillus anthracis* in animal tissues using InBios active anthrax detect rapid test lateral flow immunoassay. *Lett. Appl. Microbiol.* **2019**, *68*, 480–484. [CrossRef]
4. Kan, S.; Fornelos, N.; Schuch, R.; Fischetti, V.A. Identification of a ligand on the Wip1 bacteriophage highly specific for a receptor on *Bacillus anthracis*. *J. Bacteriol.* **2013**, *195*, 4355–4364. [CrossRef]
5. Sozhamannan, S.; McKinstry, M.; Lentz, S.M.; Jalasvuori, M.; McAfee, F.; Smith, A.; Dabbs, J.; Ackermann, H.W.; Bamford, J.K.; Mateczun, A.; et al. Molecular characterization of a variant of *Bacillus anthracis*-specific phage AP50 with improved bacteriolytic activity. *Appl. Environ. Microbiol.* **2008**, *74*, 6792–6796. [CrossRef]
6. Brown, E.R.; Cherry, W.B. Specific identification of *Bacillus anthracis* by means of a variant bacteriophage. *J. Infect. Dis.* **1955**, *96*, 34–39. [CrossRef]
7. Kolton, C.B.; Podnecky, N.L.; Shadomy, S.V.; Gee, J.E.; Hoffmaster, A.R. *Bacillus anthracis* gamma phage lysis among soil bacteria: An update on test specificity. *BMC Res. Notes* **2017**, *10*, 598. [CrossRef]
8. Dowah, A.S.A.; Clokie, M.R.J. Review of the nature, diversity and structure of bacteriophage receptor binding proteins that target Gram-positive bacteria. *Biophys. Rev.* **2018**. [CrossRef] [PubMed]
9. Dunne, M.; Loessner, M.J. Modified bacteriophage tail fiber proteins for labeling, immobilization, capture, and detection of bacteria. *Methods Mol. Biol.* **2019**, *1918*, 67–86. [CrossRef]
10. Denyes, J.M.; Dunne, M.; Steiner, S.; Mittelviefhaus, M.; Weiss, A.; Schmidt, H.; Klumpp, J.; Loessner, M.J. Modified bacteriophage S16 long tail fiber proteins for rapid and specific immobilization and detection of *Salmonella* cells. *Appl. Environ. Microbiol.* **2017**, *83*. [CrossRef] [PubMed]
11. Muangsombut, V.; Withatanung, P.; Chantratita, N.; Chareonsudjai, S.; Lim, J.; Galyov, E.E.; Ottiwet, O.; Sengyee, S.; Janesomboon, S.; Loessner, M.J.; et al. Development of a bacteriophage tail fiber-based latex agglutination assay for rapid clinical screening of *Burkholderia pseudomallei*. *Appl. Environ. Microbiol.* **2021**. [CrossRef]
12. Born, F.; Braun, P.; Scholz, H.C.; Grass, G. Specific detection of *Yersinia pestis* based on receptor binding proteins of phages. *Pathogens* **2020**, *9*, 611. [CrossRef] [PubMed]
13. Braun, P.; Wolfschläger, I.; Reetz, L.; Bachstein, L.; Jacinto, A.C.; Tocantins, C.; Poppe, J.; Grass, G. Rapid microscopic detection of *Bacillus anthracis* by fluorescent receptor binding proteins of bacteriophages. *Microorganisms* **2020**, *8*, 934. [CrossRef] [PubMed]
14. Davison, S.; Couture-Tosi, E.; Candela, T.; Mock, M.; Fouet, A. Identification of the *Bacillus anthracis* (gamma) phage receptor. *J. Bacteriol.* **2005**, *187*, 6742–6749. [CrossRef]
15. Sozhamannan, S.; Chute, M.D.; McAfee, F.D.; Fouts, D.E.; Akmal, A.; Galloway, D.R.; Mateczun, A.; Baillie, L.W.; Read, T.D. The *Bacillus anthracis* chromosome contains four conserved, excision-proficient, putative prophages. *BMC Microbiol.* **2006**, *6*, 34. [CrossRef] [PubMed]
16. Sterne, M.; Proom, H. Induction of motility and capsulation in *Bacillus anthracis*. *J. Bacteriol.* **1957**, *74*, 541–542. [CrossRef]
17. Fasanella, A.; Di Taranto, P.; Garofolo, G.; Colao, V.; Marino, L.; Buonavoglia, D.; Pedarra, C.; Adone, R.; Hugh-Jones, M. Ground Anthrax *Bacillus* Refined Isolation (GABRI) method for analyzing environmental samples with low levels of *Bacillus anthracis* contamination. *BMC Microbiol.* **2013**, *13*, 167. [CrossRef]
18. Cote, C.K.; Buhr, T.; Bernhards, C.B.; Bohmke, M.D.; Calm, A.M.; Esteban-Trexler, J.S.; Hunter, M.; Katoski, S.E.; Kennihan, N.; Klimko, C.P.; et al. A standard method to inactivate *Bacillus anthracis* spores to sterility via gamma irradiation. *Appl. Environ. Microbiol.* **2018**, *84*. [CrossRef]
19. Knüpfer, M.; Braun, P.; Baumann, K.; Rehn, A.; Antwerpen, M.; Grass, G.; Wölfel, A.R. Evaluation of a highly efficient DNA extraction method for *Bacillus anthracis* endospores. *Microorganisms* **2020**, *8*, 763. [CrossRef]
20. Antwerpen, M.H.; Zimmermann, P.; Bewley, K.; Frangoulidis, D.; Meyer, H. Real-time PCR system targeting a chromosomal marker specific for *Bacillus anthracis*. *Mol. Cell. Probes* **2008**, *22*, 313–315. [CrossRef]
21. Lane, D.J.; Pace, B.; Olsen, G.J.; Stahl, D.A.; Sogin, M.L.; Pace, N.R. Rapid determination of 16S ribosomal RNA sequences for phylogenetic analyses. *Proc. Natl. Acad. Sci. USA* **1985**, *82*, 6955–6959. [CrossRef]
22. Watanabe, K.; Kodama, Y.; Harayama, S. Design and evaluation of PCR primers to amplify bacterial 16S ribosomal DNA fragments used for community fingerprinting. *J. Microbiol. Methods* **2001**, *44*, 253–262. [CrossRef]
23. Bogaert, D.; Veenhoven, R.H.; Sluijter, M.; Sanders, E.A.; de Groot, R.; Hermans, P.W. Colony blot assay: A useful method to detect multiple pneumococcal serotypes within clinical specimens. *FEMS Immunol. Med. Microbiol.* **2004**, *41*, 259–264. [CrossRef]

24. Wielinga, P.R.; Hamidjaja, R.A.; Agren, J.; Knutsson, R.; Segerman, B.; Fricker, M.; Ehling-Schulz, M.; de Groot, A.; Burton, J.; Brooks, T.; et al. A multiplex real-time PCR for identifying and differentiating *B. anthracis* virulent types. *Int. J. Food. Microbiol.* **2011**, *145*, 137–144. [CrossRef]
25. Derzelle, S.; Mendy, C.; Laroche, S.; Madani, N. Use of high-resolution melting and melting temperature-shift assays for specific detection and identification of *Bacillus anthracis* based on single nucleotide discrimination. *J. Microbiol. Methods* **2011**, *87*, 195–201. [CrossRef]
26. Zasada, A.A.; Forminska, K.; Zacharczuk, K.; Jacob, D.; Grunow, R. Comparison of eleven commercially available rapid tests for detection of *Bacillus anthracis*, *Francisella tularensis* and *Yersinia pestis*. *Lett. Appl. Microbiol.* **2015**, *60*, 409–413. [CrossRef] [PubMed]
27. Ziegler, I.; Vollmar, P.; Knüpfer, M.; Braun, P.; Stoecker, K. Reevaluating limits of detection of 12 lateral flow immunoassays for the detection of *Yersinia pestis*, *Francisella tularensis*, and *Bacillus anthracis* spores using viable risk group-3 strains. *J. Appl. Microbiol.* **2021**, *130*, 1173–1180. [CrossRef] [PubMed]
28. Pillai, S.P.; Prentice, K.W.; Ramage, J.G.; DePalma, L.; Sarwar, J.; Parameswaran, N.; Bell, M.; Plummer, A.; Santos, A.; Singh, A.; et al. Rapid presumptive identification of *Bacillus anthracis* isolates using the Tetracore RedLine Alert Test. *Health. Secur.* **2019**, *17*, 334–343. [CrossRef]
29. Dybwad, M.; van der Laaken, A.L.; Blatny, J.M.; Paauw, A. Rapid identification of *Bacillus anthracis* spores in suspicious powder samples by using matrix-assisted laser desorption ionization-time of flight mass spectrometry (MALDI-TOF MS). *Appl. Environ. Microbiol.* **2013**, *79*, 5372–5383. [CrossRef]
30. Pauker, V.I.; Thoma, B.R.; Grass, G.; Bleichert, P.; Hanczaruk, M.; Zoller, L.; Zange, S. Improved discrimination of *Bacillus anthracis* from closely related species in the *Bacillus cereus sensu lato* group based on Matrix-Assisted Laser Desorption Ionization-Time of Flight mass spectrometry. *J. Clin. Microbiol.* **2018**, *56*. [CrossRef] [PubMed]
31. Roop, R.M., 2nd; Preston-Moore, D.; Bagchi, T.; Schurig, G.G. Rapid identification of smooth *Brucella* species with a monoclonal antibody. *J. Clin. Microbiol.* **1987**, *25*, 2090–2093. [CrossRef]
32. Hoszowski, A.; Fraser, A.D.; Brooks, B.W.; Riche, E.M. Rapid detection and enumeration of *Salmonella* in chicken carcass rinses using filtration, enrichment and colony blot immunoassay. *Int. J. Food. Microbiol.* **1996**, *28*, 341–350. [CrossRef]
33. Ramotar, K.; Henderson, E.; Szumski, R.; Louie, T.J. Impact of free verotoxin testing on epidemiology of diarrhea caused by verotoxin-producing *Escherichia coli*. *J. Clin. Microbiol.* **1995**, *33*, 1114–1120. [CrossRef] [PubMed]
34. Rohde, A.; Papp, S.; Feige, P.; Grunow, R.; Kaspari, O. Development of a novel selective agar for the isolation and detection of *Bacillus anthracis*. *J. Appl. Microbiol.* **2020**. [CrossRef]
35. Silvestri, E.E.; Feldhake, D.; Griffin, D.; Lisle, J.; Nichols, T.L.; Shah, S.R.; Pemberton, A.; Schaefer, F.W., 3rd. Optimization of sample processing protocol for recovery of *Bacillus anthracis* spores from soil. *J. Microbiol. Methods* **2016**. [CrossRef]
36. Shields, M.J.; Hahn, K.R.; Janzen, T.W.; Goji, N.; Thomas, M.C.; Kingombe, C.B.; Paquet, C.; Kell, A.J.; Amoako, K.K. Immunomagnetic capture of *Bacillus anthracis* spores from food. *J. Food. Prot.* **2012**, *75*, 1243–1248. [CrossRef]
37. Fisher, M.; Atiya-Nasagi, Y.; Simon, I.; Gordin, M.; Mechaly, A.; Yitzhaki, S. A combined immunomagnetic separation and lateral flow method for a sensitive on-site detection of *Bacillus anthracis* spores—Assessment in water and dairy products. *Lett. Appl. Microbiol.* **2009**, *48*, 413–418. [CrossRef]

7. Reoccurring bovine anthrax in Germany on the same pasture after 12 years

Reoccurring bovine anthrax in Germany on the same pasture after 12 years

Peter Braun[1], Wolfgang Beyer[2], Matthias Hanczaruk[3], Julia M. Riehm[3], Markus Antwerpen[1], Christian Otterbein[4], Jacqueline Oesterheld[1] and Gregor Grass[1]*

[1]Bundeswehr Institute of Microbiology (IMB), Department of Bacteriology and Toxinology, Munich, Germany;

[2]Department of Livestock Infectiology and Environmental Hygiene, Institute of Animal Science, University of Hohenheim, Stuttgart, Germany

[3]Bavarian Health and Food Safety Authority, Oberschleißheim, Germany

[4]Local Veterinarian Unit, District Rosenheim, Germany

*Correspondence: gregorgrass@bundeswehr.org; Tel.: +49-992692-3981

Abstract

The zoonotic disease anthrax caused by the endospore-forming bacterium *Bacillus anthracis* is very rare in Germany. In the state of Bavaria, the last case occurred in July of 2009 resulting in four dead cows. In August of 2021, the disease reemerged after heavy rains, killing one gestating cow. Notably, both outbreaks affected the same pasture, suggesting a close epidemiological connection. *B. anthracis* could be grown from blood culture and the presence of both virulence plasmids (pXO1 and pXO2) was confirmed by PCR. Also, recently developed diagnostic tools enabled rapid detection of *B. anthracis* cells and nucleic acids directly in clinical samples. The complete genome of the strain isolated from blood, designated BF-5, was DNA-sequenced and phylogenetically grouped within the B.Br.CNEVA clade that is typical for European *B. anthracis* strains. The genome was almost identical to BF-1, the isolate of 2009, separated only by three single nucleotide polymorphisms on the chromosome, one on plasmid pXO2 and three indel-regions. Further, *B. anthracis* DNA was detected by PCR from soil-samples taken from spots, where the cow had fallen onto the pasture. New tools based on phage receptor binding proteins enabled the microscopic detection and isolation of *B. anthracis* directly from soil-samples. These environmental isolates were genotyped and found to be SNP-identical to BF-5. Therefore, it seems that the BF-5 genotype is currently the prevalent one at the affected premises. The contaminated area at the cadaver was subsequently disinfected with formaldehyde.

Introduction

Bacillus anthracis, the causative agent of anthrax, resides dormant in soil as endospores. These spores can resurface after heavy rains (1) or e.g., by disturbances of animal burial-sites (2). Typically, susceptible grazing mammals become infected by ingesting spore-

contaminated soil. The anthrax pathogen is notorious for unexpectedly re-emerging after years or decades of inactivity at previous outbreak -sites (1). Such instances include outbreaks in Sweden (2), Siberia (3) or Italy (4, 5). In Germany, anthrax is very uncommon. The last human infections in 2012 were associated with illicit drug-consumption of heroin allegedly contaminated with *B. anthracis* spores (6–8). Animal cases are equally rare with small-scale bovine outbreaks recorded in 2009 (9), 2012 (10) and 2014 (11). While these animal cases involved *B. anthracis* genotypes common for Germany, the human cases raised concern as genotypes involved were distinct from any known German isolate but closely related to strains from the Near and Middle East (12). Likely, spores of this genotype were introduced via drug-trafficking activities involving contaminated by-products *en route* (6, 12). Rapid identification and genotyping of new outbreak isolates is thus of importance to differentiate natural, reoccurring outbreaks of domestic strains from deliberate release or accidental contamination.

Therefore, occurrence of bovine anthrax in August of 2021 raised initial alarm. However, this outbreak has affected the same premises as in 2009. Back then, four heifers had succumbed to the disease and one was euthanized (13). Now, a gestating cow fell with strong suspicion of anthrax.

The genome (BF-1) of the 2009 anthrax-outbreak has been published (9). This genome is closely related with other isolates of the B-branch phylogeny of *B. anthracis* (B.Br. CNEVA) (14). The B.Br. CNEVA genotype seems to be typical for mountainous areas in central Europe from France (14) to Slovakia (14) and from Sweden (2) to Switzerland (15). Also, to this group belongs a historical genome reconstructed from a microscopy-slide prepared in Germany in 1878 featuring *B. anthracis*-infected dried-up cow-blood (14).

In this report, we describe the investigation of a rare reoccurring German anthrax-outbreak in southern Bavaria. Rapid detection of *B. anthracis* associated with anthrax outbreak events using species-specific means of identification is paramount for initiation of infection-

control countermeasures. Additional genomic analysis of the causative agent may help differentiate between natural infection and deliberate release of the pathogen. The aim of this study was thus the unambiguous identification of *B. anthracis* with a diverse set of diagnostic tools targeting the anthrax pathogen's nucleic acids and proteins. Because of the very close spatial occurrence of the 2009/2021 outbreaks, the question arose, whether the *B. anthracis* strains involved were identical or different. We thus analyzed the genome-sequence of the 2021 outbreak isolate and offer conclusions on the phylogenetic relation of this *B. anthracis* strain to closely related strains.

Material and Methods

Bacterial culture and inactivation

Strain, *B. anthracis* Sterne (positive control) (16) and *B. cereus* ATCC10987 (negative control) were grown on Columbia blood agar (Becton Dickinson, Heidelberg, Germany) or trimethoprim-sulfamethoxazole-polymyxin blood agar (TSPBA) (17). *B. anthracis* was chemically inactivated with 4% (*v*/*v*) Terralin PAA (Schülke & Mayr GmbH, Norderstedt, Germany), as in (18). Blood-samples were inactivated within a class III biological safety cabinet at the Bundeswehr Institute of Microbiology BSL-3 facility by adding 50 ml 4% (v/v) Terralin PAA to 0.5 ml blood. After incubation at room temperature for 30 min, samples were washed twice by centrifugation (5000 x g, 5 min) with 10 ml phosphate-buffered saline (PBS) and finally resuspended in 0.5 ml PBS.

Initial carcass samples, diagnostic polymerase chain reaction for B. anthracis and microscopy

Blood-samples from the left nostril of the cow-carcass were taken and transferred to the federal state veterinary laboratory and the Bundeswehr Institute of Microbiology for further analysis. Sample-culture was conducted on Columbia blood agar, and grown overnight at 37°C. A single colony with typical growth morphology was cultivated, named BF-5 and used for DNA preparation (Qiagen, Hilden, Germany). Polymerase chain reaction (PCR) was performed for chromosomal and both virulence plasmids markers (pXO1 and pXO2) as described in the manufacturer's instructions (RealStar® Anthrax PCR Kit 1.0; Altona, Hamburg, Germany).

For direct PCR-based detection of *B. anthracis* in blood-samples, 100 µl inactivated blood-sample were incubated at 95°C for 10 min to lyse cells and centrifuged at 5000 x g for 2 min. Aliquots of 5 µl of the supernatant were then used as templates for 16S rRNA SNP-PCR or 16S rRNA SNP RT-PCR performed as described in (19). Alternatively, total nucleic acid extractions of blood-samples were used as templates. MasterPure Complete DNA and RNA Purification Kit (Lucigen, Middleton, WI, USA) was used for extraction of DNA and RNA from blood-samples according to the manufacturer's instructions for whole-blood-samples.

For microscopic detection of *B. anthracis* from blood-samples, receptor binding protein (RBP) derivative $RBP_{\lambda 03\square 1\text{-}120}$ was used. A volume of 0.5 ml blood was inactivated, repeatedly washed with PBS and mixed with 1 µg mCherry-$RBP_{\lambda 03\square 1\text{-}120}$ protein (18). Fluorescence microscopy was conducted as described in (18).

Collection of soil-samples

On September 6, 2021, soil-samples were collected from four spots corresponding to the head and tail area where the deceased cow had fallen and subsequently exuded spore-contaminated blood onto the pasture. Because of heavy rains in the area in the meantime (>50 l/m^2), samples were collected from approx. 10 cm below the surface. Each sample comprised duplicates of 50 ml conical tubes half-filled with soil (about 50-70 g). Samples were stored at ambient temperature.

Soil-sample analysis by PCR and culturing of B. anthracis

Soil-samples for PCR analysis were processed as described in (20). Briefly, three aliquots of soil-samples (10 g) were resuspended in 20 ml of sterile water with glass-beads (Ø5 mm) and mixed overnight at room temperature. Two of the aliquots were spiked beforehand with spores of strain *B. anthracis* Sterne 34F2 for quantification (2 x 10^2 and 5 x 10^2 spores per sample). The suspensions were filtered through sterile gauze to remove soil particles and other rough materials. After centrifugation at 4000 x g for 15 min, the pellet was washed three times in sterile water and finally re-suspended in 5 ml $aqua_{dest}$. This suspension was heated to 65-70°C for 30 min to inactivate vegetative cells. Volumes of 250 µl each were plated onto four semi-selective agar plates (TSPBA) (21). Plates were incubated overnight at 37°C. Then, the bacterial lawn from each plate was scraped off and re-suspended in 4 ml of 0.9 % (*w/v*) NaCl-solution. An aliquot (ca. 1 ml) of this suspension was boiled for 20 min in a heating block to release DNA from cells, centrifuged at 12,000 x g for 15 min and the supernatant filtered through a 0.45 µm Luer-lock filter. Aliquots of 5 µl of the filtered supernatant were used for PCR analysis (20). If PCR-positive, dilutions of the original suspension were plated and grown on TSPBA (17) for isolation and verification of suspicious *B. anthracis* colonies (20). DNA from a picked colony was tested by PCR for *B. anthracis* specific markers as described in (1). Additional enrichment of *B. anthracis*

from soil-samples was achieved by culturing on semi-selective CEFOMA agar "*Bacillus CEreus sensu lato* group-specific antibiotics, FOsfomycin, Macrolides Agar" according to [22].

Enrichment of B. anthracis from soil-samples by magnetic separation and culturing

For enriching *B. anthracis* from possibly spore-contaminated soil-samples, a newly developed magnetic bead-assisted magnetic separation-method was applied. In this approach $RBP_{\lambda03\square1\text{-}120}$ (18) was re-purposed to capture *B. anthracis* from soil. In short, Strep-Tactin XT protein (IBA GmbH, Göttingen, Germany) was coupled to magnetic beads (Dynabeads™ M-280 Tosylactivated, ThermoFisher, Dreieich, Germany). Then $RBP_{\lambda03\square1\text{-}120}$ protein was attached to this Strep-Tactin XT via the Twin Strep-tag epitope. Soil was processed as described in (17), i.e., a soil-sample was shaken in PBS buffer with 0.5 % (*v/v*) Tween 20 to solubilize spores. The sample was mildly centrifuged to remove solid material and the crudely cleared supernatant incubated at 62°C for 20 min to inactivate vegetative cells. The supernatant was mixed 1: 10 with Brain Heart Infusion broth (Merck, Darmstadt, Germany) with 10% (*v/v*) fetal calf serum (Merck) and incubated to allow spores to germinate and develop into vegetative cells. This germination culture was mixed and incubated with the RBP-loaded magnetic beads to separate *B. anthracis* spores from the liquid. Separation was accomplished using a magnetic stand (ThermoFisher). Beads were washed and finally plated onto TSPBA agar or Columbia blood agar plates (Becton Dickinson). Colonies were evaluated after incubating over night at 37°C. Full details on the method will be published elsewhere.

Rapid prescreening of candidate B. anthracis colonies

Blood-samples from the carcass or colonies suspicious for *B. anthracis* obtained after enrichment from soil-samples, were subjected to colorimetric Enzyme-Linked Phage Receptor Binding Protein Assay (ELPRA) as described in (23). In short, the one-step assay version was applied that utilizes recombinant HRP-coupled $RBP_{\lambda03\square1\text{-}120}$. Candidate colony material or blood was inactivated, washed twice with PBS and incubated with 0.1 µg of HRP-$RBP_{\lambda03\square1\text{-}120}$ protein. Samples were repeatedly washed with PBS and the pellet resuspended in 50 µL SeramunBlau® slow (containing 3,3′,5,5′-tetramethylbenzidin) peroxidase substrate (Seramun Diagnostica, Heidesee, Germany). Blue color development was monitored for several minutes and photo-documented. Inactivated sheep blood served as a negative control.

High quality DNA preparation from B. anthracis colony material and confirmative PCR

Single bacterial colonies grown on semi-selective agar (TSPBA) were chemically inactivated with 4% Terralin PAA and DNA isolated using the MasterPure™ Gram Positive DNA Purification kit (Lucigen, Middleton, WI, USA) with minor modifications as described in (24). DNA concentrations were quantified using the Qubit dsDNA HS Assay Kit (Thermo Fisher Scientific, Darmstadt, Germany), according to the supplier's protocol. For confirmation of *B. anthracis* DNA via PCR, the chromosomal marker *dhp61* was used as described previously (25). DNA preparations were stored at −20 °C until further use.

Whole Genome Sequencing

Nanopore sequencing was performed using SQK-LSK109 chemistry on a R10.3 SpotON Flow Cell on the GridION system (Oxford Nanopore Technologies, Oxford, UK) running system software MinKNOW 21.05.8. A total of 350,000 reads were generated using the

implemented “super-accurate base calling” model. For increasing the assembly-efficacy the amount of reads were down-sampled to 104,110 reads (N50 of 10.01 kb; mean raw quality score of Q13.5). After processing using Flye assembler V2.9 (26) three circularized high-quality replicons, corresponding to the chromosome (5,213,322 bp; coverage 174-fold) as well as both plasmids pXO1 (181,920 bp; coverage 614-fold) and pXO2 (94,735 bp; coverage 491-fold) were obtained. The scaffolds were manually checked for contaminant reads and annotated automatically by the NCBI Prokaryotic Genome Annotation Pipeline (27) after submission. All data generated or analyzed during this study are included in this published article, and its supplementary information files are publically available in the NCBI Sequence Read Archive (SRA) repository (Bioproject PRJNA171093). CanSNPer (v1.0.10) (28) was used to classify and subsequently assign the corresponding canSNP-group B.Br.CNEVA to this genome.

Analysis of whole genome sequencing data and SNP-calling

For rapid core chromosome multiple-alignment, the Parsnp tool from the Harvest Suite (version 1.1.2) was used (29). For this, a chromosome-dataset, representing genomes from public databases (Table S1) and the newly sequenced strains of *B. anthracis*, were aligned against the chromosome of *B. anthracis* ‘Ames ancestor’ (NC_007530) as a phylogenetic outgroup using Parsnp (parameters -c -e -u -C 1000). To export the identified SNP-positions, HarvestTools (version 1.2) from the same software suite was used to create a vcf-(Variant Calling File) listing all SNP-positions. In order to enhance data quality, chromosome regions with closely adjacent SNPs (<10 bp distance), and positions harboring undefined nucleotides (“N”), were removed. This curated vcf-file was used as input for HarvestTools to compile a multi-FASTA file out of the chromosome-dataset, comprising the concatenated SNPs as a multiple-sequence alignment. This concatenated sequence information was used to calculate a Maximum Likelihood tree in MEGA X

(version 10.0.5) (30, 31). A minimum spanning tree was computed in BioNumerics 6.6 (Applied Maths, Sint-Martens-Latem, Belgium) from the vcf SNP-file (in binary format) as input, and manually edited (using Powerpoint 2016, Microsoft) for style.

Analysis of the distribution of SNPs specific for B. anthracis strain BF-5 in other isolates

DNA of several additional clones retrieved from soil sampling were subjected to SNP-analysis. For this, regions covering the SNP-regions identified by genome sequencing were PCR-amplified (Primers listed in Table S2) and Sanger DNA-sequenced (Eurofin Genomics, Ebersbach, Germany). DNA-sequence analysis was conducted with Geneious Prime (Biomatters, USA).

Results

B. anthracis infection in a deceased cow was confirmed by initial in situ and PCR diagnostics

Veterinary examination of a deceased gestating cow on a pasture near Rosenheim (Bavaria, Germany) on August 24, 2021 raised suspicion of anthrax infection due to the disease-typical symptoms, i.e., sudden death and bloody discharge from all body orifices, including nostrils, eyes, vagina and anus (Figure 1A, B). PCR of DNA isolated from colonies with typical morphology grown after cultivating blood from the deceased animal gave positive results for diagnostic *B. anthracis* markers, the *dhp61*, *pag*, and *cap* genes, respectively (data not shown). Thus, anthrax disease was confirmed and an official diagnostic report released.

Detection of B. anthracis directly in blood-samples by phage RBP-based reporter and 16S rRNA SNP (RT)-PCR

Independent to initial diagnostic PCR analysis performed by state health authorities, blood taken from the left nostril of the carcass (Figure 1A) was inactivated and subjected to recently developed ultrasensitive 16S rRNA SNP (RT)-PCR (19) and phage RBP reporter-based rapid detection assays (18). Results confirmed the previous PCR tests as phage RBP $_{\lambda 03\Delta 1\text{-}120}$ reporter based ELPRA gave positive results when inactivated blood-samples from the carcass were tested (Figure 2A). Using fluorescence microscopy, mCherry-RBP$_{\lambda 03\Delta 1\text{-}120}$ reporter was found to specifically bind to bacterial chains in blood-sample as evidenced by red fluorescence (Figure 2B). This indicated that the detected cells were indeed very likely *B. anthracis*. Of note, these phage RBP-based tests can be performed in just a few minutes. Using 16S rRNA SNP-PCR, specific detection of *B. anthracis* nucleic acids directly in the blood-samples derived from the carcass as well as from nucleic acid extractions thereof, was also accomplished (Figure 2C). Dilutions (1:10 to 1:1000) of the inactivated blood-sample (without prior nucleic acid extraction) yielded Ct values from 24.9 to 31.7. Conversely, dilutions of total nucleic acid extracted from the same blood-sample yielded Ct values from 13.9 to 21.5 when testing for DNA only (Table S3). When these total nucleic acid preparations (containing DNA and RNA) were subjected to 16S rRNA SNP RT-PCR, the same samples (dilutions 1:10 to 1:1000) yielded even lower Ct values (9.7 to 17.8; Table S3). This is because the ultrasensitive RT version of the PCR not only detects 16S rRNA genes of *B. anthracis* but also their transcripts, which are more abundant in growing cells compared to their respective gene copies.

B. anthracis strains BF-1 and BF-5 are clonal, very closely related outbreak strains

Genomic DNA of *B. anthracis* strains BF-5 was subjected to sequencing resulting in three contigs (chromosome, plasmid pXO1 and pXO2) (accession # CP089993- CP089995). Comparison of the genomes of *B. anthracis* strains BF-1 and BF-5 revealed that both strains were exceptionally similar (Table 1). The chromosome of BF-5 featured only three SNPs and two single nucleotide repeat (SNR) differences (both SNRs in non-coding regions with deletions of a single “T”). While plasmid pXO1 was identical, pXO2 harbored a single additional SNP- and SNR-insertion (“T”) in three identical repeat regions, respectively. This clonality of the two outbreak strains clearly supported the hypothesis that a hitherto non-localized source of unknown origin of contamination exists on-site. This source is very likely the cause of repeated infection of grassing cows on this pasture.

Phylogenetically, strains B. anthracis BF-1 and BF-5 group with strains from the Austrian state of Tyrol

The canSNP-type of *B. anthracis* BF-5 was determined, assigning the strain to the B.Br.CNEVA clade (32). Chromosomal sequence analysis inferred the phylogenetic placement of strain BF-5 to a cluster of central European *B. anthracis* strains within the B.Br.CNEVA clade. As expected from Table 1, the closest relative was strain BF-1 (Figure 3). Other close relatives were Tyrol 4675 and Tyrol 6282, from the Austrian state of Tyrol from 1988 and 1979, respectively. Strains from a large French B.Br.CNEVA cluster (only three representatives shown in Figure 3) as well as strains from Switzerland, Slovakia, Germany and Italy were more distantly related. Not shown are additional B.Br.CNEVA genomes phylogenetically more loosely related to the focus strain, BF-5. Notably, there is a polytomy at the base of the French cluster, the clade comprising strains A016/17OD930 and Tyrol 3520 and the clade featuring BF-1, BF-5 as well as Tyrol 4674 and Tyrol 6282 (Figure 3). This clearly suggests a common ancestor of all the strains.

Both "classical", established methods and novel phage RBP reporter fusions enable direct detection and isolation of B. anthracis from soil-samples

Soil samples were retrieved (single samples each) from the site of the carcass from depths of about 5-10 cm. This corresponded to soil positions close to those of head and anus of the deceased cow (Figure 1A, B). The established analysis methods yielded positive PCR results after cultivation of original soil materials. Isolated colonies with typical morphology of *B. anthracis* were positive in PCR for *pagA*, *capC* and *saspB* (data not shown). The novel, phage protein-based magnetic enrichment approach fared equally well, yet, can be completed in much shorter time: To screen the possibly contaminated soil-samples for *B. anthracis* spores, mCherry-$RBP_{\lambda 03\Delta 1\text{-}120}$ was just added to soil supernatants pre-incubated with germination medium and the samples were subjected to fluorescence microscopy. With this method, cells of *B. anthracis* could be detected directly in soil-samples as cell chains emitted strong red fluorescence derived from the attached RBP reporter (Figure 4A). While presence of *B. anthracis* was indicated by fluorescence microscopy, isolation of *B. anthracis* from soil-samples was achieved using magnetic beads coupled with $RBP_{\lambda 03\Delta 1\text{-}120}$. After binding of the cells to the RBP-loaded magnetic beads, the buffer-washed cell-bead-complexes (Figure 4B, left panel) were agar-plated and cultured. A representative result is shown in Figure 4B (right panel). While occasionally hemolytic, non-*B. anthracis* colonies (negative in *dhp61*-PCR) also grew on the plates, suspect *B. anthracis* colonies showing no hemolysis were chemically inactivated and confirmed by ELPRA (Figure 4C). Genomic DNA from six of these additional isolates was prepared for further analysis.

Four SNPs found between B. anthracis strains BF-1 and BF-5 were interrogated in additional isolates derived from contaminated soil

In order to determine the distribution and relative abundance of the four SNPs separating *B. anthracis* strains BF-1 and BF-5 (Table1; Table S2), PCRs of the identified four SNP-regions were conducted on DNA from six *B. anthracis* soil isolates and the PCR amplicons Sanger-sequenced. We did not identify any SNP-differences in these six soil isolates relative to BF-5 (data not shown). Thus, these results indicate that the BF-5 genotype is the prevalent genotype at the affected pasture in 2021.

Discussion

Regarding risk-assessment, re-occurrence of an anthrax-outbreak after 12 years (9) at the same pasture diminished the suspicion of intentional release of the pathogen as underlying cause. Conversely, the outbreak strongly indicated that an old anthrax focus was still active. This is reminiscent to similar situations in other regions of Europe. For instance, in Sweden an outbreak in cattle occurred in a nature-reserve in 2011. Notably, records positioned an old anthrax burial-site (mid-1940s) in that area (2, 33). Remarkably, only two years later, an additional cow deceased closely to this area that had seen cattle-vaccination after the 2011 outbreak (34). The complete elimination of *B. anthracis* spores from soil within a natural focus cannot be assured by any decontamination measure (35). Therefore, German law considers the temporary closure of respective areas for grazing to prevent reinfection besides decontamination trials (German Federal Ministry of Justice/ Bundesministerium für Justiz: Verordnung zum Schutz gegen den Milzbrand und den Rauschbrand https://www.gesetze-im-internet.de/milzbrbv/BJNR011720991.html; accessed: 2022-01-06)(35). Similar to the case at hand, genome sequencing of the two Swedish outbreak isolates from 2011/2013 indicated these were clonal (2). The authors

offered as plausible explanation for this genomic identity among spatially and temporally separated outbreaks the spreading of spores by birds or wildlife. Though these Swedish outbreaks have caused public alarm for the risk of environmental contamination (2), no more cases were reported in that region since (as of November 2021). More active is the re-emerging situation in Italy where anthrax resurfaces repeatedly in the southern region of Basilicata (36, 37) and soils at outbreak-sites remained contaminated with viable spores for many years (4, 5). Finally, the phylogeny of B.Br.CNEVA is well characterized in France where this lineage is dominant and ecologically established in the regions Alps, Pyrenees and Massif Central (plus Saône-et-Loire) (38). In contrast to France, where all B.Br.CNEVA strains are monophyletic ((38) and Figure 3), the situation differs in Germany and Austria. Isolates from these countries are distributed across several closely related lineages branching off a very shallow polytomy (Figure 3). This suggests not only that the B.Br.CNEVA clade had been introduced by a single event into France as proposed earlier (38). This data also hints at a similar process of limited introduction of the branch of *B. anthracis* into central Europe. In this model, an early introduction event of the pathogen had occurred into Italy, Slovakia and parts of Germany, from which again, a likely single introduction event is linked to the ancestor of B. Br.CNEVA in France, Austria, Switzerland and Bavaria (Figure 3).

The genomes of strains BF-1 and BF-5 differ by only three chromosomal SNPs (Table 1). A recent genomic study on an anthrax-outbreak in Italy found strains differing by up to five SNPs (39). Genome analysis for epidemiological investigation of strains associated with injectional anthrax have led the authors to the conclusion that genetic variation is possibly generated as a result of infection of a single host. Nonetheless, some phylogenetic patterns might be best explained by diversity introduced through several infection-cycles of *B. anthracis* in several hosts (8). The 2021 outbreak in Bavaria seems to follow this pattern with only very few SNP-differences between strains from the same outbreak-site

separated by 12 years. Notably, all six isolates retrieved from soil surrounding the carcass-site and from 80 m away at a ditch featured the same unique SNP-positions as isolate BF-5 directly grown from the dead cow's blood. In contrast, it is very unlikely that isolate BF-1 is a direct ancestor of BF-5. Chromosomal SNP 1 differs from the ancestor-state (Ames 'Ancestor') only in BF-5 but not in BF-1. Vice versa, however, chromosomal SNP 2 and SNP 3 showed an evolved state (relative to Ames 'Ancestor') in BF-1, while being ancestral in BF-5 (Table 1).

In order to acutely diminish the local risk of surface-near spore contamination on-site, the affected pasture-site where the animal fell (Figure 1A and B), was disinfected with 10 l/m^2 10% (*v/v*) formaldehyde as similarly advised by (1). Obviously, this measure will neither be able to disinfect deeper soil horizons nor eliminate the unidentified original contamination-site presumably located somewhere on the premises. Longer term monitoring of surface-near soil on-site may be able to alert authorities in case *B. anthracis* spores can again be detected after favorable weather conditions, e.g., heavy rains followed by mild temperatures (40). Further developments related to sensitive detection of *B. anthracis* in soil could facilitate the identification and elimination of the original source of spore contamination at the affected premises.

In any case, this rare outbreak provided an ideal opportunity for real-life testing of assays developed beforehand for detection and identification of *B. anthracis*. Direct microscopy of *B. anthracis*-infected blood (Figure 2A) or germinated cells in *B. anthracis* spore-contaminated soil (Figure 4A) and rapid testing of inactivated blood (Figure 4B) or suspect colonies (23) yielded similar results with these authentic materials to previously tested spiked-in materials (unpublished).

Acknowledgements

The authors thank Malena Bestehorn-Willmann for help with genome sequencing, Rahime Terzioglu, Gabriele Echle, Linda Dobrzykowski, and Laura Madeddu for technical assistance.

Funding

This research work was supported by the Medical Biological Defense Research Program of the Bundeswehr Joint Medical Service (to GG and MA) and was partially funded through Bundeswehr Medical Service [SoFo 56Z1-S-43 1922] to MA and the German Federal Ministry of Education and Research (BMBF) [ZooSeq FKZ 01KI1905A] to MA.

Conflicts of Interest

The authors declare no conflicts of interest. Opinions, interpretations, conclusions, and recommendations are those of the authors and are not necessarily endorsed by any governmental agency, department, or other institutions. The funders had no role in the design of the study; in the collection, analyses, or interpretation of data; in the writing of the manuscript, or in the decision to publish the results.

References

1. Turnbull PC. 2008. World Health Organization. Anthrax in humans and animals. WHO Press, Geneva (CH).
2. Ågren J, Finn M, Bengtsson B, Segerman B. 2014. Microevolution during an anthrax outbreak leading to clonal heterogeneity and penicillin resistance. PLoS One 9:e89112.
3. Revich BA, Podolnaya MA. 2011. Thawing of permafrost may disturb historic cattle burial grounds in East Siberia. Global Health Action 4.
4. Fasanella A, Di Taranto P, Battisti A, Longobardi C, Panerei F, Martelli B, Garofolo G. 2011. Old animal anthrax outbreaks discovered through the analysis of soil. Giornale Italiano die Medicina Tropicale 16:1–4.
5. Braun P, Grass G, Aceti A, Serrecchia L, Affuso A, Marino L, Grimaldi S, Pagano S, Hanczaruk M, Georgi E, Northoff B, Schöler A, Schloter M, Antwerpen M, Fasanella A. 2015. Microevolution of anthrax from a young ancestor (M.A.Y.A.) suggests a soil-borne life cycle of *Bacillus anthracis*. PLoS ONE 10:e0135346.
6. Hanczaruk M, Reischl U, Holzmann T, Frangoulidis D, Wagner DM, Keim PS, Antwerpen MH, Meyer H, Grass G. 2014. Injectional anthrax in heroin users, Europe, 2000-2012. Emerg Infect Dis 20:322–3.
7. Ringertz SH, Hoiby EA, Jensenius M, Maehlen J, Caugant DA, Myklebust A, Fossum K. 2000. Injectional anthrax in a heroin skin-popper. Lancet 356:1574–5.
8. Keim P, Grunow R, Vipond R, Grass G, Hoffmaster A, Birdsell DN, Klee SR, Pullan S, Antwerpen M, Bayer BN, Latham J, Wiggins K, Hepp C, Pearson T, Brooks T, Sahl J, Wagner DM. 2015. Whole genome analysis of injectional anthrax identifies two disease clusters spanning more than 13 years. EBioMedicine 2:1613–1618.

9. Antwerpen M, Proenca DN, Ruckert C, Licht K, Kalinowski J, Hanczaruk M, Tiemann C, Grass G. 2012. Draft genome sequence of *Bacillus anthracis* BF-1, isolated from Bavarian cattle. J Bacteriol 194:6360–1.

10. Antwerpen M, Elschner M, Gaede W, Schliephake A, Grass G, Tomaso H. 2016. Genome sequence of *Bacillus anthracis* strain Stendal, isolated from an anthrax outbreak in cattle in Germany. Genome Announc 4:e00219-16.

11. Elschner MC, Busch A, Schliephake A, Gaede W, Zuchantke E, Tomaso H. 2017. High-quality genome sequence of *Bacillus anthracis* strain 14RA5914 isolated during an outbreak in Germany in 2014. Genome Announc 5.

12. Price EP, Seymour ML, Sarovich DS, Latham J, Wolken SR, Mason J, Vincent G, Drees KP, Beckstrom-Sternberg SM, Phillippy AM, Koren S, Okinaka RT, Chung W-K, Schupp JM, Wagner DM, Vipond R, Foster JT, Bergman NH, Burans J, Pearson T, Brooks T, Keim P. 2012. Molecular epidemiologic investigation of an anthrax outbreak among heroin users, Europe. Emerging Infectious Diseases 18:1307–1313.

13. BAYERISCHE, LANDESTIERÄRZTEKAMMER. 2009. Aktueller Fall von Milzbrand bei Weiderindern in Bayern. BLTK Newsletter 3:1.

14. Braun P, Knupfer M, Antwerpen M, Triebel D, Grass G. 2020. A rare glimpse into the past of the anthrax pathogen *Bacillus anthracis*. Microorganisms 8.

15. Derzelle S, Aguilar-Bultet L, Frey J. 2016. Whole genome SNP analysis of bovine *B. anthracis* strains from Switzerland reflects strict regional separation of Simmental and Swiss Brown breeds in the past. Vet Microbiol 196:1–8.

16. Sterne M. 1959. Anthrax, p. 16–52. *In* Stableforth, AW, Galloway, IA (eds.), Infectious Diseases of Animals, Disease due to Bacteria. Butterworth, London.

17. Fasanella A, Di Taranto P, Garofolo G, Colao V, Marino L, Buonavoglia D, Pedarra C, Adone R, Hugh-Jones M. 2013. Ground Anthrax *Bacillus* Refined Isolation

(GABRI) method for analyzing environmental samples with low levels of *Bacillus anthracis* contamination. BMC Microbiol 13:167.

18. Braun P, Wolfschläger I, Reetz L, Bachstein L, Jacinto AC, Tocantins C, Poppe J, Grass G. 2020. Rapid microscopic detection of *Bacillus anthracis* by fluorescent receptor binding proteins of bacteriophages. Microorganisms 8:934.

19. Braun P, Nguyen MD-T, Walter MC, Grass G. 2021. Ultrasensitive detection of *Bacillus anthracis* by real-time PCR targeting a polymorphism in multi-copy 16S rRNA genes and their transcripts. International Journal of Molecular Sciences 22:12224.

20. Beyer W, Bellan S, Eberle G, Ganz HH, Getz WM, Haumacher R, Hilss KA, Kilian W, Lazak J, Turner WC, Turnbull PC. 2012. Distribution and molecular evolution of *Bacillus anthracis* genotypes in Namibia. PLoS Negl Trop Dis 6:e1534.

21. Turnbull, Peter C. 2008. Anthrax in Humans and Animals, 4th ed. World Health Organization, Geneva. http://www.ncbi.nlm.nih.gov/books/NBK310486/. Retrieved 5 October 2021.

22. Rohde A, Papp S, Feige P, Grunow R, Kaspari O. 2020. Development of a novel selective agar for the isolation and detection of *Bacillus anthracis*. J Appl Microbiol https://doi.org/10.1111/jam.14615.

23. Braun P, Rupprich N, Neif D, Grass G. 2021. Enzyme-Linked Phage Receptor Binding Protein Assays (ELPRA) Enable Identification of Bacillus anthracis Colonies. Viruses 13:1462.

24. Knüpfer M, Braun P, Baumann K, Rehn A, Antwerpen M, Grass G, Wölfel AR. 2020. Evaluation of a highly efficient DNA extraction method for *Bacillus anthracis* endospores. Microorganisms 8.

25. Antwerpen MH, Zimmermann P, Bewley K, Frangoulidis D, Meyer H. 2008. Real-time PCR system targeting a chromosomal marker specific for *Bacillus anthracis*. Mol Cell Probes 22:313–5.

26. Kolmogorov M, Yuan J, Lin Y, Pevzner PA. 2019. Assembly of long, error-prone reads using repeat graphs. Nat Biotechnol 37:540–546.

27. Angiuoli SV, Gussman A, Klimke W, Cochrane G, Field D, Garrity G, Kodira CD, Kyrpides N, Madupu R, Markowitz V, Tatusova T, Thomson N, White O. 2008. Toward an online repository of Standard Operating Procedures (SOPs) for (meta)genomic annotation. OMICS 12:137–141.

28. Lärkeryd A, Myrtennäs K, Karlsson E, Dwibedi CK, Forsman M, Larsson P, Johansson A, Sjödin A. 2014. CanSNPer: a hierarchical genotype classifier of clonal pathogens. Bioinformatics 30:1762–4.

29. Treangen TJ, Ondov BD, Koren S, Phillippy AM. 2014. The Harvest suite for rapid core-genome alignment and visualization of thousands of intraspecific microbial genomes. Genome Biol 15:524.

30. Tamura K, Nei M. 1993. Estimation of the number of nucleotide substitutions in the control region of mitochondrial DNA in humans and chimpanzees. Mol Biol Evol 10:512–26.

31. Kumar S, Stecher G, Li M, Knyaz C, Tamura K. 2018. MEGA X: Molecular evolutionary genetics analysis across computing platforms. Mol Biol Evol 35:1547–1549.

32. Van Ert MN, Easterday WR, Huynh LY, Okinaka RT, Hugh-Jones ME, Ravel J, Zanecki SR, Pearson T, Simonson TS, U'Ren JM, Kachur SM, Leadem-Dougherty RR, Rhoton SD, Zinser G, Farlow J, Coker PR, Smith KL, Wang B, Kenefic LJ, Fraser-Liggett CM, Wagner DM, Keim P. 2007. Global genetic population structure of *Bacillus anthracis*. PLoS One 2:e461.

33. Lewerin SS, Elvander M, Westermark T, Hartzell LN, Norstrom AK, Ehrs S, Knutsson R, Englund S, Andersson AC, Granberg M, Backman S, Wikstrom P, Sandstedt K. 2010. Anthrax outbreak in a Swedish beef cattle herd--1st case in 27 years: Case report. Acta Vet Scand 52:7.

34. Elvander M, Persson B, Sternberg Lewerin S. 2017. Historical cases of anthrax in Sweden 1916-1961. Transbound Emerg Dis 64:892–898.

35. Willis EA. 2009. Landscape with dead sheep: What they did to Gruinard Island. null 25:320–331.

36. Fasanella A. 2013. *Bacillus anthracis*, virulence factors, PCR, and interpretation of results. Virulence 4.

37. Fasanella A, Garofolo G, Galante D, Quaranta V, Palazzo L, Lista F, Adone R, Jones MH. 2010. Severe anthrax outbreaks in Italy in 2004: considerations on factors involved in the spread of infection. New Microbiol 33:83–6.

38. Girault G, Blouin Y, Vergnaud G, Derzelle S. 2014. High-throughput sequencing of *Bacillus anthracis* in France: investigating genome diversity and population structure using whole-genome SNP discovery. BMC Genomics 15:288.

39. Abdel-Glil MY, Chiaverini A, Garofolo G, Fasanella A, Parisi A, Harmsen D, Jolley KA, Elschner MC, Tomaso H, Linde J, Galante D. 2021. A whole-genome-based gene-by-gene typing system for standardized high-resolution strain typing of *Bacillus anthracis*. J Clin Microbiol 59:e0288920.

40. Van Ness GB. 1971. Ecology of anthrax. Science 172:1303–7.

Tables

Table 1: DNA sequence differences between genomes of *B. anthracis* BF-1 and BF-5.

Reference (BF-1)	Position	BF-1 nucleotide sequence (ancestor state)	BF-5 nucleotide sequence (derived state)	Kind of change
CP047131.1 (chromosome)	519877	C	T	SNP (SNP1)
CP047131.1	1434950	CTTTTTTTTTTTTTTG TAAATAA	CTTTTTTTTTTTTTGT AAATAA	Deletion
CP047131.1	1625072	A	C	SNP (SNP2)
CP047131.1	1878269	GTTTTTTTTTTTTTTT GTAAAATTAA	GTTTTTTTTTTTTTTG TAAAATTAA	Deletion
CP047131.1	2472315	T	C	SNP (SNP3)
CP047133.1 (plasmid pX02)	29759 31759 30759	CTTTTTTTAT	CTTTTTTTTAT	Insertion
CP047133.1 (plasmid pX02)	62640	A	G	SNP (SNP4)

Figure legends

Figure 1: *In situ* presentation of a cow deceased of anthrax. A two year old gestating cow fallen to anthrax on a pasture in southern Bavaria (Germany) in August of 2021 (A and B). Close up of the head with bloody discharge out of eyes and left nostril (A) and rear view with bloody anus and vagina (B).

Figure 2: Direct detection of *B. anthracis* cells in blood from a diseased cow and molecular PCR diagnostics. A: Horseradish peroxidase (HRP) conjugated $RBP_{\lambda 03\Delta 1\text{-}120}$ was added directly to inactivated blood (taken from the carcass' left nostril) (right reaction tube) as well as to inactivated sheep blood which served as a negative control (left reaction tube). After washing, chromogenic HRP substrate was added and color development photo-documented after 1 min. **B**: Recombinant fusion protein mCherry-$RBP_{\lambda 03\Delta 1\text{-}120}$ was added to 100 µl of blood and directly subjected to fluorescence microscopy. Shown are merged images of transmission and fluorescent light (wavelengths: excitation 594 nm, emission: 610 nm). Scale bar: 5 µm. **C**: Dilutions of the inactivated cow blood (1 – 1:10, 2 – 1:100, 3 – 1:1000) as well as dilutions of isolated DNA (4 – 1:10, 5 – 1:100, 6 – 1:1000) from the blood-samples were subjected to 16S rRNA SNP-PCR. Shown are representative realtime PCR amplification-curves.

Figure 3: Phylogeny of new *B. anthracis* isolate BF-5 among its close relatives of the B.Br.CNEVA canonical SNP-clade. A rooted phylogenetic tree of representatives of the B.Br.CNEVA canonical single-nucleotide polymorphisms (canSNP) clade of *B. anthracis* is shown (A). The tree is based on 1558 chromosomal SNPs used to construct a Maximum Likelihood tree (bootstrap confidence from 500 permutations were generated and the tree with the highest likelihood is shown). Isolate names and countries of origin are indicated at branch termini (red: sequenced in this study; black: sequences from public databases, Table S1). A Minimum-spanning tree of close relatives of strain BF-5 within the B.Br.CNEVA canSNP-clade of *B. anthracis* derived from chromosomal SNPs is shown (B). Indicated are numerical SNP-differences (logarithmic scale) between chromosomes. Both trees are rooted to the reference chromosome, *B. anthracis* strain Ames 'Ancestor' that belongs to the A.Br.Ames canSNP-clade.

Figure 4: Direct detection and isolation of *B. anthracis* from contaminated soil-samples associated with a deceased cow. Soil-samples were shaken in PBST buffer to solubilize spores, centrifuged and the supernatant mixed with BHI broth containing fetal calf serum and incubated to allow spores to germinate. **A**: Recombinant fusion protein mCherry-$RBP_{\lambda 03\Delta 1\text{-}120}$ was added to pre-incubated soil supernatants and directly subjected to fluorescence microscopy. Shown are two merged images of transmission and fluorescent light (wavelengths: excitation 594 nm, emission: 610 nm). Scale bar: 5 µm. **B**: Magnetic beads coupled with $RBP_{\lambda 03\Delta 1\text{-}120}$ were added to pre-incubated soil supernatants to capture *B. anthracis* cells. A sample was taken for brightfield microscopy (left panel, Scale bar: 5 µm) and the remainder of the bead suspension buffer-washed, plated on blood agar plates and incubated at 37°C overnight (right panel). **C**: Rapid RBP reporter-based assay on inactivated suspicious colony material from enrichment plates. Inactivated colony material was incubated with $RBP_{\lambda 03\Delta 1\text{-}120}$ covalently linked to horseradish peroxidase for colorimetric identification with chromogenic substrate. Positive control (+) was *B. anthracis* Sterne and negative control (-) *B. cereus* ATCC10987. Results were scored after about 1 min as positive (blue color development) or negative (no color development).

Figures

Figure 1

A. 

B. 

Figure 2

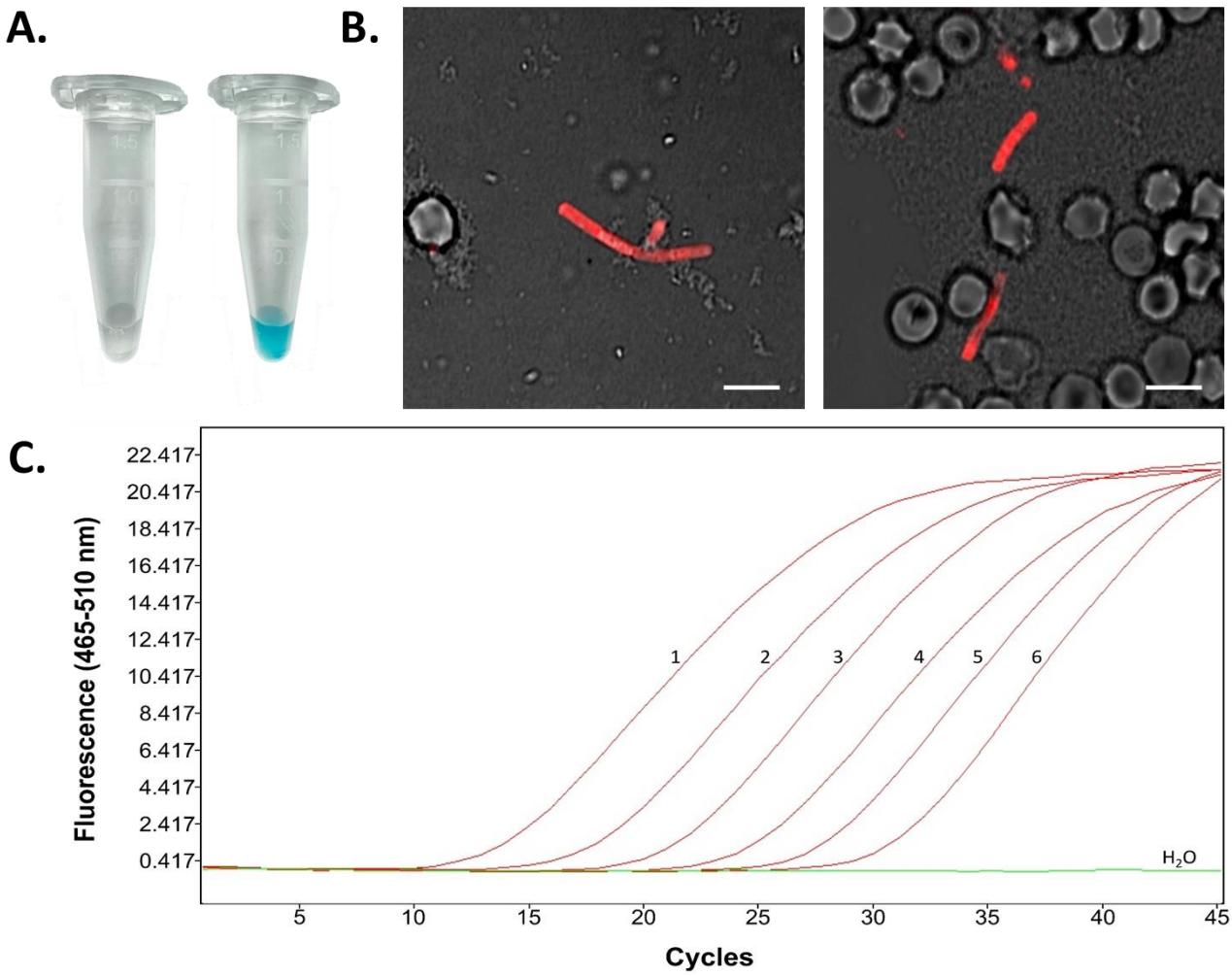
A.
B.
C.
Fluorescence (465-510 nm)
22.417
20.417
18.417
16.417
14.417
12.417
10.417
8.417
6.417
4.417
2.417
0.417
1
2
3
4
5
6
H2O
5
10
15
20
25
30
35
40
45
Cycles

Figure 3

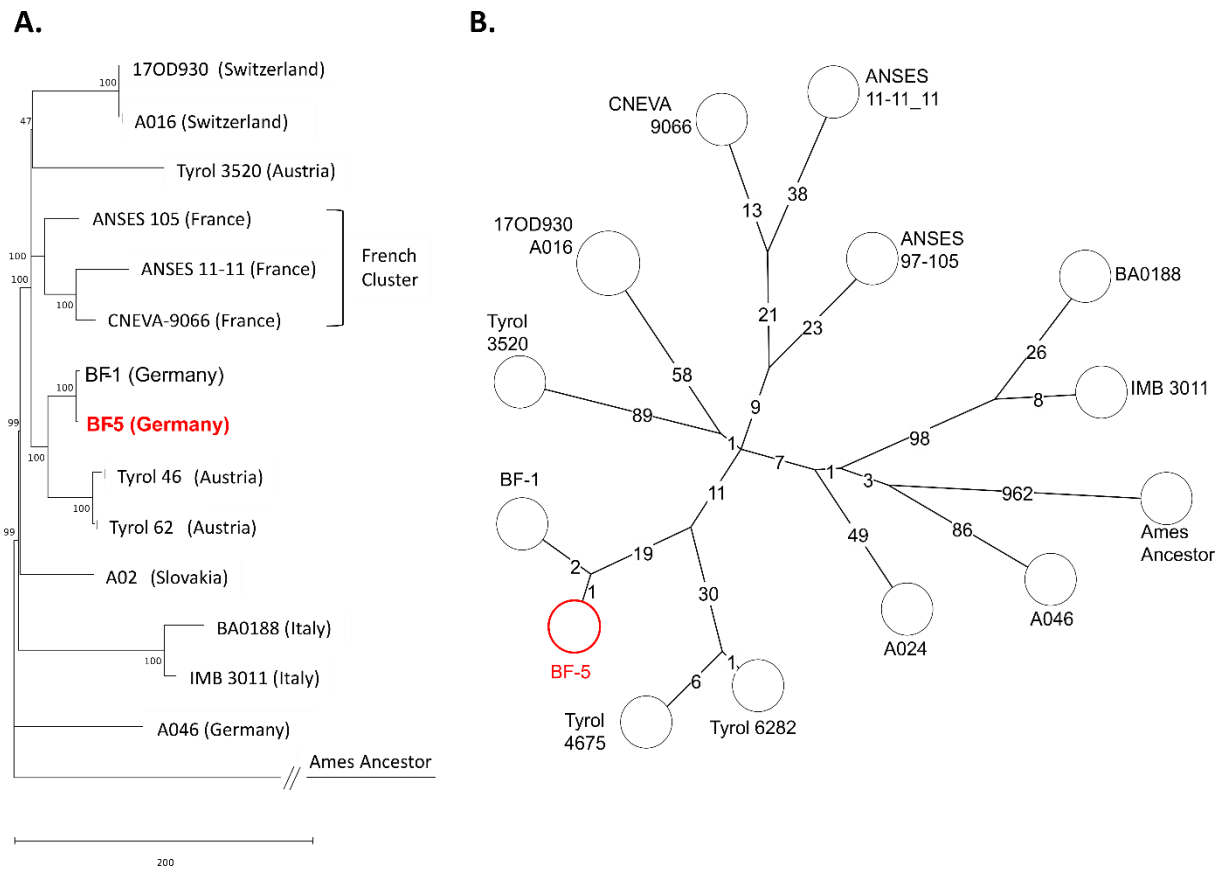
A.
17OD930 (Switzerland)
A016 (Switzerland)
Tyrol 3520 (Austria)
ANSES 105 (France)
ANSES 11-11 (France)
CNEVA-9066 (France)
French Cluster
BF1 (Germany)
BF5 (Germany)
Tyrol 46 (Austria)
Tyrol 62 (Austria)
A02 (Slovakia)
BA0188 (Italy)
IMB 3011 (Italy)
A046 (Germany)
Ames Ancestor
200
B.
CNEVA 9066
ANSES 11-11_11
17OD930 A016
ANSES 97-105
BA0188
Tyrol 3520
IMB 3011
BF-1
Ames Ancestor
BF-5
A046
A024
Tyrol 4675
Tyrol 6282

Figure 4

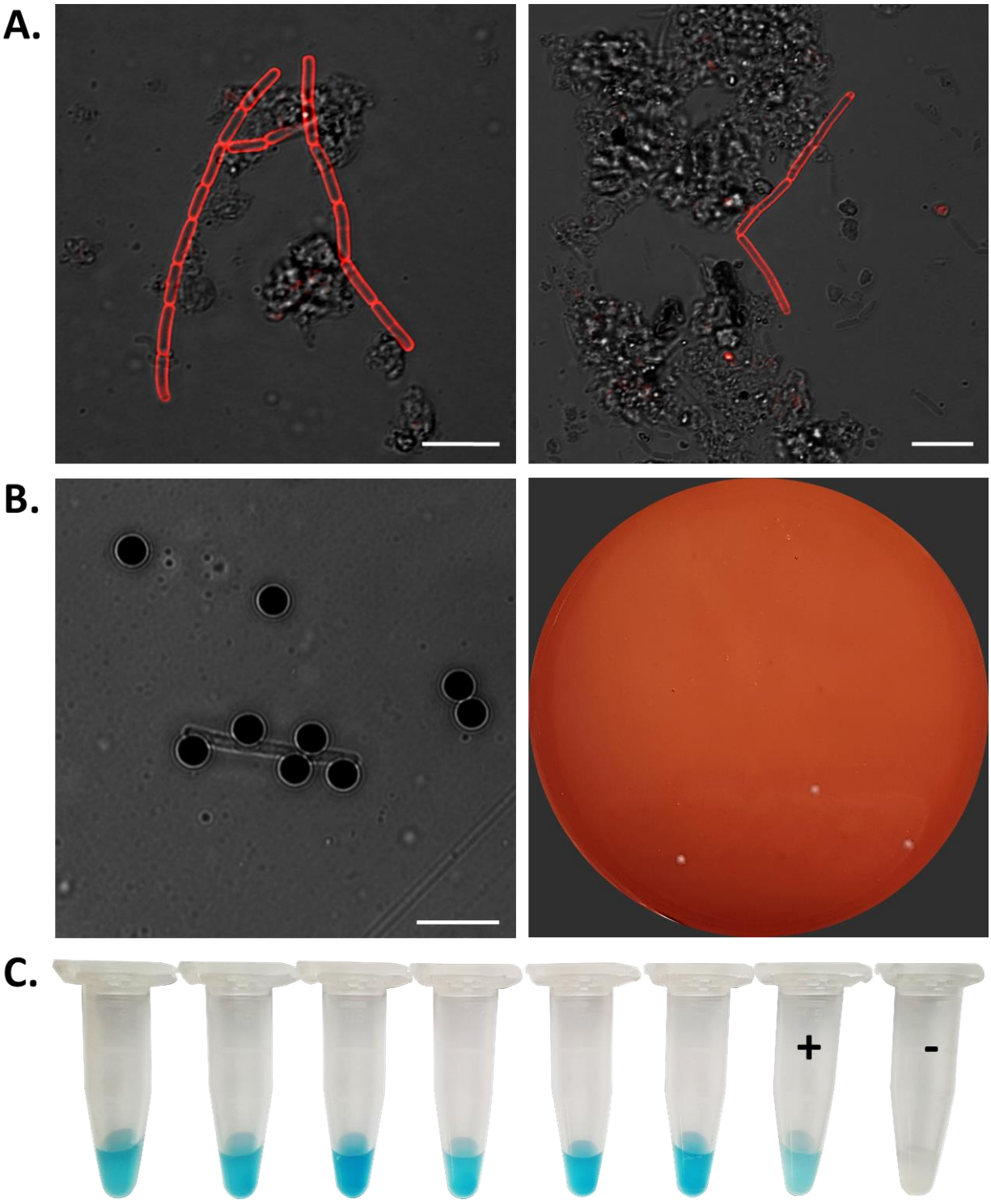

8. Concluding Discussion

8.1. Historical *B. anthracis* specimens facilitate more accurate future bioforensics

Accurate bioforensics of anthrax outbreaks, i.e., tracing back the causes of the outbreak, requires knowledge of the naturally occurring genotype in the affected region. While genotyping of live strains isolated centuries ago may be easy, these bacteria often lack associated metadata. In addition, it is usually impossible to determine how often a strain has undergone laboratory passaging and which selection pressure (antibiotics) has been applied since the time of initial isolation. All these influences can, of course, affect genotyping due to the accumulation of laboratory-acquired mutations (Pilo and Frey 2011; Van Ert et al. 2007). This is, for example, likely the case for a set of strains isolated in the 1930s in Denmark and South Africa that had been cultured ever since and were sequenced in recent years (Derzelle et al. 2015; Lekota et al. 2020). In contrast, genomic data retrieved from authentic historical samples such as the historical genome described in this work provides reliable information about the natural phylogeography of a certain area since the biological material has been inactive since fixation and thus, not been able to acquire any mutations (except by random DNA degradation over time) that would otherwise skew genotyping. In addition to the exact year, properly documented metadata of the sample from 1878 also provided information about the sample type, the location and the author (Figure 8-1). At that time, the Saxonian veterinarian Dr. Zimmermann prepared collections of microscopy slides, which he then sold for use in teaching (Thümen 1879). Among these was the specimen described in this work containing blood of a cow diseased with anthrax (Chapter 2).

Figure 8-1: The original label of the historic *B. anthracis* sample. The label provides informative metadata (Sachsen: Chemnitz im Blut von Rindern. Ist die Ursache des „Milzbrandes“ 1878 - Engl.: Saxony: Chemnitz in the blood of cattle. Is the cause of "anthrax" 1878).

The fact that this historic *B. anthracis* genome termed “Chemnitz 1878” was genotyped and grouped to the B.Br.CNEVA clade was not very surprising as many recent outbreak strains in Central Europe were found to belong to this group, such as the strain BF-5 from the recent outbreak in southern Bavaria (Fouet et al. 2002; Vergnaud et al. 2016; Pilo and Frey 2011). However, due to the expansion of global trade at the beginning of the 20th century, these genotypes gained from extant organisms could represent imported ones from other regions of the world and thus would not represent the local autochthonous population (Pilo and Frey 2011). Now, the identification of a B.Br.CNEVA genome from 1878 provides strong evidence, that this branch indeed represents a naturally occurring genotype in Central Europe. Thus, from a bioforensic perspective, a future outbreak caused by a *B. anthracis* strain from the B.Br.CNEVA group can be assumed to be likely a natural infection while the isolation of a *B. anthracis* strain from a canSNP group for which a non-European origin is very likely (e.g., B.Br.Kruger) should be investigated more carefully, as this may indicate an intentional release of the pathogen. For example, the recent anthrax outbreak in southern Bavaria did not raise concern as it was also caused by a B.Br.CNEVA strain closely related to the historical genome from 1878. Overall, the work at hand shows that a glimpse into the past of the notorious anthrax pathogen *B. anthracis* allows for more accurate bioforensics in the future. Yet, this approach is just at

the beginning with its full spectrum largely unexplored. It is indeed, astonishing that historical *B. anthracis* has received very little attention by the research community in contrast to e.g., other notorious pathogesns such as *Yersinia pestis*, the etiological agent of plague, the Syphilis-causing spirochaete *Treponema palidum* or the tuberculosis bacillus *Mycobacterium tuberculosis*. Genotyped and even genome-typed specimens for these bacteria do not span a mere ~150 years as is the current maximum for *B. anthracis* (Chapter 2) but reach back a couple of hundred years, in case of *T. palidum* (Majander et al. 2020), or even thousands of years, as do ancient genomes of *M. tuberculosis* (Susat et al. 2021) and *Y. pestis* (Kerner et al. 2021).

8.2. The elusive dissemination of *B. anthracis* in soil and the reemerging anthrax conundrum

Although once a major plague to humans and animals in Central Europe, anthrax is now very rare here. The scattered cases are often confined to small endemic areas, where mostly minor outbreaks occur in cattle or other grazing animals, while humans are almost never affected. This was also the case in the recent anthrax outbreak in southern Bavaria in 2021 in which two cows fell from the disease (Chapter 7). The location of the outbreak was no surprise to the local veterinary authorities as an outbreak had occurred on the same farm 12 years ago (Antwerpen et al. 2012). This sporadic reoccurrence of the disease in certain areas after years up to decades is typical for anthrax (Turnbull 2008; Braun et al. 2015; Hugh-Jones and Blackburn 2009). Usually these reoccurring outbreaks are preceded by periods of heavy rainfall and high temperatures in the affected region and many researchers in this field assume that these extreme weather conditions lead to physical accumulations of endospores and thus to new infections in grazing animals (Hugh-Jones and Blackburn 2009). However, this sporadic return of the disease after hot-humid weather can be more easily explained by a soil-borne lifecycle of *B. anthracis* where

germination of endospores and multiplication occur under favorable environmental conditions in nutrient rich near-surface soil, especially around plant roots (Turnbull 2008). This hypothesis is supported by experimental data, for instance, Saile and Koehler found that *B. anthracis* is able to persist and multiply in the rhizosphere of grass plants (Saile and Koehler 2006). Additionally, in a study by Turner et al. the authors measured the concentration of *B. anthracis* spores at a carcass site over five years (Turner et al. 2016). Near waterholes or soil surrounding a carcass location the concentration of endospores rapidly declined over the years while the endospore concentration around plant roots significantly increased. In another study, the genetic diversity of *B. anthracis* isolates from a ten-year-old burial site was found to be higher in near-surface isolates compared to isolates from deeper soil layers close to the buried carcass. This also suggested soil-borne proliferation as a cause for acquired mutations (Braun et al. 2015). In the case of the recent anthrax outbreak in southern Bavaria (Chapter 7), the months leading up to the outbreak were also dominated by high temperatures and heavy rainfall but this is not uncommon for Bavarian summers. This might have led to germination and proliferation and thus, to local accumulation of *B. anthracis* spores, which have been present in soil since the last outbreak 12 years ago. These accumulations might then have caused an increased uptake of spores by the grazing cows exceeding the infectious dose required for the disease to manifest. Why an outbreak occured in 2021 on this farm but not in any other year between 2012 and present is a conundrum.

Once infected, rapid diagnostics of anthrax disease is crucial to be able to initiate therapy and prevent further infections by e.g. disinfection of exposed areas. However, of the numerous methods described for the detection of *B. anthracis*, only very few are tested on genuine clinical or environmental samples. Most assays have been developed under laboratory conditions using attenuated strains that have been in culture for decades and thus, may not compare well to wildtype outbreak strains (Leiser et al. 2018). In addition,

due to lack of clinical samples, these assays have been tested mostly with spiked-in material, which does also not compare well to authentic clinical samples. Therefore, the validity and applicability of these methods might be questionable. In contrast, the recent outbreak of anthrax among cattle in southern Bavaria provided a unique opportunity to test and evaluate novel detection methods developed throughout this work (Chapter 7), such as the identification of *B. anthracis* by a unique SNP in its 16S rRNA genes.

8.3. *B. anthracis* bears a unique 16S rRNA allele variation – the "16S-BA-allele"

8.3.1. The ribosomal RNA operon copy numbers of *B. anthracis* are more variable than previously anticipated

Since their introduction as phylogenetic marker molecule in 1977 by Woese, 16S rRNA genes play a pivotal role in the study of microbial evolution and ecology and in diagnostics of diseases caused by bacterial pathogens (Woese and Fox 1977). These genes encoding the small ribosomal subunit are typically part of a chromosomally encoded operon consisting of three ribosomal RNA genes (16S, 23S and 5S), intergenic spacer regions and tRNAs. Bacterial genomes have been demonstrated to harbor between 1 and 15 rRNA operon copies (Schmidt 1998; Klappenbach et al. 2000; Stoddard et al. 2015). Interestingly, the *rrn* operon number correlates well with the growth rate and growth efficiency of bacteria and thus their ability to quickly react to changing environmental conditions such as resource availability (Roller et al. 2016; Klappenbach et al. 2000).

In the work at hand work, it was demonstrated that *B. anthracis* harbors between 9 and 11 rRNA-operons (Chapter 3). Regardless of these variations, the high rRNA-operon copy numbers places *B. anthracis* at the upper range of the scale. This observation fits well with

the lifestyle of this pathogen, which relies on the capacity to react quickly to favorable conditions (e.g. after uptake of endospores by a host and germination). Interestingly, it has already been shown for related *B. subtilis* that the deletion of a single rRNA operon can negatively affect the doubling time and growth efficacy (Yano et al. 2013). However, the deletion of an operon can hardly be compared to natural variations in *rrn* operon copy numbers. In the growth experiments described in chapter 3, only *B. anthracis* strains with 11 rRNA-operons were compared. Thus, it would be interesting to elucidate in further studies if *B. anthracis* strains with 10 or 9 rRNA-operons, respectively, show different growth dynamics compared to representatives with 11 rRNA-operons.

8.3.2. No specific function can be assigned to the *B. anthracis*-specific SNP in 16S-BA-alleles

Other than for modifications of the 23S rRNA (Green and Noller 1999), changes in the 16S rRNA are not always essential for proper ribosome assembly (Krzyzosiak et al. 1987). Hence, it is tempting to speculate that alterations in the 16S rRNA could facilitate the functional diversification of ribosomes. It has been shown that even a single mutation in the 16S gene can lead to a conformational switch in the 16S rRNA affecting the codon-anticodon arrangement and proper selection of tRNA at the ribosomal A site (Lodmell and Dahlberg 1997). In previous studies, the ribosome has been attributed with a sensor-role in the prokaryotic heat and cold shock response, respectively (Prüß et al. 1999; VanBogelen and Neidhardt 1990). Several studies indicate that rRNA heterogeneity converts the protein synthesis machinery into a regulatory hub that modulates the cellular proteomic profile in response to environmental cues. Hence, rRNA heterogeneity might represent a bacterial stress-response mechanism (Kurylo et al. 2018). However, secondary structure predictions using the rnafold webtool (http://rna.tbi.univie.ac.at/cgi-bin/RNAWebSuite/RNAfold.cgi) did not show any changes in the secondary structure for the 16S-BA/BC-alleles (data not shown). In addition to this, none of the known 16S rRNA

directed antibiotics is relevant for the *B. anthracis* specific SNP position in 16S-BA-alleles. Therefore, it is highly unlikely that this SNP confers any antibiotic resistances to *B. anthracis* as it has been previously described for different SNPs found in 16S rRNA genes of other species (Galimand et al. 2011).

8.3.3. All *B. anthracis* rRNA alleles are constantly expressed - yet in different ratios

FISH and RT-dPCR results (Chapter 3) demonstrated that all rRNA operons are transcribed across different growth stages of *B. anthracis*. However, striking differences in the temporal expression ratios were observed. Results indicated that the genomic ratios of different alleles of the investigated 16S rRNA genes are mirrored on the transcript level when comparing different strains with 2/9, 3/8 and 4/7 (16S-BA-alleles/-BC-alleles) alleles, respectively. A lower genomic 16S-BA-allele content is strongly associated with a respective lower transcript content, certainly as a consequence of the gene dose effect. Interestingly, however, one or several of the 16S-BA-alleles seem to be preferentially transcribed. This was evidenced by a 1.5 fold average overexpression of the 16S-BA-allele of what the gene ratios of the two alleles would predict. This overexpression increased in the course of growth experiments from lag, exponential and stationary phase, where a further change in the expression level ratio in favor of the 16S-BA-allele (up to 2.5 fold) was measured over time. This points towards a differential regulation of the different operons. There are two non-exclusive explanations for the observed differences: 1. All 16S-BA-alleles are upregulated due to the SNP or 2. a single 16S-BA-allele bearing operon is upregulated because of co-transcribed essential genes in direct genomic vicinity. With the methods employed thus far, it was not possible to gain deeper insight into this open question. Although a specific function could not be assigned to the SNP this does not mean that there is none. As mentioned before, rRNA heterogeneity can affect gene expression (Kurylo et al. 2018). Thus, it is well conceivable that the 16S-BA-alleles are

specifically upregulated because of the SNP. However, there are also clues for the single operon-related upregulation hypothesis. Whereas no conspicuous regulatory genes in the proximity of 16S-BA-allele bearing operons could be identified (data not shown), operon *rrnE* features a striking accumulation of tRNAs located upstream. This one specific 16S-BA-allele bearing operon is the only operon-type, which is present in all analyzed *B. anthracis* strains. Strikingly, this particular rRNA operon is not fitting in the classification by Candelon et al. who stated that there are only two classes of rRNA operons within the *B. cereus* group, those with tRNAs interspersed in the intergenic spacer regions (i.e. after the 16S rRNA gene) and those without (Candelon et al. 2004). Instead, for *rrnE* the tRNA accumulation is located directly upstream of the 16S rRNA gene. It is tempting to speculate that the tRNAs are the cause for the relative overabundance of 16S-BA-allele transtripts. In summary, more research is needed to elucidate the functional role of the SNP and to unravel the reasons for the differential expression of the *rrn* operons in *B. anthracis*. Herein, it would be quite interesting to investigate which individual 16S rRNA genes are highly expressed and which are not or if this expression changes under different conditions (such as growth in synthetic media vs. blood).

8.3.4. The 16S-BA-allele provides new possibilities for anthrax diagnostics

This work provided the opportunity to identify *B. anthracis* using multi-copy markers that are used in principle in a standard approach for the identification of many other bacteria as well. Unfortunately, due to oversight, these markers have previously been considered not species-specific for *B. anthracis*: the 16S rRNA genes and transcpirts. This opened up the possibility to expand the existing toolbox for detection of *B. anthracis.* It is now possible to detect and identify *B. anthracis* with FISH, PCR and 16S rRNA sequencing (Chapter 3). Although FISH has its limitations regarding sensitivity (10^3 cells / ml), it has certain advantages compared to PCR or sequencing (Daims et al. 2005). For example, as a

minimum of approximately 400 intact ribosomes per cell are needed for a detectable FISH-conferred signal (Hoshino et al. 2008), this method allows for differentiation between living and dead cells.

Furthermore, a set of new PCR based approaches was established on the basis of the 16S-BA-allele described here, such as digital PCR (dPCR) (Chapter 3). Due to the ability of absolute quantification, excellent precision and high accuracy, dPCR has been widely used for pathogen detection and quantification in recent years (Kuypers and Jerome 2017). In this study, dPCR served as reliable tool for the detection and quantification of 16S rRNA alleles on transcript level, by means of a RT duplex assay, as well as on genomic level where a tetraplex assay using single color multiplexing was developed. Despite labor-intensive titration of primers and probes in order to achieve accurate clustering of droplets, single color multiplexing has already been successfully employed for simultaneous detection of genetically modified organisms (Lindström et al. 2001). Since dPCR is typically too time-consuming and expensive for testing of clinical samples where only the presence or absence of a pathogen has to be interrogated, a diagnostic (RT) PCR assay has been developed as part of the work at hand based on the 16S rRNA SNP dPCR assay for *B. anthracis* (Chapter 4).

In an *in silico* analysis using approximately 100 PCR primers and labeled ssDNA probes against *B. anthracis*, only four assays yielded 100% specificity and were thus further tested in an interlaboratory comparison (Ågren et al. 2013). Only three of the four *in silico* validated markers, *dhp61* (Antwerpen et al. 2008), *PL3* (Wielinga et al. 2011), and *BA5357* (Letant et al. 2011) yielded 100% specificity when tested with the respective diagnostic realtime PCR assays (Ågren et al. 2013). *In silico* analysis of the new 16S rRNA SNP (RT)-PCR assay also yielded 100% specificity for *B. anthracis*, but compared to the study of Agren et al., where only 134 *Bacillus* spp. genomes were used for the analysis, the 16S-BA-allele was present in all of the 959 tested *B. anthracis* genomes and was not found

among all other non-*B. anthracis*-sequences present in the nucleotide database of the National Center for Biotechnology Information (NCBI). In addition to the 100% specificity, the 16S rRNA SNP assay was also convincing in terms of sensitivity. (Chapter 4) shows that the 16S rRNA SNP-PCR was approximately 4-8 (2^2-2^3) times more sensitive than established assays targeting *dhp61* and *PL3* when pure DNA was tested, and up to 10,000 times more sensitive when both DNA and RNA was used as template due to high abundance of ribosomes per cell (van Dijk-Salkinoja and Planta 1971). These properties not only allow for the ultrasensitive detection of *B. anthracis* nucleic acids and thus, possibly for early diagnostics of anthrax disease in patients, but for the differentiation between living and dead cells. While growing cells contain up to 10,000 ribosomes, rRNA content of dead cells rapidly decreases due to the instability of ribonucleic acids (van Dijk-Salkinoja and Planta 1971). Comparing Ct values of 16S rRNA SNP-PCR and 16S rRNA SNP RT-PCR of a single sample can thus provide information about *B. anthracis* cell viability, as a sample containing only dead, rRNA deficient cells will result in small, close to zero ΔCt ($Ct_{RT\text{-}PCR}$-Ct_{PCR}) values due to predominant contribution of amplification of genomic DNA in both reactions. In contrast, when a sample is tested containing viable- or freshly inactivated cells with many ribosomes, Ct values of 16S rRNA SNP RT-PCR, compared to those of 16S rRNA SNP-PCR, will be significantly decreased (i.e., ΔCt ($Ct_{RT\text{-}PCR}$-Ct_{PCR}) will be markedly negative. This could already be shown when cow blood from the recent bovine anthrax outbreak was tested with the two PCR approaches (Chapter 7). In addition to that, the cow blood was directly used as a sample for 16S rRNA SNP-PCR without further processing steps such as nucleic acid purification. Notably, a 1:10 dilution of the blood (to dilute potential inhibiting substances) resulted in impeccable amplification curves and Ct values of 25. This further demonstrated the stability of the assay and insensitivity towards blood derived inhibitors and undoubtedly attests the applicability of the newly developed 16S rRNA SNP (RT)-PCR for the diagnostics of anthrax diseases directly in clinical samples. Along with the 16S rRNA SNP (RT)-PCR, the real-life clinical

samples from the outbreak were also a test bed for a new type of anthrax diagnostics: receptor binding proteins (RBPs) of bacteriophages (described in the following chapter).

8.4. Phage RBPs are versatile tools for detection o*f* *B. anthracis*

Bacteriophages, or short phages, are the most abundant biological entities on earth with an estimated number of phage particles of ≥ 10^{31} (Ackermann and Prangishvili 2012). Phages are viruses that exclusively infect bacteria and depend on their host for replication. Phages vary in sizes and shapes (Sharma et al. 2017). A wide variety of classifications have been proposed to date. Currently, a nucleic acid- and morphology-based system is commonly used. Most phages possess an icosahedral head and a tail, and thus, belong to the Myoviridae, Siphoviridae, or Podoviridae family (Ackermann and Prangishvili 2012).

Three life cycles have been described for phages: the lytic, lysogenic and pseudolysogenic cycle. The lytic cycle consists of six steps, starting with the adsorptionof the phage to a potential host. When a phage finds a suitable host and infects it by injecting its DNA (penetration), the host cell is being forced into phage production by replication of the phage DNA and proteins. Thereupon, among other things, the phage capsids are assembled and packed with the genetic material (maturation). Finally, the host cell is lysed to release the new phage particles, which restart the infection cycle (Maciejewska et al. 2018). For many phages, this lytic cycle is the only pathway of reproduction. Temperate phages, on the other hand, also possess an alternative life cycle. Here, the host cell survives the initial phage infection as the phage genome physically incorporates into the host genome. The phage genome stays in a dormant form (prophage) and replicates integrated with the host genome until environmental cues trigger the activation of the phage and initiate the lytic cycle (Campbell 2003). In the third manifestation of phage life cycle, pseudolysogeny, the phage DNA is present in the cell, after host-infection, as an episome (i.e., a plasmid-like

structure). Thus, in this case, the host is only a carrier of the phage similar to lysogeny, but the episome is distributed asymmetrically to the daughter cells during cell division (Maciejewska et al. 2018). In the lysogenic and pseudolysogenic cycle, new phage particles are typically only formed when triggered by external signals such as stress (Campbell 2003).

The first crucial step for successful infection is the interaction and binding to a receptor on the surface of the host cell, which is mediated by proteins typically located at the distal end of the phage, the receptor binding proteins (RBPs). This initial interaction is highly specific and enables the phage to attach to the host cell, thereby determining the breadth (broad or narrow) of host range of this phage (de Jonge et al. 2019; Nobrega et al. 2018). RBPs can interact with different types of host surface receptors, e.g. single proteins, teichoic acids, surface polysaccharides, pili, flagella, or even the capsule of the host cells (Dunne et al. 2018; Nobrega et al. 2018). The structure of RBPs, which might be phage tail-spikes or tail-fibers, is often similar. RBPs frequently form homotrimers (Figure 8-2), are N-terminally anchored to the phage (also called the shoulder domain), and possess a C-terminal host binding domain (also called the head domain). The shoulder- and head-domain are connected by the neck domain (Nobrega et al. 2018). Phage RBPs have been shown to be very stable and exhibit high resistance to proteases and detergents, presumably because these proteins have evolved to be functional in harsh natural environments such as soil, sludge, manure etc. (Simpson et al. 2016).

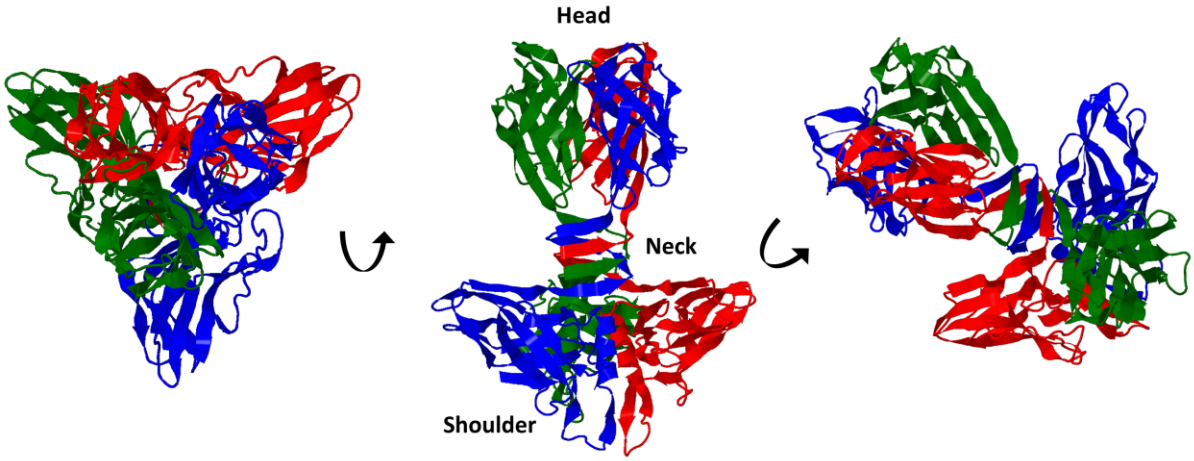

Figure 8-2: Ribbon model of the structure of *Lactococcus lactis* phage p2 RBP (Tremblay et al. 2006). Three monomers, depicted in red, blue and green, form a homotrimer. While the N-terminal shoulder domain is anchored to the phage, the C-terminal head domain binds to the host receptor. Head and shoulder domain are linked by the neck domain, which mediates trimerization. Visualization of the structure (Protein Data Bank: 1ZRU) was performed using Geneious Prime (Biomatters, USA).

This high stability together with binding-affinity and -specificity of RBPs towards host bacteria have led to the use of RBPs as detection probes in biosensors for diagnostics of infectious disease agents (Simpson et al. 2016). A typical biosensor has a probe element of biological origin that provides detection specificity, and a transducer element or reporter, which converts the interaction between the target and the probe into a measurable signal (Singh et al. 2010). Various reporters can be integrated, e.g. by generation of fusion protein, into RBP-based biosensors such as fluorescent proteins, peroxidases or luciferases. Alternatively, RBPs might also be coupled to magnet beads or immobilized in microtiter plates to enable enrichment or isolation prior to detection. This has already been used for *Pseudomonas aeruginosa* enrichment and detection. He et al. used RBP coupled magnetic beads with RBPs for enrichment and also developed a RBP-based biosensor using a fluorescently labeled recombinant tail fiber protein of *P. aeruginosa* specific phage P069 (He et al. 2018). In another study, enrichment with magnetic particles and

simultaneous detection of *Salmonella enterica sv.* Typhimurium was achieved using recombinant RBPs of phage S16 (Denyes et al. 2017). Here, enrichment of *S. enterica sv.* Typhimurium by RBP-based magnetic separation was possible even with low concentrations of the target bacterium in a high background of other microorganisms. A similar system was developed by Poshtiban et al. to enrich and detect *Camptylobacter jejuni* (Poshtiban et al. 2013). For this, recombinant RBPs fused to glutathione S-transferase were either directly coupled to magnetic particles or indirectly via glutathione coupled beads. The recovery rate for *Campylobacter jejuni* cells was approximately 80% and the detection limit 100 bacteria/ml sample (Poshtiban et al. 2013). Furthermore, Kunstmann et al. developed a RBP-based detection system for *Shigella flexneri*, which was named ELISA like tailspike absorption assay (ELITA). The tail spike protein of phage Sf6 (Sf6TSP) was adsorbed to the surface of microtiter plates enabling the subsequent immobilization of *S. flexneri* cells. Following incubation with Sf6TSP fused to a Strep-Tag epitope this system allowed the detection of cell-bound Sf6TSP and thus of *S. flexneri* cells by Strep-Tactin-HRP (Kunstmann et al. 2018). In this work, the RBPs of the *B. anthracis* phages Wip1 and AP50c as well as RBP of prophage λ03 were heterologously produced in *E. coli* and then utilized to develop the first phage RBP-based biosensors for *B. anthracis* detection (Figure 8-3, Chapters 5 and 6).

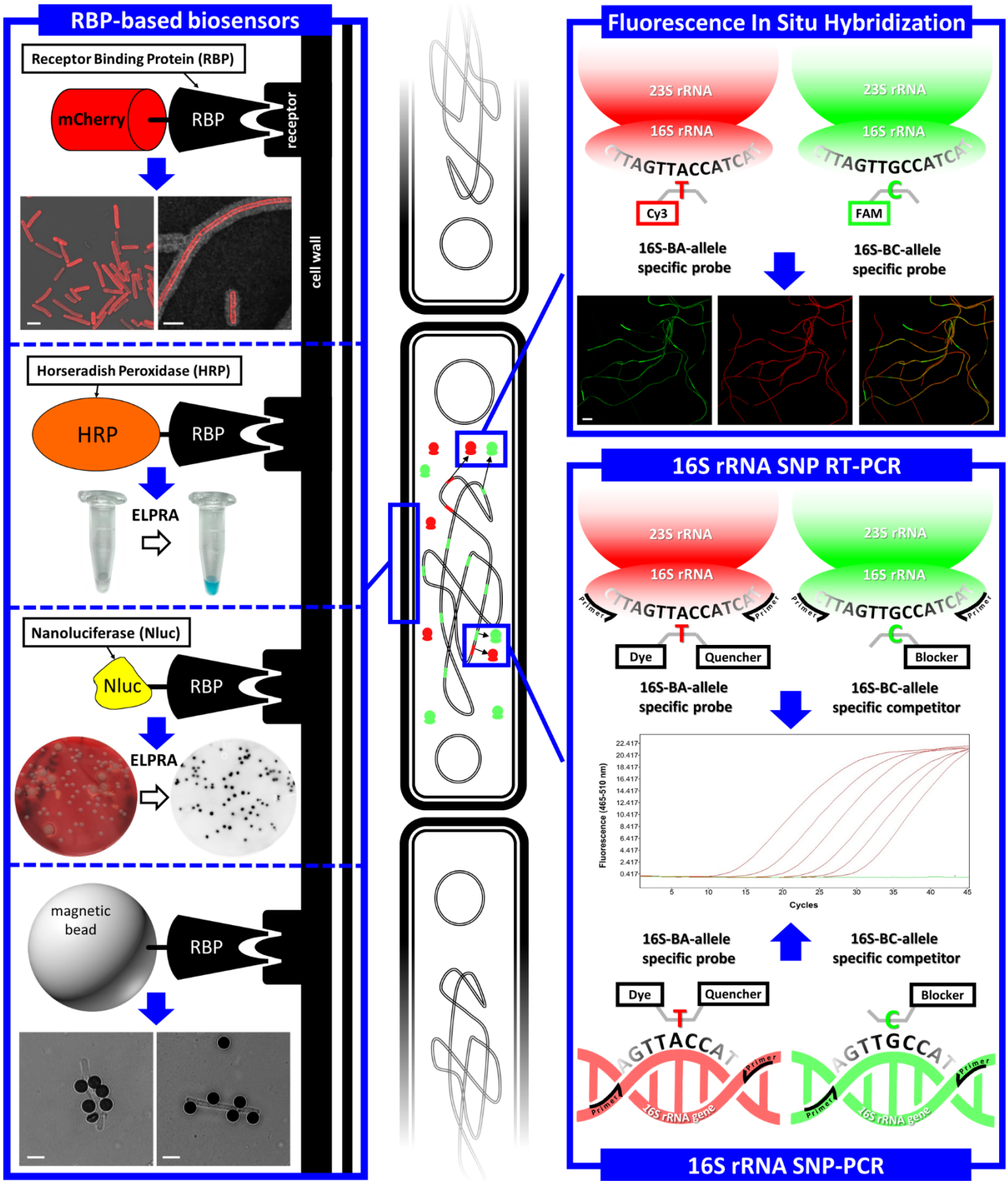

Figure 8-3: Novel tools for detection of *B. anthracis* based on phage RBPs and 16S rRNA genes and transcripts. The central panel of the figure shows a chain of *B. anthracis* cells with plasmids, a chromosome on which 16S-BA-allele- and BC-allele containing rRNA operons are highlighted as red and green segments, and respectively ribosomes derived from these operons. The *B. anthracis* specific single nucleotide variation of the

16S-BA-allele enabled the development of new detection methods (right panel) such as fluorescence in situ hybridization (FISH), where oligonucleotide probes labeled with fluorescent dyes are used to detect 16S-BA-allele (Cy3, red) or 16S-BC-allele (6-FAM, green) ribosomes by fluorescence microscopy. In addition, the 16S rRNA SNP-PCR targets 16S rRNA genes using amplification primers and a 16S-BA-allele specific hydrolysis probe and a 16S-BC-allele specific competitor probe. Converted to a 16S rRNA SNP RT-PCR this assay detects both 16S rRNA genes and their transcripts. In contrast, nucleic acid independent *B. anthracis* identification can be achieved by utilizing the binding of phage RPBs to specific surface receptors of *B. anthracis* cells (left panel). Fluorescent biosensors, consisting of RBPs fused to fluorescent protein mCherry, can be used to identify *B. anthracis* cells by fluorescence microscopy. A enzyme linked phage RBP assays (ELPRA) allow for the identification of *B. anthracis* colonies on overgrown agar plates using luminescent RBP-biosensors (RBP fused to Nanoluciferase) and for the rapid colorimetric detection of *B. anthracis* cells in a one-tube approach when horseradish peroxidase coupled RBPs are used. Moreover, RBPs coupled to magnet beads enable enrichment and isolation of *B. anthracis* from complex environmental samples such as soil.

AS a proof-of-principle approach, fluorescent biosensors were generated by genetically fusing RBP genes with those of fluorescent protein mCherry. These protein fusions were then successfully used to detect *B. anthracis* cells by fluorescence microscopy (Chapter 5). Together with the new FISH assay described in this work (Chapter 3), the first reliable microscopy based detection methods for *B. anthracis* have been developed. These assays even complement each other as the FISH assay targets nucleic acids while the RBP-based approach detects specific cell-surface receptors (Figure 8-3). Earlier microscopy based approaches mostly lack specificity, as the hitherto existing FISH assay was found to suffer from unspecific probe binding (Weerasekara et al. 2013). The only other yet published microscopic detection method relies on immunofluorescence (De et al. 2002). However, for 100% specificity two different antibodies, one of which binds to the capsule of *B. anthracis*, have to bind to the target cells in two separate, time-consuming assays. In addition, if *B. anthracis* was grown under conditions that inhibit capsule formation, this

assay will turn out negative. In contrast, both of the assays described in the work at hand (Chapter 5) feature a combined 100% specificity for *B. anthracis.* Even though none of the RBP-based fluorescent biosensors exceeded 98% specificity when tested alone, combining all three of them in one approach resulted in 100% specificity for *B. anthracis.* As proven by the successful application in the recent anthrax outbreak in southern Bavaria, the RBP-based assay can be performed directly in clinical and environmental samples, and results can be obtained in less than 10 min, making this approach a highly valuable tool for rapid identification of *B. anthracis* and diagnostics of anthrax.

When RBP binding was tested for bacterial growth-stage dependency, $RBP_{\lambda03\Delta1\text{-}120}$, compared to RBP_{Wip} and RBP_{AP50}, was found to bind to *B. anthracis* cells over a wide range independently of their growth phase. Therefore, $RBP_{\lambda03\Delta1\text{-}120}$ was used to develop further biosensors for enzyme-linked phage RBP assays (ELPRA, Figure 8-3). Using the miniature-sized “nano”luciferase nanoluc (Nluc) as transducer, instead of fluorescent proteins, enabled the identification of *B. anthracis* colonies on overgrown agar plates, e.g. from environmental samples, by emission of bioluminescence (Chapter 6). In a next step, horseradish peroxidase (HRP) was combined with $RBP_{\lambda03\Delta1\text{-}120}$ to generate a biosensor capable of producing a colorimetric ELPRA signal. When a chromogenic HRP substrate is used, the ELPRA readout can be performed by simple visual inspection without any dependence on an electronic detecting devise (Chapter 6). This enabled the rapid identification of *B. anthracis* cells in a one-tube approach when isolated colonies from environmental samples of the recent anthrax outbreak were tested (Chapter 7). They assay even performed well when inactivated blood from a diseased cow was used as a sample proving the applicability of the approach directly with authentically infected animal material. Compared to fluorescent or bioluminescent biosensors, this colorimetric biosensor might even be applied in a field laboratory environment since no advanced

laboratory equipment is needed such as a fluorescence microscope or a luminescence reader.

Inspired by earlier work (He et al. 2018; Denyes et al. 2017; Poshtiban et al. 2013), a RBP-based enrichment method was also developed utilizing $RBP_{\lambda03\Delta1\text{-}120}$ coupled magnetic beads to catch and isolate *B. anthracis* cells by magnetic separation (Figure 8-3, Chapter 7). An alternative approach using antibody coupled beads to enrich *B. anthracis* spores from food samples has already been published a decade ago (Shields et al. 2012). Although very high recovery rates of up to 100% were reported for this system, it is most likely unsuitable for environmental samples, especially for soil, as polyclonal antibodies were used to capture *B. anthracis* spores. This is due to the lack of specificity of polyclonal antibodies towards *B. anthracis* (De et al. 2002) combined with the high abundance of cells of closely related *B. cereus s. l.* strains in soil, which will most likely be co-enriched using this technique. In contrast, owed to the high specificity of $RBP_{\lambda03\Delta1\text{-}120}$ of >95% towards *B. anthracis* cells, the RBP-based enrichment approach described in the work at hand enables the isolation of *B. anthracis* from lowly contaminated environmental samples. This opens up the possibility to screen and, if present, isolate *B. anthracis* from soil samples of areas where anthrax no longer or very rarely occurs, e.g. old anthrax foci in Central Europe. Strains isolated in these areas could then be genotyped and added to the phylogeographic map of autochthonous *B. anthracis* strains. This increased phylogeographic resolution could eventually significantly improve bioforensics in case of a future anthrax outbreak, i.e. facilitate the distinction between a natural anthrax outbreak and a deliberate release of the pathogen.

8.5. Conclusion - Anthrax outbreak investigation 2.0

This work opens up three new avenues for modern anthrax outbreak investigation: i) the analysis of historical anthrax samples that facilitate future bioforensics, ii) the use of 16S rRNA gene- and transcript-based ultraspecific identification systems and iii) recombinant phage RBPs that allow for nucleic acid-independent detection and isolation of *B. anthracis.* This work not only adds new techniques to the hitherto existing toolbox for the identification and detection of *B. anthracis*, but also provides new insights into the genetics of rRNA genes and their transcripts of *B. anthracis.* In particular, the intra- and intergenomic diversity of rRNA operons has, to this point, never before been investigated for a single species in such detail. Further, three phage RBPs of *B. anthracis* specific (pro)phages have been identified and experimentally tested for their specificity towards *B. anthracis* as well as for their receptor availability in different growth phases of *B. anthracis*. In relation to previous methods, the new set of assays can be expected to aid the unequivocal identification and detection of *B. anthracis.* For instance, the new 16S rRNA SNP (RT)-PCR is superior in specificity and sensitivity compared to most established assays and is therefore likely to become the new gold standard for *B. anthracis* PCR thus improving anthrax diagnostics. With the novel 16S rRNA FISH approach and the phage RBP-based fluorescent biosensors, the first reliable microscopy based detection assays for *B. anthracis* have been developed. Together with the enzyme based RBP-biosensors used for ELPRA, these RBP assays can be ideally applied not only to detect intact *B. anthracis* cells but also as DNA-independent approaches to confirm PCR results. Finally, phage RBP-based magnetic separation can now be used to enrich and isolate *B. anthracis* from environmental samples. This groundbreaking technique can be used to increase the resolution of global phylogeography by adding more *B. anthracis* isolates from previously unavailable sources (e.g., lowly contaminated soils). Along with genetic information obtained from historical specimen, new *B. anthracis* isolates will most likely improve

anthrax bioforensics. Combined with the novel rapid and ultrasensitive detection methods developed in this work, that have already been successfully tested with actual clinical and environmental samples, modern anthrax outbreak investigations will be dramatically modernized building the foundation for "anthrax outbreak investigation 2.0".

8.6. References of Concluding Discussion

Ackermann, H.-W., and D. Prangishvili. 2012. “Prokaryote Viruses Studied by Electron Microscopy.” *Archives of Virology* 157 (10): 1843–49. https://doi.org/10.1007/s00705-012-1383-y.

Ågren, J., R. A. Hamidjaja, T. Hansen, R. Ruuls, S. Thierry, H. Vigre, I. Janse, et al. 2013. “In Silico and in Vitro Evaluation of PCR-Based Assays for the Detection of *Bacillus anthracis* Chromosomal Signature Sequences.” *Virulence* 4 (8): 671–85. https://doi.org/10.4161/viru.26288.

Antwerpen, M. H., P. Zimmermann, K. Bewley, D. Frangoulidis, and H. Meyer. 2008. “Real-Time PCR System Targeting a Chromosomal Marker Specific for *Bacillus anthracis*.” *Mol Cell Probes* 22 (5–6): 313–15. https://doi.org/S0890-8508(08)00041-8 [pii] 10.1016/j.mcp.2008.06.001.

Antwerpen, M., D. N. Proenca, C. Ruckert, K. Licht, J. Kalinowski, M. Hanczaruk, C. Tiemann, and G. Grass. 2012. “Draft Genome Sequence of *Bacillus anthracis* BF-1, Isolated from Bavarian Cattle.” *J Bacteriol* 194 (22): 6360–61. https://doi.org/10.1128/JB.01676-12 194/22/6360 [pii].

Braun, Peter, Gregor Grass, Angela Aceti, Luigina Serrecchia, Alessia Affuso, Leonardo Marino, Stefania Grimaldi, et al. 2015. “Microevolution of Anthrax from a Young Ancestor (M.A.Y.A.) Suggests a Soil-Borne Life Cycle of *Bacillus anthracis*.” *PLoS ONE* 10 (8): e0135346. https://doi.org/10.1371/journal.pone.0135346.

Campbell, Allan. 2003. “The Future of Bacteriophage Biology.” *Nature Reviews. Genetics* 4 (6): 471–77. https://doi.org/10.1038/nrg1089.

Candelon, B., K. Guilloux, S. D. Ehrlich, and A. Sorokin. 2004. “Two Distinct Types of rRNA Operons in the *Bacillus cereus* Group.” *Microbiology* 150 (Pt 3): 601–11. https://doi.org/10.1099/mic.0.26870-0.

Daims, H., K. Stoecker, and M. Wagner. 2005. “Fluorescence in Situ Hybridisation for the Detection of Prokaryotes.” In *Molecular Microbial Ecology*, edited by Mark Osborn and Cindy Smith, 213–39. London, United Kingdom: Taylor & Francis.

De, B. K., S. L. Bragg, G. N. Sanden, K. E. Wilson, L. A. Diem, C. K. Marston, A. R. Hoffmaster, et al. 2002. “A Two-Component Direct Fluorescent-Antibody Assay for Rapid Identification of *Bacillus anthracis*.” *Emerg Infect Dis* 8 (10): 1060–65. https://doi.org/10.3201/eid0810.020392.

Denyes, J. M., M. Dunne, S. Steiner, M. Mittelviefhaus, A. Weiss, H. Schmidt, J. Klumpp, and M. J. Loessner. 2017. “Modified Bacteriophage S16 Long Tail Fiber Proteins

for Rapid and Specific Immobilization and Detection of *Salmonella* Cells." *Appl Environ Microbiol* 83 (12). https://doi.org/10.1128/aem.00277-17.

Derzelle, S., G. Girault, B. Kokotovic, and O. Angen. 2015. "Whole Genome-Sequencing and Phylogenetic Analysis of a Historical Collection of *Bacillus anthracis* Strains from Danish Cattle." *PLoS One* 10 (8): e0134699. https://doi.org/10.1371/journal.pone.0134699 PONE-D-14-56572 [pii].

Dijk-Salkinoja, M. S. van, and R. J. Planta. 1971. "Rate of Ribosome Production in *Bacillus licheniformis*." *Journal of Bacteriology* 105 (1): 20–27. https://doi.org/10.1128/jb.105.1.20-27.1971.

Dunne, M., M. Hupfeld, J. Klumpp, and M. J. Loessner. 2018. "Molecular Basis of Bacterial Host Interactions by Gram-Positive Targeting Bacteriophages." *Viruses* 10 (8). https://doi.org/10.3390/v10080397.

Fouet, A., K. L. Smith, C. Keys, J. Vaissaire, C. Le Doujet, M. Levy, M. Mock, and P. Keim. 2002. "Diversity among French *Bacillus anthracis* Isolates." *Journal of Clinical Microbiology* 40 (12): 4732–34. https://doi.org/10.1128/jcm.40.12.4732-4734.2002.

Galimand, Marc, Emmanuelle Schmitt, Michel Panvert, Benoît Desmolaize, Stephen Douthwaite, Yves Mechulam, and Patrice Courvalin. 2011. "Intrinsic Resistance to Aminoglycosides in *Enterococcus faecium* Is Conferred by the 16S rRNA M5C1404-Specific Methyltransferase EfmM." *RNA (New York, N.Y.)* 17 (2): 251–62. https://doi.org/10.1261/rna.2233511.

Green, Rachel, and Harry F. Noller. 1999. "Reconstitution of Functional 50S Ribosomes from in Vitro Transcripts of *Bacillus stearothermophilus* 23S rRNA." *Biochemistry* 38 (6): 1772–79. https://doi.org/10.1021/bi982246a.

He, Yong, Yanli Shi, Mengli Liu, Yingran Wang, Lin Wang, Shuguang Lu, and Zhifeng Fu. 2018. "Nonlytic Recombinant Phage Tail Fiber Protein for Specific Recognition of Pseudomonas aeruginosa." *Analytical Chemistry* 90 (24): 14462–68. https://doi.org/10.1021/acs.analchem.8b04160.

Hoshino, T., L. S. Yilmaz, D. R. Noguera, H. Daims, and M. Wagner. 2008. "Quantification of Target Molecules Needed to Detect Microorganisms by Fluorescence in Situ Hybridization (FISH) and Catalyzed Reporter Deposition-FISH." *Appl Environ Microbiol* 74 (16): 5068–77. https://doi.org/10.1128/aem.00208-08.

Hugh-Jones, Martin, and Jason Blackburn. 2009. "The Ecology of *Bacillus anthracis*." *Molecular Aspects of Medicine* 30 (6): 356–67. https://doi.org/10.1016/j.mam.2009.08.003.

Jonge, P. A. de, F. L. Nobrega, S. J. J. Brouns, and B. E. Dutilh. 2019. “Molecular and Evolutionary Determinants of Bacteriophage Host Range.” *Trends Microbiol* 27 (1): 51–63. https://doi.org/10.1016/j.tim.2018.08.006.

Kerner, Gaspard, Guillaume Laval, Etienne Patin, Stéphanie Boisson-Dupuis, Laurent Abel, Jean-Laurent Casanova, and Lluis Quintana-Murci. 2021. “Human Ancient DNA Analyses Reveal the High Burden of Tuberculosis in Europeans over the Last 2,000 Years.” *The American Journal of Human Genetics* 108 (3): 517–24. https://doi.org/10.1016/j.ajhg.2021.02.009.

Klappenbach, J. A., J. M. Dunbar, and T. M. Schmidt. 2000. “rRNA Operon Copy Number Reflects Ecological Strategies of Bacteria.” *Appl Environ Microbiol* 66 (4): 1328–33. https://doi.org/10.1128/aem.66.4.1328-1333.2000.

Krzyzosiak, W., R. Denman, K. Nurse, W. Hellmann, M. Boublik, C. W. Gehrke, P. F. Agris, and J. Ofengand. 1987. “In Vitro Synthesis of 16S Ribosomal RNA Containing Single Base Changes and Assembly into a Functional 30S Ribosome.” *Biochemistry* 26 (8): 2353–64. https://doi.org/10.1021/bi00382a042.

Kunstmann, S., T. Scheidt, S. Buchwald, A. Helm, L. A. Mulard, A. Fruth, and S. Barbirz. 2018. “Bacteriophage Sf6 Tailspike Protein for Detection of *Shigella flexneri* Pathogens.” *Viruses* 10 (8). https://doi.org/10.3390/v10080431.

Kurylo, Chad M., Matthew M. Parks, Manuel F. Juette, Boris Zinshteyn, Roger B. Altman, Jordana K. Thibado, C. Theresa Vincent, and Scott C. Blanchard. 2018. “Endogenous rRNA Sequence Variation Can Regulate Stress Response Gene Expression and Phenotype.” *Cell Reports* 25 (1): 236-248.e6. https://doi.org/10.1016/j.celrep.2018.08.093.

Kuypers, J., and K. R. Jerome. 2017. “Applications of Digital PCR for Clinical Microbiology.” *J Clin Microbiol* 55 (6): 1621–28. https://doi.org/10.1128/jcm.00211-17.

Leiser, O. P., J. K. Blackburn, T. L. Hadfield, H. W. Kreuzer, D. S. Wunschel, and C. J. Bruckner-Lea. 2018. “Laboratory Strains of *Bacillus anthracis* Exhibit Pervasive Alteration in Expression of Proteins Related to Sporulation under Laboratory Conditions Relative to Genetically Related Wild Strains.” *PLoS ONE* 13 (12): e0209120. https://doi.org/10.1371/journal.pone.0209120.

Lekota, Kgaugelo Edward, Ayesha Hassim, Evelyn Madoroba, Charles A. Hefer, and Henriette van Heerden. 2020. “Phylogenomic Structure of *Bacillus anthracis* Isolates in the Northern Cape Province, South Africa Revealed Novel Single Nucleotide Polymorphisms.” *Infection, Genetics and Evolution* 80 (June): 104146. https://doi.org/10.1016/j.meegid.2019.104146.

Letant, S. E., G. A. Murphy, T. M. Alfaro, J. R. Avila, S. R. Kane, E. Raber, T. M. Bunt, and S. R. Shah. 2011. “Rapid Viability Polymerase Chain Reaction Method for Detection of Live Virulent *Bacillus anthracis* from Environmental Samples.” *Appl Environ Microbiol*, July. https://doi.org/AEM.00623-11 [pii] 10.1128/AEM.00623-11.

Lindström, M., R. Keto, A. Markkula, M. Nevas, S. Hielm, and H. Korkeala. 2001. “Multiplex PCR Assay for Detection and Identification of *Clostridium botulinum* Types A, B, E, and F in Food and Fecal Material.” *Appl Environ Microbiol* 67 (12): 5694–99. https://doi.org/10.1128/AEM.67.12.5694-5699.2001.

Lodmell, J. Stephen, and Albert E. Dahlberg. 1997. “A Conformational Switch in *Escherichia Coli* 16*S* Ribosomal RNA During Decoding of Messenger RNA.” *Science* 277 (5330): 1262–67. https://doi.org/10.1126/science.277.5330.1262.

Maciejewska, B., T. Olszak, and Z. Drulis-Kawa. 2018. “Applications of Bacteriophages versus Phage Enzymes to Combat and Cure Bacterial Infections: An Ambitious and Also a Realistic Application?” *Appl Microbiol Biotechnol* 102 (6): 2563–81. https://doi.org/10.1007/s00253-018-8811-1.

Majander, Kerttu, Saskia Pfrengle, Arthur Kocher, Judith Neukamm, Louis du Plessis, Marta Pla-Díaz, Natasha Arora, et al. 2020. “Ancient Bacterial Genomes Reveal a High Diversity of *Treponema pallidum* Strains in Early Modern Europe.” *Current Biology* 30 (19): 3788-3803.e10. https://doi.org/10.1016/j.cub.2020.07.058.

Nobrega, F. L., M. Vlot, P. A. de Jonge, L. L. Dreesens, H. J. E. Beaumont, R. Lavigne, B. E. Dutilh, and S. J. J. Brouns. 2018. “Targeting Mechanisms of Tailed Bacteriophages.” *Nat Rev Microbiol* 16 (12): 760–73. https://doi.org/10.1038/s41579-018-0070-8.

Pilo, P., and J. Frey. 2011. “*Bacillus anthracis*: Molecular Taxonomy, Population Genetics, Phylogeny and Patho-Evolution.” *Infect Genet Evol*, May. https://doi.org/S1567-1348(11)00201-2 [pii] 10.1016/j.meegid.2011.05.013.

Poshtiban, S., M. A. Javed, D. Arutyunov, A. Singh, G. Banting, C. M. Szymanski, and S. Evoy. 2013. “Phage Receptor Binding Protein-Based Magnetic Enrichment Method as an Aid for Real Time PCR Detection of Foodborne Bacteria.” *Analyst* 138 (19): 5619–26. https://doi.org/10.1039/c3an01100c.

Prüß, Birgit M., Kevin P. Francis, Felix von Stetten, and Siegfried Scherer. 1999. “Correlation of 16S Ribosomal DNA Signature Sequences with Temperature-Dependent Growth Rates of Mesophilic and Psychrotolerant Strains of the *Bacillus cereus* Group.” *Journal of Bacteriology* 181 (8): 2624–30.

Roller, B. R., S. F. Stoddard, and T. M. Schmidt. 2016. “Exploiting rRNA Operon Copy Number to Investigate Bacterial Reproductive Strategies.” *Nat Microbiol* 1 (11): 16160. https://doi.org/10.1038/nmicrobiol.2016.160.

Saile, E., and T. M. Koehler. 2006. “*Bacillus anthracis* Multiplication, Persistence, and Genetic Exchange in the Rhizosphere of Grass Plants.” *Appl Environ Microbiol* 72 (5): 3168–74. https://doi.org/72/5/3168 [pii] 10.1128/AEM.72.5.3168-3174.2006.

Schmidt, T. M. 1998. “Multiplicity of Ribosomal RNA Operons in Prokaryotic Genomes.” In *Bacterial Genomes*, edited by F. J. de Bruijn, J. R. Lupski, and G. M. Weinstock. Boston, MA: Springer.

Sharma, S., S. Chatterjee, S. Datta, R. Prasad, D. Dubey, R. K. Prasad, and M. G. Vairale. 2017. “Bacteriophages and Its Applications: An Overview.” *Folia Microbiol (Praha)* 62 (1): 17–55. https://doi.org/10.1007/s12223-016-0471-x.

Shields, M. J., K. R. Hahn, T. W. Janzen, N. Goji, M. C. Thomas, C. B. Kingombe, C. Paquet, A. J. Kell, and K. K. Amoako. 2012. “Immunomagnetic Capture of *Bacillus anthracis* Spores from Food.” *J Food Prot* 75 (7): 1243–48. https://doi.org/10.4315/0362-028X.JFP-12-048.

Simpson, D. J., J. C. Sacher, and C. M. Szymanski. 2016. “Development of an Assay for the Identification of Receptor Binding Proteins from Bacteriophages.” *Viruses* 8 (1). https://doi.org/10.3390/v8010017.

Singh, Amit, Sunil K. Arya, Nick Glass, Pejman Hanifi-Moghaddam, Ravendra Naidoo, Christine M. Szymanski, Jamshid Tanha, and Stephane Evoy. 2010. “Bacteriophage Tailspike Proteins as Molecular Probes for Sensitive and Selective Bacterial Detection.” *Biosensors & Bioelectronics* 26 (1): 131–38. https://doi.org/10.1016/j.bios.2010.05.024.

Stoddard, S. F., B. J. Smith, R. Hein, B. R. Roller, and T. M. Schmidt. 2015. “rrnDB: Improved Tools for Interpreting rRNA Gene Abundance in Bacteria and Archaea and a New Foundation for Future Development.” *Nucleic Acids Res* 43 (Database issue): D593-8. https://doi.org/10.1093/nar/gku1201.

Susat, Julian, Harald Lübke, Alexander Immel, Ute Brinker, Aija Macāne, John Meadows, Britta Steer, et al. 2021. “A 5,000-Year-Old Hunter-Gatherer Already Plagued by *Yersinia pestis*.” *Cell Reports* 35 (13): 109278. https://doi.org/10.1016/j.celrep.2021.109278.

Thümen, FKAEJ. 1879. “*Herbarium Mycologicum Oeconomicum*.”

Tremblay, Denise M., Mariella Tegoni, Silvia Spinelli, Valérie Campanacci, Stéphanie Blangy, Céline Huyghe, Aline Desmyter, Steve Labrie, Sylvain Moineau, and Christian Cambillau. 2006. “Receptor-Binding Protein of *Lactococcus lactis*

Phages: Identification and Characterization of the Saccharide Receptor-Binding Site." *Journal of Bacteriology* 188 (7): 2400–2410. https://doi.org/10.1128/JB.188.7.2400-2410.2006.

Turnbull, P. C. 2008. *World Health Organization. Anthrax in Humans and Animals*. Geneva (CH): WHO Press.

Turner, W. C., K. L. Kausrud, W. Beyer, W. R. Easterday, Z. R. Barandongo, E. Blaschke, C. C. Cloete, et al. 2016. "Lethal Exposure: An Integrated Approach to Pathogen Transmission via Environmental Reservoirs." *Sci Rep* 6: 27311. https://doi.org/10.1038/srep27311 srep27311 [pii].

Van Ert, M. N., W. R. Easterday, L. Y. Huynh, R. T. Okinaka, M. E. Hugh-Jones, J. Ravel, S. R. Zanecki, et al. 2007. "Global Genetic Population Structure of *Bacillus anthracis*." *PLoS One* 2 (5): e461. https://doi.org/10.1371/journal.pone.0000461.

VanBogelen, R. A., and F. C. Neidhardt. 1990. "Ribosomes as Sensors of Heat and Cold Shock in *Escherichia coli*." *Proceedings of the National Academy of Sciences of the United States of America* 87 (15): 5589–93. https://doi.org/10.1073/pnas.87.15.5589.

Vergnaud, G., G. Girault, S. Thierry, C. Pourcel, N. Madani, and Y. Blouin. 2016. "Comparison of French and Worldwide *Bacillus anthracis* Strains Favors a Recent, Post-Columbian Origin of the Predominant North-American Clade." *PLoS One* 11 (2): e0146216. https://doi.org/10.1371/journal.pone.0146216 PONE-D-15-00424 [pii].

Weerasekara, M. L., N. Ryuda, H. Miyamoto, T. Okumura, D. Ueno, K. Inoue, and T. Someya. 2013. "Double-Color Fluorescence in Situ Hybridization (FISH) for the Detection of *Bacillus anthracis* Spores in Environmental Samples with a Novel Permeabilization Protocol." *J Microbiol Methods* 93 (3): 177–84. https://doi.org/10.1016/j.mimet.2013.03.007 S0167-7012(13)00101-2 [pii].

Wielinga, P. R., R. A. Hamidjaja, J. Agren, R. Knutsson, B. Segerman, M. Fricker, M. Ehling-Schulz, et al. 2011. "A Multiplex Real-Time PCR for Identifying and Differentiating *B. anthracis* Virulent Types." *Int J Food Microbiol* 145 Suppl 1 (March): S137-44. https://doi.org/10.1016/j.ijfoodmicro.2010.07.039 S0168-1605(10)00449-6 [pii].

Woese, C. R., and G. E. Fox. 1977. "Phylogenetic Structure of the Prokaryotic Domain: The Primary Kingdoms." *Proceedings of the National Academy of Sciences* 74 (11): 5088–90. https://doi.org/10.1073/pnas.74.11.5088.

Yano, Koichi, Tetsuya Wada, Shota Suzuki, Kazumi Tagami, Takashi Matsumoto, Yuh Shiwa, Taichiro Ishige, et al. 2013. "Multiple rRNA Operons Are Essential for

Efficient Cell Growth and Sporulation as Well as Outgrowth in *Bacillus subtilis*." *Microbiology* 159 (Pt_11): 2225–36. https://doi.org/10.1099/mic.0.067025-0.

Acknowledgements

First of all, I thank Prof. Dr. Ralf Heermann for supervising my doctoral thesis. I also want to thank the thesis committee, especially Prof. Dr. Heinrich Jung for being the second examiner of my thesis.

I would especially like to thank my friend and mentor PD Dr. Gregor Grass, the external supervisor of this work, for his guidance, support, and advice throughout the years but also for giving me the possibility to work as autonomously as possible.

I also want to thank my office-mate Philipp and all the other colleagues and comrades for making this institute a great place to work.

Special thanks are due to Linda, Rahime, Sinan, Inga and all the students who worked on the projects of this thesis and without whose help this work would not have been possible.

Finally, I want to thank my family and my dear Simone for their constant support.